

PEOPLE'S DEMOCRATIC REPUBLIC OF ALGERIA
MINISTRY OF HIGHER EDUCATION AND SCIENTIFIC RESEARCH

UNIVERSITE DES FRERES MENTOURI - CONSTANTINE 1
FACULTY OF EXACT SCIENCES
DEPARTMENT OF CHEMISTRY

Ranking N°: 141 / D3C / 20158

Serial N°: 27 / CH / 2018

Thesis

Presented for Doctorate Degree third cycle (LMD).

Specialty: Pharmaceutical Chemistry.

Option: Physicochemical Analysis, Quality Control and Synthesis
of Bioactive Substances.

By

KHALFAOUI Ayoub

**Isolation, Structural Determination of Secondary
Metabolites and Biological Activities of *Asphodelus
tenuifolius* (Liliaceae)**

Members of jury

Prof. AKKAL Salah	University brothers Mentouri, Constantine 1	President
Prof. BOUHEROUM Mohamed	University brothers Mentouri, Constantine 1	Supervisor
Prof. BEHLOUL Cherif	University brothers Mentouri, Constantine 1	Examiner
Prof. BELKHIRI Abdelmalik	University Salah Boubnider, Constantine 3	Examiner
M.C.A. BENMEKHBI Lotfi	University Salah Boubnider, Constantine 3	Examiner

13/12/2018

Acknowledgements

First, I would like to thank and blessing ALLAH for giving me strength, health, energy and patience to do all this work.

I would like to express my heartfelt gratitude to my supervisor Prof. BOUHEROUM Mohamed, for offering me the remarkable opportunity to join his research group. I sincerely appreciate his genial supervision and valuable support during my PhD studies.

I am grateful to all the jury members: Prof. AKKAL Salah and Prof. BEHLOUL Cherif from university of Constantine 1, Prof. BELKHIRI Abdelmalik and M. C. A. BENMEKHBI Lotfi from university of Constantine 3 for accepting discussing and correcting my thesis.

I would like to express my acknowledgment to Prof. BENAYACHE Samir for offering me the opportunity to join his research unit (VARENBIOMOL).

I am very thankful to Prof. Guiseppe BIFULCO from University of Salerno (ITALY), for accepting my in his research group and for his constructive discussions, expert suggestions and continuous encouragement. A special thank to the entire laboratory members: Maria, Antonio, Lauro, Simone, Carmen, Stefania, Alessandra and especially to Maria Giovanna CHINI for all the knowledge and techniques she taught me, as well as for her precious help and patient direction, without her I could not make my study in Italy so far.

I would like to express my special appreciation to Prof. Ines MANCINI from University of Trento (ITALY), for accepting me to during a short-term internship at her laboratory, a special thank to Andrea DEFANT and all the technical staff.

I am indebted to both Dr. Mejdi SNOUSSI and Dr. Emira NOUMI of University of Monastir (TUNISIA), for the generous help performing for the different biological assays on various organic extracts.

I am deeply indebted to Soumia BELAABED, a special college, a special wife and a special woman, Thank you for your advice, continuous encouragement, support, being always close to me and for all your understand.

I would like also to acknowledge all my colleges, PhD students and all the staff members in our research unit (VARENBIOMOL).

At the end, I want to thank all the people who supported me from near and far, throughout my entire scientific career.

To all of you, **THANK YOU so much!**

DEDICATION

I dedicate my thesis to my dearest lovely wife SOUMIA, who gave and still giving me all the support, encouragement, understand, love and happiness.

To my special parents MAHFOUD & BADIA for their sacrifices, advice and for being always with me during all my study career with support and encourage till I finish all my studies.

To my beloved child FADY, my source of love and happiness.

To my wonderful sister IKHLASS and brothers HOUDEIFA & ASSIL.

To my brother LOKMANE, his wife IMENE and his sweet daughter LAMAR.

To my special aunt SOUMIA.

To all my wife family, uncle BRAHIM, aunt ZOUBEIDA, AMEL, SARA, MOURAD, HOUDA, MIRAL, ALINE, and BASSEM.

To all my big family, friends and colleges.

Ayoub

TABLE OF CONTENTS

List of Figures.....	
List of Tables.....	
List of Abbreviations.....	
General Introduction.....	1
References.....	3

CHAPTER I : SECONDARY METABOLITES IN PLANTS

I.1. Generalities on polyphenols.....	4
I.2. Polyphenols in health	6
I.3. Classification.....	7
I.3.1. Phenolic acids	7
I.3.2. Flavonoids	9
I.3.2.1. Generalities on flavonoids.....	9
I.3.2.2. Flavonoids and bioactivities in plants.....	15
➤ Antioxydant activity.....	15
➤ Antibacterial activity.....	15
➤ Anticancer activity.....	15
➤ Antiviral activity.....	15
➤ Hepatoprotective activity.....	16
➤ Anti-inflammatory activity.....	16
I.3.2.3. Role of flavonoids in plant physiology.....	16
I.3.2.4. Flavonoids and health benefits.....	17
I.3.3. Anthraquinones.....	17
I.3.3.1. Generalities on anthraquinones.....	17
I.3.3.2. Protective benefit of anthraquinones.....	18
➤ Laxative activity.....	19
➤ Anticancer activity.....	19
➤ Hepatoprotective activity.....	19
➤ Antimicrobial activity.....	19
➤ Antifungal activity.....	19
➤ Antiviral activity.....	19
➤ Antidiabetic activity.....	20
➤ Antioxidant activity.....	20
➤ Industrial applications.....	20
I.3.3.3. Classification of anthraquinones.....	21
a - Anthracene / anthraquinone glycosides.....	21
b - Sennosides.....	22
c - Cascarosides.....	22

I.3.3.4. Biosynthesis of anthraquinones glycosides.....	23
I.1.3.4. Tannins	24
I.1.3.5. Stilbenes.....	25
I.1.3.6. Sterols.....	25
I.1.3.7. Phytosterol.....	25
I.1.3.7.1. Biological activities of phytosterols.....	26
References.....	28

CHAPTER II : BIBLIOGRAPHIC STUDY ON *A. TENUIFOLIUS* PLANT

II.1. Botanic aspect of Liliaceae family.....	35
II.1.1. Description.....	35
II.1.2. Characters of Liliaceae.....	35
II.1.2.1. Vegetative characters.....	35
II.1.2.2. Floral characters.....	36
II.1.3. Principal secondary metabolites of Liliaceae.....	36
II.1.4. Economic importance of Liliaceae family.....	36
II.2. Botanic aspect of <i>asphodelus</i> genus.....	37
II.2.1. Description.....	37
II.2.2. Previous phytochemical studies on <i>asphodelus</i> genus.....	38
II.2.3. Previous biological studies on <i>asphodelus</i> genus.....	49
II.2.4. <i>Asphodelus tenuifolius</i> Cavase specie.....	50
II.2.4.1. Morphological aspect.....	50
II.2.4.2. Classification.....	51
II.2.4.3 Geographic distribution.....	51
II.2.4.4. Toxicity action	51
II.2.4.5. Traditional and Medicinal uses.....	52
References.....	53

CHAPTER III : MATERIALS AND METHODS

III.1. Plant material and extraction methods of <i>Asphodelus tenuifolius</i>	56
III.1.1. Plant collection.....	56
III.1.2. Preparation of extracts.....	56
III.1.3. Determination of Total Phenolic Content (TPC).....	56
III.1.4. Determination of Total Flavonoids Content (TFC).....	57
III.1.5. Determination of Total Tannins Content (TTC).....	57
III.1.6. Separation and purification.....	57
III.1.6.1. Chloroform extract of <i>A. tenuifolius</i>	57
• Study of fractions 22 and 23.....	60
• Study of fractions 21.....	61
• Study of fractions 15.....	61
• Study of fractions 10.....	62
• Study of fractions 9.....	62

• Study of fractions 2.....	63
III.1.6.2. Ethyl Acetate extract of <i>A. tenuifolius</i>	63
• Study of fractions 1.....	64
• Study of fractions 3.....	64
• Study of fractions 5.....	65
• Study of fractions 7.....	65
• Study of fractions 8.....	65
III.2. General experimental procedures.....	66
References.....	67

CHAPTER IV: RESULTS & DISCUSSIONS

IV.1. Determination of Total Phenolic Content (TPC).....	68
IV.2. Determination of Total Flavonoids Content (TFC).....	69
IV.3. Determination of Total Tannins Content (TTC).....	69
IV.4. LC-MS Analysis.....	70
IV.4.1. LC-MS analysis of Chloroform extract.....	70
IV.4.2. LC-MS analysis of Ethyl Acetate extract.....	73
IV.5. Identification of the isolated compounds from <i>A. Tenuifolius</i>	75
IV.5.1. Identification of compound 1.....	75
IV.5.2. Identification of compound 2.....	79
IV.5.3. Identification of compound 3.....	87
IV.5.4. Identification of compound 4.....	96
IV.5.5. Identification of compound 5.....	102
IV.5.6. Identification of compound 6.....	111
IV.5.7. Identification of compound 7.....	116
IV.5.8. Identification of compound 8.....	121
IV.5.9. Identification of compound 9.....	125
IV.5.10. Identification of compound 10.....	129
IV.5.11. Identification of compound 11 (New compound).....	138
IV.5.12. Identification of compound 12 (New compound).....	149
IV.5.13. Identification of compound 13.....	162
IV.5.14. Identification of compound 14.....	169
References	179

CHAPTER V: EVALUATION OF BIOLOGICAL ACTIVITIES ON *A. TENUIFOLIUS*

V.1. Antioxidant activities.....	181
V.1.1. DPPH radical scavenging assay.....	181
V.1.1.1. Results & discussion.....	182
V.1.2. β -Carotene Bleaching assay.....	184
V.1.2.1. Results & discussion.....	185
V.1.3. Conclusion.....	186

V.2. Antibacterial and antifungal activities.....	186
V.2.1. Disk diffusion assay	187
V.2.2. Microdilution assay: MICs and MBCs determinations.....	188
V.2.3. Results & discussion.....	188
V.3. Cytotoxic activities.....	191
V.3.1. Results & discussion.....	192
V.4. Antiviral activity.....	192
V.5. MTT assay.....	193
V.5.1. Cell viability assay.....	193
V.5.2. Analysis of cell cycle and hypodiploidy by flow cytometry.....	194
V.5.3. Conclusion.....	195
References.....	196
General Conclusion.....	199
Abstract.....	201
ملخص	202
Résumé	203
Article.....	

LIST OF FIGURES

Figure I.1.	Biosynthesis of phenolic compounds	5
Figure I.2.	Structure of the most important naturally occurring phenolic acids.....	8
Figure I.3.	Structure of flavonoid molecule.....	9
Figure I.4.	Structure of major classes of flavonoids.	10
Figure I.5.	Anthracene, anthracene derivatives skeleton.....	21
Figure I.6.	Anthraquinone derivatives skeleton.....	21
Figure I.7.	Dimeric anthraquinone derivatives skeleton.....	22
Figure I.8.	Sennoside (anthraquinone glycoside) derivatives skeleton.....	22
Figure I.9.	Cascarosides derivatives skeleton.....	23
Figure I.10.	Acylpolymalonate pathway.....	23
Figure I.11.	Shikimic acid pathway.....	24
Figure I.12.	Structure of Cholesterol	25
Figure I.13.	Chemical structures of Sterols	26
Figure I.14.	Chemical structures of Stanols	26
Figure II.1.	<i>Asphodelus acaulis</i> Desf	38
Figure II.2.	<i>Asphodelus aestivus</i> Brot	38
Figure II.3.	<i>Asphodelus albus</i> Mill.....	38
Figure II.4.	<i>Asphodelus macrocarpus</i> Parl.....	38
Figure II.5.	<i>Asphodelus fistulosus</i> L.....	38
Figure II.6.	<i>Asphodelus lutea</i>	38
Figure II.7.	<i>A. tenuifolius</i> floral diagram.....	50
Figure II.8.	<i>A. tenuifolius</i> Cav.	50
Figure II.9.	Geographic distribution (in Red) of <i>Asphodelus tenuifolius</i> Cav.....	51
Figure III.1.	<i>A. tenuifolius</i> Cav. (2011)	56
Figure III.2.	Plan of separation and purification of the compounds isolated from <i>A. tenuifolius</i>	58
Figure III.3.	TLC of subfraction 3 of Fraction (22+23) eluted with (CHCl ₃ / MEOH, 90:10, v/v) by treating with a Ce (SO ₄) ₂ /H ₂ SO ₄ before HPLC separation.....	60
Figure III.4.	RP- HPLC Separation chromatogram of fraction (22+23) with acetonitrile / H ₂ O (50:50, v/v).....	60
Figure III.5.	TLC of separated compounds 16, 12, 17 and 11	60
Figure III.6.	RP-HPLC Separation chromatogram of fraction 21 with Acetonitrile / H ₂ O (50:50, v/v).....	61
Figure III.7.	TLC of separated compounds 13, 14 and 15.....	61
Figure III.8.	TLC of Fraction 15 eluted with (Hexane / EtOAc, 90:10, v/v) by treating with a Ce(SO ₄) ₂ / H ₂ SO ₄	62
Figure III.9.	TLC of Fraction 9 eluted with (CHCl ₃ / MeOH, 90:10, v/v) by treating with a Ce(SO ₄) ₂ / H ₂ SO ₄	62
Figure III.10.	TLC of subfraction (1+2) from fraction 9 eluted with (CHCl ₃ / MeOH, 90:10, v/v) by treating with a Ce (SO ₄) ₂ / H ₂ SO ₄	63

Figure III.11.	RP-HPLC Separation chromatogram of fraction 1 with MeOH/H ₂ O (5% to 100%).....	64
Figure III.12.	TLC of subfraction 3 from fraction 3 eluted with (CHCl ₃ / MeOH, 90:10, v/v) by treating with a Ce (SO ₄) ₂ / H ₂ SO ₄	64
Figure III.13.	RP-HPLC Separation chromatogram of fraction 7 with MeOH /H ₂ O (5% to 100%).....	65
Figure IV.1.	Total Phenol Content (TPC) of <i>A. tenuifolius</i> extracts (expressed as mg GAE/g of DW)	68
Figure IV.2.	Total Flavonoids Content (TFC) of <i>A. tenuifolius</i> extracts (expressed as mg CE/g of DW)	69
Figure IV.3.	Total condensed Tannin Content (TTC) of <i>A. tenuifolius</i> (expressed as mg CE/g of DW)	70
Figure IV.4.	LC-MC profile in negative mode of Chloroform extract of <i>A. tenuifolius</i>	71
Figure IV.5.	Mass spectrums in negative mode of LC-MS detected compounds of Chloroform extract at different retention times.....	72
Figure IV.6.	LC-MS profile in negative mode of Ethyl Acetate extract of <i>A. tenuifolius</i>	73
Figure IV.7.	Mass spectrums of LC-MS detected compounds of Ethyl Acetate extract at different retention times.....	74
Figure IV.8.	Structure of compound 1	75
Figure IV.9.	HRESI-MS spectrum in negative ion mode of compound 1.....	75
Figure IV.10.	¹ H-NMR Spectrum (250 MHz, CD ₃ COCD ₃) of compound 1.....	76
Figure IV.11.	¹ H-NMR Spectrum (250 MHz, CD ₃ COCD ₃) of compound 1 (From 0.50 ppm to 2.50 ppm).....	77
Figure IV.12.	¹ H-NMR Spectrum (250 MHz, CD ₃ COCD ₃) of compound 1 (From 3.00 ppm to 5.50 ppm)	77
Figure IV.13.	¹³ C NMR Spectrum (250 MHz, CD ₃ COCD ₃) of compound 1.....	78
Figure IV.14.	Structure of compound 2	79
Figure IV.15.	ESI-MS in positive ion mode of compound 2.	80
Figure IV.16.	ESI-MS spectrum in negative ion mode of compound 2	80
Figure IV.17.	IR Spectrum of compound 2	81
Figure IV.18.	¹ H-NMR Spectrum (400 MHz, CD ₃ COCD ₃) of compound 2	81
Figure IV.19.	¹ H-NMR Spectrum (400 MHz, CD ₃ COCD ₃) of compound 2 (From 6.20 ppm to 7.50 ppm)	82
Figure IV.20.	¹ H-NMR Spectrum (400 MHz, CD ₃ COCD ₃) of compound 2 (From 2.40 ppm to 4.00 ppm)	82
Figure IV.21.	HSQC NMR Spectrum (400 MHz, CD ₃ COCD ₃) of compound 2.....	83
Figure IV.22.	HSQC-NMR Spectrum (400 MHz, CD ₃ COCD ₃) of compound 2 (From 6.20 ppm to 7.60 ppm)	84
Figure IV.23.	HSQC-NMR Spectrum (400 MHz, CD ₃ COCD ₃) of compound 2 (From 2.50 ppm to 4.20 ppm)	84
Figure IV.24.	HMBC-NMR Spectrum (400 MHz, CD ₃ COCD ₃) of compound 2	85

Figure IV.25.	Structure of compound 3	87
Figure IV.26.	ESI-MS spectrum in negative ion mode of compound 3	88
Figure IV.27.	¹ H-NMR Spectrum (400 MHz, CD ₃ COCD ₃) of compound 3	88
Figure IV.28.	¹ H-NMR Spectrum (400 MHz, CD ₃ COCD ₃) of compound 3 (From 7.20 ppm to 8.00 ppm)	89
Figure. IV.29.	¹ H NMR Spectrum (400 MHz, CD ₃ COCD ₃) of compound 3 (From 1.00 ppm to 3.00 ppm)	90
Figure IV.30.	HSQC-NMR Spectrum (400 MHz, CD ₃ COCD ₃) of compound 3	90
Figure IV.31.	HSQC-NMR Spectrum (400 MHz, CD ₃ COCD ₃) of compound 3 (From 7.10 ppm to 8.10 ppm)	91
Figure IV.32.	HSQC-NMR Spectrum (400 MHz, CD ₃ COCD ₃) of compound 3 (From 1.10 ppm to 3.00 ppm)	92
Figure IV.33.	HMBC-NMR Spectrum (400 MHz, CD ₃ COCD ₃) of compound 3	92
Figure IV.34.	HMBC-NMR Spectrum (400 MHz, CD ₃ COCD ₃) of compound 3 (From 7.10 ppm to 8.10 ppm)	93
Figure IV.35.	IR Spectrum of compound 3	95
Figure IV.36.	Structure of compound 4	96
Figure IV.37.	ESI-MS spectrum in negative ion mode of compound 4	97
Figure IV.38.	UV-Visible analysis spectrums of compound 4	97
Figure IV.39.	¹ H-NMR Spectrum (600 MHz, CD ₃ OD) of compound 4	98
Figure IV.40.	HSQC-NMR Spectrum (600 MHz, CD ₃ OD) of compound 4	99
Figure IV.41.	HMBC-NMR Spectrum (600 MHz, CD ₃ OD) of compound 4	100
Figure IV.42.	Structure of compound 5	102
Figure IV.43.	UV-Visible analysis spectrums of compound 5	102
Figure IV.44.	ESI-MS spectrum in negative ion mode of compound 5	103
Figure IV.45.	¹ H-NMR Spectrum (400 MHz, DMSO- <i>d</i> ₆) of compound 5	104
Figure IV.46.	¹ H-NMR Spectrum (400 MHz, DMSO- <i>d</i> ₆) of compound 5 (From 6.20 ppm to 7.50 ppm)	104
Figure IV.47.	¹ H-NMR Spectrum (400 MHz, DMSO- <i>d</i> ₆) of compound 5 (From 3.00 ppm to 5.50 ppm)	105
Figure IV.48.	HSQC-NMR Spectrum (400 MHz, DMSO- <i>d</i> ₆) of compound 5.....	106
Figure IV.49.	HMBC-NMR Spectrum (400 MHz, DMSO- <i>d</i> ₆) of compound 5.....	107
Figure IV.50.	HMBC-NMR Spectrum (400 MHz, DMSO- <i>d</i> ₆) of compound 5 (From 6.00 ppm to 7.80 ppm).	107
Figure IV.51.	HMBC-NMR Spectrum (400 MHz, DMSO- <i>d</i> ₆) of compound 5 (From 2.60 ppm to 5.30 ppm).	109
Figure IV.52.	¹ H- ¹ H COSY-NMR Spectrum (400 MHz, DMSO- <i>d</i> ₆) of compound 5..	109
Figure IV.53.	Structure of compound 6.....	111
Figure IV.54.	ESI-MS spectrum in negative ion mode of compound 6.....	111
Figure IV.55.	¹ H-NMR Spectrum (400 MHz, CDCl ₃) of compound 6.....	112
Figure IV.56.	¹ H-NMR Spectrum (400 MHz, CDCl ₃) of compound 6 (From 7.00 ppm to 8.00 ppm).	112
Figure IV.57.	HSQC-NMR Spectrum (400 MHz, CDCl ₃) of compound 6.....	113

Figure IV.58.	HMBC-NMR Spectrum (400 MHz, CDCl ₃) of compound 6.....	114
Figure IV.59.	HMBC-NMR Spectrum (400 MHz, CDCl ₃) of compound 6 (From 7.00 ppm to 8.00 ppm).	115
Figure IV.60.	Structure of compound 7.....	116
Figure IV.61.	ESI-MS data in positive ion mode of compound 7.....	117
Figure IV.62.	¹ H-NMR Spectrum (600 MHz, CD ₃ OD) of compound 7.....	117
Figure IV.63.	¹³ C-NMR Spectrum (600 MHz, CD ₃ OD) of compound 7.....	118
Figure IV.64.	HSQC-NMR Spectrum (600 MHz, CD ₃ OD) of compound 7.....	118
Figure IV.65.	¹ H- ¹ H COSY-NMR Spectrum (600 MHz, CD ₃ OD) of compound 7 (From 3.00 ppm to 5.10 ppm).	119
Figure IV.66.	HMBC-NMR Spectrum (600 MHz, CD ₃ OD) of compound 7 (From 0.50 ppm to 6.50 ppm).	120
Figure IV.67.	Structure of compound 8	121
Figure IV.68.	¹ H-NMR Spectrum (400 MHz, DMSO-d ₆) of compound 8.....	122
Figure IV.69.	¹³ C-NMR Spectrum (100 MHz, DMSO-d ₆) of compound 8.....	122
Figure IV.70.	HSQC-NMR Spectrum (400 MHz, DMSO-d ₆) of compound 8.....	123
Figure IV.71.	HMBC-NMR Spectrum (400 MHz, DMSO-d ₆) of compound 8.....	124
Figure IV.72.	Structure of compound 9.....	125
Figure IV.73.	¹ H-NMR Spectrum (600 MHz, CD ₃ OD) of compound 9.....	126
Figure IV.74.	¹ H-NMR Spectrum (600 MHz, CD ₃ OD) of compound 9 (From 7.20 ppm to 8.80 ppm).	126
Figure IV.75.	¹³ C-NMR Spectrum (150 MHz, CD ₃ OD) of compound 9.....	127
Figure IV.76.	HSQC-NMR Spectrum (600 MHz, CD ₃ OD) of compound 9.....	127
Figure IV.77.	HMBC-NMR Spectrum (600 MHz, CD ₃ OD) of compound 9.....	128
Figure IV.78.	Structure of compound 10.....	129
Figure IV.79.	ESI-MS (+) and (-) ion mode of compound 10.....	130
Figure IV.80.	¹³ C-NMR spectrum of compound 10.....	130
Figure IV.81.	¹ H-NMR Spectrum (600 MHz, CD ₃ OD) of compound 10.....	131
Figure IV.82.	¹ H-NMR Spectrum (600 MHz, CD ₃ OD) of compound 10 (From 5.00 ppm to 7.90 ppm)	132
Figure IV.83.	¹ H-NMR Spectrum (600 MHz, CD ₃ OD) of compound 10 (From 2.00 ppm to 4.50 ppm)	132
Figure IV.84.	HSQC-NMR Spectrum (600 MHz, CD ₃ OD) of compound 10	133
Figure IV.85.	¹ H- ¹ H COSY NMR Spectrum (600 MHz, CD ₃ OD) of compound 10	134
Figure IV.86.	HMBC-NMR Spectrum (600 MHz, CD ₃ OD) of compound 10.....	135
Figure IV.87.	HMBC-NMR Spectrum (600 MHz, CD ₃ OD) of compound 10 (From 5.00 ppm to 8.00 ppm).....	135
Figure IV.88.	HMBC-NMR Spectrum (600 MHz, CD ₃ OD) of compound 10 (From 1.50 ppm to 5.50 ppm).....	137
Figure IV.89.	Structure of compound 11.....	138
Figure IV.90.	HR-ESIMS spectrum in negative ion mode of compound 11	139
Figure IV.91.	¹ H-NMR Spectrum (600 MHz, CDCl ₃) of compound 11.....	139
Figure IV.92.	¹ H-NMR Spectrum (600 MHz, CDCl ₃) of compound 11 (From 6.70	

	ppm to 7.70 ppm).....	140
Figure IV.93.	¹ H-NMR Spectrum (600 MHz, CDCl ₃) of compound 11 (From 2.90 ppm to 4.30 ppm).....	141
Figure IV.94.	HSQC-NMR Spectrum (600 MHz, CDCl ₃) of compound 11.....	142
Figure IV.95.	HSQC-NMR Spectrum (600 MHz, CDCl ₃) of compound 11 (From 6.75 ppm to 7.75 ppm)	143
Figure IV.96.	HSQC-NMR Spectrum (600 MHz, CDCl ₃) of compound 11 (From 1.90 ppm to 3.80 ppm).....	144
Figure IV.97.	HMBC-NMR Spectrum (600 MHz, CDCl ₃) of compound 11.....	144
Figure IV.98.	HMBC-NMR Spectrum (600 MHz, CDCl ₃) of compound 11 (From 11.55 ppm to 12.75 ppm)	145
Figure IV.99.	HMBC-NMR Spectrum (600 MHz, CDCl ₃) of compound 11 (From 6.00 ppm to 7.70 ppm).....	146
Figure IV.100.	HMBC-NMR Spectrum (600 MHz, CDCl ₃) of compound 11 (From 0.50 ppm to 4.30 ppm).....	146
Figure IV.101.	¹ H- ¹ H COSY NMR Spectrum (600 MHz, CDCl ₃) of compound 11.(From 2.50 ppm 4.70 ppm).....	147
Figure IV.102.	IR Spectrum of compound 11.....	147
Figure IV.103.	Structure of compound 12.....	149
Figure IV.104.	HRESI-MS spectrum in negative ion mode of compound 12.....	150
Figure IV.105.	¹ H-NMR Spectrum (600 MHz, CDCl ₃) of compound 12.....	150
Figure IV.106.	¹ H-NMR Spectrum (600 MHz, CDCl ₃) of compound 12 (From 6.70 ppm to 7.80 ppm)	151
Figure IV.107.	¹ H-NMR Spectrum (600 MHz, CDCl ₃) of compound 12 (From 2.90 ppm to 4.30 ppm).....	151
Figure IV.108.	HSQC-NMR Spectrum (600 MHz, CDCl ₃) of compound 12.....	152
Figure IV.109.	HSQC-NMR Spectrum (600 MHz, CDCl ₃) of compound 12 (From 6.60 ppm to 7.90 ppm).....	153
Figure IV.110.	HSQC-NMR Spectrum (600 MHz, CDCl ₃) of compound 12 (From 2.10 ppm to 3.90 ppm).....	153
Figure IV.111.	HMBC-NMR Spectrum (600 MHz, CDCl ₃) of compound 12.....	155
Figure IV.112.	HMBC-NMR Spectrum (600 MHz, CDCl ₃) of compound 12 (From 11.75 ppm to 12.70 ppm).....	155
Figure IV.113.	HMBC-NMR Spectrum (600 MHz, CDCl ₃) of compound 12 (From 6.75 ppm to 7.70 ppm).....	156
Figure IV.114.	HMBC-NMR Spectrum (600 MHz, CDCl ₃) of compound 12 (From 1.80 ppm to 4.00 ppm).....	156
Figure IV.115.	¹ H- ¹ H COSY NMR Spectrum (600 MHz, CDCl ₃) of compound 12 (From 2.50 ppm to 4.70 ppm).....	157
Figure IV.116.	Proposed stereo-assignment of compounds 11 and 12.....	160
Figure IV.117.	Comparison of the experimental ECD spectra of compounds 11 and 12 with the TDDFT-predicted curves of compounds 11a, 11b, 12a and 12b	161

Figure IV.118.	Structures of compounds 11 (<i>M</i> , 10' <i>S</i>) and 12 (<i>P</i> , 10' <i>S</i>).....	162
Figure IV.119.	Structure of compound 13.....	162
Figure IV.120.	ESI-MS spectrum in negative ion mode of compound 13	163
Figure IV.121.	¹ H-NMR Spectrum (400 MHz, CD ₃ COCD ₃) of compound 13.....	163
Figure IV.122.	¹ H-NMR Spectrum (400 MHz, CD ₃ COCD ₃) of compound 13 (From 6.50 ppm to 8.00 ppm).....	164
Figure IV.123.	¹ H-NMR Spectrum (400 MHz, CD ₃ COCD ₃) of compound 13 (From 1.70 ppm to 4.20 ppm).....	164
Figure IV.124.	¹³ C-NMR Spectrum (400 MHz, CD ₃ COCD ₃) of compound 13.....	165
Figure IV.125.	HSQC-NMR Spectrum (400 MHz, CD ₃ COCD ₃) of compound 13.....	166
Figure IV.126.	HSQC-NMR Spectrum (400 MHz, CD ₃ COCD ₃) of compound 13 (From 6.60 ppm to 8.10 ppm).....	166
Figure IV.127.	HSQC-NMR Spectrum (400 MHz, CD ₃ COCD ₃) of compound 13 (From 1.80 ppm to 3.90 ppm).....	167
Figure IV.128.	Experimental (Green for compound 13) spectrum compared to the calculated (Black) ECD spectrum of compound 13.....	169
Figure IV.129.	Structure of compound 14	169
Figure IV.130.	ESI-MS spectrum in negative ion mode of compound 14.....	170
Figure IV.131.	¹ H-NMR Spectrum (400 MHz, CD ₃ COCD ₃) of compound 14.....	171
Figure IV.132.	¹ H-NMR Spectrum (400 MHz, CD ₃ COCD ₃) of compound 14 (From 6.70 ppm to 7.90 ppm).....	171
Figure IV.133.	¹ H-NMR Spectrum (400 MHz, CDCl ₃) of compound 14.....	172
Figure IV.134.	¹ H-NMR Spectrum (400 MHz, CDCl ₃) of compound 14 (From 2.10 ppm to 3.90 ppm)	173
Figure IV.135.	HSQC-NMR Spectrum (400 MHz, CDCl ₃) of compound 14.....	173
Figure IV.136.	HSQC-NMR Spectrum (400 MHz, CDCl ₃) of compound 14.....	174
Figure IV.137.	HMBC-NMR Spectrum (400 MHz, CDCl ₃) of compound 14 (From 11.40 ppm to 12.70 ppm).....	175
Figure IV.138.	HMBC-NMR Spectrum (400 MHz, CDCl ₃) of compound 14 (From 1.30 ppm to 4.60 ppm).....	175
Figure IV.139.	HMBC-NMR Spectrum (400 MHz, CDCl ₃) of compound 14 (From 4.80 ppm to 7.90 ppm).....	176
Figure IV.140.	Experimental (Blue for compound 13 and Pink for compound 14) spectrum compared to the calculated (Black) ECD spectrum of compound 13.....	177
Figure V.1.	Structure of DPPH [•] radical and its reduction by an antioxidant (AO-H)	182
Figure V.2.	Scavenging effect of different extracts of <i>A. tenuifolius</i> on DPPH radical (%)	184
Figure V.3.	Scavenging effect of different extracts of <i>A. tenuifolius</i> on β-Carotene bleaching (BCB%).....	186
Figure V.4.	Compounds 11 and 12 affects A375 human melanoma cell viability and cell cycle progression.....	194

LIST OF TABLES

Table I.1.	Classification of phenolic compounds in plants.....	6
Table I.2.	Flavonoids, classes, sub-classes and different sources	11
Table II.1.	Isolated compounds from <i>Asphodelus</i> genus.....	39
Table III.1.	Results of chromatographic separation of Chloroform extract by silica gel column with Hexane/ EtOAc.....	59
Table III.2.	Results of chromatographic separation of Ethyl Acetate extract by silica gel column with CHCl ₃ / MeOH.....	63
Table IV.1.	Total Phenol Contents (TPC) (expressed as mg Gallic Acid Equivalents/g Dry Weight) of <i>A. tenuifolius</i> extracts.....	68
Table IV.2.	Total Flavonoids Contents (TFC) (expressed as mg Catechin Equivalents/g of Dry Weight) in <i>A. tenuifolius</i> extracts.....	69
Table IV.3.	Total Tannins Contents (TTC) (expressed as mg Catechin Equivalents/g Dry Weight) in <i>A. tenuifolius</i>	70
Table IV.4.	Bioactive compounds detected and identified by LC-MS of Chloroform extract of <i>A. tenuifolius</i>	73
Table IV.5.	Bioactive compounds detected and identified by LC-MS of Ethyl Acetate extract of <i>A. tenuifolius</i>	74
Table IV.6.	¹ H and ¹³ C NMR data (250 MHz) of compound 1 (CD ₃ COCD ₃).....	78
Table IV.7.	¹ H, ¹³ C and HMBC NMR data (400 MHz) of compound 2 (CD ₃ COCD ₃)	86
Table IV.8.	¹ H, ¹³ C and HMBC NMR data (400 MHz) of compound 3 (CD ₃ COCD ₃).....	95
Table IV.9.	UV-Visible data of compound 4.....	98
Table IV.10.	¹ H, ¹³ C and HMBC NMR data (600 MHz) of compound 4 (CD ₃ OD)...	101
Table IV.11.	UV-Visible data of compound 5.....	103
Table IV.12.	¹ H, ¹³ C and HMBC NMR data (400 MHz) of compound 5 (DMSO- <i>d</i> ₆).....	110
Table IV.13.	¹ H NMR, ¹³ C and HMBC data (600 MHz)of compound 6 (CDCl ₃)....	115
Table IV.14.	¹ H NMR and ¹³ C data (600 MHz) of compound 7 (CD ₃ OD).....	120
Table IV.15.	¹ H NMR, ¹³ C and HMBC data (400 MHz) of compound 8 (DMSO- <i>d</i> ₆).....	124
Table IV.16.	¹ H, ¹³ C and HMBC NMR data (600 MHz) of compound 9 (CD ₃ OD)...	129
Table IV.17.	¹ H, ¹³ C and HMBC NMR data (600 MHz) of compound 10 (CD ₃ OD)...	137
Table IV.18.	¹ H, ¹³ C and HMBC NMR data of compound 11 (CDCl ₃).....	148
Table IV.19.	¹ H, ¹³ C and HMBC NMR data of compound 12 (CDCl ₃).....	157
Table IV.20.	¹ H, ¹³ C and HMBC NMR data of compound 13 (CD ₃ COCD ₃).....	167
Table IV.21.	¹ H, ¹³ C and HMBC NMR data of compound 14 (CDCl ₃).....	176
Table V.1.	Antioxidant activity (%) of the various extracts of <i>A. Tenuifolius</i> measured by the scavenging of DPPH radicals.....	183
Table V.2.	Antioxidant activity of the different extracts of <i>A. tenuifolius</i> and standard assayed by β -Carotene linoleate bleaching.....	185
Table V.3.	Antibacterial and antifungal activities (expressed as diameter of	

	Inhibition Zone (IZ), on mm), MIC and MBC values (mg/ml) of the different extracts from <i>A. tenuifolius</i> (Values expressed as the means $IZ \pm SD$ (Standard Deviation)).....	190
Table V.4.	The CC_{50} of the cytotoxicity assay of <i>A. tenuifolius</i> extracts on VERO cells.....	192

LIST OF ABBREVIATIONS

approx.	approximately
<i>brs</i>	broad sigulet
CC	Column Chromatography
¹³ C-NMR	Carbon Nuclear Magnetic Resonance.
COSY	Correlation Spectroscopy
CHCl ₃	Chloroform
CDCl ₃	Chloroform deuterated
<i>d</i>	doublet
<i>dd</i>	double of doublets
<i>ddd</i>	double double of doublets
<i>dt</i>	double of triplets
DEPT	distortionless enhancement by polarization transfer
DMSO-d ₆	dimethyl sulphoxide deuterated
DNA	deoxyribonucleic acid
DPPH	2,2-diphenyl-1-picrylhydrazyl
DW	Dry weight
δ _C	Carbon chemical shift
δ _H	proton chemical shift
EC 50	half maximal effective concentration
e.g.	exempli gratia (for the sake of example)
EI	electron impact
ESI	electro spray ionization
<i>et al.</i>	(and others)
EtOH	ethanol
EtOAc	ethyl acetate
ECD	Electronic Circular Dichroism
Fr	fraction
g	gramme
Glu	glucose
h	hours
Kg	Kilogramme
¹ H-NMR	proton Nuclear Magnetic Resonance.
HMBC	heteronuclear multiple bond connectivity
HPLC	high performance liquid chromatography
HSQC	heteronuclear single quantum coherence
Hz	hertz
HR-MS	high resolution mass spectroscopy
IC50	half maximal inhibitory concentration
IZ	Inhibition zone
<i>J</i>	Coupling constant.
L	liter
LC-MS	Liquid chromatography-mass spectrometer

M	Molarity
<i>m</i>	multiplet
CD ₃ OD	methanol deuterated
MeOH	methanol
μg	microgramme
mm	millimeter
mg	milligramme
MHz	Mega hertz
min	minute
mL	millilitre
MS	mass spectroscopy
MTT	3-(4,5-dimethylthiazol-2-yl)-2,5-diphenyltetrazolium bromide
<i>m/z</i>	mass per charge
<i>m</i>	multiplet
μL	microlitre
MW	Molecular Weight
n-BuOH	n-butanol
n.d.	not determined
nm	nanometer
NMR	nuclear magnetic resonance
ppm	part per million
<i>q</i>	quartet
RP	reversed phase
<i>s</i>	singlet
<i>t</i>	triplet
TLC	Thin layer chromatography.
UV	Ultraviolet.

GENERAL INTRODUCTION

Human beings have used plants for the treatment of diverse ailments for thousands of years [1]. Medicinal plants have been used as sources of medicine in virtually all cultures [2]. A large number of them are used without side effects when compared with synthetic drugs. Each plant whether it may be shrub, herbs, algae have its own significance in pharmaceutical, medicinal, agricultural, industrial, biochemical and chemical sciences.

In recent years, phytochemicals in vegetables and plants have received a great deal of attention mainly on their role in preventing diseases caused as a result of oxidative stress which releases reactive oxygen species such as singlet oxygen and various radicals as a damaging side effect of aerobic metabolism. Characterization of extracts of medicinal plants is necessary, due to its numerous benefits to science and society. The information obtained, makes pharmacological studies possible. It also enabled structure-related activity studies to be carried out, leading to the possible synthesis of more potent drug with reduced toxicity. The mode of action of the plants producing the therapeutic effect can also be better investigated if the active ingredients are characterized.

The most essential of these bioactive constituents of medicinal plants are alkaloids, tannins, flavonoids, anthraquinones and phenolic compounds. Many of the indigenous medicinal plants are used as spices and food [3].

The study on natural products encompasses the investigation into their molecular structure, biogenesis, and biological functions in the organism, therapeutic applications and other uses. Studies on natural products have become more and more important with the realization that plants provide a source of useful chemicals that may be used directly or as templates for the development of drugs responsible for defense or protection against various diseases.

African medicinal plants have a long history of providing important sources of healing drugs to local populations. In certain African countries, up to 80% of the population (OMS) still relies exclusively on plants as a source of medicines [4]. In Algeria, North African country with its large variety of soils (littoral, steppe, mountains and desert) and climates, possesses a rich flora (more than 3000 species, 123 botanic family and 1000 genders) [5], This richness make the study of the algerian flora presenting a scientific interest for more knowledge in the field of ethnobotany, traditional pharmacopoeia and in the field of valorization of natural substances. These findings led us to explore these resources in terms of phytochemistry and pharmacology.

In this context, and in continuity of our research program at the VARENBIOMOL research unit on Algerian saharian plants, the aim of this work focused firstly on the structural determination of common and new compounds with potential biological activity, and secondly, on the evaluation of different biological activities of the various organic extracts of *Asphodelus tenuifolius* plant which belongs to the Liliaceae family. The selection of this species was based on its endemism and on the fact that this Algerian plant had never been a subject of any phytochemical investigations.

Our works reported in this manuscript are divided into five chapters:

- The first describe the main families of secondary metabolites isolated from plants, In particular, phenolic acids, flavonoids, Anthraquinones, sterols. This study will include definitions, classifications, their biosynthesis as well as their biological activities.
- The second concern a bibliographic study of the Liliaceae family, *Asphodelus* genus and the studied plant *Asphodelus tenuifolius*.
- The third is devoted to all the personal phytochemical works. This chapter describes the isolation, the purification methods and the structural characterization, as well as the chromatographic and spectroscopic techniques used during this study.
- The fourth present the identification and structural determination of the isolated compounds from this species, LC-MS profiles of the studied organic extracts, explications and discussion of the obtained results from the spectroscopic data released using the different NMR experiments (^1H , ^{13}C , HSQC, HMBC, COSY...), ECD spectra, UV-Visible and Mass spectroscopic analysis.
- The last chapter included the various biological analysis results of the different organic extracts of *Asphodelus tenuifolius* plant (antioxydant, antibacterial, antifungal, cytotoxic and antiviral activities) and the MTT assay on two new isolated compounds to evaluate the potential anti-proliferative and cytotoxic activity in A375 (human melanoma) cancer cell line.

REFERENCES

- [1] Sofowara, A., **1982**. Medicinal plants and traditional medicine in Africa. John Wiley, Chichester, 179.
- [2] Anwanni, H. G., Atta, R., *J. Ethnopharmacol*, **2013**, *100*, 43-49
- [3] Amin, M. M., Sawhney, S. S., Jassal, M. M. S., *Wudpecker Journal of Pharmacy and Pharmacology*, **2013**. *2*, 1-5.
- [4] Hostettmann, K., Wolfender, J. L., Terreaux, C., *Pharmaceutical Biology*, **2001**, *39*, 18-32.
- [5] Lakehal, S., Meliani, A., Benmimoune, S., Bensouna, S. N., Benrebiha, F. Z., Chaouia, C., *Medicinal chemistry*, **2016**, *6*, 435-439.

CHAPTER I

SECONDARY METABOLITES

IN PLANTS

I.1. Generalities on Polyphenols

Plants are rich sources of functional dietary micronutrients, fibers and phytochemicals, such as ascorbic acid, carotenoids, and phenolic compounds, that individually, or in combination, may be beneficial for health since they demonstrate antioxidative activity *in vitro* [1-2].

Phenolic compounds are secondary metabolites, which are produced in the shikimic acid of plants and pentose phosphate through phenylpropanoid metabolization [3]. They contain benzene rings, with one or more hydroxyl substituent, and range from simple phenolic molecules to highly polymerized compounds [4].

In the biosynthesis of phenolic compounds, the first procedure is the commitment of glucose to the Pentose Phosphate Pathway (PPP) and transforming glucose-6-phosphate irreversibly to ribulose-5-phosphate (**Fig. I.1**). The first committed procedure in the conversion to ribulose-5-phosphate is put into effect by glucose-6-phosphate dehydrogenase (G6PDH). On the one hand, the conversion to ribulose-5-phosphate produces reducing equivalents of nicotinamide adenine dinucleotide phosphate (NADPH) for cellular anabolic reactions. On the other hand, PPP also produces erythrose-4-phosphate along with phosphoenolpyruvate from glycolysis, which is then used through the phenylpropanoid pathway to generate phenolic compounds after being channeled to the shikimic acid pathway to produce phenylalanine [5-6].

These phenolic compounds, one of the most widely occurring groups of phytochemicals, are of considerable physiological and morphological importance in plants. These compounds play an important role in growth and reproduction, providing protection against pathogens and predators [7]. They are widespread groups of substances in flowering plants, occurring in all vegetative organs, as well as in flowers and fruits, vegetables, cereals, grains, seeds and drinks. Despite this structural diversity, the groups of compounds are often referred to as “polyphenols” [8-9]. Plant genetics and cultivar, soil composition and growing conditions, maturity state and post-harvest conditions are effective on the quantity and quality of the polyphenols present in plant foods [10].

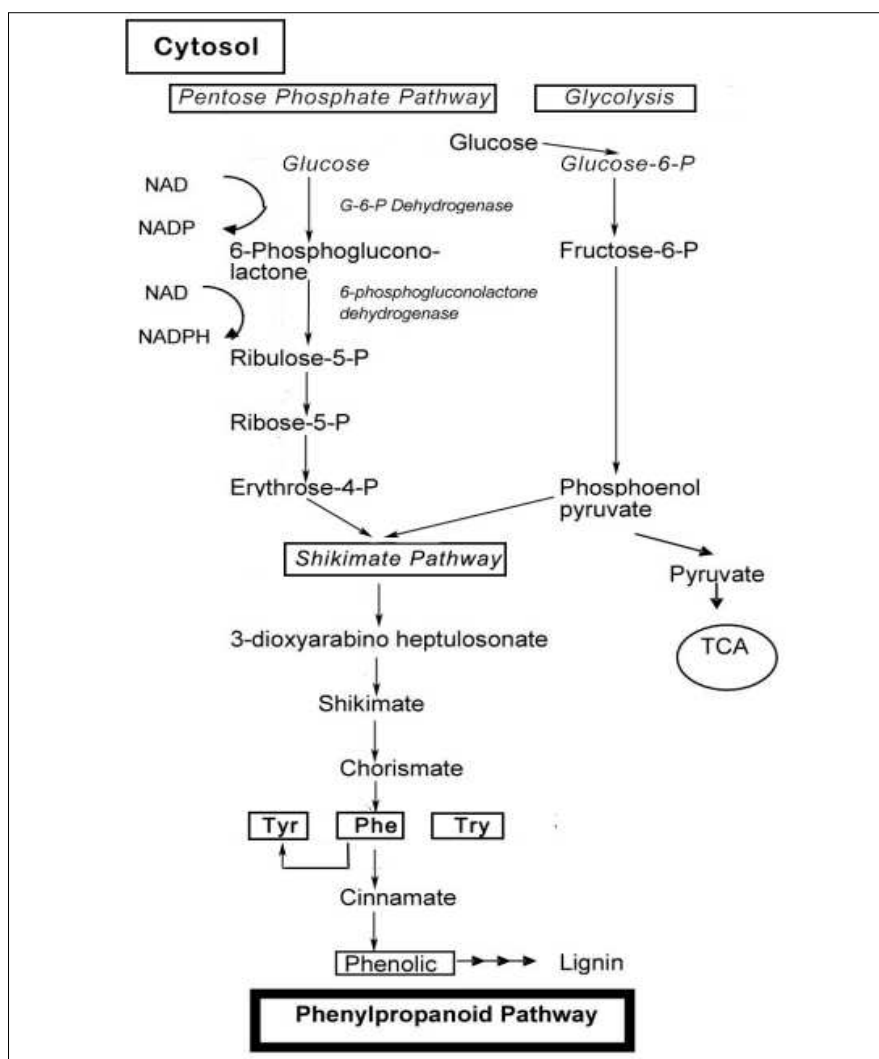


Figure I.1. Biosynthesis of phenol compounds (modified by Vatter *et al.*, 2005 [5] and Lin *et al.* 2010 [6]).

These phenolic substances and polyphenols, contain numerous varieties of compounds (**Table. I.1**): simple flavonoids, phenolic acids, complex flavonoids and colored anthocyanins [11]. These phenolic compounds are usually related to defense responses in the plant. However, phenolic metabolites play an important part in other processes, for instance incorporating attractive substances to accelerate pollination, coloring for camouflage and defense against herbivores, as well as antibacterial and antifungal activities [12-13].

Table I.1. Classification of phenolic compounds in plants.

<i>Classes</i>	<i>Structure</i>
Simple phenolics, benzoquinones	C ₆
Hydroxybenzoic acids	C ₆ -C ₁
Acetophenones, phenylacetic acids	C ₆ -C ₂
Hydroxycinnamic acids, phenylpropanoids (Coumrins, isocoumarins, chromones, chromenes)	C ₆ -C ₃
Napthaquinones	C ₆ -C ₄
Xanthones	C ₆ -C ₁ -C ₆
Stilbenes, anthraquinones	C ₆ -C ₂ -C ₆
Flavonoids, Isoflavonoids	C ₆ -C ₃ -C ₆
Lignans, neolignans	(C ₆ -C ₃) ₂
Biflavonoids	(C ₆ -C ₃ -C ₆) ₂
Lignins	(C ₆ -C ₃) _n
Condensed tannins (proanthocyanidins or flavons)	(C ₆ -C ₃ -C ₆) _n

Phenolic compounds confer unique taste, flavour, and health promoting properties found in plants, vegetables and fruits [14].

I.2. Polyphenols in Health

In recent years, the importance of antioxidant activities of phenolic compounds and their potential usage in processed foods as a natural antioxidant compounds has reached a new level and some evidence suggests that the biological actions of these compounds are related to their antioxidant activity [15].

Phenolic compounds exhibit a wide range of physiological properties; many studies have reported many advantages such as: anti-allergenic, anti-atherogenic, anti-inflammatory, anti-microbial, antioxidant, anti-thrombotic, cardioprotective and vasodilatory effects [16-20].

The chemical constituents extracted from plants, can inhibit the absorption of amylase in the treatment of carbohydrate absorption, such as diabetes [21]. In addition to the adjustment of the above, there are relevant antioxidant enzymes to counter oxidants [22-23]. The possible health benefits of dietary phenolics depend on their absorption and metabolism, which in turn are determined by their structure including their conjugation with other phenolics, degree of glycosilation / acylation, molecular size and solubility. The metabolites of polyphenols are rapidly eliminated from plasma, thus, daily consumption of plant products is essential in order to supply high metabolite concentrations in the blood [24-25].

Up to now epidemiological knowledge emphasize that polyphenols display important functions, like inhibition of pathogens and decay microorganisms, anti-

deposition of triglycerides, reduce the incidence of non-transmissible diseases such as cardiovascular diseases, diabetes, cancer and stroke, anti-inflammation and anti-allergic effect through processes involving reactive oxygen species. These protective effects are attributed, in part, to phenolic secondary metabolites [26-27].

Phenolic acids, hydrolysable tannins, and flavonoids have anti-carcinogenic and anti-mutagenic effects since they act as protective agents of DNA against free radicals, by inactivating carcinogens, inhibiting enzymes involved in pro-carcinogen activation and by activating of xenobiotics detoxification enzymes. In particular flavonoids and L-ascorbic acid have a synergistic protective effect towards oxidative damages of DNA in lymphocytes [28-29]. Block *et al.* [30] stated that a diet rich in vegetables reduces the risk for colon cancer. Both chlorogenic and caffeic acids are antioxidants *in vitro*, and they are potential inhibitors for the formation of mutagenic and carcinogenic N-nitroso compounds *in vitro* [31]. Flavonoids, catechins and their derivatives are considered as therapeutic agents in studies focused on degenerative diseases and brain aging processes, and serve as possible neuroprotective agents in progressive neurodegenerative disorders such as Parkinson's and Alzheimer's diseases [32-33]. High flavonoid intakes lead a decrease in LDL oxidation [34-35].

I.3. Classification

The structure, the number of aromatic nuclei and structural elements which bind these nuclei are the dominant features of the classification of polyphenols which can distinguish the following main groups [36]:

I.3.1. Phenolic Acids

Phenolic acids are aromatic secondary plant metabolites broadly distributed throughout the plant kingdom. The term “phenolic acids”, in general, designates phenols that possess one carboxylic acid functionality, moreover the reason for including phenolic acids in the family of plant polyphenols lies in the fact that they are bioprecursors of polyphenols and, more importantly, they are metabolites of polyphenols. Naturally occurring phenolic acids contain two distinctive carbon frameworks: the hydroxycinnamic and hydroxybenzoic structures. Hydroxybenzoic acids include gallic, *p*-hydroxybenzoic, protocatechuic, vanillic and syringic acids, which in common have the (C6–C1) structure (**Fig. I.2**). Hydroxycinnamic acids, on the other hand, are aromatic compounds with a three-carbon side chain (C6–C3), with caffeic, ferulic, *p*-coumaric and sinapic acids being the most common (**Fig. I.2**).

The main sources of phenolic acids are blueberry, cranberry, pear, cherry (sweet), apple, orange, grapefruit, cherry juice, apple juice, lemon, peach, potato, lettuce, spinach, coffee beans, tea, coffee and cider. Hydroxycinnamic acids are a major class within the phenolic compounds [37-38].

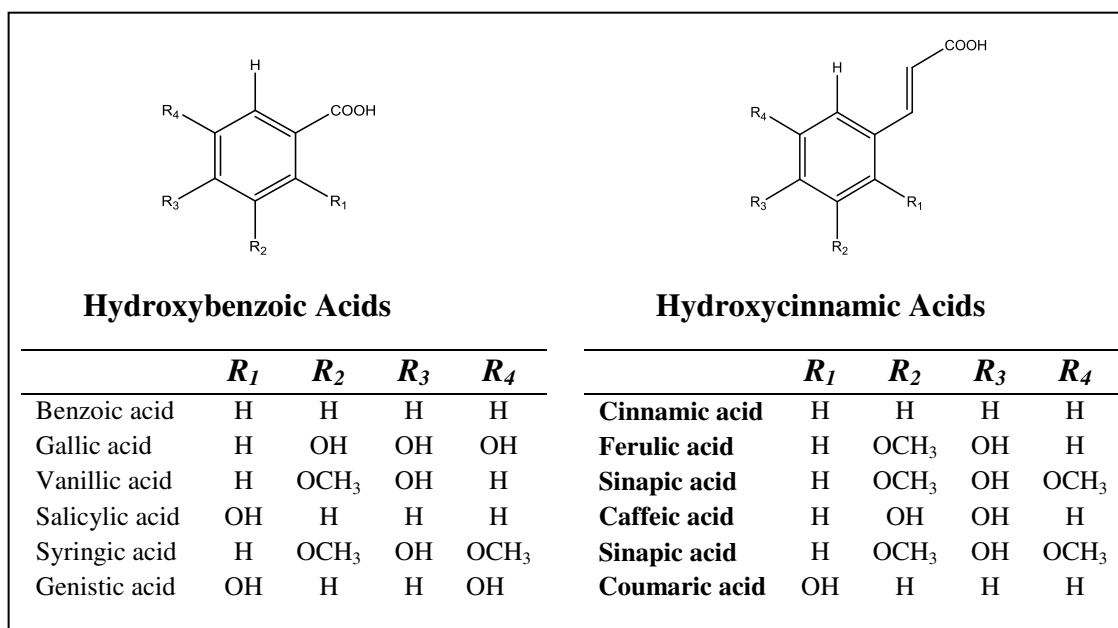


Figure I.2. Structure of the most important naturally occurring phenolic acids.

Many papers and reviews described studies on bioavailability of phenolic acids, emphasizing both the direct intake through food consumption and the indirect bioavailability deriving by gastric, intestinal and hepatic metabolism [39]. In addition Phenolic acid compounds and functions have been the subject of a great number of agricultural, biological, chemical and medical studies.

Also, these phenols acids which are present in a significant amount in fruits and vegetables are scavengers of free radicals (antioxidants) playing a recognized role in the maintenance of a good state of health. These compounds could participate in the prevention of pathologies partly related to an excess of free radicals and oxidative stress [40].

Various phenolic acids have been found during the different stages of maturation [41] while growing conditions are known to have an impact on the phenolic acid content [42]. Many of the phenolic acids like cinnamic and benzoic acid derivatives exist in all plant and plant-derived foods (*e.g.*, fruits, vegetables, and grains) [43]. Although much knowledge is to be obtained with respect to the role of phenolic acids in plants, they have been associated with diverse functions, including nutrient uptake, protein synthesis, enzyme activity, photosynthesis, structural components and allelopathy [44].

I.3.2. Flavonoids

I.3.2.1. Generalities on flavonoids

Flavonoids are the most abundant polyphenols in human diets, accounting for over half of the eight thousand naturally occurring phenolic compounds found mainly in blackberries, black currant, blueberries, grape, strawberries, cherries, plums, cranberry, pomegranate, and raspberry. The flavonoids, the derivatives of 1, 3-diphenylpropane, are a large group of natural products which are widespread in higher plants but also found in some lower plants, including algae. They are low molecular weight compounds, consisting of fifteen carbon atoms; bear the C6–C3–C6 structure (**Fig. I.3**). They are mainly divided into two classes: (a) anthocyanins (glycosylated derivative of anthocyanidin, present in colorful flowers and fruits); (b) anthoxanthins (a group of colorless compounds further divided in several categories, including flavones, flavans, flavonols, isoflavones and their glycosides) [37-45-46]. Flavonoids occur both in the free state and as glycosides.

Essentially the structure consists of two benzene or aromatic rings A and B, joined by a 3-carbon bridge, usually in the form of a heterocyclic ring C (**Fig. I.3**). The aromatic ring A is derived from the acetate / malonate pathway, while ring B is derived from phenylalanine through the shikimate pathway [47-48]. Variations in substitution patterns to ring C result in the major flavonoid classes, i.e., flavonols, flavones, flavanones, flavanols, isoflavones, flavanonols, and anthocyanidins (**Fig. I.4**) [49], of which flavones and flavonols are the most widely occurring and structurally diverse [50]. Substitutions to rings A and B give rise to the different compounds within each class of flavonoids [51]. These substitutions may include oxygenation, alkylation, glycosylation, acylation, and sulfation [47-49].

Major dietary sources of Flavonoids in the form of flavonols, flavones, isoflavones, flavanones are, tea, red wine, apple, tomato, cherry, onion, thyme, parsley, soyabeans, and other legumes, grape fruit, orange, lemon and ginkgo [52].

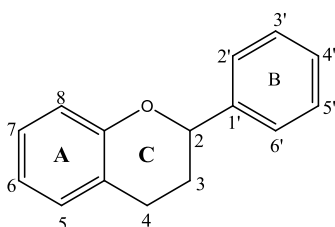


Figure I.3. Structure of flavonoid molecule.

Most flavonoids are yellow compounds, and contribute to the yellow color of the flowers and fruits, where they are usually present as glycosides and within any one class may be characterized as monoglycosidic, diglycosidic and so on. There are over 2000 glycosides of the flavones and flavonols isolated to date. Both *O*- and *C*-

glycosides are common in plant flavonoids; *e.g.*, rutin is an *O*-glycoside, whereas isovitexin is a *C*-glycoside. Sulphated conjugates are also common in the flavone and flavonol series, where the sulphate conjugation may be on a phenolic hydroxyl and / or on an aliphatic hydroxyl of a glycoside moiety.

Flavonoids are responsible for red and dark blue color of berries, as well as orange and yellow coloring citrus fruits. In the human body they play a similar role as vitamins [53-54].

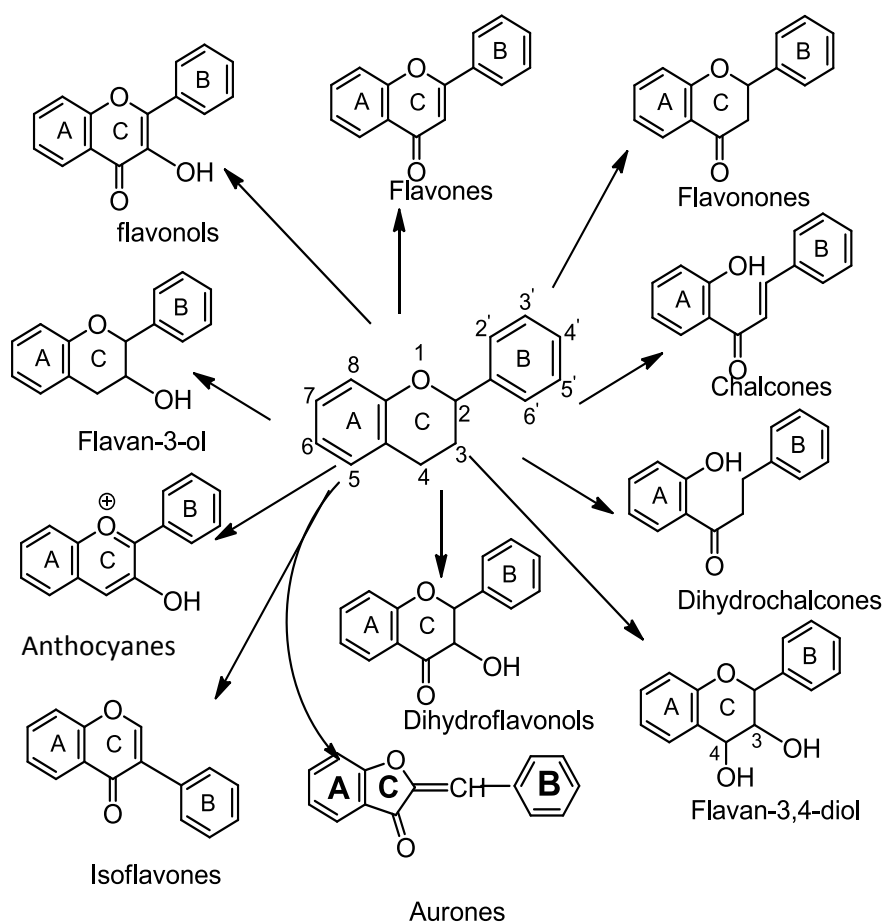
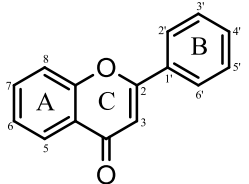
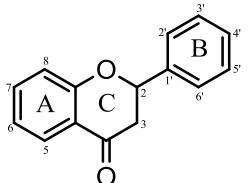
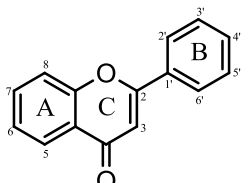
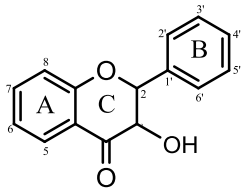
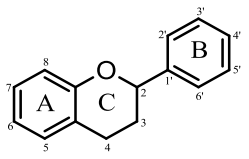
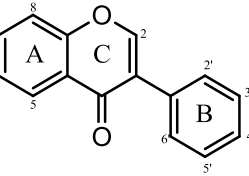
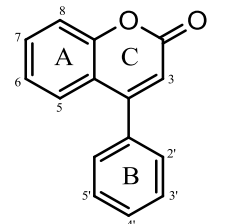
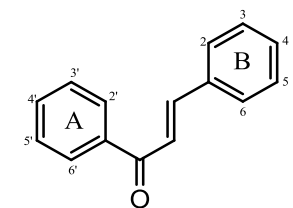
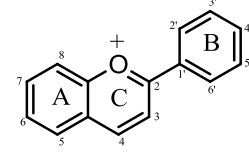


Figure I.4. Structure of major classes of flavonoids.

Table I.2. Flavonoids, classes, subclasses and different sources.

Class name, Sub-class name and backbone structure	Examples	Position of Hydroxyl groups / substituted hydroxyl groups / other substituents												Some Sources	Ref.	
		2	3	4	5	6	7	8	2'	3'	4'	5'	6'			
Flavones 	- Luteolin - Apigenin - Chrysin - Baicalein	-	-	-	OH	-	OH	-	-	OH	OH	-	-	<i>Cichorium endivia.</i> <i>Medicago sativa.</i> <i>Oroxylum indicum.</i>	[55-56], [57-58], [59-60].	
		-	-	-	OH	-	OH	-	-	-	OH	-	-			
		-	-	-	OH	-	OH	-	-	-	-	-	-			-
		-	-	-	OH	OH	OH	-	-	-	-	-	-			-
Flavanones 	- Hesperitin - Naringenin	-	-	-	OH	-	OH	-	-	OH	OCH ₃	-	-	Citrus and grape fruit peels.	[61-62], [63].	
		-	-	-	OH	-	OH	-	-	-	OH	-	-			
Flavonols 	- Quercetin	-	OH	-	OH	-	OH	-	-	OH	OH	-	-	Propolis, honey, chamomile and linden, <i>Ginkgo biloba</i> , Blue gum eucalyptus.	[64-65], [66-67].	
	- Kaempferol	-	OH	-	OH	-	OH	-	-	-	OH	-	-			
	- Galangin	-	OH	-	OH	-	OH	-	-	-	-	-	-			
	- Fisetin	-	OH	-	-	-	OH	-	-	OH	OH	-	-			
	- Myricetin	-	OH	-	OH	-	OH	-	-	OH	OH	OH	-			
	- Morin	-	OH	-	OH	-	OH	-	OH	-	OH	-	-			
	- Hyperoside	-	O-Gal	-	OH	-	OH	-	-	OH	OH	-	-			
	- Heliosin	-	O-diGal	-	OH	-	OH	-	-	OH	OH	-	-			

Class name, Sub-class name and backbone structure	Examples	Position of Hydroxyl groups / substituted hydroxyl groups / other substituents												Some Sources	Ref.
		2	3	4	5	6	7	8	2'	3'	4'	5'	6'		
Flavanonols 	- Taxifolin	-	OH	-	OH	-	OH	-	-	OH	OH	-	-	<i>Larix gmelinii</i> and Chinese lacquer tree.	[68-69]
	- Fustin	-	OH	-	-	-	OH	-	-	OH	OH	-	-		
Flavan-3-ols 	- (+) Catechin	-	β OH	-	OH	-	OH	-	-	OH	OH	-	-	Green tea, black tea, cocoa.	[70-71], [72].
	- (-) Epicatechin	-	α OH	-	OH	-	OH	-	-	OH	OH	-	-		
	- (-) Epigallo catechin	-	α OH	-	OH	-	OH	-	-	OH	OH	OH	-		
	- (-) Epicatechin - 3-gallate	-	α O-Gallate	-	OH	-	OH	-	-	OH	OH	-	-		
	- (-) Epigallo catechin-3-gallate	-	α O-Gallate	-	OH	-	OH	-	-	OH	OH	OH	-		
Isoflavonoids 	- Genistein	-	-	-	OH	-	OH	-	-	-	OH	-	-	Leguminous family plants (soybean), red clover.	[73-74], [75-76], [77-78].
	- Genistin	-	-	-	OH	-	OGl	-	-	-	OH	-	-		
	- Daidzein	-	-	-	-	-	OH	-	-	-	OH	-	-		
	- Daidzin	-	-	-	-	-	OGl	-	-	-	OH	-	-		
	- Biochanin	-	-	-	OH	-	OH	-	-	-	OCH ₃	-	-		
	- Formononetin	-	-	-	-	-	OH	-	-	-	OCH ₃	-	-		

Class name, Sub-class name and backbone structure	Examples	Position of Hydroxyl groups / substituted hydroxyl groups / other substituents												Some Sources	Ref.
		2	3	4	5	6	7	8	2'	3'	4'	5'	6'		
Neoflavonoids (4-phenyl coumarine) 	- Dalbergin	-	-	-	-	OH	OCH ₃	-	-	-	-	-	-	Widely distributed in plant kingdom.	[79-80].
	- Calophyllolide	Complex structure													
	- Inophyllums B, P, G, F	Complex structure													
Chalcones 	- Isoliquiritigenin	-	-	OH	-	-	-	-	OH	-	OH	-	-	Apples, flowers, hop, beer.	[77-81], [82-83], [84].
	- Flavokawain A	-	-	OCH ₃	-	-	-	-	OH	-	OCH ₃	-	OCH ₃		
	- Flavokawain B	-	-	-	-	-	-	-	OH	-	OCH ₃	-	OCH ₃		
	- Flavokawain C	-	-	OH	-	-	-	-	OH	-	OCH ₃	-	OCH ₃		
	- Gymnogrammene	-	-	OCH ₃	-	-	-	-	OH	-	OCH ₃	-	OH		
Anthocyanidins 	- Cyanidin	-	OH	-	OH	-	OH	-	-	OH	OH	-	-	Red and blue flowers petals, fruits and vegetables.	[85-86], [51].
	- Pelargonidin	-	OH	-	OH	-	OH	-	-	-	OH	-	-		
	- Peonidin	-	OH	-	OH	-	OH	-	-	OCH ₃	OH	-	-		
	- Delphinidin	-	OH	-	OH	-	OH	-	-	OH	OH	OH	-		
	- Petunidin	-	OH	-	OH	-	OH	-	-	OH	OH	OCH ₃	-		
	- Malvidin	-	OH	-	OH	-	OH	-	-	OCH ₃	OH	OCH ₃	-		

		2	3	4	5	6	7	8	2'	3'	4'	5'	6'		
	Anthocyanins														
	- Cyanidin-3-glucoside	-	OGl	-	OH	-	OH	-	-	OH	OH	-	-		
	- Cyanidin-3-rutinoside	-	ORu	-	OH	-	OH	-	-	OH	OH	-	-		
	- Cyanin	-	OGl	-	OGl	-	OH	-	-	OH	OH	-	-		
	- Pelargonidin-3-glucoside.	-	OGl	-	OH	-	OH	-	-	-	OH	-	-		

I.3.2.2. Flavonoids and Bioactivities in plants

Several flavonoids possess antioxidant, antimicrobial, anticancer, anti-inflammatory, antiviral, hepatoprotective, antihepatotoxic and antitumour properties. Many traditional medicines and medicinal plants contain flavonoids as the bioactive compounds. The antioxidant properties of flavonoids present in fresh fruits and vegetables are thought to contribute to their preventative effect against cancer and heart diseases. We describe here in details each propriety:

➤ **Antioxydant Activity:** Flavonoids are well known for their antioxidant activity, they are specific compounds that protect human, animal and plant cells against the damaging effects of free radicals. An imbalance between antioxidants and free radicals results in oxidative stress will / may lead to cellular damage [86]. The capacity of flavonoids to act as antioxidants depends upon their molecular structure. The position of hydroxyl groups and other features in the chemical structure of flavonoids are important for their antioxidant and free radical scavenging activities. The acknowledged dietary antioxidants are vitamin C, vitamin E, selenium and carotenoids. However, recent studies have demonstrated that flavonoids found in fruits and vegetables may also act as antioxidants [87]. On the other hand flavonoids such as luteolin and catechins, are better antioxidants than the nutrients antioxidants such as vitamin C, vitamin E and β -carotene [88]. The function of an antioxidant is to intercept and react with free radicals at a rate faster than the substrate. Since free radicals are able to attack at a variety of target including lipids, fats and proteins, it is believed that they may damage organisms, leading to disease and poisoning [89].

➤ **Antibacterial Activity:** Flavonoids are known to be synthesized by plants in response to microbial infection; thus it should not be surprising that they have been found *in vitro* to be effective antimicrobial substances against a wide array of microorganisms. Flavonoid rich plant extracts from different species have been reported to possess antibacterial activity [90-93].

➤ **Anticancer Activity:** Dietary factors play an important role in the prevention of cancers. Fruits and vegetables having flavonoids have been reported as cancer chemopreventive agents [91-94]. Consumption of onions and/or apples, two major sources of the flavonol quercetin, is inversely associated with the incidence of cancer of the prostate, lung, stomach, and breast. In addition, moderate wine drinkers also seem to have a lower risk to develop cancer of the lung, endometrium, esophagus, stomach, and colon [95].

➤ **Antiviral Activity:** Naturally occurring flavonoids with antiviral activity have been recognized since the 1940s and many reports on the antiviral activity of various flavonoids are available. Search of effective drug against human immunodeficiency virus (HIV) is the need of hour. Most of the work related with antiviral compounds revolves around inhibition of various enzymes associated with the life cycle of

viruses. Structure function relationship between flavonoids and their enzyme inhibitory activity has been observed. Gerdin and Srenso [96] demonstrated that flavan-3-ol was more effective than flavones and flavonones in selective inhibition of HIV-1, HIV-2, and similar immunodeficiency virus infections.

➤ **Hepatoprotective Activity:** Several flavonoids such as catechin, apigenin, quercetin, naringenin, rutin, and venoruton are reported for their hepatoprotective activities [97]. Different chronic diseases such as diabetes may lead to development of hepatic clinical manifestations.

➤ **Anti-Inflammatory Activity:** Inflammation is a normal biological process in response to tissue injury, microbial pathogen infection, and chemical irritation; certain members of flavonoids significantly affect the function of the immune system and inflammatory cells [98]. A number of flavonoids such as hesperidin, apigenin, luteolin, and quercetin are reported to possess anti-inflammatory and analgesic effects. Flavonoids may affect specifically the function of enzyme systems critically involved in the generation of inflammatory processes [99].

Like as phenolic acids, flavonoids are secondary metabolites of plants with polyphenolic structure thus flavonoid groups of polyphenolic compounds have low toxicity in mammals and are widely distributed in plant kingdom [100].

The role of flavonoids in flowers is to provide colors attractive to plant pollinators [101] and in leaves, these compounds are increasingly believed to promote physiological survival of the plant, protecting it from, for example, fungal pathogens and UV-radiation [102].

In addition, flavonoids are involved in photosensitization, energy transfer, the actions of plant growth hormones and growth regulators, control of respiration and photosynthesis, morphogenesis and sex determination [103], Although flavonoids are amongst of the chemicals that give the plant a rich taste and the flavor may act as an attractant or repellent to pollinators or pests [104].

I.3.2.3. Role of flavonoids in plant physiology

Flavonoids are universal within the plant kingdom; they are the most common plant pigments next to chlorophyll and carotenoids. They are recognized as the pigments responsible for autumnal leaf colors as well as for the many shades of yellow, orange and red in flowers. Their functions include protection of plant tissues from damaging UV radiation, acting as antioxidants, enzyme inhibitors, pigments and light screens. The compounds are involved in photo-sensitization and energy transfer, action of plant growth hormones and growth regulators, as well as defense against infection [105]. The plant response to injury results in increased synthesis of flavonoid aglycones (including phytoalexins) at the site of injury or infection.

Flavonoids can be considered as important constituents of the human diet average consumption are estimated at approximately 1 g flavonoids per person per day, although the amount of absorbed flavonoids may be much lower. Flavonoid aglycones that reach the large bowel are subject to ring fission by intestinal bacteria, a process in which the middle (non-aromatic) carbon ring is split apart into smaller fission metabolites. These metabolites are readily absorbed and some are known to possess therapeutic benefits in their own right [106].

I.3.2.4. Flavonoids and health benefits

Experiments have proven flavonoids affect the heart and circulatory system and strengthen the capillaries. They are often referred to as ‘biological stress modifiers’ since they serve as protection against environmental stress [105]. They are also known to have synergistic effects with ascorbic acid. Their protective actions are mainly due to membrane stabilising and antioxidant effects.

In the Zutphen Elderly Study (in Holland) carried out on 805 men aged 65–84 years, dietary intake of flavonoids was calculated during a five-year period. The study indicates that the intake of flavonoids is inversely associated with mortality from coronary heart disease and, to a lesser extent, myocardial infarct. The main sources of flavonoids in the men’s diets were tea, onions and apples. These flavonoids include quercetin, kaempferol and myricetin as well as the catechin- type condensed tannins found in black tea [107].

Epidemiological studies with dietary flavonoids have also demonstrated an inverse association with incidence of stroke [108].

I.3.3. Anthraquinones

I.3.3.1. Generalities on anthraquinones

Anthraquinone derivatives are the largest group of natural quinones. Other natural quinones are naphthoquinones and benzoquinones. Anthraquinones also constitute one of the largest group of natural pigments with about 700 compounds described, in which the compounds most frequently reported are emodin, physcion, catenarin and rhein. Around 200 of these compounds are issued from flowering plants while the rest of them are produced by lichens and fungi [109]. They can be found in all parts of the plants: roots, rhizomes, fruits, flowers and leaves.

Anthraquinones are yellow-brown pigments, most commonly occurring as *O*-glycosides or *C*-glycosides. Their aglycones consist of two or more phenols linked by a quinone ring. Hydroxyl groups always occur at positions 1 and 8, that is, 1, 8-dihydroxyanthraquinones.

For the first time, in 1835, scientist Laurent synthesized anthraquinone via oxidation of anthracene though the researchers did not take interest on this for a long time [110]. Later in 1868, the importance of anthraquinones and its derivatives for the dye industry was recognised, when Graebe and Liebermann prepared anthracene from alizarin (1, 2-dihydroxyanthraquinone) also, alizarin via anthraquinone. Since then, there was a rapid growth in the chemistry of anthraquinone by discovering many anthraquinone dyes. Plenty of studies on the spectral characteristics of the anthraquinone were available in literature [111].

Most of these compounds are derivatives of the basic structure 9, 10-anthracenedione, a tricyclic aromatic organic compound with formula $C_{14}H_8O_2$. The latter is a yellow solid crystalline powder that absorbs visible light and is the basic structure of a large class of dyes and pigments [112]. Glycosylated anthraquinones are also present within the plant, for instance in rhizomes to favour their accumulation and storage in the plant [113], but they are converted into aglycone anthraquinones by -glucosidases or oxidative processes. However, some studies only report the presence of non-glycosylated anthraquinones in varied seeds [114-117]. Many anthraquinones are especially common in the families of Fabaceae (*Cassia*), Liliaceae (*Aloe*), Polygonaceae (*Rheum*, *Rumex*), Rhamnaceae (*Rhamnus*), Rubiaceae (*Asperula*, *Coelospermum*), and Scrophulariaceae (*Digitalis*) [117]. A wide body of literature has demonstrated that natural anthraquinones possess a broad range of bioactivities such as anticancer, anti-inflammatory, immunosuppressive, antimicrobial, diuretic, cathartic, laxative, vasorelaxing, antioxidant and phytoestrogen activities [118-120]. Anthraquinone derivatives such as rhein, the main active substance of traditional Chinese herb rhubarb have demonstrated several interesting biological properties, notably immunosuppressive and anti-inflammatory [121]. In addition, anthraquinones also have an important role in the electron transport chain to maintain biological functions of plants. According to Strotmann et al. the anthraquinone dyes inhibit energy transfer in the photosynthesis process [122].

This compound is also a potential candidate for DNA interaction with subsequent positive and / or negative effects [123]. Thus, the analysis of natural anthraquinones is significant to various fields including the investigation of physiological properties of anthraquinones, to evaluate the risks and potentialities on human health, and therapeutic monitoring.

I.3.3.2. Protective benefit of anthraquinones

Natural anthraquinones are distinguished by a large structural variety, wide range of biological activity and low toxicity. Bioactive properties well known of anthraquinones are laxative properties. However, other activities are described in the literature.

➤ **Laxative activity:** Anthraquinone derivatives are well-known for their laxative action, as was shown in a number of plants: *folia sennae*, *rhizome rhein*, *cortex frangulae* and *aloe*. For example, depending on the administered dose, 1, 8-anthraquinone induces laxative or purgative activity. At therapeutic doses, they are stimulant laxatives by directly stimulating colonic smooth muscles [124-125].

➤ **Anticancer activity:** In addition, physcion and emodin are kinase and tyrosinase inhibitors and have demonstrated cytotoxicity against cancer cells. Another study including six anthraquinones (nordamnacanthal, alizarin-1-methyl ether, rubiadin, soranjidiol, lucidin-methyl ether and morindone) isolated from cell cultures of *Morinda elliptica* were assayed for antitumor and antioxidant activities at the concentration of 2.0 g/ml. Moreover, aloe emodin showed a significant antileukemic activity against the P-388 lymphocytic leukemia in mice, corresponding to a tumor-inhibitory activity. This component was isolated from the seeds of *Rhamnus frangula* L. [125].

➤ **Hepatoprotective activity:** Isolated from the roots of *Berchemia* genus, several anthraquinones comprising physcion, aloe emodin, xanthorin, chrysophanol and 1, 5, 8-trihydroxy-3-methyl-anthraquinone had a positive effect against D-galactosamine-induced toxicity in rat hepatic epithelial cells [125].

➤ **Antimicrobial activity:** Two anthraquinones isolated from *Kniphofia foliosa* roots yielded high inhibition for the malaria parasite (*Plasmodium falciparum*) with ED₅₀ valued of 0.260 and 0.537 g/ml [126]. In addition, emodin isolated from *Cassia nigricans* leaves demonstrated an efficient antimicrobial activity against *Staphylococcus aureus*, *Corynebacterium pyogenes*, *Streptococcus pyogenes*, *Bacillus subtilis*, *Salmonella typhi*, *Escherichia coli*, *Pseudomonas aeruginosa*, *Candida albicans*, *Neisseria gonorrhoea*, and *Klebsiella pneumoniae*: it showed significant antimicrobial activity on some common pathogens. The LC₅₀ (lower – upper limits) of the emodin was 42.77 (11.80–72.94) g/ml [127].

➤ **Antifungal activity:** Rhein, physcion, aloe-emodin and chrysophanol extracted from *Rheum* showed an antifungal activity against *Candida albicans*, *Cryptococcus neoformans*, *Trichophyton mentagrophytes* and *Aspergillus fumigates* [125]. Another study has revealed the antifungal activity of root and leaf extracts of *Coccoloba mollis*, this plant activity was tested against *Botryosphaeria ribis*, *Botryosphaeria rhodina*, *Lasiodiplodia theobromae* and several *Fusarium* sp. And showed promising results for their use as fungicides, where emodin was the most active compound [128].

➤ **Antiviral activity:** Chrysophanol from the *Dianella* genus has revealed an antiviral activity against poliovirus through *in-vitro* essays. It has been found to inhibit the replication of poliovirus types 2 and 3 *in vitro*. It inhibited poliovirus-induced cytopathic effects with IC₅₀ of 0.21 and 0.02 µg/mL for poliovirus types 2

and 3, respectively. Compared to rhein, aloë emodin, emodin and 1, 8-dihydroxyanthraquinone, chrysophanol was the most effective antiviral component against poliovirus type 3 [125].

➤ **Antidiabetic activity:** Chrysophanol and its glycoside form have shown an antidiabetic effect. The antidiabetic activity was examined by glucose transport activity. Chrysophanol and Chrysophanol-8-O- β -d-glucopyranoside up to 100 μ M and 25 μ M exerted mild Glucose transport activity. These two anthraquinones from *rhubarb rhizome* have anti-diabetic properties and could play metabolic roles in the insulin-stimulated glucose transport pathway [129].

➤ **Antioxidant activity:** The antioxidant activity of the compounds isolated from the AtOAc extract of the *Muehlenbeckia hastulata* plant was measured by bleaching of the DPPH (1, 1-diphenyl-2-picryl hydrazyl) radical scavenging method. Three anthraquinones, emodin, physcion and emodin-8- β -d-idopyranoside were isolated from the leaves of this plant. The antioxidant activity assays show that physcion was the most active compound. Emodin had weaker activity, possibly because of the formation of intermolecular hydrogen bridges which may inactivate its antioxidant property. Moreover, emodin-8- β -d-idopyranoside was more active than emodin. The presence of the glycoside moiety increases the radical scavenging activity by 48.9% [130].

➤ **Industrial applications:** Anthraquinones may be used as color agents and represent the biggest group of quinone dyes. Different dye groups are employed: natural and synthetic. Until the 19th century, natural dyes were mostly used to color textiles, hides and animal skins, and had a great interest in the cosmetic, pharmaceutical and food-processing fields. Some natural anthraquinones are colorless. But natural anthraquinoid dyes' colorations are the results of synergistic action (anthraquinones together with other molecules present in the matrix) or of reaction products issued from transformation processes. Consequently, these molecules can include a large variety of forms and natures or being originally [131-132]. Moreover, the effects of substituents on the electronic spectrum of anthraquinone show that the nature and number of the substituents, as well as their position, play a major role in coloring properties. Nowadays, with increasing awareness of the adverse effects of synthetic chemicals, natural dyes have a real interest for the formulation of varied products. Anthraquinones have been associated to lichens and mushrooms to stain several matters in colors varying from yellow to orange.

I.3.3.3. Classification of anthraquinones

a - Anthracene / anthraquinone glycosides

The aglycones of anthracene glycosides belong to structural category of anthracene derivatives. Most of them possess an anthraquinone skeleton, and are called anthraquinone glycosides, *e.g.* rhein 8-*O*-glucoside and aloin (a *C*-glucoside) [133]. The most common sugars present in these glycosides are glucose and rhamnose (**Fig. I.5**).

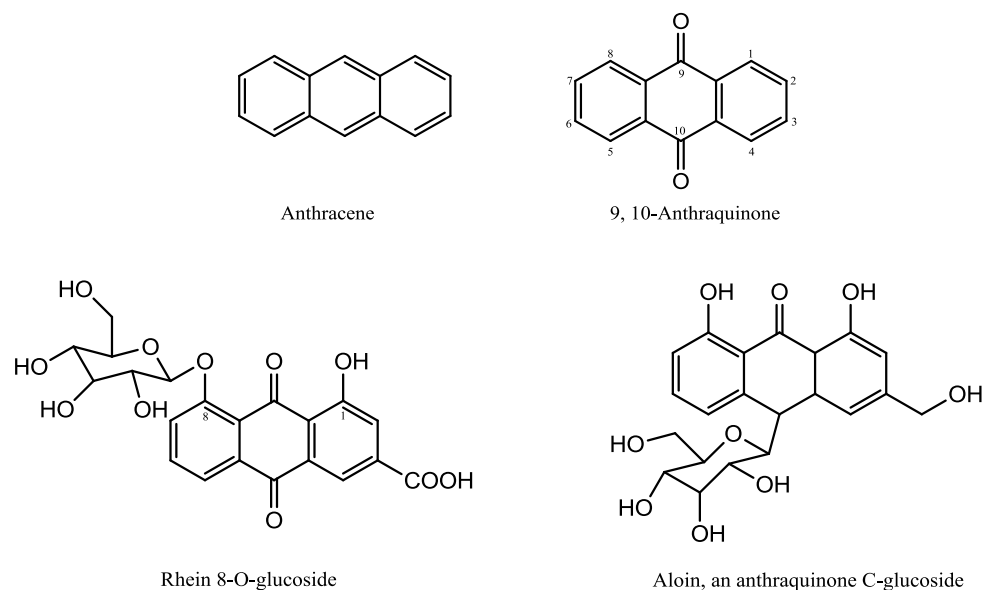


Figure I.5. Anthracene, anthracene derivatives skeleton

The following structural variations within anthraquinone aglycones are most common in nature [133] (**Fig. I.6**).

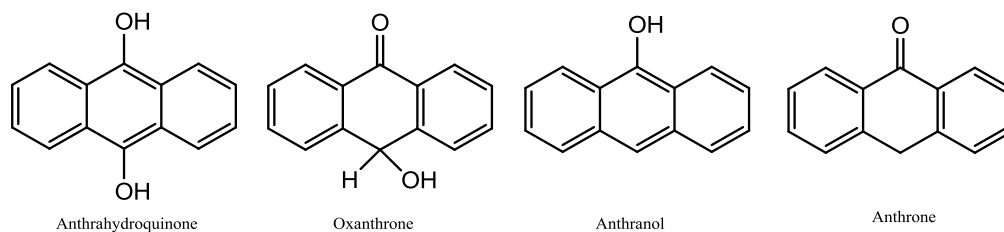


Figure I.6. Anthraquinone derivatives skeleton

Dimeric anthraquinone and their derivatives are also present as aglycones in anthraquinone glycoside found in the plant kingdom [133] (**Fig. I.7**).

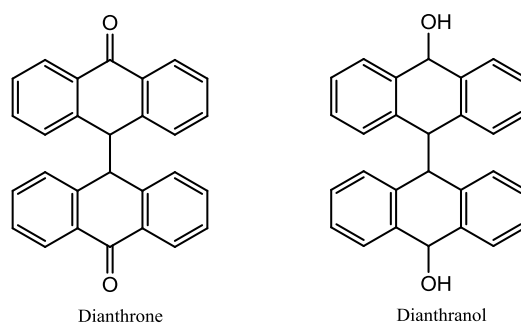


Figure I.7. Dimeric anthraquinone derivatives skeleton

b - Sennosides

The most important anthraquinone glycosides are sennosides, found in the *senna* leaves and fruits (*Cassia senna* or *Cassia angustifolia*). These are, in fact, dimeric anthraquinone glycosides [133]. However, monomeric anthraquinone glycosides are also present in this plant (**Fig. I.8**).

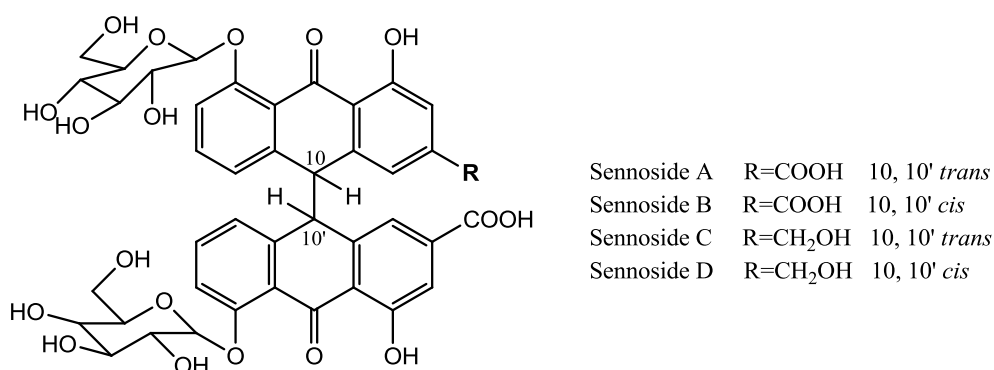


Figure I.8. Sennoside (anthraquinone glycoside) derivatives skeleton

c - Cascarosides

Cascara bark (*Rhamnus purshianus*) contains various anthraquinone *O*-glycosides, but the main components are the *C*-glycosides, which are known as cascariosides. Rhubarb (*Rheum palmatum*) also contains several different *O*-glycosides and cascariosides. *Aloe vera* mainly produces anthraquinone *C*-glycosides, *e.g.* aloin [133].

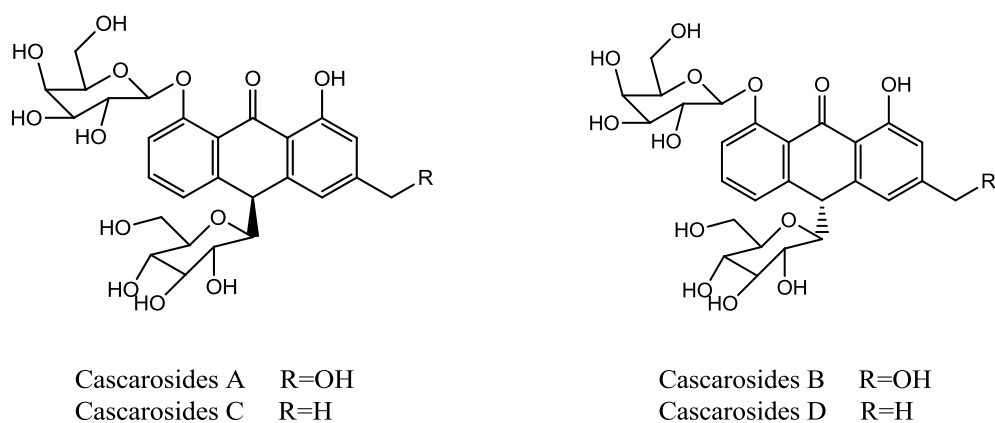


Figure I.9. Cascarosides derivatives skeleton

I.3.3.4. Biosynthesis of anthraquinones glycosides

In higher plants, anthraquinones are biosynthesized either via acylpolymalonate (as in the plants of the families Polygonaceae and Rhamnaceae) or via shikimic acid pathways (as in the plants of the families Rubiaceae and Gesneriaceae) as presented in the following biosynthetic schemes (**Fig. I.10** and **Fig. I.11**).

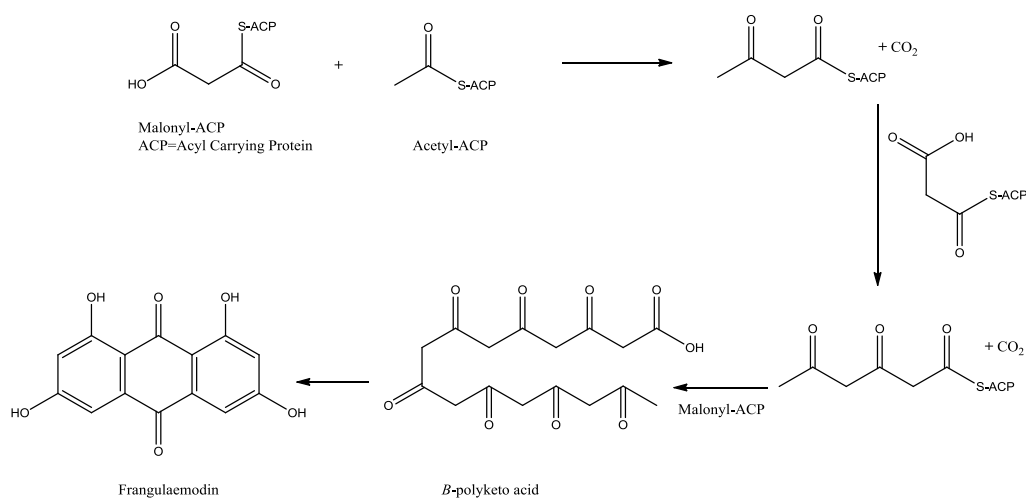


Figure I.10. Acylpolymalonate pathway

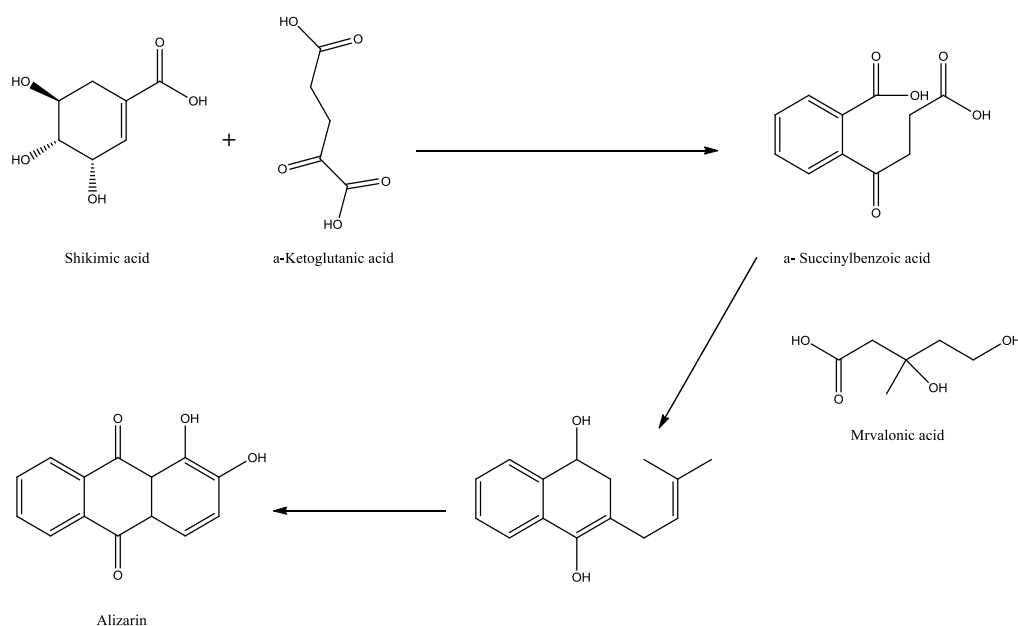


Figure I.11. Shikimic acid pathway

I.1.3.4. Tannins

Tannins, the relatively high molecular weight compounds found in complexes with alkaloids, polysaccharides and proteins, are a group of water-soluble polyphenols. They may be subdivided into hydrolysable and condensed tannins. The hydrolysable tannins are esters of gallic acid (gallo- and ellagi-tannins), while the latter (also known as proanthocyanidins) are polymers of polyhydroxyflavan-3-ol monomers. A third subdivision, the phlorotannins consisting entirely of phloroglucinol, has been isolated from several genera of brown algae [134], but these are not significant in the human diet [7]. They are found grape (dark/light) seed/skin, apple juice, strawberries, blackberry, olive, plum, chick pea, black-eyed peas, lentils, haricot bean, red/white wine, cocoa, chocolate, tea, coffee, immature fruits are the main sources of tannins [37-135].

Tannins, commonly referred as tannic acid, have been reported to be responsible for decreases in feed intake, growth rate, feed efficiency, net metabolizable energy, and protein digestibility in experimental animals. Therefore, tannins-rich foods, such as betel nuts and herbal teas, are considered to be of low nutritional value. However, many researches indicated that the major effect of tannins was not due to their inhibition on food consumption or digestion but rather the decreased efficiency in converting the absorbed nutrients to new body substances. The anticarcinogenic and antimutagenic potentials of tannins may be related to their antioxidative property, which is important in protecting cellular oxidative damage, including lipid peroxidation. Tannins have also been reported to exert other physiological effects,

such as to accelerate blood clotting, reduce blood pressure, decrease the serum lipid level, produce liver necrosis, and modulate immunoresponses [136-137].

I.1.3.5. Stilbenes

Stilbenes are structurally characterized by the presence of a 1, 2-diphenylethylene nucleus with hydroxyl groups substituted on the aromatic rings. They exist in the form of monomers or oligomers. The best known compound is *trans*-resveratrol, possessing a trihydroxystilbene skeleton [138], it's found in various plants (grapes, berries, peanuts, cocoa), as well as in red wine. The major dietary sources of stilbenes include grapes, wine, soy, peanuts, and peanut products [139].

Due to their various biological activities, such as antioxidant, anti- cancer, estrogenic, and antibacterial actions, *trans*-resveratrol has attracted the attention of many researchers [140-141].

I.1.3.6. Sterols

The majority of steroids are alcohols; they called sterols [142]. Sterols are steroids derived from triterpenes and forming a whole group of solid alcohols [143]. These are tetracyclic compounds most often containing 27, 28, or 29 carbon atoms. The perhydrocyclopentanophenanthrene nucleus most often has a double bond frequently in 5, but can be found in 7, much more rarely in C-8 or C-9. The methyl groups 18 and 19, the alcohol function at 3 and the side chain at 17 are in β configuration. The side chain which may be saturated or have one or two double bonds has 8, 9 or 10 carbon atoms. They are the constituents of the membranes of various cellular metabolites and the most characteristic of which is cholesterol [144] (**Fig. I.12**).

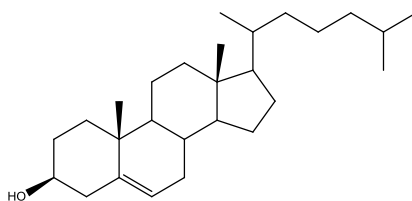


Figure I.12. Structure of Cholesterol

I.1.3.7. Phytosterol

Phytosterols, which include plant sterols and stanols, are steroid compounds that occur in plants and are similar to cholesterol but vary only in carbon side chains and / or presence or absence of a double bond, and may lower blood cholesterol levels [145]. Thus, phytosterols are considered as plant cholesterol; for they are plant-derived lipid compounds that are similar in structure and functions to cholesterol

[146]. Plant cholesterol are naturally-occurring in the parts of all plants and there are claims by researchers that they may promote the health of man and animals when consumed regularly for a reasonable period either in natural foods or in enriched food supplements.

Phytosterols have been classified into two: (1) Sterols, which have a double bond in the sterol ring, so are unsaturated compounds (**Fig. I.13**) and (2) Stanols, which lack a double bond in the sterol ring, so are saturated molecules (**Fig. I.14**). The most abundant sterols in plants and human diets are Sitosterols and Campesterols. Stanols are also present in plants, but they form only 10% of total dietary phytosterols.

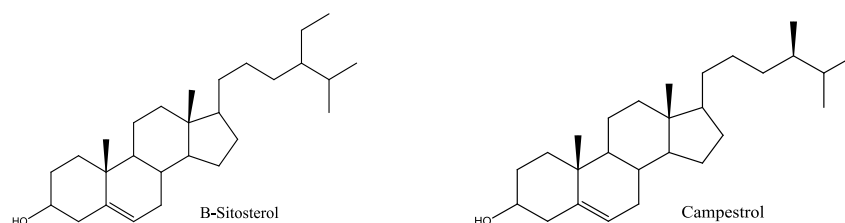


Figure I.13. Chemical structures of Sterols.

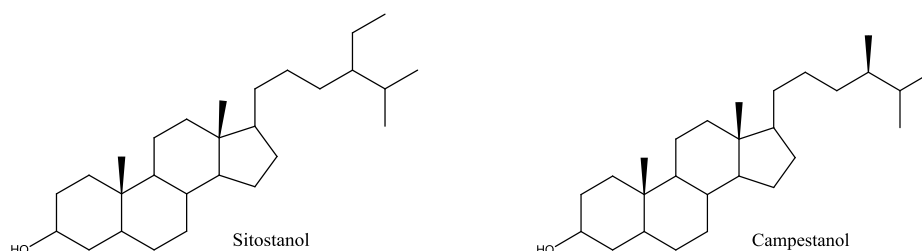


Figure I.14. Chemical structures of Stanols.

I.1.3.7.1. Biological activities of Phytosterols

➤ **Anti-inflammatory Effects:** Limited data from cell culture and animal studies suggest that phytosterols may attenuate the inflammatory activity of immune cells, including macrophages and neutrophils [147]. Thus, they may have anti-inflammatory activities in living systems.

➤ **Safety:** In the United States, plant sterols and stanols added to a variety of food products are generally recognized as safe (GRAS) by the FDA (Food and Drug Administration). The scientific committee on foods of the EU also concluded that plant sterols and stanols added to various food products are safe for human use [148]. However, the committee also recommended that intakes of plant sterols and stanols from food products should not exceed 3 g / day because there is no evidence of health

benefits at higher intakes and there might be undesirable effects when they are consumed in high amounts.

Limited data from animal studies suggest that very high intakes of phytosterols, particularly sitosterol, may inhibit the growth of breast and prostate cancers [149-150]. Some epidemiological studies have found that higher intakes of plant foods containing phytosterols are associated with reduced cancer risk; however it is not certain whether the protective factors are phytosterols or other compounds in the plant foods. Nevertheless, it is reported that phytosterols may inhibit lung, stomach, ovarian and breast cancers [151].

REFERENCES

- [1] Liu, R. H., *Journal of Nutrition*, **2004**, *134*, 3479-3485.
- [2] Yahia, E. M., *Wiley- Blackwell*, **2009**, *1*, 3-51.
- [3] Randhir, R., Lin, Y. T., Shetty, K., *Process Biochem*, **2004**, *39*, 637-646.
- [4] Velderrain-Rodríguez, G. R., Palafox-Carlos, H., Wall-Medrano, A., Ayala Zavala, J. F., Chen, C. Y. O., Robles-Sanchez, M., Astiazaran-García, H., Alvarez-Parrilla, E., González-Aguilar, G. A., *Food Funct*, **2014**, *5*, 189-197.
- [5] Vatter, D. A., Randhir, R., Shetty, K., *Process. Biochem.*, **2005**, *40*, 2225-2238.
- [6] Lin, D. R., Hu, L. J., You, H., Sarkar, D., Xing, B. S., Shetty, K., *J. Soils Sediment*, **2010**, *10*, 923-932.
- [7] Bravo, L., *Nutrition Reviews*, **1998**, *56*, 317-333.
- [8] Duthie, G. G., Duthie, S. J., Kyle, J. A. M., *Nutrition Research Review*, **2000**, *13*, 79-106.
- [9] Pinto, G., Pollio, A., *Molecules*, **2011**, *16*, 1486-1507.
- [10] Jaffery, E. H., Brown, A. F., Kurilich, A. C., Keek, A. S., Matusheski, N., Klein, B. P., *J. Food Composition and Analysis*, **2003**, *16*, 323-330.
- [11] Babbar, N., Oberoi, H. S., Sandhu, S. K., Bhargav, V. K., *J. Food Sci. Technol*, **2014**, *51*, 2568-2575.
- [12] Alasalvar, C., Grigor, J. M., Zhang, D. L., Quantick, P. C., Shahidi, F., *J. Agric. Food Chem*, **2001**, *49*, 1410-1416.
- [13] Edreva, A., Velikova, V., Tsonev, T., Dagnon, S., Gürel, A. L., Aktas, L., *Gen. Appl. Plant. Physiol*, **2008**, *34*, 67-78.
- [14] Tomas-Barberan, F., Espin, J. C., *J. Sci Food Agric*, **2001**, *81*, 853-876.
- [15] Gryglewski, R. J., Korbut, R., Robak, J., *Biochemical Pharmacol.*, **1987**, *36*, 317-321.
- [16] Benavente-Garcia, O., Castillo, J., Marin, F. R., Ortuno, A., Del Rio, J. A., *J. of Agricultural and Food Chemistry*, **1997**, *45*, 4505-4515.
- [17] Manach, C., Mazur, A., Scalbert, A., *Current Opinions in Lipidology*, **2005**, *16*, 77-84.
- [18] Middleton, E., Kandaswami, C., Theoharides, T. C., *Pharmacological Reviews*, **2000**, *52*, 673-751.
- [19] Puupponen-Pimia, R., Nohynek, L., Meier, C., Kahkonen, M., Heinonen, M., Hopia, A., *J. Applied Microbiology*, **2001**, *90*, 494-507.
- [20] Samman, S., Lyons Wall, P. M., Cook, N. C., In Rice-Evans & L. Packer (Eds.), *Flavonoids in health and disease*, New York: Marcel Dekker, **1998**, 469-482
- [21] Sales, P. M., Souza, P. M., Simeoni, L. A., Magalhães, P. O., Silveira, D., *J. Pharm. Pharm. Sci.*, **2012**, *15*, 141-183.
- [22] Shukitt-Hale, B., Lau, F. C., Joseph, J. A., *J. Agric. Food Chem.*, **2008**, *56*, 636-641
- [23] Moo-Huchin, V. M., Moo-Huchin, M. I., Estrada-León, R. J., Cuevas-Gloryc, L., Estrada-Motaa, I. A., Ortiz-Vázquez, E., Betancur-Anconad, D., Sauri-Duchc, E., *Mexico Food Chem.*, **2015**, *166*, 17-22.

- [24] Crozier, A. A., Jaganath, I. B., Clifford, M. N., *Natural Product Reports*, **2009**, 26, 1001-1043.
- [25] Manach, C., Williamson, G., Morand, C., Scalbert, A., Rémésy, C., *American Journal of Clinical Nutrition*, **2005**, 81, 230-242.
- [26] Alberto, M. R., Gómez-Cordovés, C., Manca De Nadra, M. C., *J. Agriculture and Food Chemistry*, **2004**, 52, 6465-6469.
- [27] Graf, B. A., Milbury, P. E., Blumberg, J. B., *J. Medicinal Food*, **2005**, 8, 281-290.
- [28] Noroozi, M., Angerson, W. J., Lean, M. E. J., *American Journal of Clinical Nutrition*, **1998**, 67, 1210-1218.
- [29] Lairon, D., Amiot, M. J., *Current Opinion Lipidology*, **1999**, 10, 23-28.
- [30] Block, G., Patterson, B., Subar, A., *A review of the epidemiological evidence, Nutrition and Cancer*, **1992**, 18, 1-29.
- [31] Mennen, L. I., Walker, R., Bennetau-Pelissero, C., Scalbert, A., *American Journal of Clinical Nutrition*, **2005**, 81, 326-329.
- [32] Yang, F., De Villiers, W. J., McClain, C. J., Varilek, G. W., *Journal of Nutrition*, **1998**, 128, 2334-2340.
- [33] Dai, Q., Borenstein, A. R., Wu, Y., *American Journal of Clinical Nutrition*, **2006**, 119, 751-759.
- [34] Appel, L. J., Moore, T. J., Obarzanek, E., *The New England Journal of Medicine*, **1997**, 336, 1117-1124.
- [35] Williams, R. J., Spencer, J. P. E., Rice-Evans, C., *Free Radical Biology and Medicine*, **2004**, 36, 838-849.
- [36] Ross, R. W., *Polyphenols in plants: Isolation, purification and extract preparation. Academic Press, USA*, **2014**.
- [37] Balasundram, N., Sundram, K., Samman, S., *Food Chemistry*, **2006**, 99, 191-203.
- [38] Gonthier, M. P., Remesy, C., Scalbert, A., Cheynier, V., Souquet, J. M., Poutanen, K., Aura, A. M., *Biomedicine & Pharmacotherapy*, **2006**, 60, 536-540.
- [39] Lafay, S., Gil-Izquierdo, A., *Phytochem Rev.*, **2008**, 7, 301-311.
- [40] Pantelidis, G. E., Vasilakakis, M., Manganaris, G. A., Diamantidis, G., *Food Chemistry*, **2007**, 102, 777-783.
- [41] Ellnain-Wojtaszek, Kurczynski, M., Kasprzak, Z., *J. Acta Pol Pharm.*, **2001**, 58, 205-209.
- [42] Zheng, W., Wang, S. Y., *J. Agric Food Chem.*, **2001**, 49, 4977-4982.
- [43] Shahidi, F., Nacsk, M., *Technomic Publishing Company Inc Lancaster*, **1995**, 27, 245-278.
- [44] Einhellig, F. A., Putnam, A. R., Tang, C. S., *The Science of Allelopathy. John Wiley and Sons New York*, **1986**, 163, 171-189.
- [45] Rice-Evans, C. A., Miller, N. J., Paganga, G., *Trends in Plant Science*, **1997**, 2, 152-159.
- [46] Lotito, S. B., Frei, B., *Free Radical Biology and Medicine*, **2006**, 4, 1727-1746.
- [47] Bohm, B. A., *Introduction to flavonoids. Amsterdam: Harwood Academic Publishers*, **1998**.

- [48] Merken, H. M., Beecher, G. R., *J. Agricultural and Food Chemistry*, **2000**, *48*, 577-599.
- [49] Hollman, P. C. H., Katan, M. B., *Food and Chemical Toxicology*, **1999**, *37*, 937-942.
- [50] Harborne, J. B., Baxter, H., Moss, G. P., *Handbook of bioactive compounds from plants (2nd ed.)*. London: Taylor & Francis, **1999**.
- [51] Pietta, P. G., *J. Natural Products*, **2000**, *63*, 1035-1042.
- [52] Beecher G. R., *J. Nut.*, **2003**, *133*, 3248-3254.
- [53] Mitek, M., Gasik, A., *Przem Spoż.*, **2009**, *5*, 34-39.
- [54] Ostrowska, J., Skrzydlewska, E., *Post Fitoter*, **2005**, *3*, 71-79.
- [55] Kawai, S., Tomono, Y., Katase, E., Ogawa, K., Yano, M., *J. Agric. Food Chem.*, **1999**, *47*, 3565-3571.
- [56] Chen, L. J., Games, D. E., Jones, J., *J. Chromatogr A*, **2003**, *988*, 95-105.
- [57] Barros, L., Duenas, M., Pinela, J., Carvalho, A. M., Buelga, C. S., Ferreira, I. C., *Plant Foods Hum. Nutr.*, **2012**, *67*, 229-234.
- [58] El-Shafey, N. M., Abdelgawad, H., *Acta Physiol Plant*, **2012**, *34*, 2165-2177.
- [59] Mishima, K., Kawamura, H., Kawakami, R., Shota, I. T., Inoue, Y., Hirota, T., Harada, T., Sharmin, T., Misumi, M., Suetsugu, T., Mishima, K., *Solvent Extr. Res. Dev.*, **2015**, *22*, 177-186.
- [60] Kim, J. H., Ahn, D. U., Eun, J. B., Moon, S. H., *Antioxidants (Basel)*, **2016**, *5*, 21-31.
- [61] Lien, T. F., Yeh, H. S., Su, W. T., *Arch. Anim. Nutr.*, **2008**, *62*, 33-43.
- [62] Mullen, W., Archeveque, M. A., Edwards, C. A., Matsumoto, H., Crozier, A., *J. Agric. Food Chem.*, **2008**, *56*, 11157-11164.
- [63] Tomas-Navarro, M., Vallejo, F., Tomas-Barberan, *Polyphenols in human health and disease*. San Diego: Academic Press, **2014**, 537-551.
- [64] Chan, P. C., Xia, Q., Fu, P. P., *J. Environ Sci. Health C Environ Carcinog Ecotoxicol Rev.*, **2007**, *25*, 211-44.
- [65] Bertelli, D., Papotti, G., Bortolotti, L., Marcazzan, G. L., Plessi, M., *Phytochem. Anal.*, **2012**, *23*, 260-266.
- [66] Kurtagic, H., Redzic, S., Memic, M., Sulejmanovic, J., *Bull Chem Technol Bosnia Herzegovina*, **2013**, *40*, 25-30.
- [67] Sanlia, S., Lunte, C., *Anal. Methods*, **2014**, *6*, 3858-3864.
- [68] Kim, J., Kwon, Y., Chun, W., Kim, T., Sun, J., Yu, C., Kim, M., *Food Chem.*, **2010**, *120*, 539-543.
- [69] Liu, Z., Jia, J., Chen, F., Yang, F., Zu, Y., Yang, L., *Molecules*, **2014**, *19*, 19471-19490.
- [70] Zaveri, N. T., *Life Sci.*, **2006**, *78*, 2073-2080.
- [71] Subhashini, R., Mahadeva-Rao, U. S., Sumathi, P., Gunalan, G., *Indian J. Sci. Technol.*, **2010**, *3*, 188-192.
- [72] Gadkari, P. V., Balaraman, M., *Food Bioprod. Proc.*, **2015**, *93*, 122-138.
- [73] Wang, H. J., Murphy, P. A., *J. Agric. Food Chem.*, **1994**, *42*, 1666-1673.
- [74] Mazur, W. M., Duke, J. A., Wahala, K., Rasku, S., Adlercreutz, H., *J. Nutr. Biochem.*, **1998**, *9*, 193-200.

- [75] Dixon, R. A., Ferreira, D., *Phytochemistry*, **2002**, *60*, 205-211.
- [76] Tsao, R., Yang, R., Young, J. C., *J. Agric. Food Chem.* **2003**, *51*, 6445-6451.
- [77] Kim, E. H., Kim, S. L., Kim, S. H., Chung, I. M., *J. Agric. Food Chem.*, **2012**, *60*, 10196-10202.
- [78] Kuligowski, M., Pawłowska, K., Jasinska, K. I., Nowak, J., *Cyta. J. Food*, **2017**, *15*, 27-33.
- [79] Garazd, M. M., Garazd, Y. L., Khilya, V. P., *Chem. Nat. Compd.*, **2003**, *39*, 54-121.
- [80] Laure, F., Raharivelomanana, P., Butaud, J. F., Bianchini, J. P., Gaydou, E. M., *Anal. Chim. Acta.*, **2008**, *624*, 147-153.
- [81] Tsao, R., McCallum, J., *Fruit and vegetable phytochemicals: chemistry, nutritional value and stability. Ames, IA, USA: Blackwell Publishing*, **2009**, 131-153.
- [82] Aksoz, B. E., Ertan, R., *J. Pharm. Sci.*, **2012**, *37*, 205-216.
- [83] Suwito, H., Mustofa, J., Kristanti, A. N., Puspaningsih, N. N. T., *J. Chem. Pharm. Res.*, **2014**, *6*, 1076-1088.
- [84] Phang, C. W., Karsani, S. A., Sethi, G., Abdmalek, S. N., *PLoS One*, **2016**, *11*, e0148775.
- [85] Mazza, G., *Crit. Rev. Food Sci. Nutr.*, **1995**, *35*, 341-371.
- [86] Kukic, J., Petrovic, S., Niketic, M., *Biol. Pharmaceut. Bull.*, **2006**, *29*, 725-729.
- [87] Sies, H., Stahl, W., Sundquist, A. R., *Annals of the New York Academy of Science*, **1992**, *669*, 7-20.
- [88] Herrmann, K., *J. Food Technol.*, **1976**, *11*, 433-448.
- [89] Pietta, P. G., Rice-Evans, C. A., Packer, L., *Marcel Dekker, Inc New York*, **1998**, *23*, 61-110.
- [90] Mishra, A., Kumar, S., Pandey, A. K., *The Scientific World Journal*, **2013**, Art.ID 292934.
- [91] Mishra, A., Sharma, A. K., Kumar, S., Saxena, A. K., Pandey, A. K., *BioMed. Research International*, **2013**, Art. ID 915436.
- [92] Mishra, A., Kumar, S., Bhargava, A., Sharma, B., Pandey, A. K., *Cellular and Molecular Biology*, **2011**, *57*, 16-25.
- [93] Pandey, A. K., Mishra, A. K., Mishra, A., Kumar, S., Chandra, A., *International Journal of Biological and Medical Research*, **2010**, *1*, 228-233.
- [94] Ho, C. T., Osawa, T., Huang, M. T., Rosen, R. T., *American Chemical Society, Oxford University Press*, **1994**.
- [95] Koen, B., Ruth, V., Guido, V., Johannes, V. S., *Journal of Biological Chemistry*, **2005**, *280*, 5636-5645.
- [96] Gerdin, B., Srenso, E., *International Journal of Microcirculation, Clinical and Experimental*, **1983**, *2*, 39-46.
- [97] Tapas, A. R., Sakarkar, D. M., Kakde, R. B., *Tropical Journal of Pharmaceutical Research*, **2008**, *7*, 1089-1099.
- [98] Middleton, E., Kandaswami C., *Biochemical Pharmacology*, **1992**, *43*, 1167-1179.
- [99] Hunter, T., *Cell*, **1995**, *80*, 225-236.

- [100] Manach, C., Scalbert, A., Morand, C., Remesy, C., Jimenez, L., *American Jour. Clinical Nut.*, **2004**, 79, 727-747.
- [101] Harborne, J. B., *TW Goodwin Ed., Academic press, New York*, **1976**, 67, 736-778.
- [102] Harborne, J. B., *London UK Chapman and Hall*. **1993**, 134, 543-553.
- [103] Harborne, J. B., Baxter, H., *The handbook of natural flavonoids. Chichester John Wiley and Sons*, **1999**, 96, 612-632.
- [104] Harborne, J. B., Williams, C. A., *Phytochemistry*, **2000**, 55, 481-504.
- [105] Middleton, J. E., *Herbs, Spices & Medicinal Plants, Oryx Press, Phoenix, Arizona*, **1988**, 3, 103-144.
- [106] Bone, K., *Mediherb Conference, Sydney*, **1997**.
- [107] Hertog, M. G., Feskens, J. M., Hollman, P. C. H., Katan, M. B. Kromhout, D. *The Lancet*, **1993**, 342, 1007-1011.
- [108] Rice-Evans, C., *Current Medicinal Chemistry*, **2001**, 8, 797-807.
- [109] Seigler, D. S., *Plant Secondary Metabolism. Springer Science & Business Media*, **2012**.
- [110] Bien, H. S., Stawitz, J., Wunderlich, K., Wiley-VCH Verlag GmbH & Co., **2000**, 355.
- [111] Navas-Diaz, A., *J. Photochem. Photobiol.*, **1990**, 53, 141-167.
- [112] Dave, H., Ledwani, L., *Indian J. Nat. Prod. Resour.*, **2012**, 3, 291-319.
- [113] Pandith, S. A., Hussain, A., Bhat, W. W., Dhar, N., Qazi, A. K., Rana, S., Razdan, S., Wani, T. A., Shah, M. A., Bedi, Y. S., Hamid, A., Lattoo, S. K., *South Afr. J. Bot.*, **2014**, 95, 1-8.
- [114] Wang, N., Su, M., Liang, S., Sun, H., *Food Chem.*, **2016**, 199, 1-7.
- [115] Xie, Y., Liang, Y., Chen, H., Zhang, T., Ito, Y., *J. Liq. Chromatogr. Relat. Technol.*, **2007**, 30, 1475-1488.
- [116] Kim, Y. M., Lee, C. H., Kim, H. G., Lee, H. S., *J. Agric. Food Chem.*, **2004**, 52, 6096-6100.
- [117] Tala, M. F., Talontsi, F. M., Wabo, H. K., Lantovololona, J. E. R., Tane, P., Laatsch, H., *Biochem. Syst. Ecol.*, **2013**, 50, 310-312.
- [118] Chien, S. C., Wu, Y. C., Chen, Z. W., Yang, W. C., *Evid. Based Complement. Alternat. Med.*, **2015**, Art. 357357.
- [119] Locatelli, M., **2011**, *Curr. Drug Targets*, 12, 366-380.
- [120] Reynolds, T., *Medicinal and Aromatic Plants - Industrial Profiles. CRC Press.*, **2004**.
- [121] Spencer, C. M., Wilde, M. I., *Drugs*, **1997**, 53, 98-106.
- [122] Strotmann, H., Brendel, K., Boos, K. S., Schlimme, E., *FEBS Lett.*, **1982**, 145, 11-15.
- [123] Schrader, K. K., Dayan, F. E., Allen, S. N., de Regt, M. Q., Tucker, C. S., Paul, J., Rex, N., *Int. J. Plant Sci.*, **2000**, 161, 265-270.
- [124] Jean, B., *Pharmacognosy, Phytochemistry, Medicinal Plants, 2^{eme} ed. Retirage broch. Lavoisier*, **2008**.
- [125] Singh, A., *Herbal Drugs as Therapeutic Agents. CRC Press*, **2014**.

- [126] Wube, A. A., Bucar, F., Asres, K., Gibbons, S., Rattray, L., Croft, S. L., *Phytother. Res.*, **2005**, *19*, 472-476.
- [127] Ayo, R., Amupitan, J., Zhao, Y., *Afr. J. Biotechnol.*, **2007**, *6*, 1276-1279.
- [128] Barros, I. B., Daniel, J. F., Pinto, J. P., Rezende, M. I., Braz Filho, R., Ferreira, D. T., *Braz. Arch. Biol. Technol.*, **2011**, *54*, 535-541.
- [129] Lee, M. S., Sohn, C. B., *Biol. Pharm. Bull.*, **2008**, *31*, 2154-2157.
- [130] Mellado, M., Madrid, A., Pena-Cortes, H., Lopez, R., Jara, C., Espinoza, L., *J. Chil. Chem. Soc.*, **2013**, *58*, 1767-1770.
- [131] Bechtold, T., Mussak, R., *Handbook of Natural Colorants, Wiley Series in Renewable Resource. Wiley.*, **2009**.
- [132] Saxena, S., Raja, A., *Roadmap to Sustainable Textiles and Clothing. Springer*, **2014**, 37-80.
- [133] Satyajit, S., Lutfun, N., *Chemistry for Pharmacy Students General, Organic and Natural Product Chemistry. New York, NY John Wiley & Sons*, **2013**.
- [134] Porter, L. J., *Tannins. In J. B. Harborne (Ed.), Methods in plant biochemistry: Plant phenolics London: Academic Press*, **1989**, *1*, 389-419.
- [135] Rangkadilok, N., Sitthimonchai, S., Worasuttayangkurn, L., Mahidol, C., Ruchirawat, M., Satayavivad, J., *Food and Chemical Toxicology*, **2007**, *45*, 328-336.
- [136] Chung, K. T., Wong, T. Y., Wei, C. I., Huang, Y. W., Lin, Y., *Critical Reviews in Food Science and Nutrition*, **1998**, *38*, 421-464.
- [137] Okuda, T., *Tannins, a new family of bioactive natural organic compounds (questions and answers), Yakugaku Zasshi*, **1995**, *115*, 81-100.
- [138] Han, X., Shen, T., Lou, H., *International Journal Molecular Sciences*, **2007**, *8*, 950-988.
- [139] Cassidy, A., Hanley, B., Lamuela-Raventos, R. M., *Journal of the Science and Food Agriculture*, **2000**, *80*, 1044-1062.
- [140] Gorham, J., Tori, M., Asakawa, Y., *The biochemistry of the stilbenoids. London: Chapman & Hall*, **1995**.
- [141] Zhang, N. L., Zhu, Y. H., Huang, R. M., Fu, M. Q., Su, Z. W., Cai, J. Z., Hu, Y. J., Qiu, S. X., *Z Naturforsch B*, **2012**, *67*, 1314-1318.
- [142] Chappell, J., *Current Opinion in Plant Biology*, **2002**, *5*, 151-157.
- [143] Goldstein, J. L., Brown, M. S., *Nature*, **1990**, *343*, 425-430.
- [144] Mann, J., Davidson, R. S., Hobbs, J. B., Banthorpe, D. V., Harborne, J. B., *Natural products: Their chemistry and biological significance, Longman, England*, **1994**, *1*, 331-334
- [145] Wayn, B. J., *Mosby's Dictionary of Complementary and Alternative Medicine*, **2005**.
- [146] Ostlund, RE. J., *Annu. Rev. Nutr.*, **2002**, *22*, 533-549.
- [147] Awad, A. B., Toczek, J., Fink, C. S., *Prostaglandins Leukot Essent Fatty Acids*, **2004**, *70*, 511-520.
- [148] SCF, Scientific Committee on Food, **2003**.
- [149] Awad, A. B., Downie, A., Fink, C. S., Kim, U., *Anticancer Res.*, **2000**, *20*, 821-824.

[150] Awad, A. B., Fink, C. S., Williams, H., Kim, U., *Eur. J. Cancer Prev.*, **2001**, *10*, 507-513.

[151] Woyengo, T. A., Ramprasath, V. R., Jones, P. J. H., *Eur. J. Clin. Nutr.*, **2009**, *63*, 813-20.

CHAPTER II

BIBLIOGRAPHIC STUDY ON *ASPHODELUS TENUIFOLIUS* PLANT

II.1. Botanic aspect of Liliaceae family

II.1.1. Description

The diversity of characteristics complicates any description of the Liliaceae morphology, and confused taxonomic classification for centuries. The diversity is also of considerable evolutionary significance, as some members emerged from shaded areas and adapted to a more open environment [1]. They are cosmopolitan in distribution, majority of them are found in tropical regions.

The Liliaceae “Lily family” is mostly perennial herbs from starchy rhizomes, corms or bulbs comprising about 289 genera and 4000 species [2] contains many important medicinal, edible and ornamental plants.

Liliaceae family is classified as follow:

- Kingdom : **Plantae**
- Subkingdom : **Tracheobionta**
- Superdivision : **Spermatophyta**
- Division : **Magnoliophyta**
- Class : **Liliopsida**
- Subclass : **Liliidae**
- Order : **Liliales**
- Family : **Liliaceae (Lily family)**

II.1.2. Characters of Liliaceae

The Liliaceae family are characterized as monocotyledonous, perennial, herbaceous, bulbous (or rhizomatous in the case of Medeoleae) [3] flowering plants with simple trichomes (root hairs) and contractile roots [4].

II.1.2.1. Vegetative characters

Liliaceae family plants are mostly herbs (like: *Asphodelus*), perennating by rhizome (like: *Aloe*), bulb (like: *Lilium*), trees (like; *Dracena*), climber (like: *Asparagus* and *Smilax*), xerophytic plants (like: *Yucca*); cladodes in *Asparagus* and *Ruscus*. Their main morphological character of the different parts is presented as follows:

- **Roots:** are Fibrous adventitious, sometimes tuberous (like: *Asparagus*).
- **Stems:** are Herbaceous, or woody, solid or fistular, underground; aerial climbing or erect; underground stem may be corm, bulb or rhizome.
- **Leaves:** are Alternate, opposite or whorled, radical and cauline, sessile or petiolate, sheathing leaf base; shape is variable scale-like (*Asparagus*), thick succulent and mucilaginous in *Aloe*.

- **Fruits:** A capsule that is usually loculicidal as in the *Lilioideae*, but occasionally septicidal in the *Calachortoideae* and wind dispersed, although the *Medeoleae* form berries (baccate) [1].
- **Seeds:** are endospermic; endosperm horny or cartilagenous.

The family has close affinity with Amaryllidaceae from which it can be distinguished by the presence of superior ovary, and absence of corona. It is also close to Juncaceae as in both the seeds have albumen but differs from Juncaceae in petaloid perianth.

II.1.2.2. Floral characters

Liliaceae family plants main floral characters are presented as follows:

- **Inflorescence:** The flowers are arranged in a cluster or rarely are subumbellate (like: *Gagea*) or a thyse (spike) [5]. Variable-solitary (like: *Tulipa*, *Fritillaria*), paniced raceme (like: *Asphodelus*), solitary axillary (like: *Gloriosa*).
- **Flowers:** Hermaphroditic, actinomorphic (radially symmetric) or slightly zygomorphic (bilaterally symmetric). The perianth is undifferentiated, formed from six tepals arranged into two separate whorls of three parts (trimerous) each. The perianth is either homochlamydeous (all tepals equal, like *Fritillaria*) or dichlamydeous (two separate and different whorls, like *Calochortus*) and may be united into a tube. Nectar is produced in perigonal nectaries at the base of the tepals [5-8].
- **Pollination:** Entomophilous rarely self-pollination

II.1.3. Principal secondary metabolites of Liliaceae

The Liliaceae family is a rich source of natural products displaying a vast range of structural diversity. A multitude of natural products have been isolated and characterized from Liliaceae including, dimeric ent-kaurane diterpenes [9-10] flavonoid glycosides [11-12], anthocyanins [13-14], stilbenes [15] phenolics [16], phenolic glucosides [17], phenolic amides [18], carotenoids [19], sterols [20], alkaloids [21] and sulfur-containing compounds [22].

II.1.4. Economic importance of Liliaceae family

Many plants belonging to this family are useful as: good ornamentals (like: *tulipa*, *Lilium*, *Ruscus*, *Gloriosa*, *Dracaena*...), in medicine like: *Smilax*, *Aloe*, *Gloriosa*, *Veratrum*, *Colchicum*, *Scilla* and *Urginea* which yield many useful drugs, Rat poison is obtained from *Urginea* and the bulbs of *Scilla*. *Aloe vera* yields the “Aloin”, the roots of *Asparagus* yield a tonic and from *Colchicum*, colchicine is obtained), as

vegetables and food (*Allium cepa* (Onion), *Allium sativum* (Garlic) and *Asparagus*), colchicine (*Colchicum autumnale*). As Fibres (*Yucca*, *Phormium tenax* yield fibres used in commerce) and as a source of resin (*Dracaena* and *Xanthorrhoea* yield resin, from the acrid resin of *Xanthorrhoea* sealing wax is prepared).

II.2. Botanic aspect of *Asphodelus* genus

II.2.1. Description

Asphodelus is a genus of mainly perennial plants first described for modern science in 1753. The genus is native to temperate Europe, the Mediterranean, Africa, the Middle East, and the Indian Subcontinent, and now naturalized in other places (New Zealand, Australia, Mexico, southwestern United States). The word is a loanword from Greek.

The Asphodelaceae consists of the sub-families Asphodeloideae and Alo-oideae. Accordingly the genus *Asphodeline*, *Asphodelus*, *Bilbine*, *Bulbinella*, *Eremurus*, *Hemiphlacus*, *Jodrellia*, *kniphofia*, *Paradisea*, *Simethis* and *Trachandra* are placed in the sub-family Asphodeloideae while *Aloe*, *Gasteria*, *Haworthia*, *Lomatophyllum* and *Poellnitzia* are placed in the *Alo-oideae* [23]. On the other hand, some workers consider the above two sub-families as distinct families i.e the Asphodelaceae and the Aloaceae [24].

Asphodels are also popular garden plants, which grow in well-drained soils with abundant natural light [25]. The genus was formerly included in the lily family (Liliaceae) [26]. This genus comprises 16 species distributed in Eurasia and the Mediterranean: [27-28] *Asphodelus acaulis* Desf. (Known as Branched asphodel) (**Fig. II.1**) found in Algeria, Morocco and Tunisia, *Asphodelus aestivus* Brot. (Known as Common asphodel and Silver rod) (**Fig. II.2**) found in southern Europe from Portugal to Turkey, *Asphodelus albus* Mill. (Known as White asphodel, also known as Rimmed lichen) (**Fig. II.3**) and *Asphodelus macrocarpus* Parl. (**Fig. II.4**) found in some Mediterranean regions, *Asphodelus ayardii* Jahand. & Maire, found in France, Spain, Italy, Algeria, Morocco, Tunisia and Canary Islands. *Asphodelus bakeri* Breistr. Found in western Himalayas of northern India and northern Pakistan. *Asphodelus bento-rainhae* P.Silva and *Asphodelus serotinus* Wolley-Dod found in Spain and Portugal. *Asphodelus cerasiferus* J.Gay. found in France, Spain, Sardinia, Algeria, Morocco and Tunisia. *Asphodelus fistulosus* L. (also known as Onion-leaved asphodel or Onionweed) (**Fig. II.5**) found in Mediterranean, naturalized in New Zealand, Mexico and southwestern United States, *Asphodelus gracilis* Braun-Blanq. & Maire found in Morocco, *Asphodelus lusitanicus* Cout. Found in Spain and Portugal, *Asphodelus ramosus* L., found in southern Europe, northern Africa, the Middle East and Canary Islands, *Asphodelus refractus* Boiss. found in North Africa and Arabian Peninsula from Mauritania, Morocco to Saudi Arabia, *Asphodelus roseus* Humbert & Maire found in Spain and Morocco, *Asphodelus*

viscidulus Boiss. Found in North Africa, Middle East and Arabian Peninsula. *Asphodelus tenuifolius* Cav. (**Fig. II.6**), found in Southeast Europe and northern Africa from the Mediterranean south to Mali, Chad, Sudan, Somalia; south-central Asia from Caucasus to India.



Figure II.1. *Asphodelus acaulis* Desf. [29]



Figure II.2. *Asphodelus aestivus* Brot. [30]



Figure II.3. *Asphodelus albus* Mill. [31]



Figure II.4. *Asphodelus macrocarpus* Parl. [32]



Figure II.5. *Asphodelus fistulosus* L. [33]

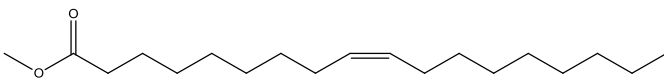
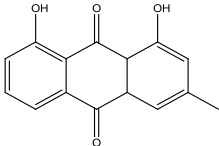
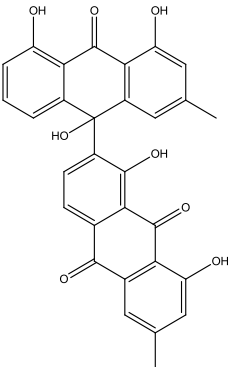
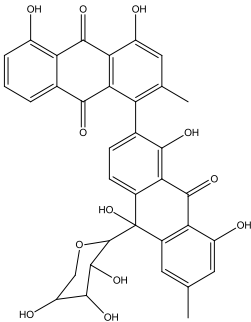


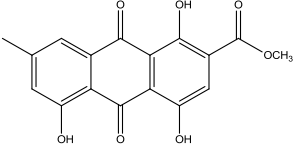
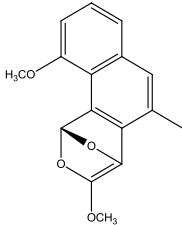
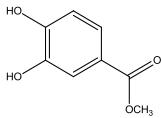
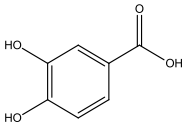
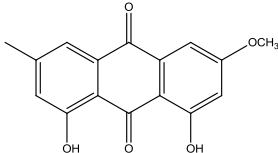
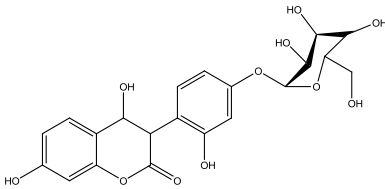
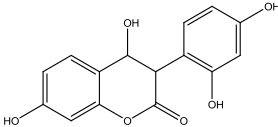
Figure II.6. *Asphodelus lutea*. [34]

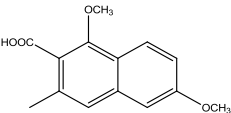
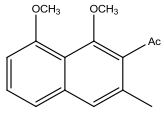
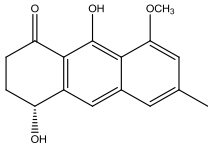
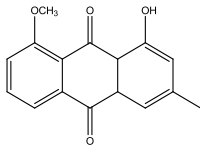
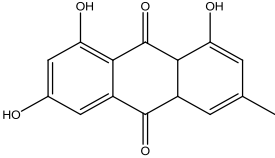
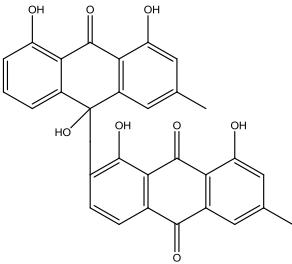
II.2.2. Previous phytochemical studies on *Asphodelus* genus

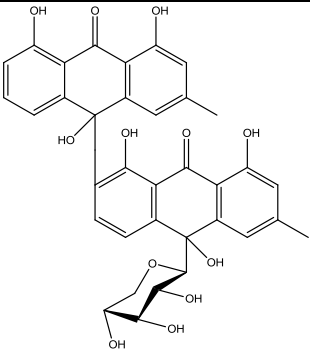
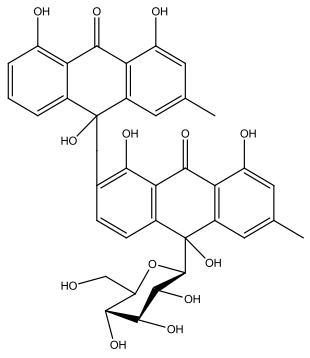
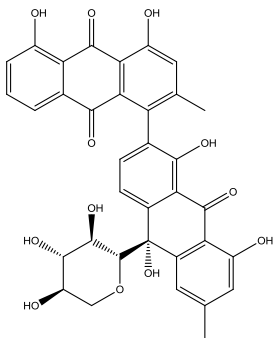
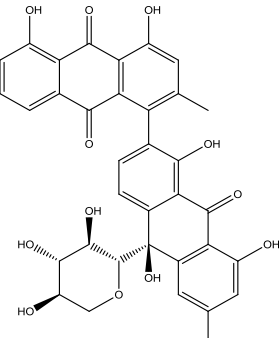
Previous studies have shown the *Asphodelus* genus contain several types of natural compounds as shown in **Table II.1**.

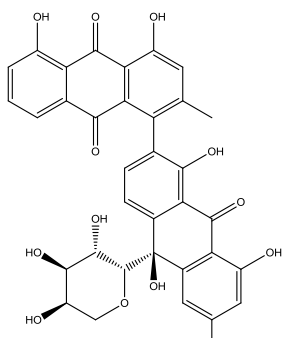
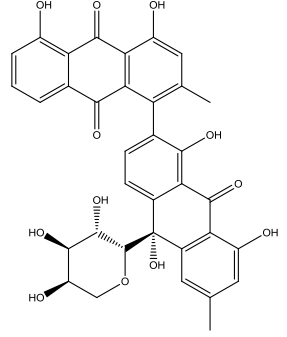
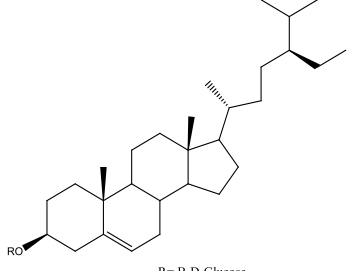
Table II.1. Isolated compounds from *Asphodelus* genus.

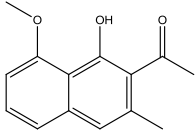
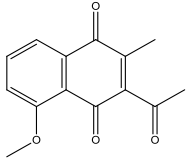
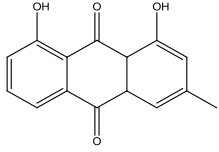
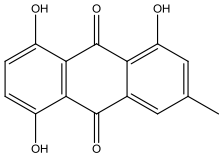
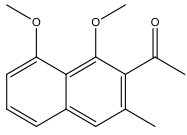
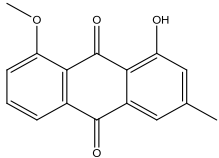
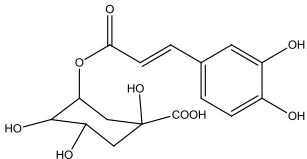
<i>Species</i>	<i>Isolated compounds</i>	<i>Part</i>	<i>Ref.</i>
<i>Asphodelus microcarpus</i>	 Oleic acid methyl ester	Leaves	[35]
	 Chrysophanol		[35-7]
	 10- (chrysophanol-7'-yl)-10-hydroxychrysophanol-9-anthrone		[35]
	 Asphodelin-10'-oxanthrone-(10'S)-D-arabinopyranoside. (asphodoside C).		[35]

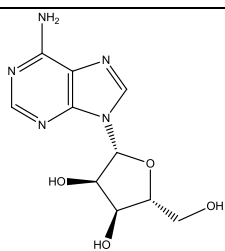
	 <p>Methyl-1,4,5-trihydroxy-7-methyl-9,10-dioxo-9,10-dihydroanthracene-2-carboxylate</p>	Tubers	[36]
	 <p>(1R) 3,10-Dimethoxy-5-methyl-1H-1,4-epoxybenzo[<i>h</i>]iso-chromene</p>		[36]
	 <p>3,4-dihydroxy-methyl benzoate</p>		[36]
	 <p>3,4-dihydroxybenzoic acid</p>		[36]
	 <p>6-methoxychry-sophanol</p>		[36]
	 <p>asphodelin A 4'-<i>O</i>-α-D-glucoside</p>	Bulbs and roots	[39]
	 <p>3-(2',4'-Dihydroxyphenyl)-4,7-dihydroxy-2H-1-benzopyran-2-one.</p>		[39]

	 <p>1, 6-dimethoxy-3-methyl-2-naphthoic acid</p>	Tubers	[41]
	 <p>2-acetyl,1,8-dimethoxy,3-methyl-naphthalene</p>		[41]
	 <p>aloesaponol III-8-methyl ether</p>		[41]
	 <p>8-methoxy- chrysophanol</p>		[41]
	 <p>emodin</p>		[41]
	 <p>10-(chrysophanol-7'-yl)-10-hydroxychrysophanol-9-anthrone</p>		[41]

	 <p>Aestivin</p>		[41]
	 <p>Ramosin</p>	whole plant	[41-42]
	 <p>Asphodelin-10'-oxanthrone-(10'R) - β - D - xylopyranoside (Asphodoside A).</p>		[47]
	 <p>Asphodelin-10'-oxanthrone-(10'S) - β - D - xylopyranoside (Asphodoside B).</p>		[47]

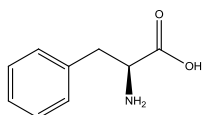
	 <p data-bbox="494 582 1069 672">Asphodelin-10'-oxanthrone-(10'S) - β - L - arabinopyrano-side (Asphodoside C).</p>		[47]
	 <p data-bbox="494 1052 1069 1142">Asphodelin-10'-oxanthrone-(10'R) - β - L - arabinopyrano-side (Asphodoside D)</p>		[47]
	 <p data-bbox="510 1456 1053 1523">β- Sitosterol-3-O- β-D-glucopyranoside</p>		[45]

<i>Asphodelus lutea</i>	 <p>2-Acetyl-1-hydroxy-8-methoxy-3-methylnaphthalene</p>  <p>2-Acetyl-8-methoxy-3-methylnaphthoquinone</p>  <p>Chrysophanol</p>  <p>1,5,8-trihydroxy-3-methylantraquinone</p>  <p>2-acetyl-1,8-dimethoxy-3-methylnaphthalene</p>  <p>1-hydroxy-8-methoxy-3-methylantraquinone</p>	Roots	<p>[37]</p> <p>[37]</p> <p>[37-41]</p> <p>[37]</p> <p>[37]</p> <p>[37]</p>
<i>Asphodelus aestivus</i>	 <p>Chlorogenic acid</p>	Leaves	[38]



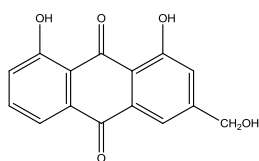
Adenosine

[38]



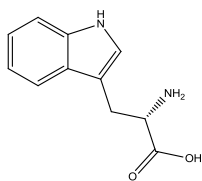
Phenylalanine

[38]



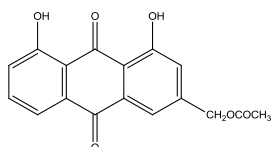
Aloe-emodin

[38]



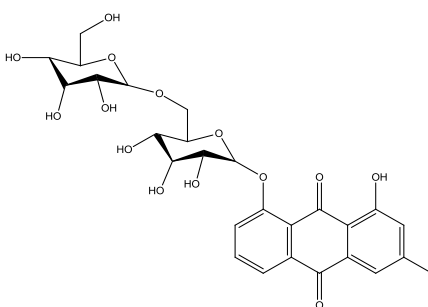
Tryptophan

[38]



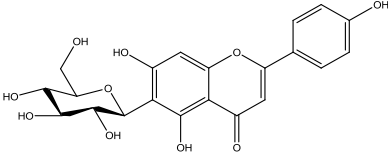
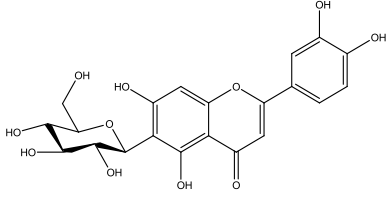
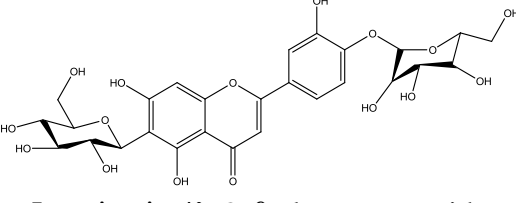
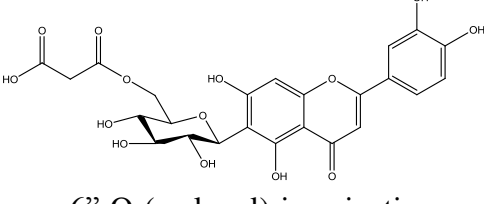
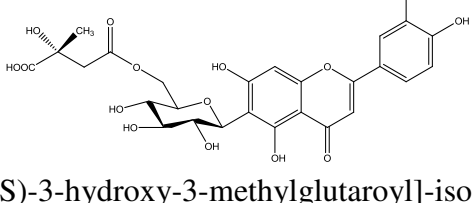
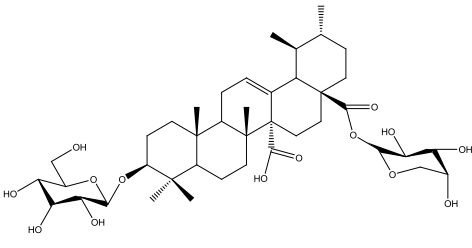
Aloe-emodin acetate

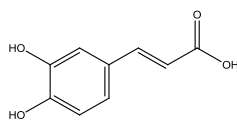
[38]



Chyrosphanol 1-O-gentiobioside

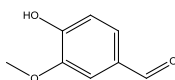
[38]

	 <p style="text-align: center;">Isovitexin</p>		[38]
	 <p style="text-align: center;">isoorientin</p>		[38]
	 <p style="text-align: center;">Isoorientin 4'-O-β-glucopyranoside</p>		[38]
	 <p style="text-align: center;">6''-O-(malonyl)-isoorientin</p>		[38]
	 <p style="text-align: center;">6''-O-[(S)-3-hydroxy-3-methylglutaroyl]-isoorientin</p>		[38]
<i>Asphodelus tenuifolius</i>	 <p style="text-align: center;">Asphorodin</p>	whole plant	[40]



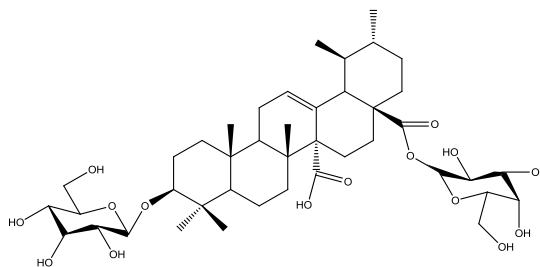
Caffeic acid

[48]



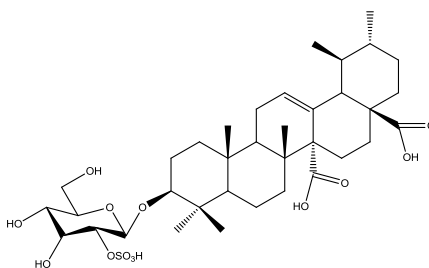
Vanillin

[48]



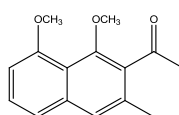
Asphorin A

[46]

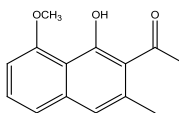


Asphorin B

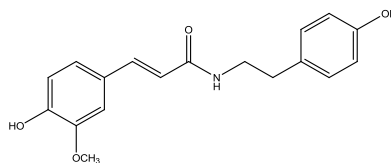
[46]

1-(1,8-dimethoxy-3-methylnaphthalen-2-yl)
ethanone.

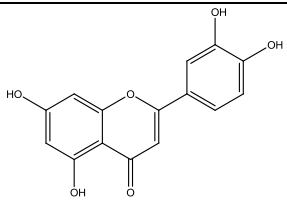
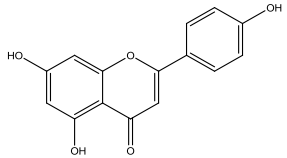
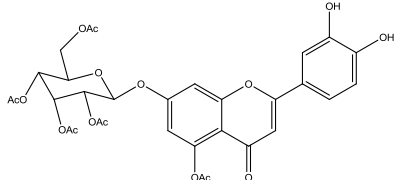
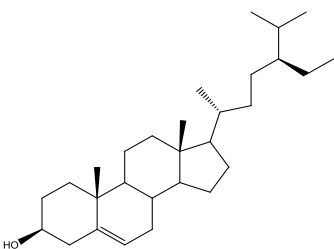
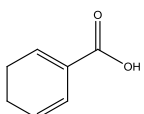
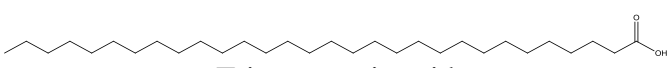
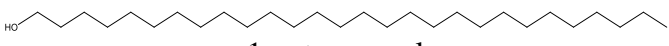
[41]

1-(1-hydroxy-8-methoxy-3-methylnaphthalen-2-yl)
ethanone

[43]

*Trans*-N- feruloyltyramine

[44]

	 <p style="text-align: center;">Luteolin</p>		[44]
	 <p style="text-align: center;">Apigenin</p>		[44]
	 <p style="text-align: center;">Luteolin 7-O-β-D-glycopyranoside tetraacetate</p>		[44]
	 <p style="text-align: center;">β-Sitosterol</p>		[45]
	 <p style="text-align: center;">3-Hydrobenzoic Acid</p>		[45]
	 <p style="text-align: center;">Triacontanoic acid</p>		[45]
	 <p style="text-align: center;">1-octacosanol</p>		[45]

II.2.3. Previous biological studies on *Asphodelus* genus

In correlation with the different traditional uses of *Asphodelus* genus plants, many plants of this genus are well known for their interesting biological activities. Various Previous biological studies were conducted to determine the different biological activities that could be exploited later for therapeutic purposes: Antioxidant, antibacterial and antifungal by using various *in vitro* systems and analysis of marker compounds HPLC of methanolic, ethanolic and petroleum ether extracts of *A. tenuifolius* Cav. were studies [48], The antimicrobial activity against some pathogenic bacteria and fungi of *A. tenuifolius* was studied [49], The antioxidant properties of the silver nanoparticles (AgNPs) using an extract from the aerial parts of *A. aestivus* Brot. were evaluated using DPPH, ABTS⁺ and hydrogen peroxide scavenging assays [50], Evaluation of antibacterial activity of wild local *A. microcarpus* and *A. lutea* crude extracts against methicillin resistant *Staphylococcus aureus* (MRSA) isolates, with the evaluation of antimicrobial activity against MRSA clinical isolates using agar wells diffusion and determination of minimum inhibitory concentration (MIC) of methanolic extract of the two plants was also performed using tetrazolium microplate assay [51], *A. aestivus* Brot. (Asphodelaceae) anthers were analyzed to provide a detailed understanding of the events that lead to pollen grain development, accompanied by cytochemical observations at different ontogenic stages [52], *In vitro* antioxidant and antifungal activities of *A. aestivus* Brot. leaves were evaluated. β -carotene bleaching effect, metal chelating ability, total antioxidant activity (DPPH), (ABTS), N,N-dimethyl-p-phenylenediamine dihydrochloride (DMPD), superoxide, hydroxyl and nitric oxide (NO) scavenging assays and antifungal activities of water and ethanol extracts were determined [53], Different antioxidant tests were employed in order to evaluate the antioxidant activities of methanolic and acetone extracts of *A. aestivus* Brot. leaves [54], Evaluation of the bio-herbicidal potential of *A. microcarpus* L. on *Chenopodium album* L.; a major wheat pest (*Triticum aestivum* L.) [55], Aqueous-ethanol extract of *A. tenuifolius* was investigated for hypotensive and diuretic activities using *in vivo* and *in vitro* models [56], Potential antioxidant activities of crude extracts from *A. aestivus* Brot. tubers were evaluated by 2,2-diphenyl-1-picrylhydrazyl (DPPH) scavenging assay, cytotoxic and apoptotic activity of the extracts on MCF-7 breast cancer cells were evaluated [57], Evaluation of the biological activity of *A. microcarpus*, antioxidant, anti-inflammatory and antibacterial activities in ethanolic extract were evaluated [58], Determination of vitamins, essential elements and antioxidant activity of *A. aestivus* L. extracts [59], Fatty-acid profiles and antimicrobial activity of *A. aestivus* seeds were examined [60], and finally the evaluation of the antibacterial, antiviral activity and antibiofilm susceptibility of *A. microcarpus* leaves extract [61].

II.2.4. *Asphodelus tenuifolius* Cavase specie

Asphodelus: generic name of Asphodel indicating in Latin and Greek several species of Liliaceae, dedicated to the Gods of hell and death who were supposed to eat the tubers. The plant is known by vernacular name:

- English: **Asphodel** and **Onion weed** [62]
- Arabic: **Tazia**, **Acheub el Ibel**, **Barwaq** [63]
- French: **Asphodèle à petites feuilles** [63]
- Urdu language: **Piazi** and **Basri** [63]
- Targui: **Izayan** [63]

II.2.4.1 Morphological aspect

Asphodelus tenuifolius Cav. is an erect annual, monocotyledonous herb; root yellowish in young plants and dark brown at maturity, superficially has the appearance of the taproot system of dicotyledons, in fact the ridged and furrowed organ is a hard and compacted bundle of fibrous roots, which may sometimes twist to give a rope-like appearance; leaves numerous, all basal, hollow, gradually acuminate to a point, 10 to 40 cm long, sparse dichotomous branching in upper region, stout, 3 mm in diameter (Fig. II.7).

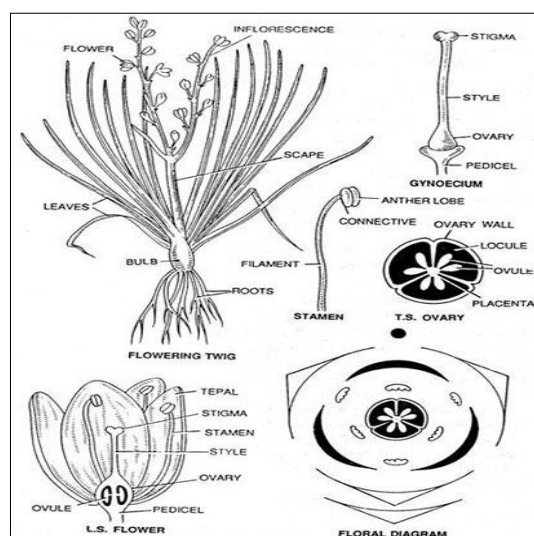


Figure II.7. *A. tenuifolius* floral diagram

Flowers campanulate, white with pink or purple stripe, short pedicel may be jointed; petals 1.5 cm long in six perianth segments; stamens six; simple, superior; flowering progressing upward in the inflorescence over a period of weeks, normally flowers do not open until late afternoon and unless conditions are dull and cool will close and wither before the next day; fruit, a 3-valved globular capsule, dehiscent at partitions into the cavity, transversely wrinkled, about 3 mm long; seeds 3-angled, blackish, finely pebbled texture, deep irregular dents on face and back (Fig. II.8). Flowering takes place in early spring from March to May.



Figure II.8. *A. tenuifolius* Cav.

The most significant morphological differences between *A. fistulosus* and *A. tenuifolius* are that the latter is annual and more dwarfs, its scape is somewhat

scabrous at the base, its tepals are smaller, the fruit is proportionally smaller, and the peduncles are articulated in the lower half [58].

II.2.4.2 Classification

Asphodelus tenuifolius specie is classified as follow [26]:

- Kingdom: **Plantae**
- Phylum : **Angiosperms**
- Sub-phylum : **Monocotyledous**
- Order : **Asparagales**
- Family : **Liliaceae (Xanthorrhoeaceae)**
- Sub-family : **Asphodeloideae**
- Genus : ***Asphodelus***
- Species : ***Asphodelus tenuifolius***

II.2.4.3 Geographic distribution

Asphodelus tenuifolius Cav. is a native to the Mediterranean region, Canary Islands, Madeira, North Africa, South Europe, but it is widespread, extending from Mediterranean region east through the Arabian Peninsula to the Indian Subcontinent, also in Malaysia, Australia, Chile, New Zealand, Mexico, United States of America [63] until Mascarene Islands [65] (**Fig. II.9**).

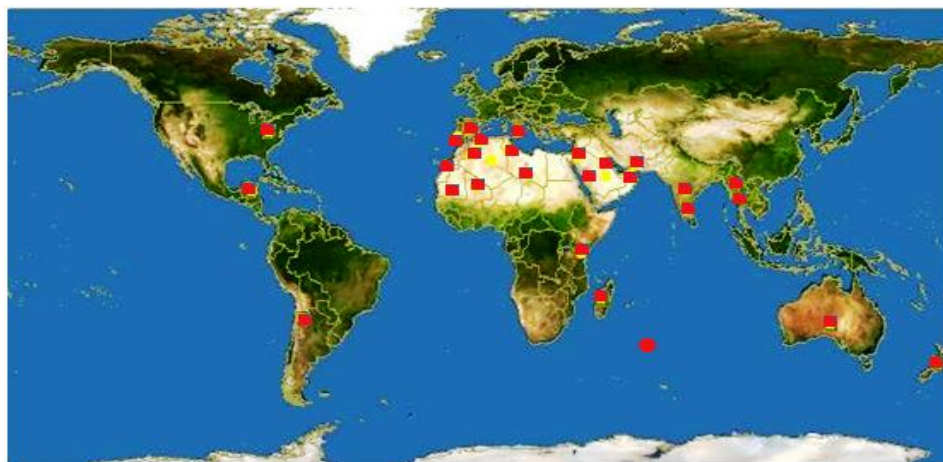


Figure II.9. Geographic distribution (in **Red**) of *Asphodelus tenuifolius* Cav.

II.2.4.4. Toxicity action

The plant is not reported as toxic by nomads. Eaten in big quantities, it can provoke indigestion [63].

II.2.4.5. Traditional and Medicinal uses

Asphodelus tenuifolius Cav. is used as vegetable [63], the small *asphodelus* is also widely used for various culinary purposes. The leaves are either boiled or cooked in oil, and the young shoots are added raw to food to enhance the taste. This plant is little appreciated as pasture. The leaves and fruits are collected in spring and prepared by maceration in olive oil; the seeds are crushed. The crushed seeds are taken internally, mixed with honey or olive oil; the liquid obtained from the macerated leaves is used externally as a massage [63].

In Egypt, the seeds are reported to be diuretic and are eaten with yoghurt. Similar uses as in Algeria are reported for Morocco. The seeds are mixed with cereals to make traditional bread and are also eaten as delicacies when mixed with dates. The leaves are fried or boiled and are sometimes put in the sauce for couscous [63].

As a medicinal plant, Seeds, roots and whole plant are used for medicinal purposes as diuretic, cure ulcer and inflamed parts [66], anti-inflammatory, insecticide, treatment for skin diseases, constipation [67], diarrhea, epilepsy, diabetes [68], paralysis [69], narcotic, sedative, sexual problems [70], cold, cough, fever, piles [71], swellings, hypertension, it is also used as antihypertensive. It is believed to be condiment and reduce blood pressure and jaundice [72]. Leaf decoction is given in kidney stone while leaf paste is applied on swellings, Taken for colds and hemorrhoids (seeds), a febrifuge, used for rheumatic pain [73].

REFERENCES

- [1] Patterson, T. B., Givnish, T. J., *Evolution*, **2002**, 56, 233-252.
- [2] Bashir, A., *African Journal of Biotechnology*, **2010**, 9, 5762-5766.
- [3] Tamura, M. N., *Liliaceae*, In Kubitzki. **1998**, 343-353.
- [4] Rodolphe, S., Mathieu, P., *Systematic Botany of Flowering Plants*, Lausanne Science Publishers, **2004**.
- [5] Simpson, M. G., *Plant Systematics*, Academic Press, **2011**, ISBN : 978-0-08-051404-8.
- [6] Mabberley, D. J., *Mabberley's Plant-Book (3ed.)*. Cambridge University Press, **2013**, ISBN : 1-107-78259-7.
- [7] Singh, G., *Liliaceae*. In Singh, **2004**, 351-352. ISBN : 9781578083510.
- [8] Weberling, F., **1992**, *Morphology of Flowers and Inflorescences*, Cambridge University Press, England, 87.
- [9] Wu, J. Z., Morizane, C., Iida, A., Ueda, S., Zhou, Z. L., Xu, M., Zhang, M., Li, R. M., Fujita, T., *Chemical and pharmaceutical bulletin*, **1995**, 43, 1448-1453.
- [10] Kitajima, J., Komori, T., Kawasaki, T., *Chem Pharm Bull*, **1982**, 30, 3912-3921.
- [11] Fattorusso, E., Iorizzi, M., Lanzotti, V., Taglialatela-Scafati, O., *J. agricultural and food chemistry*, **2002**, 50, 5686-5690.
- [12] Francis, J. A., Rumbelha, W., Nair, M. G., *Life sciences*, **2004**, 76, 671-683.
- [13] Takeda, K., Harborne, J. B., Self, R., *Phytochemistry*, **1986**, 25, 2191-2192.
- [14] Nørbæk, R., Kondo, T., *Phytochemistry*, **1999**, 50, 1181-1184.
- [15] Zhou, C. X., Tanaka, J., Cheng, C. H., Higa, T., Tan, R. X., *Planta medica*, **1999**, 65, 480-482.
- [16] Shimomura, H., Sashida, Y., Mimaki, Y., *Phytochemistry*, **1986**, 25, 2897-2899.
- [17] Shoyama, Y., Hatano, K., Nishioka, I., Yamagishi, T., *Phytochemistry*, **1987**, 26, 2965-2968.
- [18] Park, J. B., *J. agricultural and food chemistry*, **2009**, 57, 8868-8872.
- [19] Tsukida, K., Ikeuchi, K., *Bitamin*, **1965**, 32, 222-226.
- [20] Itoh, T., Tamura, T., Mitsunashi, T., Matsumoto, T., *Phytochemistry*, **1977**, 16, 140-141.
- [21] Shimomura, H., Sashida, Y., Mimaki, Y., Minegishi, Y., *Phytochemistry*, **1987**, 26, 582-583.
- [22] Lanzotti, V., *J. chromatography A*, **2006**, 1112, 3-22.
- [23] Dahlgren, R. M. T., Clifford, H. T., Yeo, P. F., *The Families of the Monocotyledons*, Springer-Verlag, Berlin, **1985**.
- [24] Brummitt, R. K., *Visceral Plant Families and Genera*, Royal Botanic Gardens, Kew, **1992**.
- [25] Bailey, L. H., Bailey, E. Z., *Hortus Third i-xiv, 1-1290*. MacMillan, New York, **1976**.
- [26] Angiosperm Phylogeny Group, *Botanical Journal of the Linnean Society*. **2016**, 181, 1-20.
- [27] Días Lifante, Z., Valdés B., *Revisión del género Asphodelus L. (Asphodelaceae) en el Mediterráneo Occidental Boissiera*, **1996**, 52, 11-189.

- [28] Lifante, Z. D., *Grana*, **1996**, 35, 24-32.
- [29] <https://www.pinterest.fr/pin/417145984215814155/?lp=true>. (08.2018).
- [30] [https://commons.wikimedia.org/wiki/File:Asphodelus_aestivus_\(flower_spike\).jpg](https://commons.wikimedia.org/wiki/File:Asphodelus_aestivus_(flower_spike).jpg)
- [31] <https://www.florealpes.com/comparaison.php?zoomph2=7&PHPSESSID=hr9p7p sgighcf6bcqrk6jeoi20#visiga>. (08.2018).
- [32] http://dryades.units.it/casentinesi/index.php?procedure=taxon_page&id=6748&num=26989. (08.2018).
- [33] https://keyserver.lucidcentral.org/weeds/data/media/html/asphodelus_fistulosus.htm. (08.2018).
- [34] <https://jardinage.ooreka.fr/plante/voir/248/asphodeline-lutea>. (08.2018).
- [35] El-Sayed, M. E. G., *J. Pharmacognosy and Phytochemistry*, **2017**, 6, 259-264.
- [36] Ghoneim, M. M., Elokely, K. M., El-Hela, A. A., Mohammad, A. I., Jacob, M. Cutler, S. J., Doerksen, R. J., Ross, S. A., *Med. Chem. Res.*, **2014**, 23, 3510-3515.
- [37] Todorova, G., Lazarova, I., Mikhova, B., Kostova, I., *Chemistry of Natural Compounds*, **2010**, 46, 322-323.
- [38] Ihsan, C., S. Birincioglu, S., Kırmızıbekmez, H., Pfeiffer, B., Heilmann, J., *Z. Naturforsch*, **2006**, 61b, 1304-1310.
- [39] Hesham, R. E. S., *J. Nat. Prod.*, **2007**, 70, 118-120.
- [40] Safder, M., Imran, M., Mehmood, R., Malik, A., Afza, N., Iqbal, L., Latif, M., *J. Asian Natural Products Research*, **2009**, 11, 945-950.
- [41] Ghoneim, M. M., Guoyi, M., Atef, A. E., Mohammad, A. I., Kottob, S., El-Ghaly, S., Cutler, S. J., Ross, S. A., *Nat. Prod. Communications*, **2013**, 8, 1117-1119.
- [42] Adinolfi, M., Corsaro, M. M., Lanzetta, R., Parriili, M., Scopa, A., *Phytochemistry*, **1989**, 28, 284-288.
- [43] Abdel-Mogib, M., Basaif, S. A., *Pharmazie*, **2002**, 57, 286-287.
- [44] Khaled, F., Saoussen, H., Abdelkader, B. S., Ridha, E. M., Mariem, G., Maha, M., Mohamed, G., Melika, T. A., Orazio, T. S., Zine, M., *J. Med. Plant Res.*, **2014**, 8, 550-557.
- [45] Safder, M., Riaz, N., Irman, M., Nawaz, H., Malik, A., Jabran, A., *J. Chem. Soc. Pak.*, **2009**, 31, 122-125.
- [46] Safder, M., Mehmood, R., Ali, B., Mughal, U. R., Malik, A., Jabbar, A., *Helvetica Chimica Acta*, **2012**, 95, 144-151.
- [47] Ghoneim, M. M., Elokely, K. M., El-Hela, A. A., Mohammad, A.-E.I., Jacob, M., Radwan, M. M., Doerksen, R. J., Cutler, S. J., Ross, A., S.A., *Phytochemistry*, **2014**, 105, 79-84.
- [48] Eddine, L. S., Segni, L., Ridha, O. M., *Int. J. Pharm. Clin. Res.*, **2015**, 7, 119-125.
- [49] Dangi, A. S., Aparna, Sharma, M., Yadav, J. P., Arora, D. R., Chaudhary, U., *J. Evolution of Medical and Dental Sciences*, **2013**, 2, 5663-5668.
- [50] Fafal, T., Taştan, P., Tüzün, B. S., Ozyazici, M., Kivcak, B., *South African Journal of Botany*, **2017**, 112, 346-353.
- [51] Al-Kayali, R., Kitaz, A., Haroun, M., *International Journal of Pharmacognosy and Phytochemical Research*, **2016**, 8, 1964-1968.

- [52] Vardar, F., İsmailoğlu, I., Ünal, M., *Turk. J. Bot.*, **2013**, *37*, 306-315.
- [53] Peksel, A., Altas-Kiyamaz, N., Imamoglu, S., *Journal of Medicinal Plants Research*, **2012**, *6*, 253-265.
- [54] Peksel, A., Imamoglu, S., Altas Kiyamaz, N., Orhan, N., *International Journal of Food Properties*, **2013**, *16*, 1339–1350.
- [55] Masarrat, M., Amal, F., Azhar, A., *Athens Journal of Sciences*, **2015**, *2*, 275-286.
- [56] Naveed, A., Janbaz, K. H., Jabeen, Q., *Bangladesh J. Pharmacol*, **2016**, *11*, 830-837.
- [57] Özlem, S., Aslantürk, Çelik, T. A., *African Journal of Pharmacy and Pharmacology*, **2013**, *7*, 610-621.
- [58] Razik, A., Adly, F., Lahlou, F. A., Hmimid, F., Fahde, S., Moussaid, M., Elamrani, A., Noureddine, B., Loutfi, M., *World Journal of Pharmaceutical Research*, **2016**, *5*, 666-673.
- [59] Ilkay, U., Olcay, K. I., *Instrumentation Science and Technology*, **2017**, *45*, 469-478.
- [60] Fafal, T., Yilmaz, F. F., Birincioğlu, S. S., Hoşgör-Limoncu, M., Kivçak, B., *HVM Bioflux*, **2016**, *8*, 103-107.
- [61] Di Petrillo, A., Fais, A., Pintus, F., Santos-Buelga, C., González-Paramás, A. M., Piras, V., Orrù, G., Mameli, A., Tramontano, E., Frau, A., *BMC Microbiology*. **2017**, *17*, 159-167.
- [62] Nasir, E., Ali, S. I., *Flora of Pakistan, No.132-190. Islamabad, Karachi. 1980-1989* (Eds.).
- [63] IUCN, *A Guide to Medicinal Plants in North Africa, Malaga, Spain*, IUCN Centre for Mediterranean Cooperation, **2005**, 49-50.
- [64] Rejon, C. R., Blanca, G., Cuetro, M., Lozano, R., Rejon, M. R., *Plant Systematics and Evolution*, **1990**, *169*, 1-12.
- [65] Aslam, N., Janbaz, K. H., Jabeen, Q., *Bangladesh Journal of Pharmacology*, **2016**, *11*, 830-837.
- [66] Jabeen, N., Ahmed, M., *Pak. J. Bot.*, **2009**, *41*, 1677-1683.
- [67] Quattrocchi, U., *CRC World dictionary of medicinal and poisonous plants: Common names, scientific names, eponyms, synonyms and etymology*, Boca Raton, USA, CRC Press, **2012**, 451-452.
- [68] Ahmed, N., Mahmood, A., Tahir, S. S., Bano, A., Malik, R. N., Hassan, S., Ashraf, A., *J. Ethnopharmacol*, **2014**, *155*, 1263-1275.
- [69] Abu-Rabia, A., *Chin Med.*; **2012**, *3*, 157-166.
- [70] Ahmed, N., Mahmood, A., Mahmood, A., Sadeghi, Z., Farman, M., *J. Ethnopharmacol*, **2015**, *168*, 66-78.
- [71] Ahmed, N., Mahmood, A., Mahmood, A., Tahir, S. S., Bano, A., Malik, R. N., Hassan, S., Ishtiaq, M., *J. Ethnopharmacol*, **2014**, *155*, 509-523.
- [72] Yaseen, G., Ahmad, M., Sultana S., Suleiman, A. A., Hussain, J., Zafar, M., Shafiq, U. R., *J. Ethnopharmacol*, **2015**, *163*, 43-59.
- [73] Mahmood, A., Mahmood, A., Shaheen, H., Qureshi, R., Sangi, Y., Gilani, S., *J. Med. Plant Res.*, **2011**, *5*, 2346-2360.

CHAPTER III

MATERIALS AND METHODS

III.1. Plant material and extraction methods of *A. tenuifolius*

III.1.1. Plant collection

Aerial parts of *A. tenuifolius* (**Fig. III.1**) were collected two times on May 2010 and April 2011 from the region of Bechar, Southwest of Algeria. The plant was identified by M. Mohamed Benabdelhakem (Ex-Director of the National Agency of Preservation of Natural Resources, Bechar, Algeria). An authenticated voucher specimen, with the identification number (AS10TEN) was deposited at the herbarium of the VARENBIOMOL research unity, University Mentouri of Constantine, Algeria.



Figure III.1. *A. tenuifolius* Cav. (2011).

III.1.2. Preparation of extracts

A total of 1860 g air-dried and powdered aerial parts of *A. tenuifolius* were extracted with EtOH/H₂O (80:20, v/v) for 48 hours, three times at room temperature. After filtration, the filtrates were concentrated by a rotary evaporator. The combined ethanolic extract was evaporated up to 38°C and to give a residue (105.5 g) which was suspended in distilled water. Each resulting solution was extracted successively with chloroform (3 x 400 ml), ethylacetate (3 x 400 ml) and *n*-butanol (6 x 400 ml). The organic phases were filtered using common filter paper and concentrated in vacuum with a water bath at 38°C to obtain the following dry organic extracts: Chloroform (5.60 g), Ethyl acetate (7.77 g) and *n*-Butanol (14.41 g) (**Fig. III.2**).

III.1.3. Determination of Total Phenolic Content (TPC)

The total phenolics content of the different extracts of *A. Tenuifolius* was determined using Folin-Ciocalteu reagent according to the method of Dewanto *et al.*, 2002 [1] using gallic acid as a standard. The reaction mixture was composed by mixing 125 µl of the sample solution, 500 µl of distilled water and 125 µl of the Folin-Ciocalteu reagent. The mixture was shaken. After 3 minutes, 1250 µl of 7% Sodium Carbonate CO₃(Na)₂ was added, by adding distilled water and mixing well, final volume was made up to 3 ml and the mixture was allowed to stand for 90 minutes in

darkness at 37°C. The absorption at 760 nm was measured against a blank. The reference range is prepared with gallic acid in different concentrations of 50, 100, 200, 300, 400, 500 $\mu\text{g}\cdot\text{l}^{-1}$. The total phenolics contents were expressed as milligram Gallic Acid Equivalents (mg GAE/g) of Dry Weight (DW). All samples were analyzed in three replicates.

III.1.4. Determination of Total Flavonoids Content (TFC)

Total flavonoids content was determined using the colorimetric method introduced by Dewanto *et al.*, 2002 [1]. A volume of 250 μl of the diluted extract (concentration of 1 mg/ml of Methanol) was added to 75 μl of Sodium Nitrite (NaNO_2 (5%)). After 6 minutes, 150 μl of $\text{AlCl}_3 \cdot 6\text{H}_2\text{O}$ (10%) was added at sample solution. 5 minutes later, 500 μl NaOH (1M) was added too at sample solution. By adding distilled water (H_2O) and mixing well, final volume was made up to 2.5 ml. using blank, absorbance was measured at 510 nm. A yellow color indicated the presence of flavonoids. As this method is restricted to aglycon part, catechin was used as standard and flavonoid contents were measured as Catechin Equivalent (CE). The reference range is prepared with Catechin in different concentrations from 50 to 500 mg/l. Extract samples were calculated as catechin ($\mu\text{g}/\text{mg}$) using the calibration curve. Results were expressed as milligram Catechin Equivalents (mg CE/g) of Dry Weight (DW). Measurements were performed at least in triplicate.

III.1.5. Determination of Total Tannin Content (TTC)

Condensed tannins were estimated using the method of Sun *et al.*, 1998 [2]. To the freshly prepared extracts (0.1 ml), 0.9 ml methanol, 3 ml of 4% vanillin reagent and 1.5 ml of 9M HCl was added. The solution was mixed thoroughly and absorbance at 500 nm was recorded after 15 to 20 min of incubation at 30°C. The standard range is prepared with catechin at concentrations ranging from 50 to 600 mg/l. Condensed tannins content was calculated from the standard calibration curve based on catechin. Results were expressed as milligram Catechin Equivalents (mg CE/g) of Dry Weight (DW). Measurements were performed at least in triplicate.

III.1.6. Separation and purification

III.1.6.1. Chloroform extract of *A. tenuifolius*

The residue from Chloroform extract (5.60 g) was dissolved in 5 ml of CHCl_3 and subjected to column chromatography on silica gel (63–200 mesh, 170 g) eluted with *n*-hexane / EtOAc gradient elution and then with increasing percentages of MeOH),

Fractions of 50 ml were collected, to yield 24 fractions (F1- F24) (Table III.1) obtained by combining the different eluates based on TLC analysis.

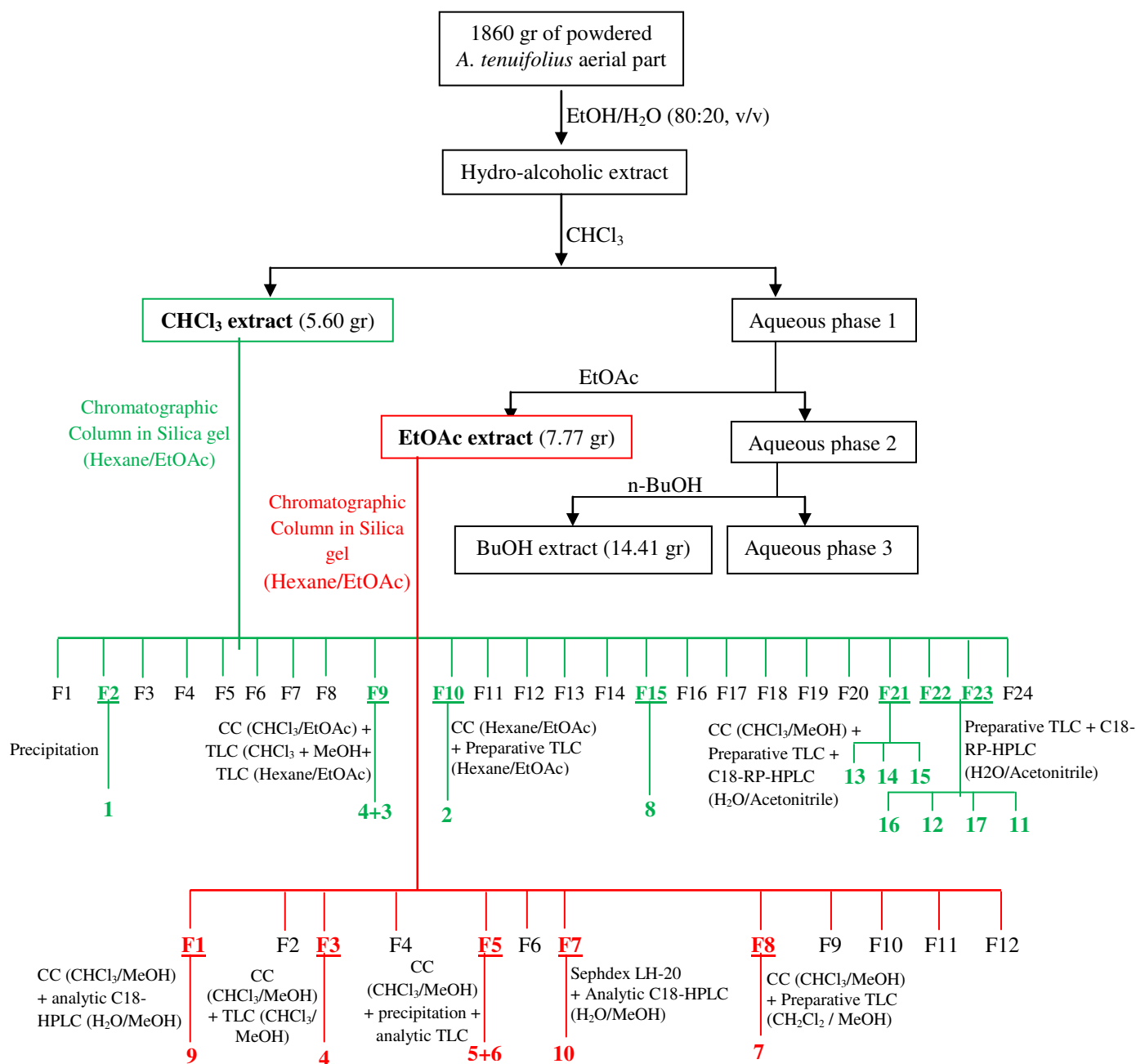


Figure III.2. Plan of separation and purification of the compounds isolated from *A. tenuifolius*

Table III.1. Results of chromatographic separation of Chloroform extract by silica gel column with Hexane / EtOAc.

° of Fractions	Collect fractions	Hexane (%)	Ethyl acetate (%)	Methanol (%)	Weight (mg)
1	1-3	100	0	0	51
2	4-6	100	0	0	55
3	7-12	98	2	0	127
4	13-28	96	4	0	141
5	29-40	95	5	0	61
6	41-44	95	5	0	71
7	45-75	95	5	0	152
8	76-90	92	8	0	45
9	91-114	92	8	0	377
10	115-126	90	10	0	181
11	127-134	90	10	0	58
12	135-146	90	10	0	153
13	147-184	90	10	0	77
14	185-189	88	12	0	101.0
15	190-197	88	12	0	390
16	198-232	85	15	0	188
17	233-250	85	15	0	94
18	251-291	80	20	0	132
19	292-329	80	20	0	79
20	330-342	80	20	0	52
21	343-353	80	20	0	104
22	354-372	75	25	0	45
23	373-399	70	30	0	57
24	400-419	60	40	0	112.5
25	420-434	50	50	0	140
26	435-446	25	75	0	109
27	447-450	10	90	50	520
28	451-460	0	0	100	360

From all these obtained fractions, some of them were chose depend on their richness on secondary metabolites using TLC check.

- **Study of fractions 22 and 23**

Fractions **22** and **23** (101.90 mg) were combined and subjected to column chromatography on a silica gel eluting with CHCl_3 / MeOH with an increasing polarity to yield 6 subfractions according to their TLC behavior. After purification on preparative TLC (Silica gel $_{254}$, CHCl_3 / MeOH, 90:10, v/v), subfraction 3 (55.10 mg) gave a mixture containing four (4) major compounds (**Fig. III.3**). This mixture was subjected to a semi preparative HPLC analysis on a reversed phase column (RP) Phenomenex Luna C18 column (250 mm x4.6 mm, 5 μm particle diameter), using acetonitrile / H_2O (50:50, v/v) at a flow rate of 1.0 ml/min and a detection at 254 nm) to give: **compound 16** (4 mg, R_t = 15 min.), **compound 12** (5 mg, R_t = 19 min.), **compound 17** (4 mg, R_t = 25 min.) and **compound 11** (4 mg, R_t = 28 min.), respectively (**Fig. III.4**).

The TLC check of the separated compounds using an elution system of CHCl_3 / MEOH, (90:10, v/v) gradient showed a single spot for each compound (**Fig. III.5**).

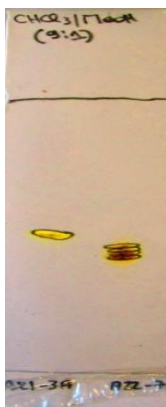


Figure III.3. TLC of subfraction 3 of Fraction (22+23) eluted with (CHCl_3 / MEOH, 90:10, v/v) by treating with a $\text{Ce}(\text{SO}_4)_2$ / H_2SO_4 (before HPLC separation).



Figure III.4. RP- HPLC Separation chromatogram of fraction (22+23) with acetonitrile / H_2O (50:50, v/v).



Figure III.5. TLC of separated compounds **16**, **12**, **17** and **11**

- **Study of fraction 21**

Fraction **21** (104 mg) was subjected to column chromatography on a silica gel eluting with CHCl_3 / MeOH with an increasing polarity to yield 2 subfractions according to their TLC behavior. After purification on preparative TLC (Silica gel ₂₅₄, CHCl_3 / MeOH, 9.5:0.5, v/v), subfraction 2 (45.50 mg) gave a mixture containing three (3) major compounds. This mixture was subjected to a semi preparative HPLC analysis on a reversed phase column (RP) Phenomenex Luna C18 column (250 mmx4.6 mm, 5 μm particle diameter), using acetonitrile / H_2O (50:50, v/v) at a flow rate of 1.0 ml/min and a detection at 254 nm to give: compound **13** (8 mg, R_t = 11 min.), compound **14** (8 mg, R_t = 12 min.) and compound **15** (6 mg, R_t = 13 min.) respectively (**Fig. III.6**).

The TLC check of the separated compounds using an elution system of CHCl_3 / MeOH, (90:10, v/v) gradient showed a single spot for each compound (**Fig. III.7**).

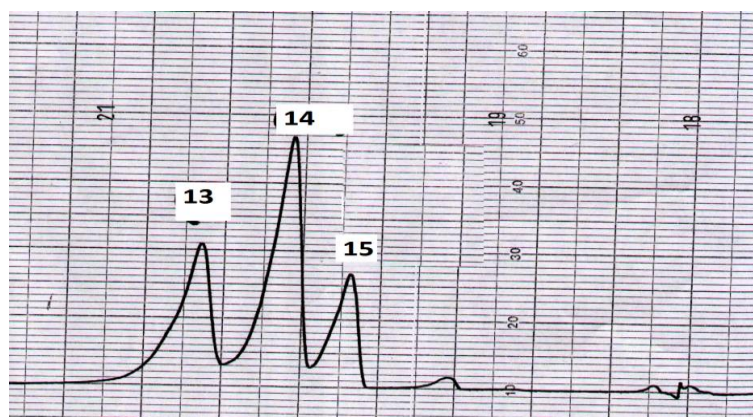


Figure III.6. RP-HPLC Separation chromatogram of fraction 21 with acetonitrile / H_2O (50:50, v/v).



Figure III.7. TLC of separated compounds **13**, **14** and **15**

- **Study of fraction 15**

A quantity of 390 mg of fraction **15** was subjected to column chromatography on silica gel eluting with Hexane / Acetone with an increasing polarity to yield 5 subfractions according to their TLC behavior (**Fig. III.8**), subfraction 1 showed a major spot in TLC with the same eluting system, a purification using a preparative TLC (Silica gel ₂₅₄, using Hexane / EtOAc, 90: 10, v/v) yield to the separation of **compound 8** (11.5 mg).



Figure III.8. TLC of Fraction 15 eluted with (Hexane / EtOAc, 90:10, v/v) by treating with a $\text{Ce}(\text{SO}_4)_2 / \text{H}_2\text{SO}_4$.

- **Study of fraction 10**

Fraction **10** (181 mg) was subjected to column chromatography on silica gel eluting with Hexane / EtOAc with an increasing polarity to yield 3 major subfractions, Chromatography of the subfraction 1 on preparative plates with n-hexane / EtOAc (80:20, v/v) allowed the isolation of the pure **compound 2** (15 mg).

- **Study of fraction 9**

Fraction **9** (377 mg) was subjected to column chromatography on silica gel eluting with CHCl_3 / EtOAc with an increasing polarity to yield 12 subfractions, subfraction 12 showed a major spot in TLC check, this spot was separated using a TLC chromatography with CHCl_3 / MeOH (90:10, v/v) elution system allowed the separation of **compound 3** (6.5 mg) (**Fig. III.9**).



Figure III.9. TLC of Fraction 9 eluted with (CHCl_3 / MeOH, 90:10, v/v) by treating with a $\text{Ce}(\text{SO}_4)_2 / \text{H}_2\text{SO}_4$.

Both subfractions 1 and 2 showed 2 major spots on TLC check (**Fig. III.10**) with Hexane / EtOAc (80:20, v/v) elution system, both spots were separated again using TLC chromatography to obtain pure **compound 4** (6.5 mg).



Figure III.10. TLC of subfraction (1+2) from fraction 9 eluted with (CHCl₃ / MeOH, 90:10, v/v) by treating with a Ce(SO₄)₂ / H₂SO₄.

- **Study of fraction 2**

A white precipitate was found in fraction 2, washing with methanol allowed us to obtain pure **compound 1** (10 mg).

III.1.6.2. Ethyl Acetate extract of *A. tenuifolius*

The residue from Ethyl Acetate extract (5.70 g) was dissolved in 10 ml of Methanol and subjected to column chromatography on silica gel (63–200 mesh, 250 g) eluted with CHCl₃ / MeOH gradient elution and then with increasing percentages of MeOH), Fractions of 50 ml were collected, to yield to 12 fractions (F1-F12) (**Table III.2**) obtained by combining the different eluates based on TLC analysis.

Table III.2. Results of chromatographic separation of Ethyl Acetate extract by silica gel column with CHCl₃ / MeOH

N° of Fractions	Collect fractions	CHCl ₃ (%)	MeOH (%)	Weight (mg)
1	1-13	100	0	551
2	14-36	100	0	155
3	37-72	98	2	327
4	73-98	95	5	141
5	99-140	90	10	291
6	141-164	85	15	171
7	165-185	80	20	459
8	186-200	75	25	245
9	201-244	70	30	377
10	245-266	70	30	181
11	267-324	50	50	358
12	135-146	0	100	453

- **Study of fraction 1**

Fraction 1 (551 mg) was subjected to column chromatography on a silica gel eluting with CHCl_3 / MeOH with an increasing polarity to yield 5 subfractions according to their TLC analysis. After purification on preparative TLC (Silica gel $_{254}$, CHCl_3 / MeOH, 9.5:0.5, v/v), subfraction 1 (54.50 mg) gave a single major spot. This spot was purified by subjecting to an analytic HPLC analysis on a reversed phase column (RP) Nucleodur C18 column (250 mm x 4.6 mm, 5 μm particle diameter), using MeOH / H_2O (from 5 to 100%) at a flow rate of 1.0 ml/min and a detection at 254 nm (**Fig. III.11**) to give: **compound 9** (5.4 mg, $R_t = 16$ min.).

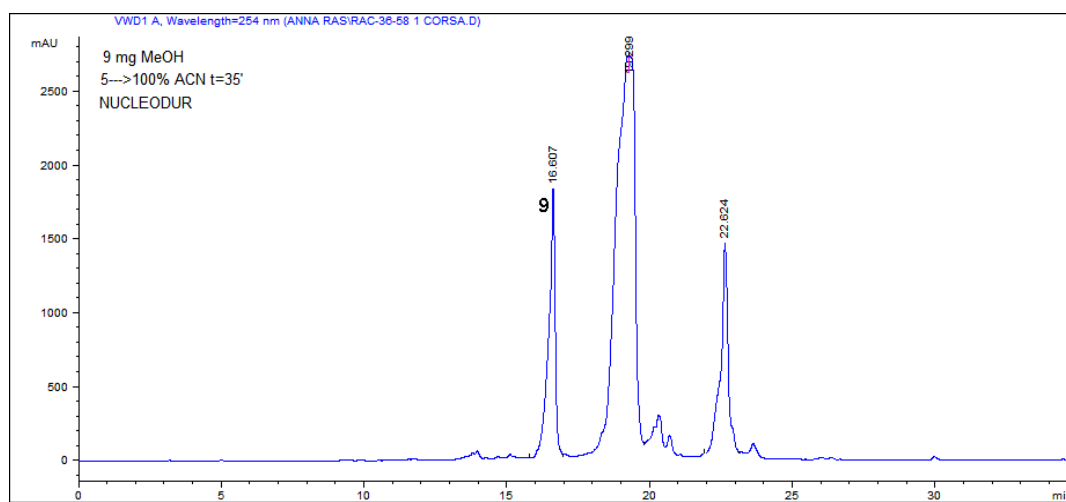


Figure III.11. RP-HPLC Separation chromatogram of fraction 1 with MeOH / H_2O (5% to 100%).

- **Study of fraction 3**

Fraction 3 (327 mg) was subjected to column chromatography on silica gel eluting with CHCl_3 / MeOH with an increasing polarity to yield 12 subfractions, subfraction 3 showed a major spot in TLC check, this spot was separated using a TLC chromatography with CHCl_3 / MeOH (95:05, v/v) elution system allowed the separation of **compound 4** (7.5 mg) (**Fig. III.12**).

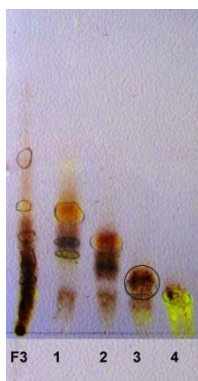


Figure III.12. TLC of subfraction 3 from fraction 3 eluted with (CHCl_3 / MeOH, 90:10, v/v) by treating with a $\text{Ce}(\text{SO}_4)_2$ / H_2SO_4 .

- **Study of fraction 5**

Fraction **5** (291 mg) was subjected to column chromatography on silica gel eluting with CHCl_3 / MeOH with an increasing polarity to yield 6 subfractions, a yellowish precipitate was observed in subfraction 2, a wash with a quantity of MeOH allowed the purification of **compound 5** (8.4 mg).

Subfraction 5 showed a major spot after TLC check, this spot was separated using TLC with CHCl_3 /MeOH, 95:05, v/v to isolate **compound 6** (10.1 mg).

- **Study of fraction 7**

Fraction **7** (459 mg) was subjected to Sephadex LH-20 column eluting with Methanol to yield 11 subfractions, subfraction 2 showed a major spot by TLC check. This spot was purified by subjecting to an analytic HPLC analysis on a reversed phase (RP) Nucleodur C18 column (250 mm x 4.6 mm, 5 μm particle diameter), using MeOH / H_2O (from 5 to 100%) at a flow rate of 1.0 ml/min and a detection at 254 nm to give **compound 10** (9.4 mg, $t_r = 19.2$ min) (**Fig. III.13**).

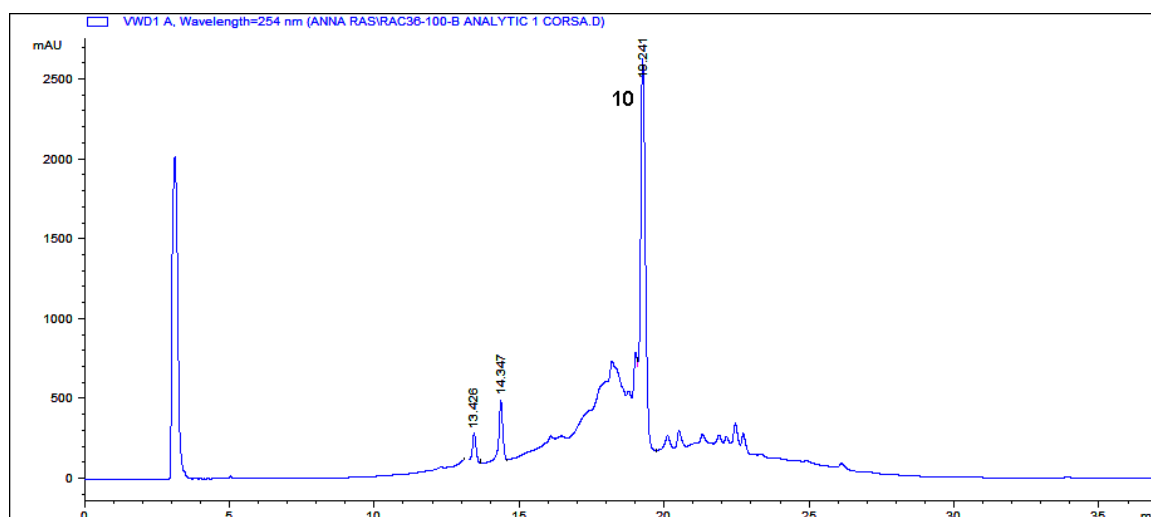


Figure III.13. RP-HPLC Separation chromatogram of fraction 7 with MeOH / H_2O (5% to 100%).

- **Study of fraction 8**

Fraction **8** (245 mg) was subjected to column chromatography on silica gel eluting with CHCl_3 / MeOH with an increasing polarity to yield 5 major subfractions, Chromatography of the subfraction 1 on preparative plates with CH_2Cl_2 / MeOH (90:10, v/v) allowed the isolation of the pure **compound 7** (10.5 mg).

III.2. General experimental procedures

NMR experiments were performed on: (1) Bruker DRX-600 spectrometer (Bruker BioSpin, Rheinstetten, Germany) equipped with a Bruker 5 mm TCI CryoProbe at 300 K. 2D NMR spectra were acquired in CDCl_3 and CDOD_3 in the phase-sensitive mode with the transmitter set at the solvent resonance and time proportional phase increment (TPPI) used to achieve frequency discrimination in the ω_1 dimension. The standard pulse sequence and phase cycling were used for DQF-COSY, HSQC and HMBC, (2) Bruker-Avance 400 spectrometer by using a 5 mm BBI probe ^1H at 400 MHz and ^{13}C at 100 MHz. **HRESI-MS** data were acquired on an LTQ Orbitrap XL mass spectrometer (Thermo Fisher Scientific, San Jose, CA, USA) operating in negative ion mode. **ESI-MS** mass spectra were taken by using a Bruker Esquire -LC spectrometer equipped with an electrospray ion source used in positive or negative ion mode by direct infusion of a methanolic solution of the sample, under the following conditions: source temperature 300 °C, drying gas N_2 , scan range 100-1000 m/z .

LC-MS profiles were performed on a Hewlett-Packard (Palo Alto, CA, USA) Model 1100 Series liquid chromatograph coupled to a Photo Diode Array detector (Agilent, Palo Alto, CA, USA) 1100 Series, and to an Esquire LC-ion trap mass spectrometer (BrukerDaltonics, Billerica, MA, USA) equipped with an electrospray ionisation (ESI) interface. The Photo Diode Array detector was set at 200-700 nm and the UV-channel at 215, 254, 300, 330 nm. The system was A= H_2O , B=Acetonitrile, with gradient: A=20%, B=80% during 30 min of analysis, then 100% of (B), the split of the column effluent was used to achieve a flow rate of 1 ml / min into the mass spectrometer. The LC-MS was run on a phenomenex Luna C18 (250 mm x 4.6 mm i.d.; 5 μm particle diameter, end-capped). High-purity nitrogen was used as the nebulizer, also as the drying gas at 300 °C at a constant flow rate of 6 l/min. Full scan spectra were acquired in negative ion mode in the region m/z 100-1000, adopting the following parameters: trap drive units, 55.1; capillary exit voltage, -113.0 V; skimmer 1 voltage, -38.3 V. MS/MS fragmentation experiments were performed on the selected precursor ion. Data Analysis (Version 3.0, BrukerDaltonik GmbH) was used to analyze the mass spectra. **FT-IR** (Fourier-transform Infrared) spectra analysis were recorded by using a FT-IR Bruker Tensor 27/37 spectrometers equipped with Attenuated Transmitter Reflection (ATR) device at 4 cm^{-1} resolution in the absorption region $\Delta\nu$ 4000 – 1000 cm^{-1} . Optical rotations were determined with an Autopol IV instrument. **Column Chromatography (CC)** separations were performed over silica gel (63-200 μm , Merck, Darmstadt, Germany). **TLC** was performed on pre-coated Kieselgel 60 F₂₅₄ plates, (0.2 mm, Merck, Darmstadt, Germany), the spots were detected by treating with a $\text{Ce}(\text{SO}_4)_2 / \text{H}_2\text{SO}_4$ (Sigma-Aldrich, Milano, Italy). **Preparative TLC** was carried out on Silica gel GF₂₅₄ (20×20 cm, 1 mm thickness). **HPLC** Merck Hitachi L-6200 equipped with a detector UVIDECE 100-V was performed using Phenomenex column Luna[®] RP-18 (5 μ , 250 mm, 4.60 mm). **UV Spectra** were recorded using a Shimadzu model UV -1700 spectrophotometer. **Optical rotations** were determined with an Autopol IV instrument.

REFERENCES

- [1] Dewanto, V., Wu, X., Adom, K. K., Liu, R. H., *J. Agric. Food Chem.*, **2002**, *50*, 3010-3014.
- [2] Sun, B., Richardo Da Silvia, J. M. I., *J. Agric. Food Chem.*, **1998**, *46*, 4267-4274.

CHAPTER IV

RESULTS & DISCUSSIONS

IV.1. Determination of Total Phenolic Content (TPC)

The Folin-Ciocalteu method is a rapid and widely used assay to determine Total Phenolic Content (TPC) [1]. This method is based on the reducing power of phenolic hydroxyl groups, but it's known that different phenolic compounds have different responses to the Folin-Ciocalteu reagent. The TPC in each extract was spectrophotometrically determined by reading the absorbance at 760 nm.

Table IV.1. Total Phenol Contents (TPC) (expressed as mg Gallic Acid Equivalents/g of Dry Weight) of *A. tenuifolius* extracts. * Values expressed as the means \pm SD.

Extracts	mg GAE/g DW
Chloroform	40,99 \pm 0.41*
Ethyl Acetate	24,04 \pm 0.55*
Butanol	10,54 \pm 0.20*

The total phenol contents (TPC) of the various extracts of *A. tenuifolius* are shown in **Table IV.1**. It was ranging from 10.54 to 40.99 mg GAE/g of DW, The maximum phenolic content was found in Chloroform extract (40.99 \pm 0.41 mg GAE/g of DW) followed by the Ethyl Acetate extract (24.04 \pm 0.55 mg GAE/g of DW) and then Butanol extract (10.54 \pm 0.20 mg GAE.g⁻¹ of DW) which contain considerably the smallest concentration of phenols (**Fig IV.1**).

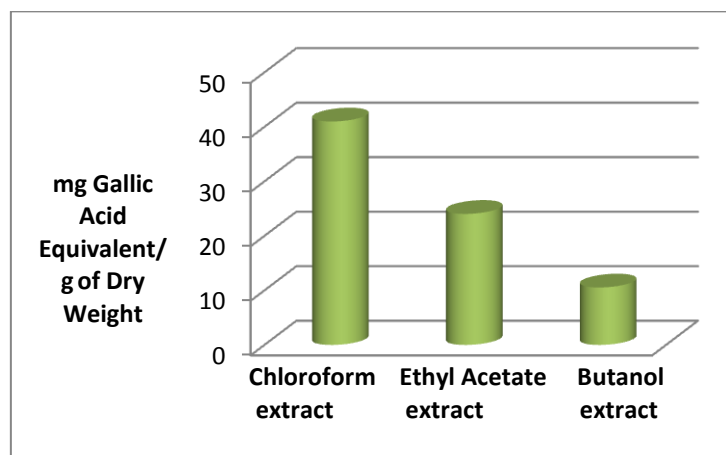


Figure IV.1. Total Phenol Content (TPC) of *A. tenuifolius* extracts (expressed as mg GAE/g of DW)

The high contents of phenolic compounds indicated that these compounds might contribute to an antioxidant activity. This result or conclusion will be confirm later in the next studies of the antioxidant evaluation assays on the different extracts.

IV.2. Determination of Total Flavonoids Content (TFC)

The concentration of flavonoids in various extracts of the *A. tenuifolius* was determined using spectrophotometric method with Aluminum Chloride (AlCl_3). The content of flavonoids was expressed in terms of Catechin Equivalent (CE/g) of Dry Weight (DW) of each extract (**Table IV.2.**). Total flavonoids content in plant extracts ranged from 62.85 to 213.07 mg CE/g of DW. Chloroform and Butanol extracts contained the highest flavonoid concentration (**Fig. IV.2**). The concentration of flavonoids in Chloroform extract was 213.07 ± 1.72 mg CE/g, which was very close to the value of Butanol extract concentration. The lowest flavonoid concentration was measured in Ethyl Acetate extract (62.85 ± 1.33).

Table IV.2. Total Flavonoids Contents (TFC) (expressed as mg Catechin Equivalents/g of Dry Weight) of *A. tenuifolius* extracts. * Values expressed as the means \pm SD.

Extracts	mg CE/g DW
Chloroform	$213,07 \pm 1.72^*$
Ethyl Acetate	$62,85 \pm 1.33^*$
Butanol	$202,89 \pm 6.15^*$

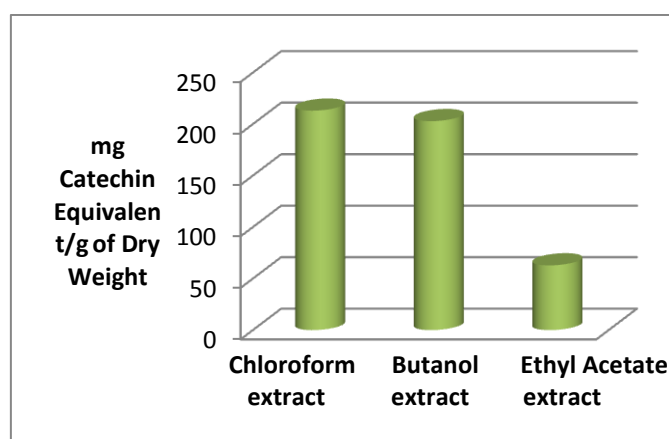


Figure IV.2. Total Flavonoids Content (TFC) of *A. tenuifolius* extracts (expressed as mg CE/g of DW)

IV.3. Determination of Total Tannin Content (TTC)

The tannins contents were examined in *A. tenuifolius* various extracts using the vanillin reagent is expressed in terms of catechin equivalent. The values obtained for the concentration of tannin contents are expressed as mg of CE/g of DW (**Table IV.3**).

Table IV.3. Total Tannins Contents (TTC) (expressed as mg Catechin Equivalents/g Dry Weight) of *A. tenuifolius*. * Values expressed as the means \pm SD.

Extracts	mg CE/g DW
Chloroform	11,13 \pm 0.25*
Ethyl Acetate	19,80 \pm 1.32*
Butanol	15,13 \pm 1.04*

The highest concentration of tannins was measured in ethyl acetate extract (19.80 mg CE/g) and the lowest was measured in Chloroform extract (11.13 mg CE/g). (**Fig IV.3.**). The Butanol extract gave a concentration about 15.13 mg CE/g.

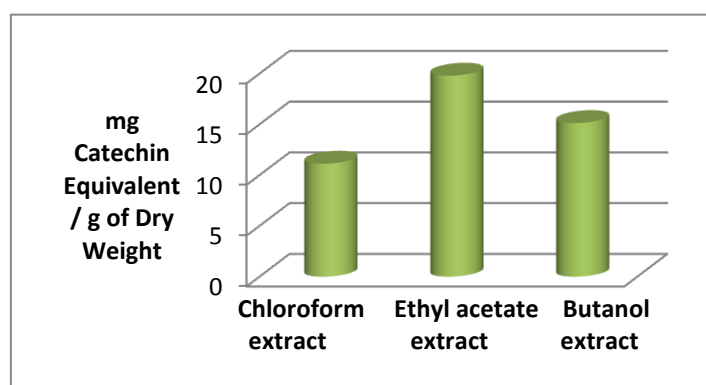


Figure IV.3. Total condensed Tannin Content (TTC) of *A. tenuifolius* (expressed as mg CE/g of DW)

IV.4. LC-MS Analysis

IV.4.1. LC-MS analysis of Chloroform extract

The LC-MS chromatogram in negative mode of Chloroform extract of *A. tenuifolius* was shown in (**Fig. IV.4**) and mass spectrums of the detected compounds were shown in (**Fig. IV.5**). It was observed that the different peaks were obtained at different retention times. In this the highest peaks are at the retention time of 37.6 min followed by 39.0 min belonging to two majority compounds.

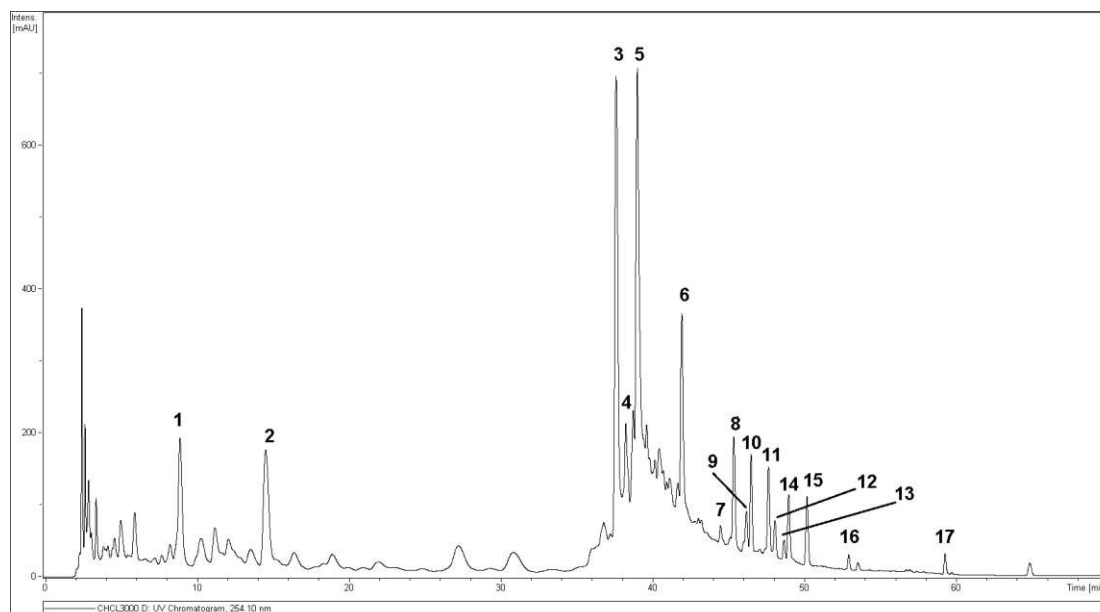


Figure IV.4. LC-MC profile in negative mode of Chloroform extract of *A. tenuifolius*

This liquid chromatographic method has been developed for the determination of these compounds. The simultaneous analysis of different classes of polyphenols was performed by a single column pass and the separation of all examined compounds was carried out in 60 min.

With the standard reference graphs, the compounds are elucidated using the molecular weight (MW).

The analysis of Chloroform extract by LC-MS (**Table IV.4**) allowed us the identification of several phenolic compounds that are already recognized by their abundance in the *Asphodelus* genus. In agreement with the literature, the phenolic compounds identified in this extract using the ESI-MS ion peaks $[M-H]^-$ were: Apigenin ($m/z = 269.0$) [2], Luteolin ($m/z = 285.0$) [3-4], Ramosin ($m/z = 671.0$) [5], Asphodeline ($m/z = 505.0$) [6-7], Tamgermantin ($m/z = 312.2$) [8-9]. However some compounds are still unidentified (peaks: **1**, **2**, **4**, **11**, **12**, **15** and **16**) and other will be identify later in this chapter (peaks: **9**, **10**, **13** and **14**).

The Mass spectrums of all LC-MS detected compounds of Chloroform extract at different retention times were representing in (**Fig. IV.5**), each peak gave their m/z , fragment ions and Retention Time.

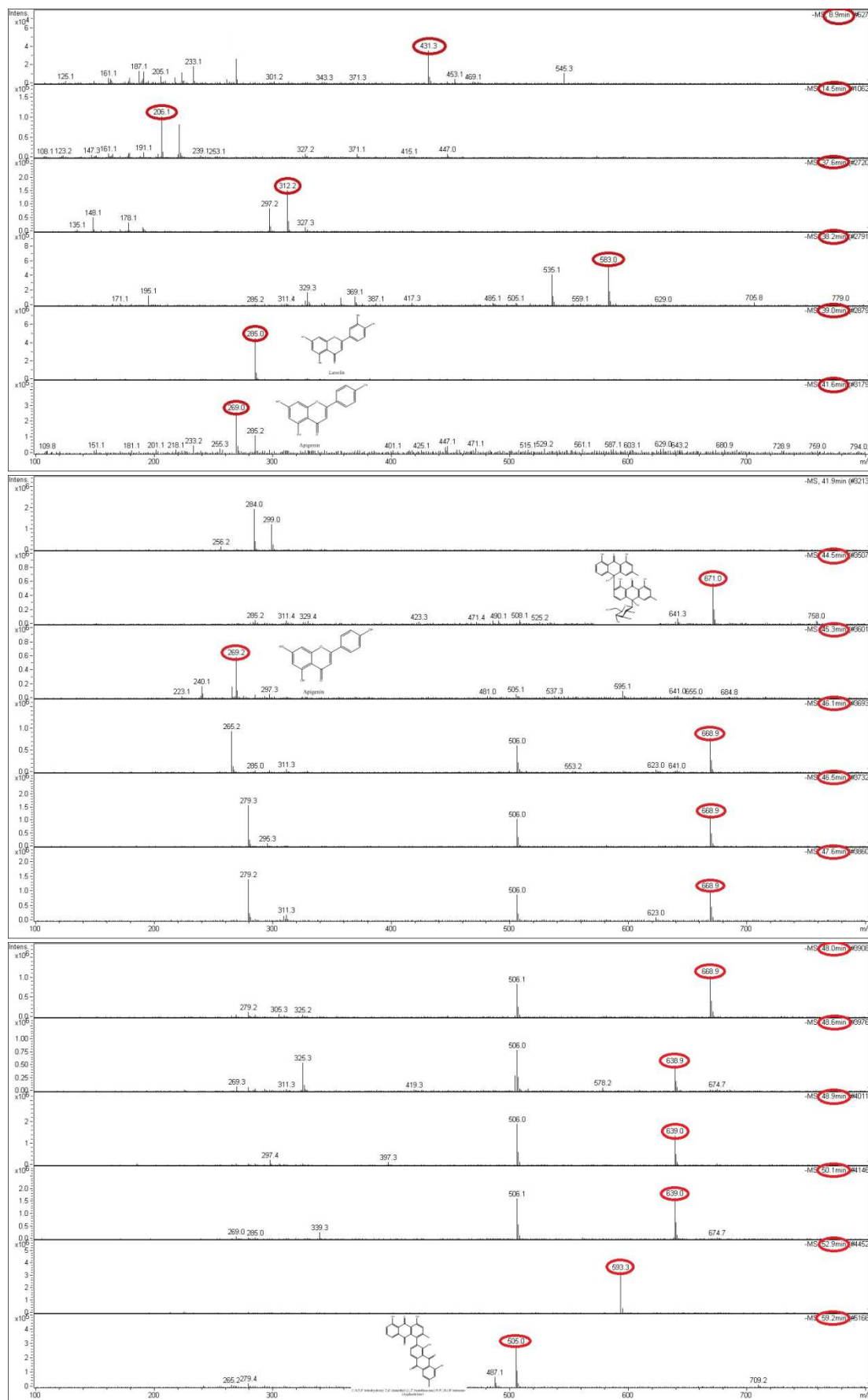


Figure IV.5. Mass spectrometry in negative mode of LC-MS detected compounds of Chloroform extract at different retention times.

Table IV.4. Bioactive compounds detected and identified by LC-MS of Chloroform extract of *A. tenuifolius*. (NI: Not Identified)

Peaks	Retention Time (min)	m/z [M-H] ⁻	Fragment Ions (m/z)	Molecular formula	Compound identification	Isolated compounds
1	8.9	431.3	269.0	NI	NI	-
2	14.5	206.1	-	NI	NI	-
3	37.6	312.2	297.2-178.1-148.1	C ₁₈ H ₁₉ O ₄ N	Tamgermanetin	2
4	38.2	583.0	535.1	NI	NI	-
5	39.0	285.0	151.1	C ₁₅ H ₁₀ O ₆	Luteolin	4
6	41.6	269.0	-	C ₁₅ H ₁₀ O ₅	Apigenin	8
7	44.5	671.0	-	C ₃₆ H ₃₂ O ₁₃	Ramosin	-
8	45.3	269.2	-	C ₁₅ H ₁₀ O ₅	Apigenin	8
9	46.1	668.9	506.0-265.2	C ₃₆ H ₃₂ O ₁₃	NI	11
10	46.5	668.9	506.0-279.3	C ₃₆ H ₃₂ O ₁₃	NI	12
11	47.6	668.9	506.0-279.2	C ₃₆ H ₃₂ O ₁₃	NI	16
12	48.0	668.9	506.1-279.2	C ₃₆ H ₃₂ O ₁₃	NI	17
13	48.6	638.9	506.0-325.3	C ₃₅ H ₂₈ O ₁₂	NI	13
14	48.9	639.0	506.0-297.4	C ₃₅ H ₂₈ O ₁₂	NI	14
15	50.1	639.0	506.1-339.3	C ₃₅ H ₂₈ O ₁₂	NI	15
16	52.9	593.3	225.1	NI	NI	-
17	59.2	505.0	487.1-279.4	C ₃₀ H ₁₈ O ₈	Asphodelin	3

IV.4.2. LC-MS analysis of Ethyl Acetate extract

The LC-MS chromatogram in negative mode of Ethyl Acetate extract of *A. tenuifolius* was performed with the same conditions used with the Chloroform extract, shown in (Fig. IV.6), Mass spectrums of the detected compounds were shown in (Fig. IV.7). It was observed that the different peaks were obtained at different retention times, In this the highest peak is at the retention time of 38.2 min belonging to an abundance compound.

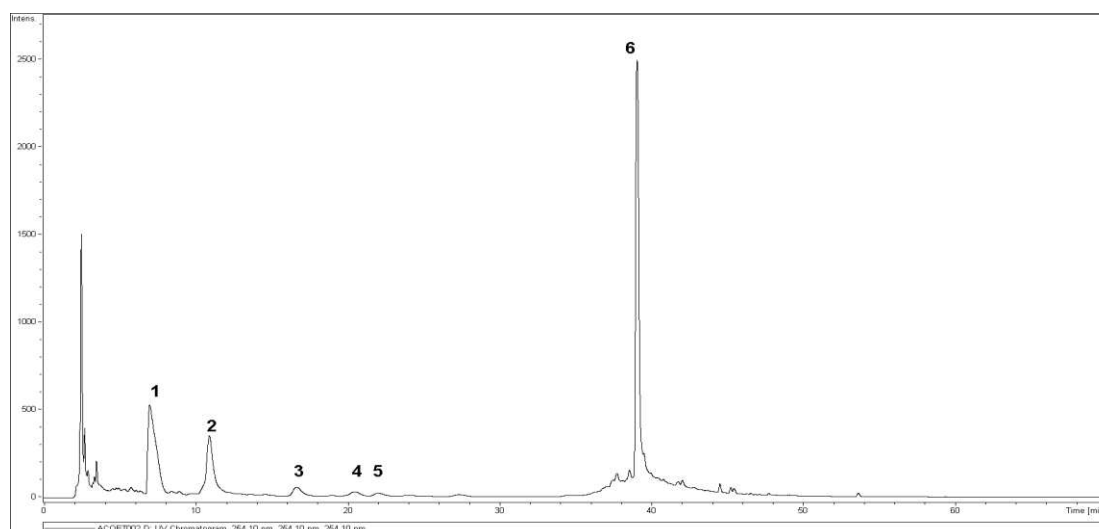


Figure IV.6. LC-MC profile in negative mode of Ethyl Acetate extract of *A. tenuifolius*.

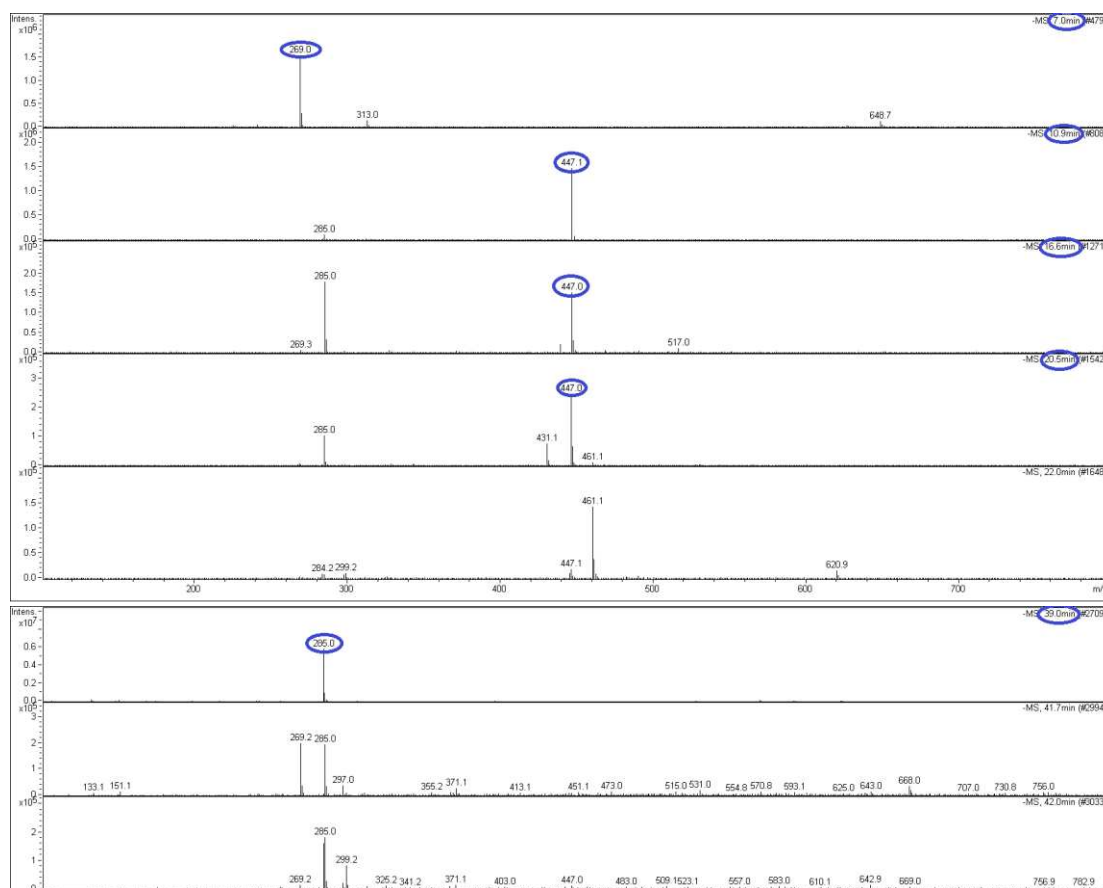


Figure IV.7. Mass spectrometry of LC-MS detected compounds of Ethyl Acetate extract at different retention times.

Table IV.5. Bioactive compounds detected and identified by LC-MS of Ethyl Acetate extract of *A. tenuifolius* (NI: Not Identified).

Peaks	Retention Time (min)	m/z [M-H]	Fragment Ions (m/z)	Molecular formula	Compound identification	Isolated compounds
1	7.0	269.0	241.2	C ₁₅ H ₁₀ O ₅	Apigenin	8
2	10.9	447.1	285.0	C ₂₁ H ₂₀ O ₁₁	Isoorientin	-
3	16.6	447.0	371.1-327.3-285.0	NI	NI	5
4	20.5	447.0	431.1-329.0-285.0	NI	NI	-
5	22.0	461.1	299.2	NI	NI	-
6	39.0	285.0	133.1	C ₁₅ H ₁₀ O ₆	Luteolin	4

The analysis of Ethyl Acetate extract by LC-MS (**Table IV.5**) allowed us the identification of phenolic compounds that are already - like Chloroform extract- recognized by their abundance in the *Asphodelus* genus. In agreement with the literature, the phenolic compounds identified in this extract were: Apigenin ($m/z = 269.0$) [2], Luteolin ($m/z = 285.0$) [4], Isoorientin ($m/z = 447.1$) [10], however some compounds are still unidentified (peaks: **4** and **5**) and one other will be identify later in this chapter (peak **3**).

IV.5. Identification of the isolated compounds from *A. tenuifolius*

IV.5.1. Identification of compound 1

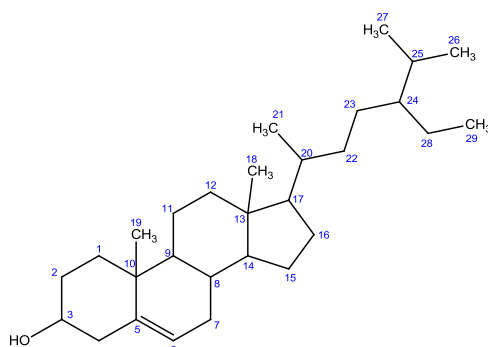


Figure IV.8. Structure of **compound 1**

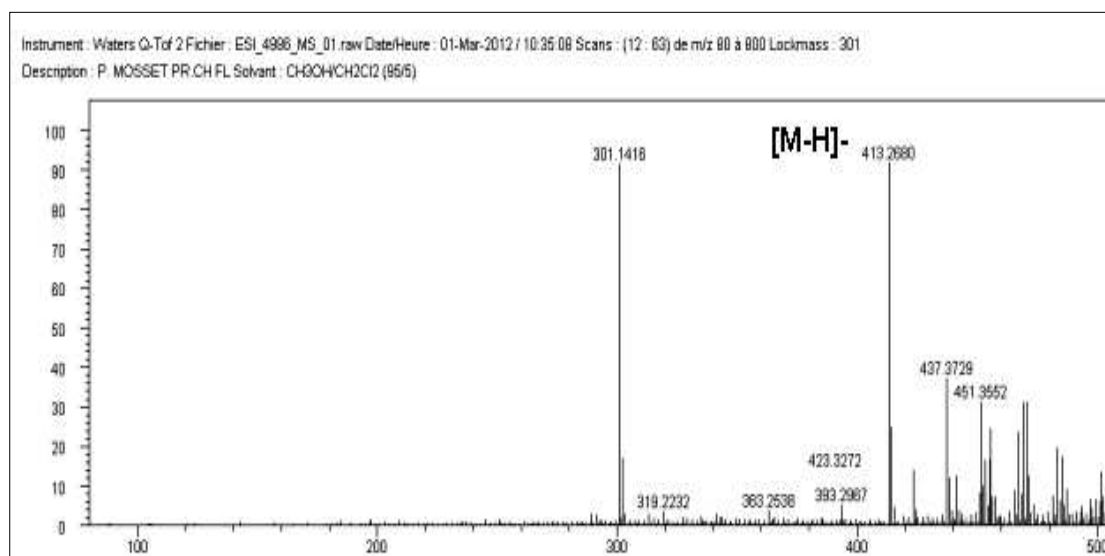


Figure IV.9. HRESI-MS spectrum in negative ion mode of **compound 1**.

Compound 1 was isolated as a white crystalline powder. The High Resolution Mass spectrum (HRESI-MS) of this compound was carried out on negative mode (**Fig. IV.9**) which presented an ion quasi-molecular at $m/z = 413.2690$ $[M-H]^-$ (calculated for $C_{29}H_{49}O$: 413.3783) which suggest a molecular mass equal to 414 amu corresponding to the molecular formula $C_{29}H_{50}O$ with 5 unsaturations.

The signals in the 1H -NMR spectrum (**Fig. IV.10**) were observed mainly in the upfield region (between δ_H 0.74 and δ_H 5.33 ppm). The spectrum exhibited only two signals with high chemical shifts values (**Fig. IV.12**); the first one resonated in the olefinic region and the other one was observed a little upfield region. The olefinic signal at δ_H 5.33 ppm (1H, *d*, $J=5.2$ Hz) appeared to be characteristic of the sterols, and it was assigned to H-6 proton in the proposed β -Sitosterol skeleton.

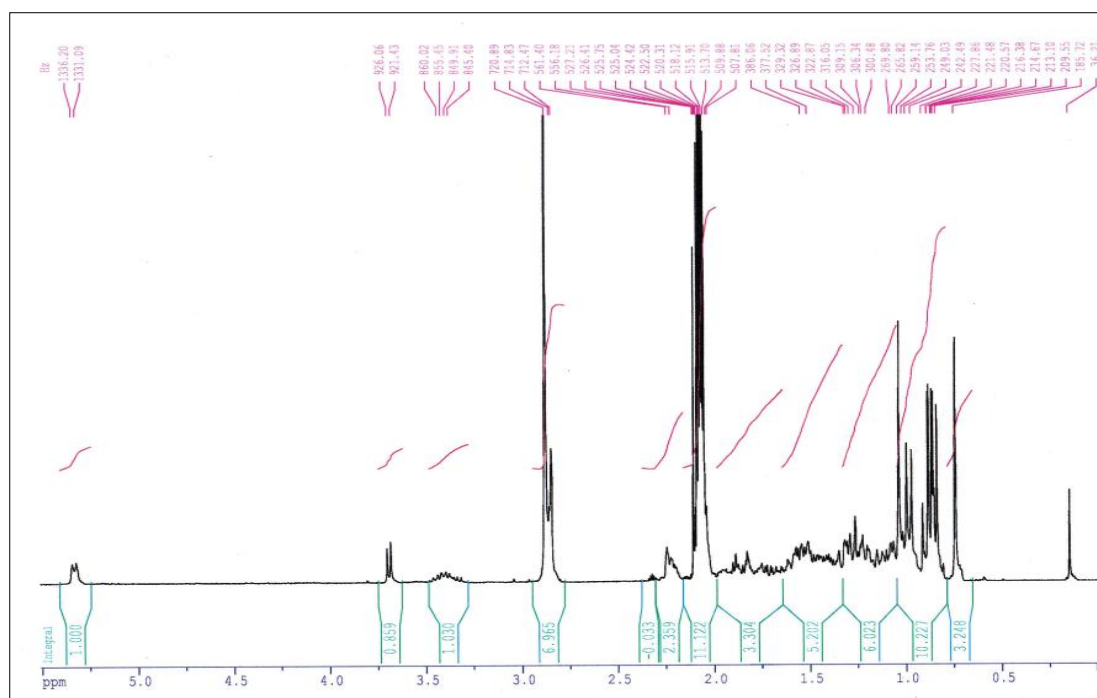


Figure IV.10. $^1\text{H-NMR}$ Spectrum (250 MHz, CD_3COCD_3) of compound **1**.

The $^1\text{H-NMR}$ spectrum of this compound exhibited also a signal corresponding to the proton connected to C-3 hydroxyl group which appeared as a multiplet at δ_{H} 3.38 ppm (1H, *m*). Six other protons with high intensity peaks were evident which include four secondary methyl groups (δ_{H} 0.98, 0.89, 0.87 and 0.85 ppm all doublets with $J = 6.6, 7.3, 6.2$ and 6.2 Hz, respectively) could be at C-21, C-29, C-26 and C-27, respectively, and two tertiary methyl groups could be at C-18 and C-19 (δ_{H} 0.74 ppm and 1.03 ppm, respectively) (**Fig. IV.11**).

The $^{13}\text{C-NMR}$ spectrum (**Fig. IV.13**) exhibited 29 carbon signals, including an oxymethine carbon signal at δ_{C} 70.7 ppm and two olefinic carbons at δ_{C} 141.4 and δ_{C} 120.6 ppm for (C5=C6) double bond, respectively. Two methylene carbon signals were present at δ_{C} 45.7 and δ_{C} 24.0 ppm for C-22 and C-23, δ_{C} 70.7 ppm for C-3 β -hydroxyl group, δ_{C} 18.8 ppm and 36.0 ppm for angular methyl carbon atoms for C-19 and C-18, respectively (**Table IV.1**).

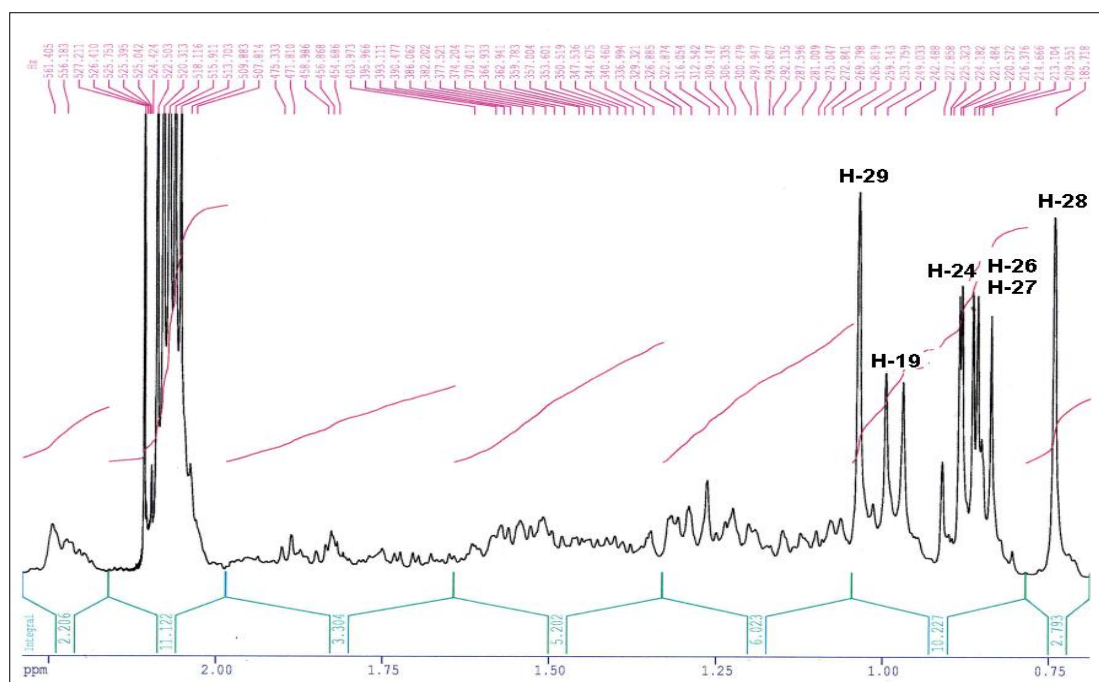


Figure IV.11. $^1\text{H-NMR}$ Spectrum (250 MHz, CD_3COCD_3) of compound **1**.
(From 0.50 ppm to 2.50 ppm)

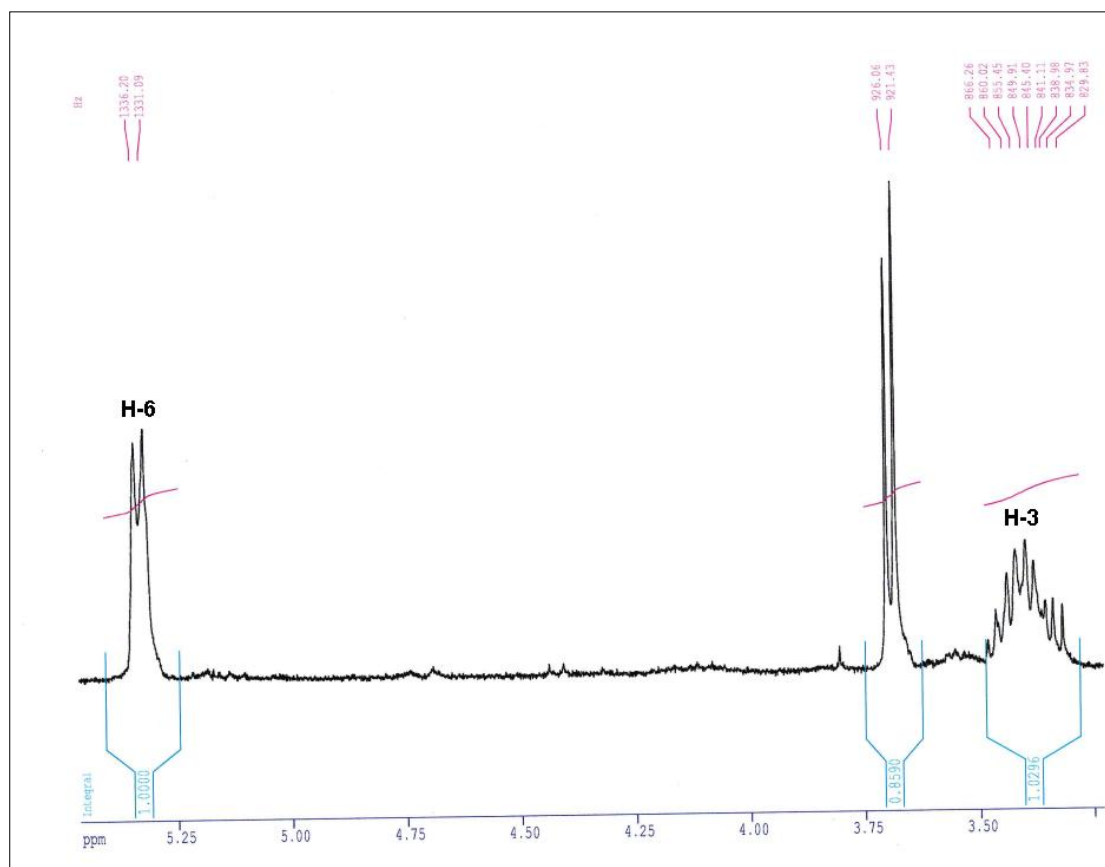


Figure IV.12. $^1\text{H-NMR}$ Spectrum (250 MHz, CD_3COCD_3) of compound **1**.
(From 3.00 ppm to 5.50 ppm)

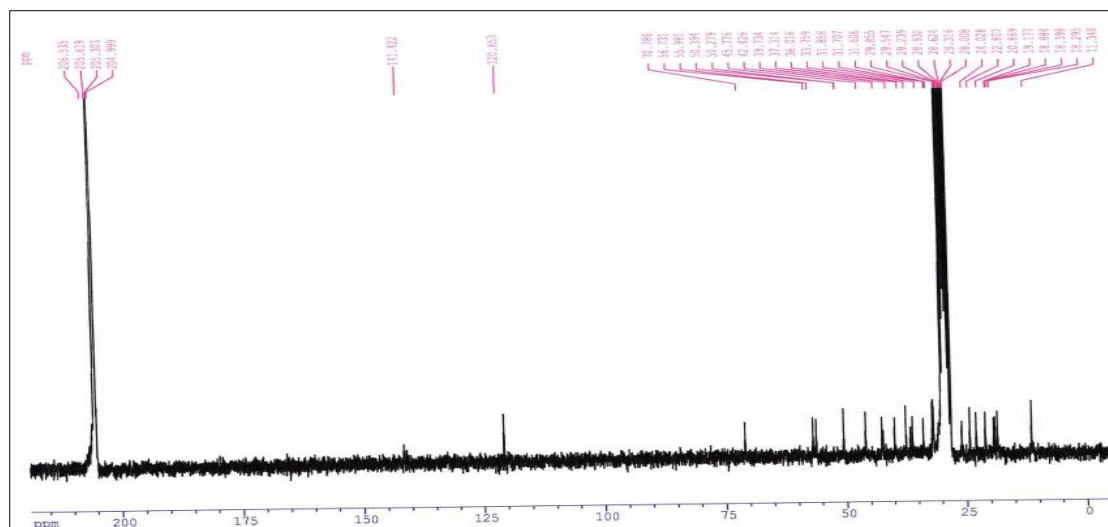


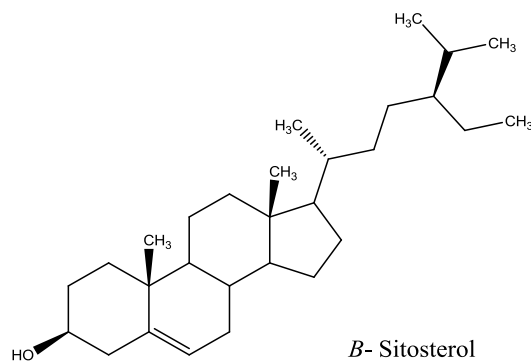
Figure IV.13. ^{13}C -NMR Spectrum (250 MHz, CD_3COCD_3) of compound **1**.

All the chemical shifts of the NMR analysis (^1H and ^{13}C) of compound **1** are summarized in the following table (**Table IV.6**).

Table IV.6. ^1H and ^{13}C -NMR data (250 MHz) of compound **1** (CD_3COCD_3).

Positions	δ_{C} (ppm)	δ_{H} (ppm), <i>mult.</i> , <i>J</i> (Hz)
1	37.3	-
2	31.6	-
3	70.7	3.38 (<i>m</i> , 1H)
4	42.1	-
5	141.4	-
6	120.6	5.33 (<i>d</i> , 1H, <i>J</i> =5.2 Hz)
7	31.8	-
8	31.8	-
9	50.2	-
10	36.3	-
11	22.8	-
12	39.7	-
13	42.7	-
14	56.7	-
15	26.3	-
16	28.5	-
17	55.9	-
18	36.0	0.74 (<i>s</i> , 3H)
19	18.8	1.03 (<i>s</i> , 3H)
20	33.7	-
21	25.7	0.98 (<i>d</i> , 3H, <i>J</i> =6.6 Hz)
22	45.7	-
23	24.0	-
24	18.2	-
25	31.7	-
26	20.8	0.87 (<i>d</i> , 3H, <i>J</i> =6.2 Hz)
27	19.1	0.85 (<i>d</i> , 3H, <i>J</i> =6.2 Hz)
28	18.3	-
29	11.3	0.89 (<i>t</i> , 3H, <i>J</i> =7.3 Hz)

These data were in agreement with the structure of **β -Sitosterol**. The NMR data of this compound **1** (**Table IV.1**) are in close agreement with the published values in literature [11-12-13], as well as it was isolated and reported previously in the *Asphodelus* genus [14].



IV.5.2. Identification of compound 2

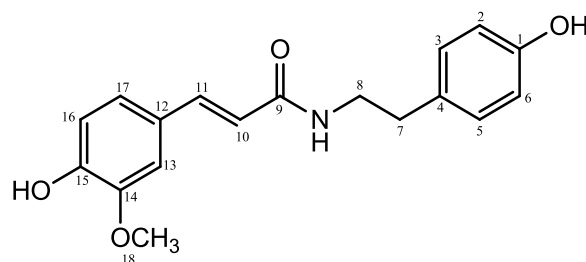


Figure IV.14. Structure of **compound 2**.

Compound 2 gave an ESI-MS ion peaks at $m/z = 312.1$ (**Fig. IV.16**) and $m/z = 336.2$ (**Fig. IV.15**) attributable to pseudo molecular cations $[M-H]^-$ and $[M+Na]^+$, respectively, indicate the possibility to have an Azote atom in the structure. These pseudo molecular cations $[M-H]^-$ and $[M+Na]^+$ are in agreement with a molecular formula of $C_{18}H_{19}O_4N$ [3] with 10 unsaturations.

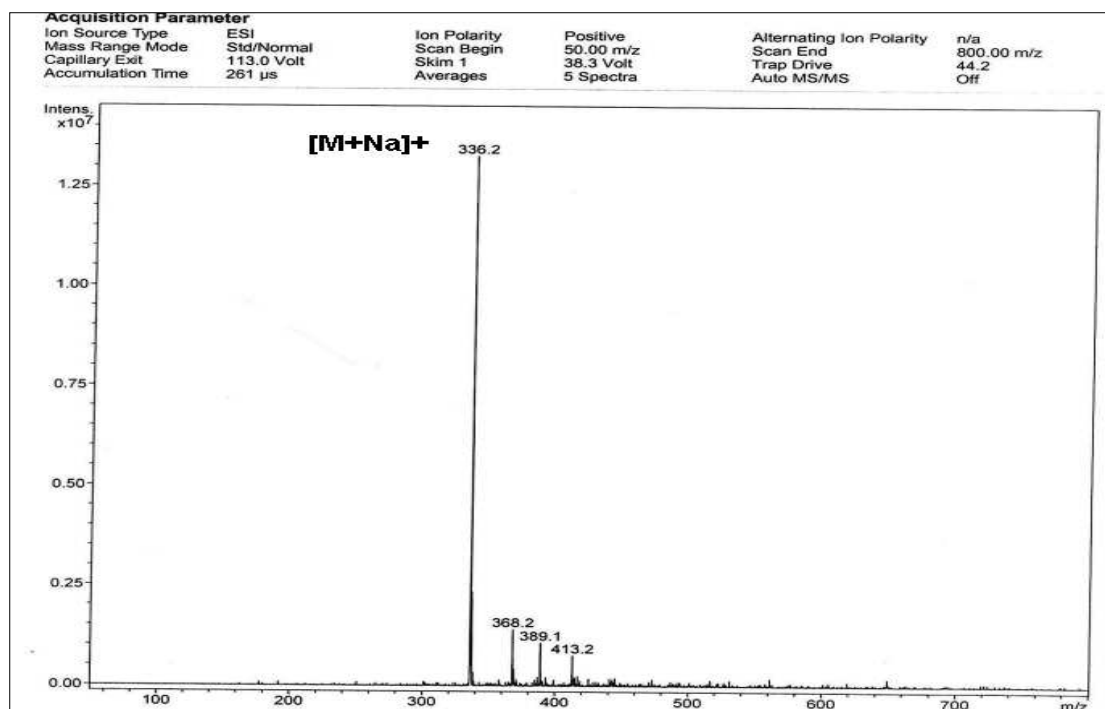


Figure IV.15. ESI-MS in positive ion mode of compound 2.

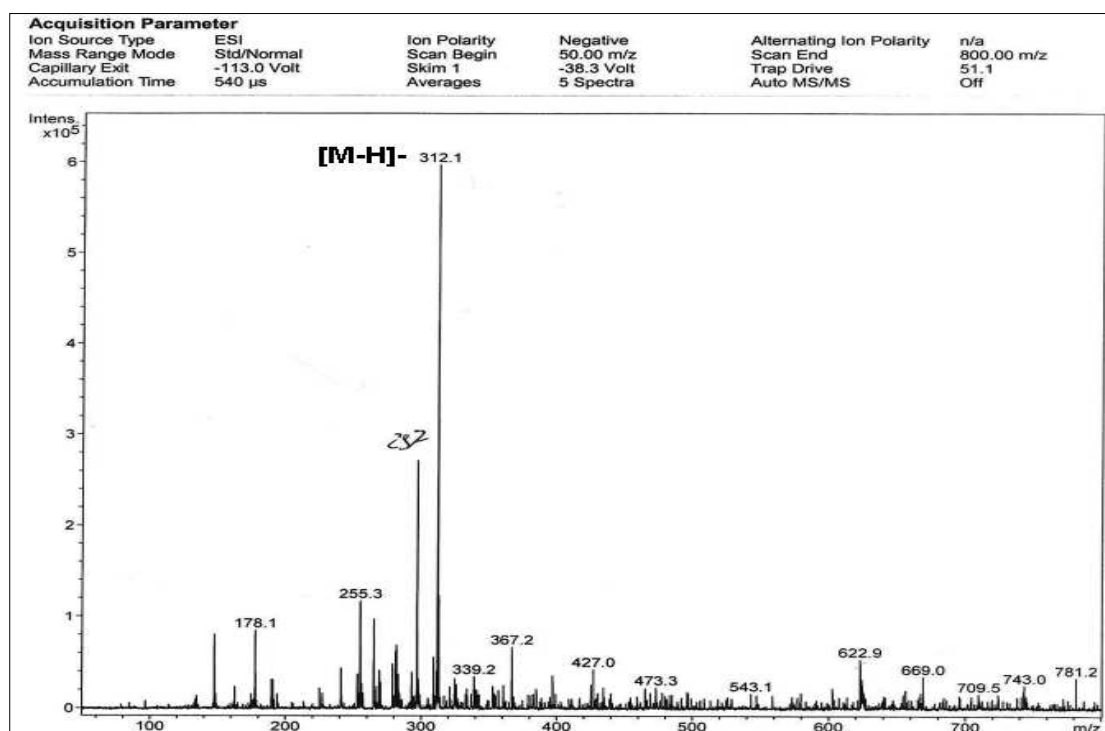


Figure IV.16. ESI-MS spectrum in negative ion mode of compound 2.

The $^1\text{H-NMR}$ spectrum of compound 2 (Fig. IV.18 and Fig. IV.20) showed two triplets at δ_{H} 2.72 ppm (2H, *t*, $J=7.3$ Hz) and δ_{H} 3.46 ppm (2H, *t*, $J=7.5$ Hz) assignable to mutually coupled methylene groups at C-7 and C-8, respectively indicative of a

four hydroxyphenyl ethyl system. In addition, signals for four aromatic protons of a *para*-substituted ring at δ_{H} 6.72 ppm (2H, *d*, H-2 and H-6), δ_{H} 7.02 ppm (2H, *d*, H-3 and H-5) as well as three others at δ_{H} 6.80 ppm (1H, *d*, $J=8.1$ Hz, H-16), δ_{H} 7.00 ppm (1H, *d*, $J=8.2$ Hz, H-17) and δ_{H} 7.12 ppm (1H, *s*, H-13) assignable to protons of a tri-substituted aromatic ring (**Fig.IV.19**). The $^1\text{H-NMR}$ spectrum further showed typical signals of two olefinic protons of a *trans*-substituted double bond resonating at δ_{H} 7.42 (1H, *d*, $J=15.6$ Hz, H-11) and δ_{H} 6.47 ppm (1H, *d*, $J=15.6$ Hz, H-10). In addition, a methoxyl singlet was assigned at δ_{H} 3.83 ppm.

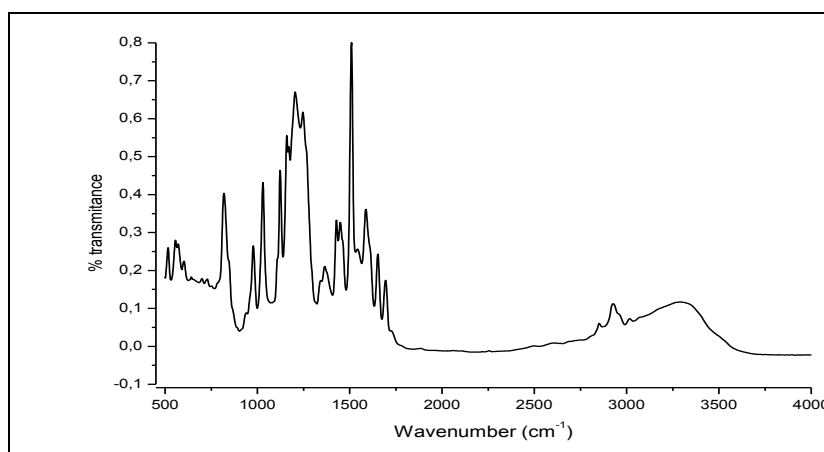


Figure IV.17. IR Spectrum of compound 2.

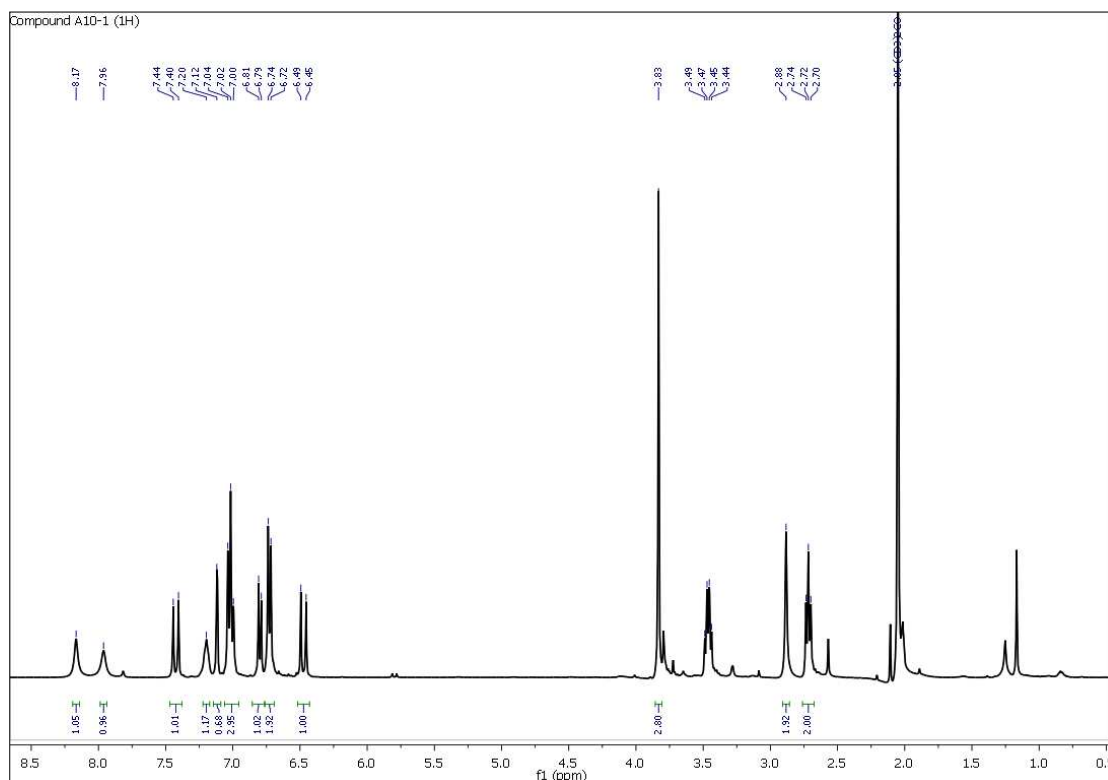


Figure IV.18. $^1\text{H-NMR}$ Spectrum (400 MHz, CD_3COCD_3) of compound 2.

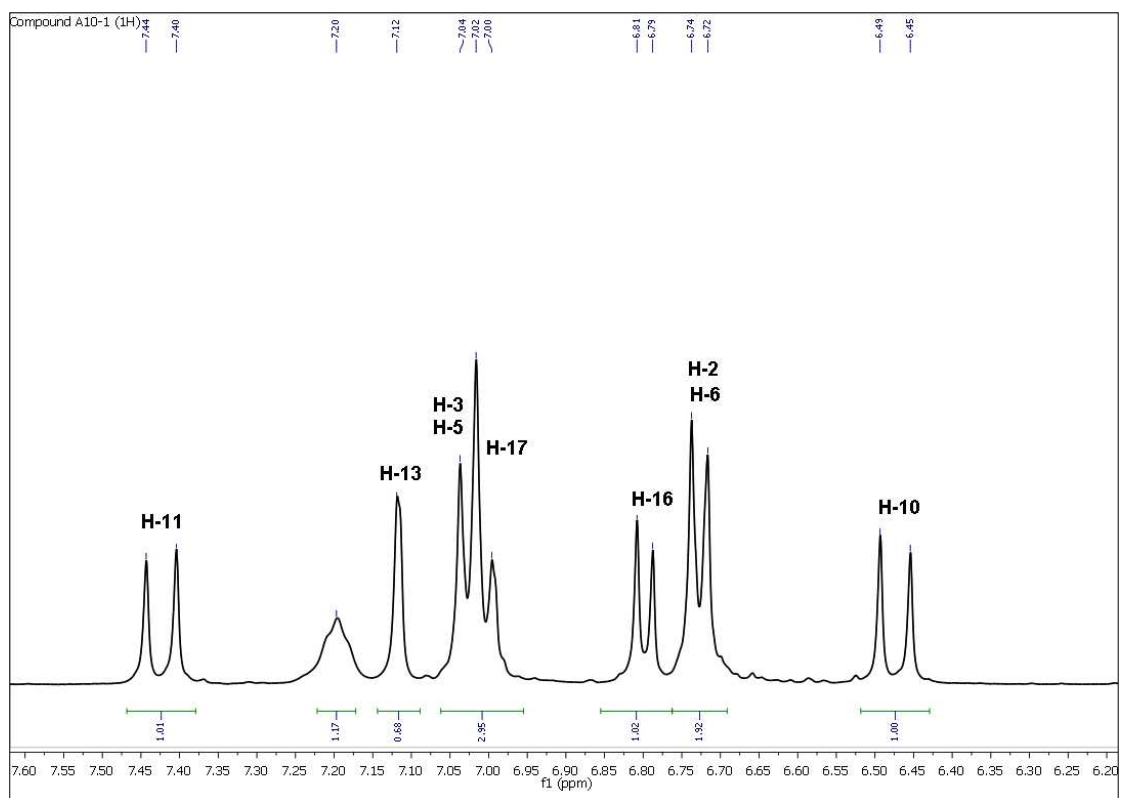


Figure IV.19. ^1H -NMR Spectrum (400 MHz, CD_3COCD_3) of compound **2**.
(From 6.20 ppm to 7.50 ppm).

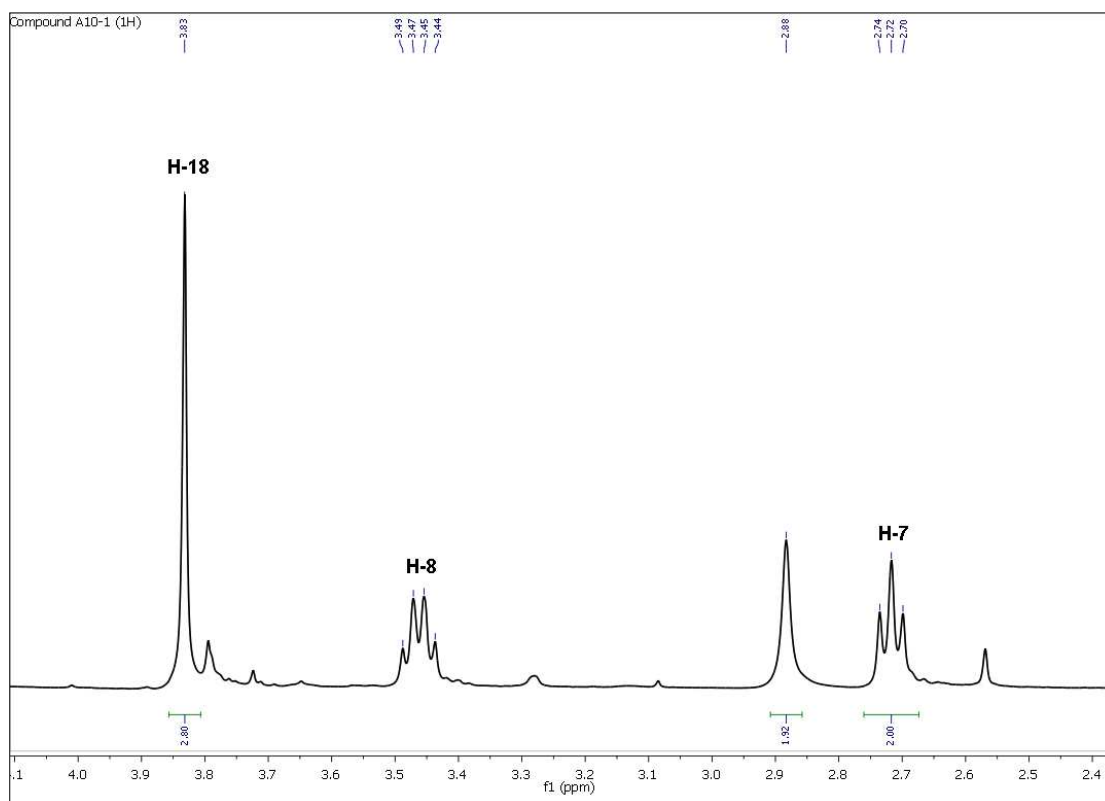


Figure IV.20. ^1H -NMR Spectrum (400 MHz, CD_3COCD_3) of compound **2**.
(From 2.40 ppm to 4.00 ppm).

The examination of the HSQC spectrum recorded in CD_3COCD_3 (**Fig. IV.21**, **Fig. IV.22** and **Fig. IV.23**) showed the presence of correlations identified as follow:

- ✓ The proton H-11 showed a correlation with the carbon C-11 at δ_{C} 139.4 ppm.
- ✓ The proton H-13 showed a correlation with the carbon C-13 at δ_{C} 110.2 ppm.
- ✓ The proton H-3 showed a correlation with the carbon C-3 at δ_{C} 129.4 ppm.
- ✓ The proton H-5 showed a correlation with the carbon C-5 at δ_{C} 115.5 ppm.
- ✓ The proton H-17 showed a correlation with the carbon C-17 at δ_{C} 121.7 ppm.
- ✓ The proton H-16 showed a correlation with the carbon C-16 at δ_{C} 115.0 ppm.
- ✓ The protons H-2 and H-6 showed a correlation with the carbon C-2/6 at δ_{C} 115.1 ppm.
- ✓ The proton H-10 showed a correlation with the carbon C-10 at δ_{C} 119.9 ppm.
- ✓ The methyl protons CH_3 -18 showed a correlation with the carbon C-18 at δ_{C} 55.1 ppm.
- ✓ The methylene protons H-8 showed a correlation with the carbon C-8 at δ_{C} 40.7 ppm.
- ✓ The methylene protons H-7 showed a correlation with the carbon C-7 at δ_{C} 34.4 ppm.

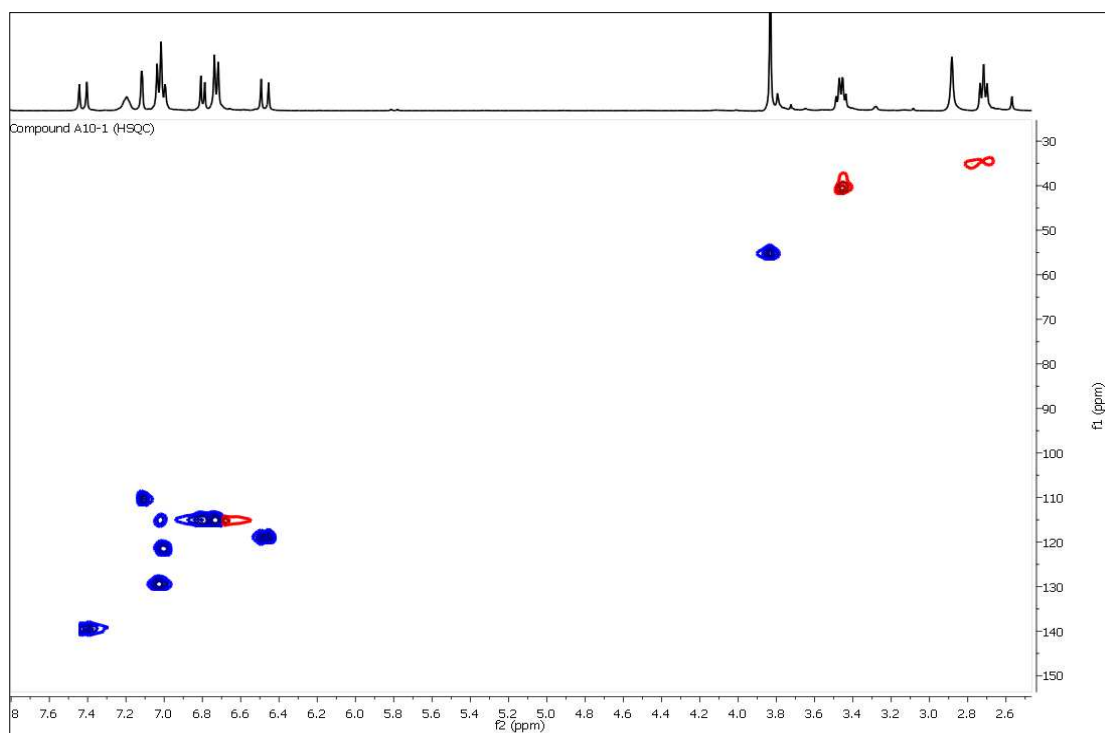


Figure IV.21. HSQC-NMR Spectrum (400 MHz, CD_3COCD_3) of compound **2**.

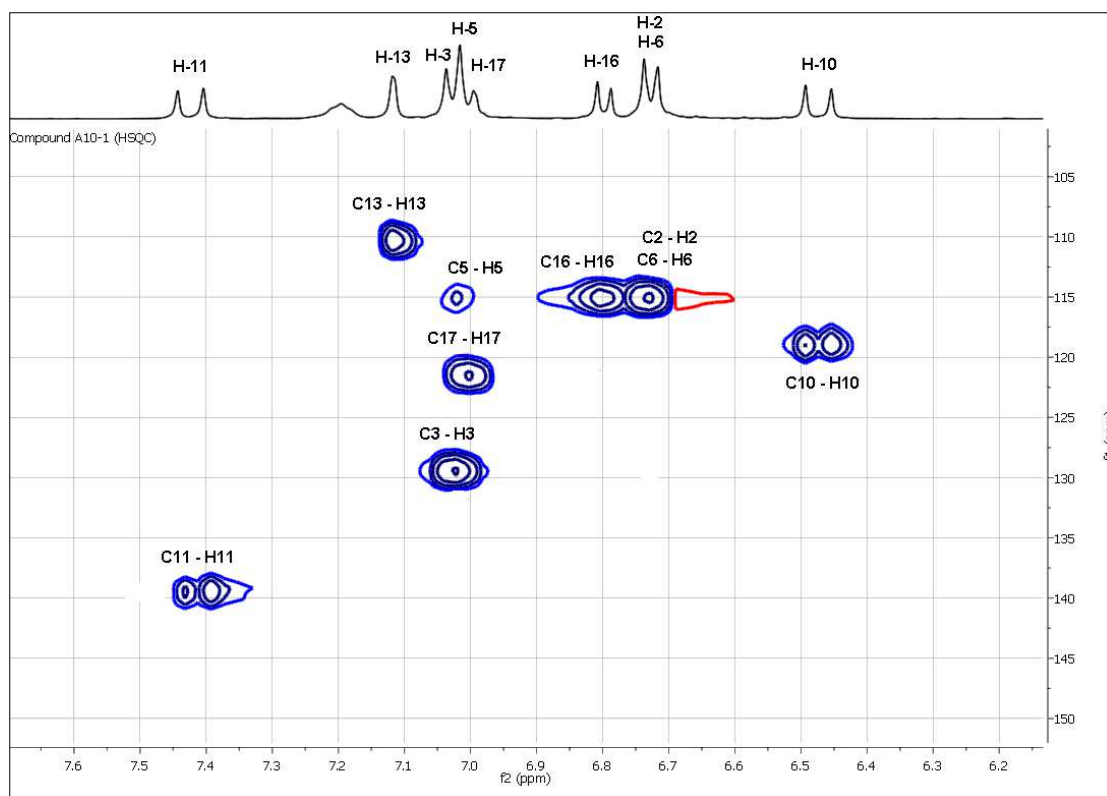


Figure IV.22. HSQC-NMR Spectrum (400 MHz, CD_3COCD_3) of compound **2**.
(From 6.20 ppm to 7.60 ppm)

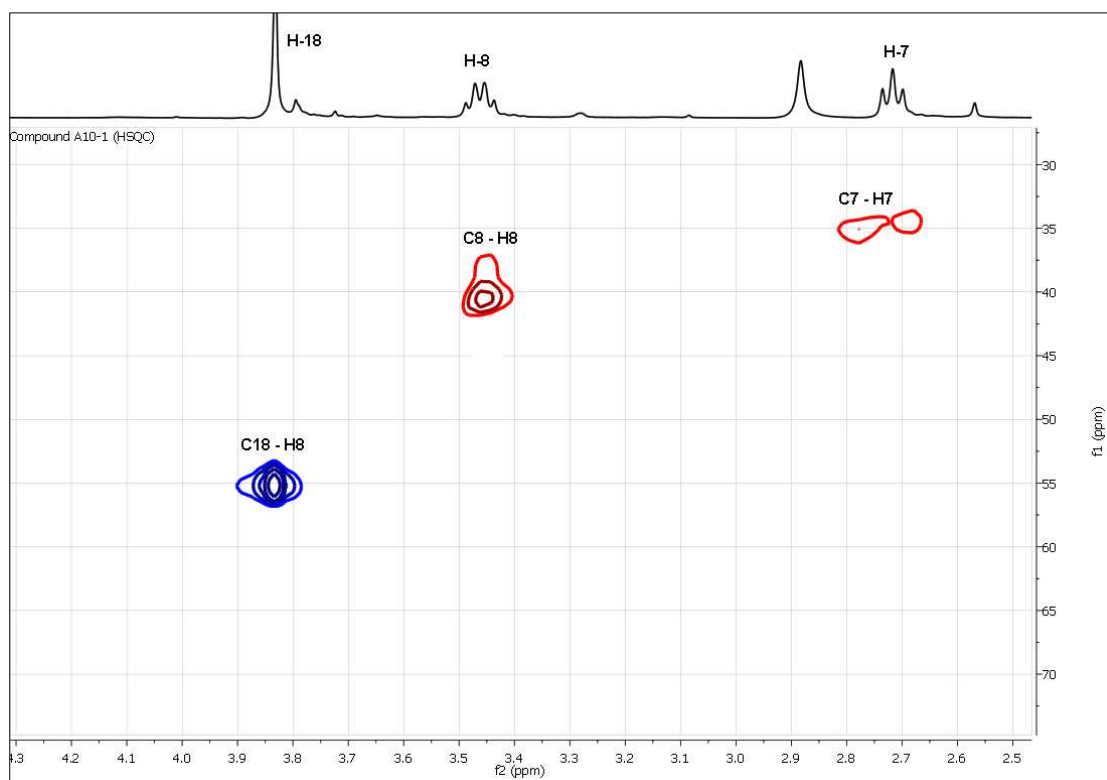


Figure IV.23. HSQC-NMR Spectrum (400 MHz, CD_3COCD_3) of compound **2**.
(From 2.50 ppm to 4.20 ppm).

Examination of the HMBC spectrum (**Fig. IV.24**) recorded in CD_3COCD_3 showed the presence of many correlations identified as follow:

- ✓ The H-11 proton showed five (5) correlations: The first with a carbon at δ_{C} 110.2 ppm, attributable to C-13, the second correlation with a carbon at δ_{C} 119.9 ppm attributable to C-10, the third correlation with carbon at δ_{C} 121.7 attributable to C-17, the fourth with carbon at δ_{C} 127.4 ppm attributable to C-12 and the last correlation with carbon of carbonyl function at δ_{C} 127.4 attributable to C-9.
- ✓ The H-13 proton showed three (3) correlations: The first with a carbon at δ_{C} 139.4 ppm, attributable to C-11, the second correlation with a carbon at δ_{C} 148.2 ppm attributable to C-15, the last correlation with carbon at δ_{C} 121.7 attributable to C-17.
- ✓ The H-3 proton showed three (3) correlations: The first with a carbon at δ_{C} 155.8 ppm, attributable to C-1, the second correlation with a carbon at δ_{C} 115.5 ppm attributable to C-5, and the last correlation with carbon of carbonyl function at δ_{C} 34.4 attributable to C-7.

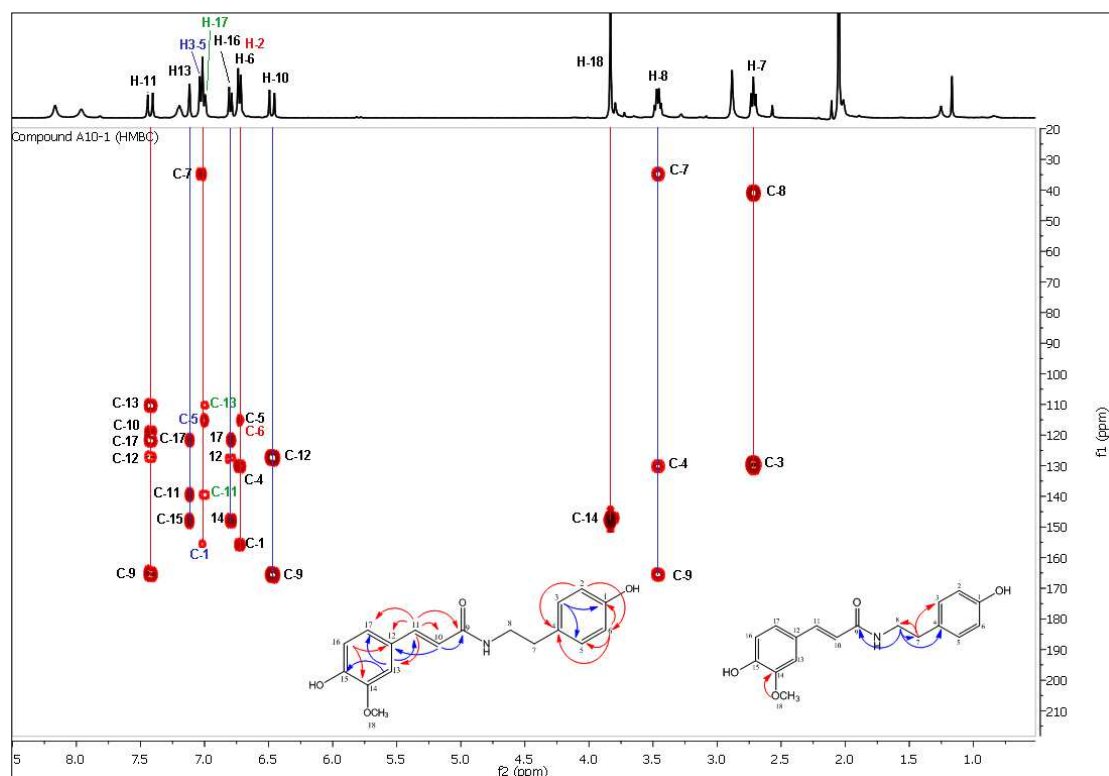


Figure IV.24. HMBC-NMR Spectrum (400 MHz, CD_3COCD_3) of compound **2**.

- ✓ The H-5 proton showed three (3) correlation: The first with a carbon at δ_{C} 155.8 ppm, attributable to C-1, the second correlation with a carbon at δ_{C} 129.4 ppm attributable to C-3, and the last correlation with carbon at δ_{C} 34.4 attributable to C-7.

- ✓ The H-17 proton showed two (2) correlations: The first with a carbon at δ_C 139.4 ppm, attributable to C-11 and the second correlation with a carbon at δ_C 110.2 ppm attributable to C-13.
- ✓ The H-16 proton showed three (3) correlations: The first with a carbon at δ_C 127.4 ppm, attributable to C-12, the second correlation with a carbon at δ_C 147.6 ppm attributable to C-14, and the last correlation with a carbon at δ_C 121.7 ppm attributable to C-17.
- ✓ The protons H-2 and H-6 showed the same correlations with a carbon at δ_C 155.8 ppm, attributable to C-1, and another correlation with a carbon at δ_C 130.2 ppm attributable to C-4, other correlation of the proton H-2 with a carbon at δ_C 115.1 ppm attributable to C-6 and other for the proton H-6 with a carbon at δ_C 115.5 attributable to C-5.
- ✓ The H-10 proton showed two (2) correlations: The first with a carbon at δ_C 165.4 ppm, attributable to the carbonyl carbon C-9, the second correlation with a carbon at δ_C 127.4 ppm attributable to C-12.
- ✓ The OCH₃-16 protons showed only one (1) possible correlation with with the carbon at δ_C 147.6 ppm, attributable to C-14, which confirm the point of attachment of the methoxyl group on C-14.
- ✓ The two protons of the methylene group at H-8 showed three (3) correlations: The first with a carbon at δ_C 34.4 ppm, attributable to the second methylene group C-7, the second correlation with a carbon at δ_C 130.2 ppm attributable to C-4 and a last one with the carbonyl function carbon at δ_C 165.4 ppm attributable to C-9.
- ✓ The other two protons of the methylene group at CH₂-7 showed two (2) correlations: The first with a carbon at δ_C 40.7 ppm, attributable to the other methylene group C-8, and a second correlation with the carbon at δ_C 129.4 ppm attributable to C-3.

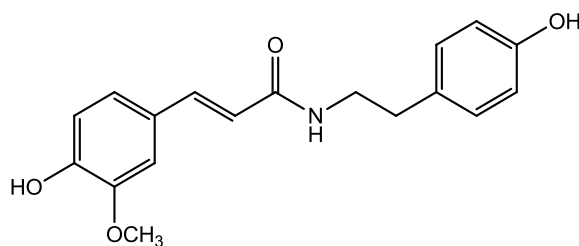
All the chemical shifts of the NMR analysis (¹H, ¹³C, HSQC and HMBC) of compound **2** are summarized in the following table (**Table IV.7**).

Table IV.7. ¹H, ¹³C and HMBC-NMR data (400 MHz) of compound **2** (CD₃COCD₃).

Positions	δ_C (ppm)	δ_H (ppm), mult., J (Hz)	HMBC
1	155,8	-	-
2	115,1	6,72 (<i>d</i> , 1H, <i>J</i> =8.4 Hz)	C-1, C-4, C-6
3	129,4	7,02 (<i>d</i> , 1H, <i>J</i> =8.2 Hz)	C-1, C-5, C-7
4	130,2	-	-
5	115,5	7,02 (<i>d</i> , 1H, <i>J</i> =8.2 Hz)	C-1, C-3, C-7
6	115,1	6,72 (<i>d</i> , 1H, <i>J</i> =8.4 Hz)	C-1, C-4, C-5
7	34,4	2,72 (<i>t</i> , 2H, <i>J</i> =7.3 Hz)	C-8, C-3
8	40,7	3,46 (<i>q</i> , 2H, <i>J</i> =7.5 Hz)	C-7, C-4, C-9
9	165,4	-	-
10	119,9	6,47 (<i>d</i> , 1H, <i>J</i> =15.6 Hz)	C-9, C-12
11	139,4	7,42 (<i>d</i> , 1H, <i>J</i> =15.6 Hz)	C-13, C-10, C-17, C-12, C-9
12	127,4	-	-
13	110,2	7,12 (<i>s</i> , 1H)	C-11, C-15, C-17

14	147,6	-	-
15	148,2	-	-
16	115,0	6,80 (<i>d</i> , 1H, <i>J</i> =8.1 Hz)	C-12, C-14, C-17
17	121,7	7,00 (<i>d</i> , 1H, <i>J</i> =8.2 Hz)	C-11, C-13
18	55,1	3,83 (<i>s</i> , 3H)	C-14

Based on all these analysis and on data of the literature [8-9], compound **2** was identified as **3-(4-hydroxy-3-methoxyphenyl)-N-(4-hydroxyphenethyl) acrylamide** (*trans*-N-feruloyltyramine), it was isolated previously from the *Asphodelus* genus [3].



trans-N- feruloyltyramine

IV.5.3. Identification of compound 3

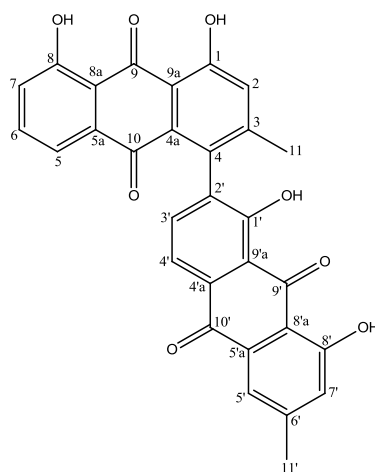


Figure IV.25. Structure of compound 3

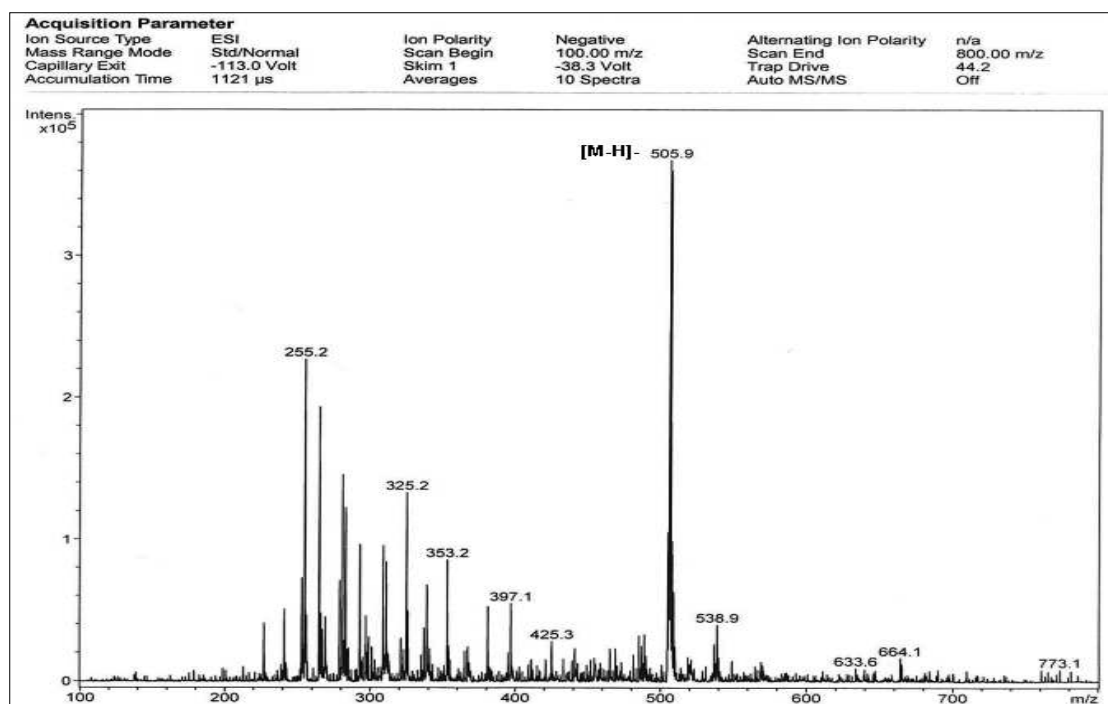


Figure IV.26. ESI-MS spectrum in negative ion mode of compound **3**.

Compound **3** was obtained as an orange powder. The ESI-MS analysis (Fig. IV.26) gave an $[M-H]^-$ ion at $m/z = 505.9$, consistent with the molecular formula $C_{30}H_{18}O_8$ with 7 unsaturations.

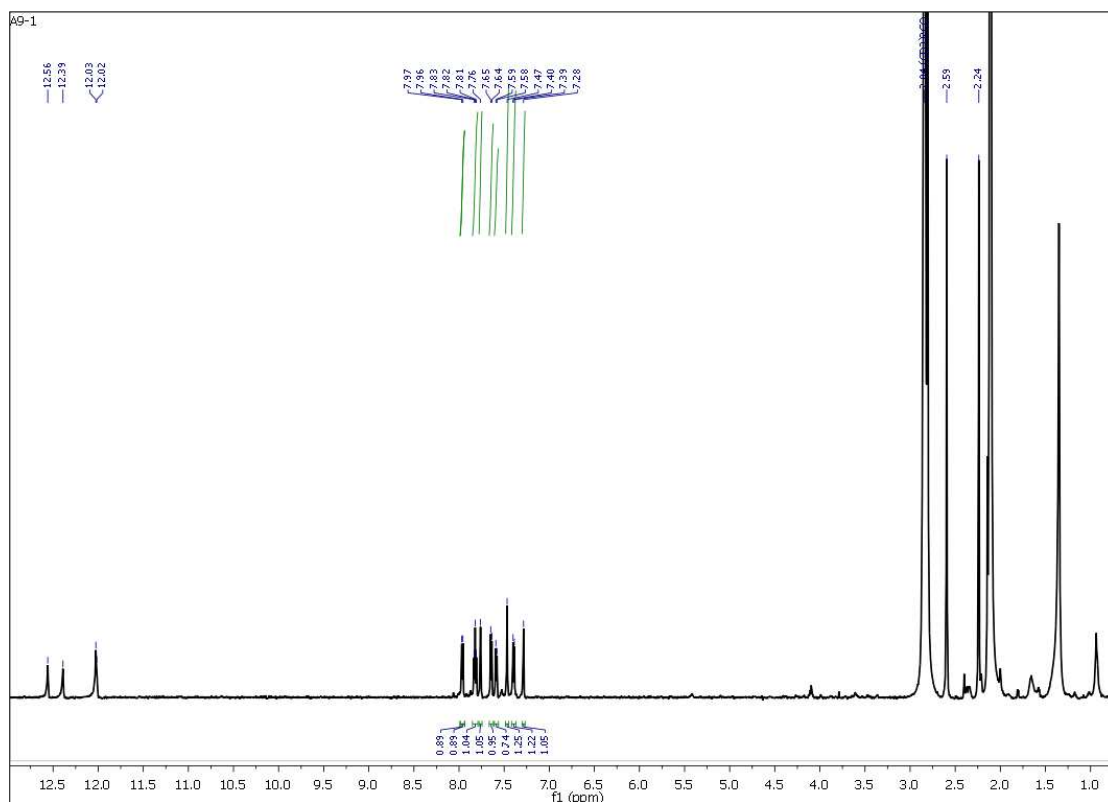


Figure IV.27. 1H -NMR Spectrum (400 MHz, CD_3COCD_3) of compound **3**.

The $^1\text{H-NMR}$ spectrums (**Fig. IV.28**, **Fig. IV.29** and **Fig. IV.30**) of compound **3** showed the presence of four highly deshielded singlets at δ_{H} 12.56 ppm, 12.39 ppm, 12.03 ppm and 12.02 ppm due to the presence of four (4) chelated hydroxyl groups; supported that the compound was a dimeric anthraquinone /anthrone derivative [15]. The $^1\text{H-NMR}$ spectrum showed also protons assigned to H-2 at δ_{H} 7.47 ppm (1H, *s*) with the C-3 attached methyl at δ_{H} 2.24 ppm (3H, *s*). In addition to an ABX spin system corresponding to three aromatic protons resonated at δ_{H} 7.58 ppm (1H, *d*, $J = 7.4$ Hz, H-5), δ_{H} 7.82 ppm (1H, *t*, $J = 7.9$ Hz, H-6) and δ_{H} 7.40 ppm (1H, *d*, $J = 7.4$ Hz, H-7) of the chrysophanol moiety as one half of the molecule. The $^1\text{H-NMR}$ spectral data of the other half of the molecule showed that it's a Chrysophanol moiety too; two *meta* coupled protons assigned to H-5' and H-7', respectively, at δ_{H} 7.76 ppm (1H, *s*) and δ_{H} 7.28 ppm (1H, *s*), with the C-6' attached methyl at δ_{H} 2.59 ppm (3H, *s*). Additionally, the ABX spin system in chrysophanol anthrone was replaced by an AX spin system in chrysophanol moiety at δ_{H} 7.64 ppm (1H, *d*, $J = 7.6$ Hz, H-3') and δ_{H} 7.96 ppm (1H, *d*, $J = 7.6$ Hz, H-4'). This indicated that the point of attachment in this half of the molecule is at C-2' (δ_{C} 141.91 ppm).

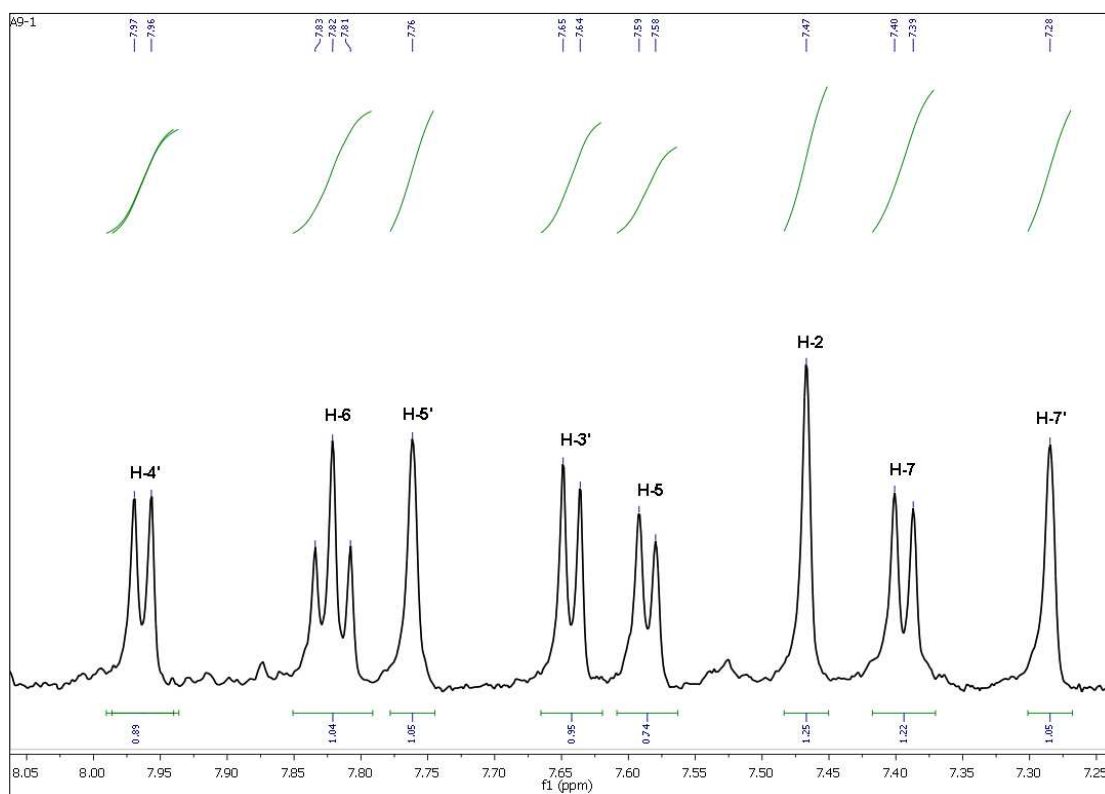


Figure IV.28. $^1\text{H-NMR}$ Spectrum (400 MHz, CD_3COCD_3) of compound **3**.
(From 7.20 ppm to 8.00 ppm).

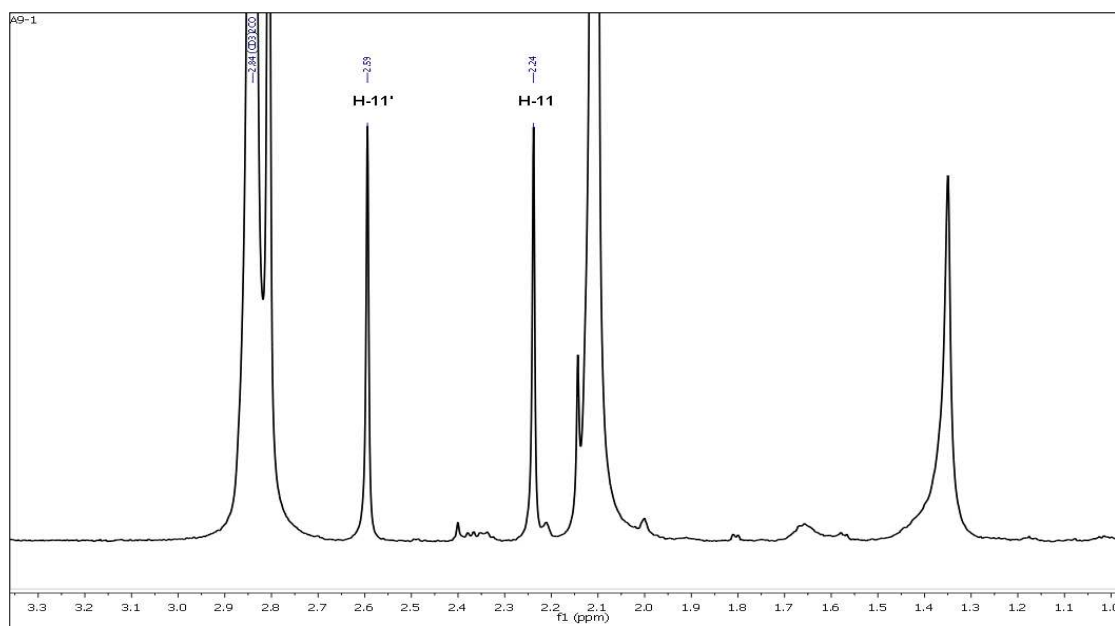


Figure. IV.29. ^1H -NMR Spectrum (400 MHz, CD_3COCD_3) of compound **3**.
(From 1.00 ppm to 3.00 ppm).

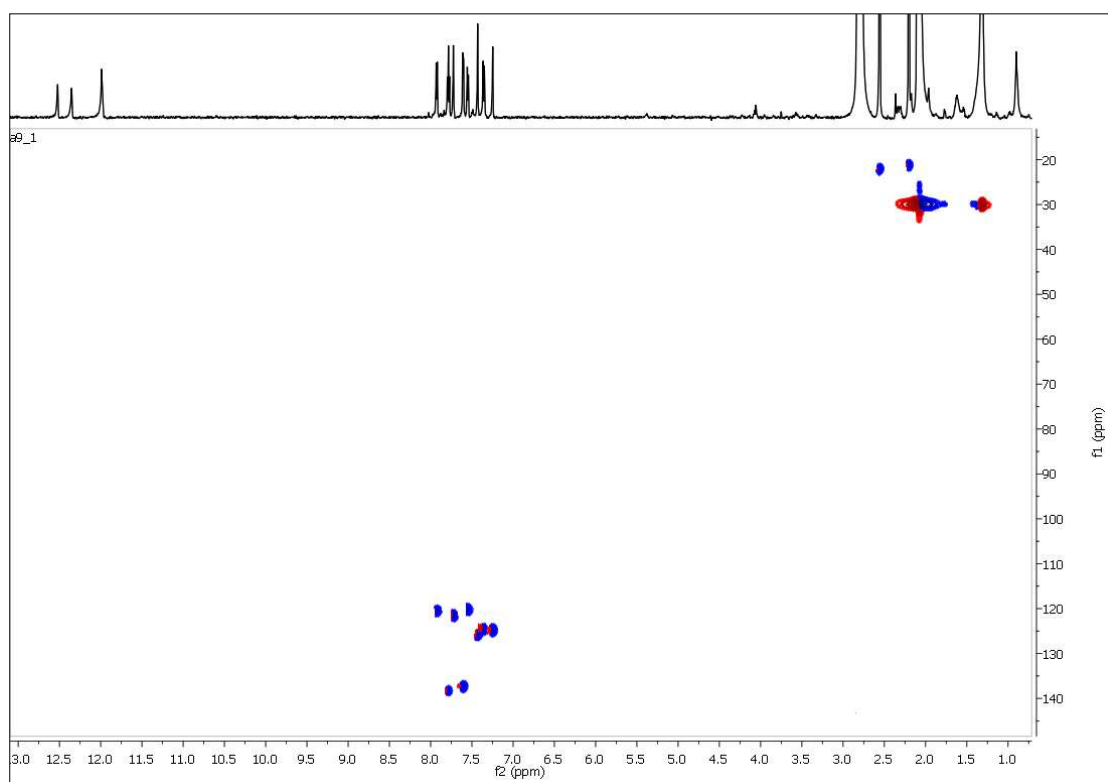


Figure IV.30. HSQC-NMR Spectrum (400 MHz, CD_3COCD_3) of compound **3**.

The examination of the HSQC spectrum (Fig. IV.30, Fig. IV.31 and Fig. IV.32) recorded in CD_3COCD_3 showed correlations identified as follow:

- ✓ The proton H-4' showed a correlation with the carbon C-4' at δ_C 120.6 ppm.
- ✓ The proton H-6 showed a correlation with the carbon C-6 at δ_C 138.3 ppm.
- ✓ The proton H-5' showed a correlation with the carbon C-5' at δ_C 122.0 ppm.
- ✓ The proton H-3' showed a correlation with the carbon C-3' at δ_C 137.4 ppm.
- ✓ The proton H-5 showed a correlation with the carbon C-5 at δ_C 120.1 ppm.
- ✓ The proton H-2 showed a correlation with the carbon C-2 at δ_C 126.1 ppm.
- ✓ The proton H-7 showed a correlation with the carbon C-7 at δ_C 124.5 ppm.
- ✓ The proton H-7' showed a correlation with the carbon C-7' at δ_C 125.1 ppm.
- ✓ The protons of the methyl group CH₃-11' showed correlations with the carbon C-11' at δ_C 22.1 ppm.
- ✓ The protons of the other methyl group CH₃-11 showed correlations with the carbon C-11 at δ_C 21.3 ppm.

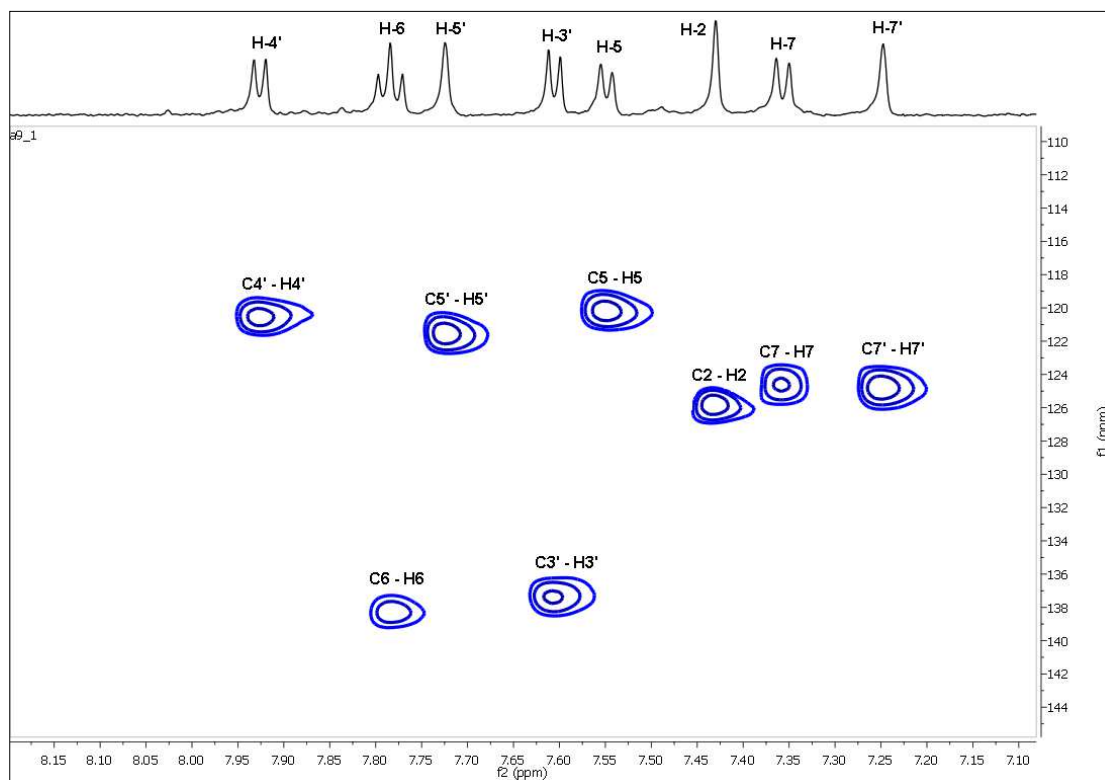


Figure IV.31. HSQC-NMR Spectrum (400 MHz, CD₃COCD₃) of compound **3**.
(From 7.10 ppm to 8.10 ppm).

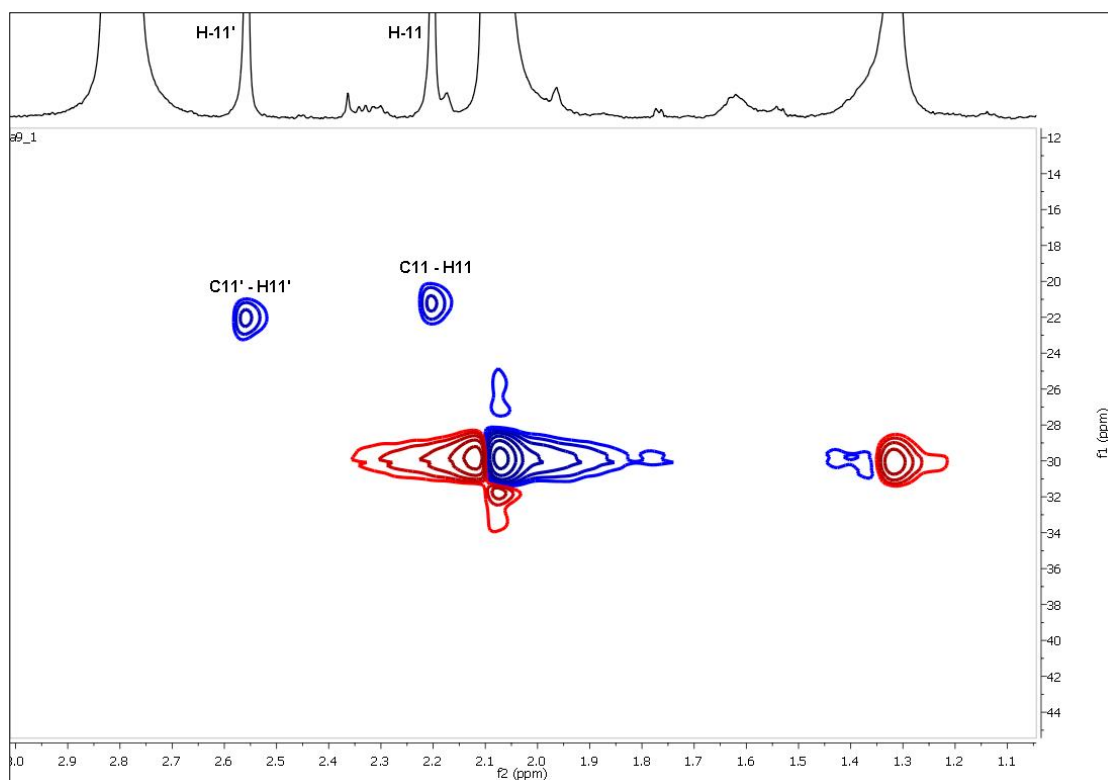


Figure IV.32. HSQC-NMR Spectrum (400 MHz, CD_3COCD_3) of compound **3**.
(From 1.10 ppm to 3.00 ppm).

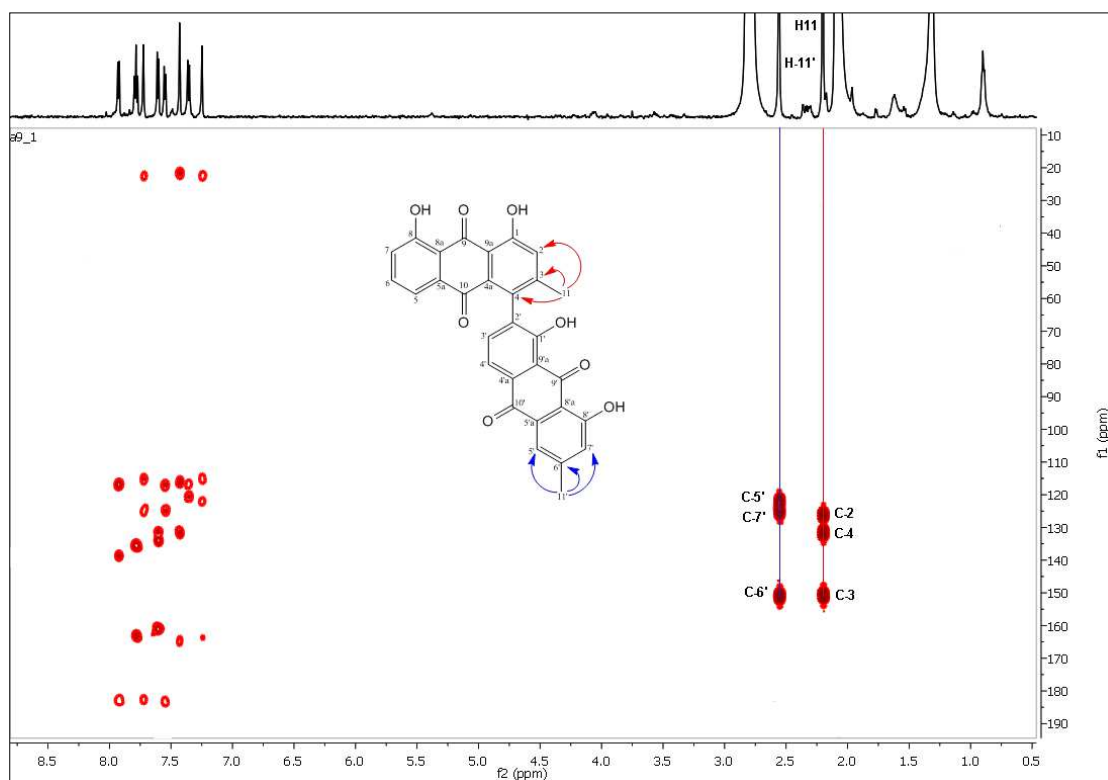


Figure IV.33. HMBC-NMR Spectrum (400 MHz, CD_3COCD_3) of compound **3**.

Examination of the HMBC spectrum (**Fig. IV.33**) recorded in CD_3COCD_3 of the upfield region showed the presence of correlations of the two methyl groups identified as follows:

- ✓ The methyl group ($-\text{CH}_3$) at δ_{H} 2.59 ppm showed three (3) correlations: the first with a carbon at δ_{C} 122.0 ppm attributable to C-5', the second with a carbon at δ_{C} 125.1 ppm attributable to C-7' and a third correlation with a carbon at δ_{C} 151.0 ppm attributable to C-6', this last correlation confirm the position of the methyl group on the carbon C-6' of the aromatic ring as proposed previously in the analysis of the ^1H -NMR spectrum.
- ✓ The second methyl group ($-\text{CH}_3$) at δ_{H} 2.24 ppm showed three (3) correlations: the first with a carbon at δ_{C} 126.1 ppm attributable to C-2, the second with a carbon at δ_{C} 131.6 ppm attributable to C-4 and a third correlation with a carbon at δ_{C} 150.7 ppm attributable to C-3, this last correlation confirm too the position of the methyl group on the carbon C-3 of the aromatic ring.

The second examination of the downfield region of the HMBC spectrum (**Fig. IV.34**) showed the presence of many correlations identified as follow:

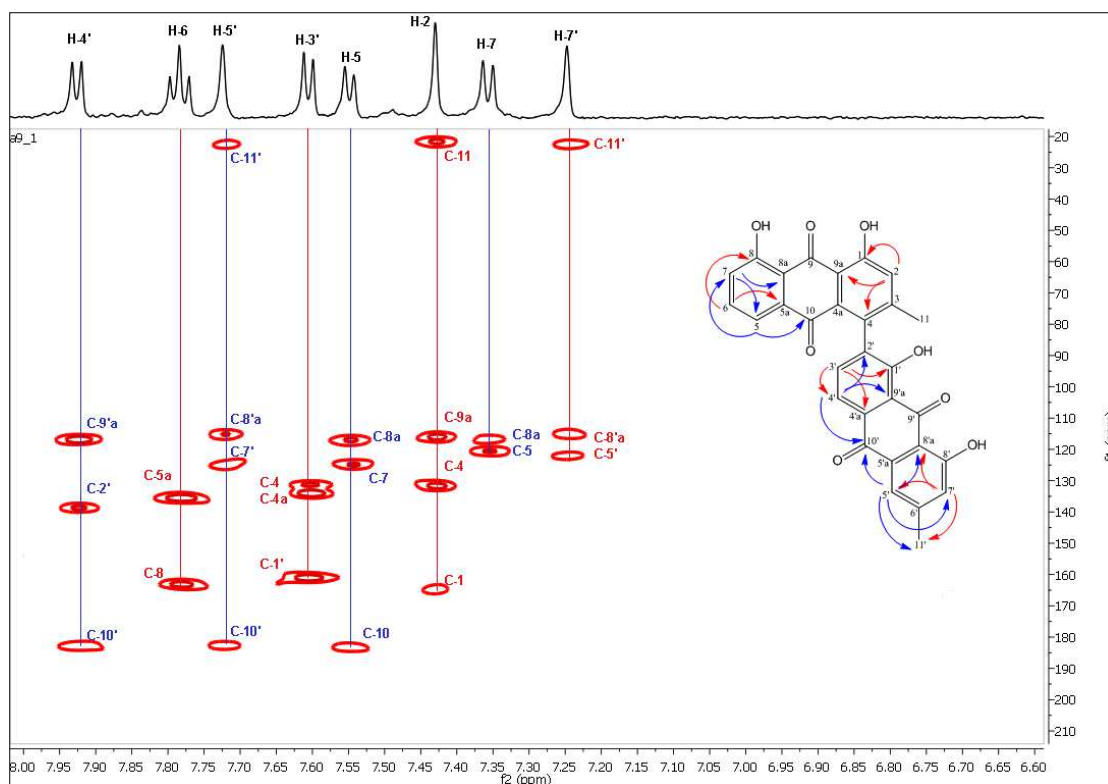


Figure IV.34. HMBC-NMR Spectrum (400 MHz, CD_3COCD_3) of compound **3**.
(From 7.10 ppm to 8.10 ppm).

- ✓ The H-4' proton showed three (3) correlations: The first with a quaternary carbon at δ_{C} 116.8 ppm, attributable to C-9'a, the second correlation with a

carbon at δ_C 138.6 ppm attributable to C-2', the third correlation with carbonyl function carbon at δ_C 182.6 ppm attributable to C-10'.

- ✓ The H-6 proton showed two (2) correlations: the first with a quaternary carbon at δ_C 135.6 ppm, attributable to C-5a, and a second correlation with a carbon at δ_C 163.1 ppm attributable to C-8 which confirms the attachment of the hydroxyl group on this carbon (C-8).
- ✓ The H-5' proton showed four (4) correlations: the first with the carbon at δ_C 22.1 ppm attributable to the methyl group, this correlation confirm the attachment point of the methyl group on C-11', the second correlation with the quaternary carbon at δ_C 115.1 ppm attributable to C-8'a, the third with a carbon at δ_C 125.1 ppm attributable to C-7', the last correlation task with a carbon at δ_C 182.6 ppm attributable to the carbon of the carbonyl group at C-10'.
- ✓ The H-5 proton showed three (3) correlations: with a quaternary carbon at δ_C 116.9 ppm attributable to C-8a, with a carbon at δ_C 124.5 ppm attributable to C-7, and a last with the carbon of the carbonyl group on C-10 at δ_C 183.2 ppm.
- ✓ The H-2 proton showed four (4) correlations: the first with the carbon at δ_C 21.3 ppm attributable to the methyl group, this correlation confirm the attachment point of the methyl group on C-11, the second correlation with the quaternary carbon at δ_C 116.0 ppm attributable to C-9a, the third with a carbon at δ_C 131.6 ppm attributable to C-4, the last correlation with a carbon at δ_C 164.7 ppm attributable to the carbon at C-1 which confirm the attachment of an hydroxyl group on the carbon (C-1).
- ✓ The H-7 proton showed two (2) correlations: The first with a quaternary carbon at δ_C 116.9 ppm, attributable to C-8a, and a second correlation with a carbon at δ_C 120.1 ppm attributable to C-5 which confirms the attachment of the hydroxyl group on this carbon (C-8).
- ✓ The H-7' proton showed three (3) correlations: the first with the carbon at δ_C 22.1 ppm attributable to the methyl group, this correlation confirm again the attachment point of the methyl group on C-11', the second correlation with the quaternary carbon at δ_C 115.1 ppm attributable to C-8'a, the third with a carbon at δ_C 122.0 ppm attributable to C-5'.
- ✓ The H-3' proton showed three (3) correlations: The first with a quaternary carbon at δ_C 135.6 ppm, attributable to C-4a, the second with a carbon at δ_C 131.6 ppm attributable to C-4, this cross-peak observed in the HMBC spectrum between H-3' and C-4 indicates the site of attachment was between C-4 of the first chrysophanol and C-2' of the second chrysophanol. The last correlation with a carbon at δ_C 161.1 ppm attributable to C-1' which confirm the attachment of a hydroxyl group on this carbon (C-1').

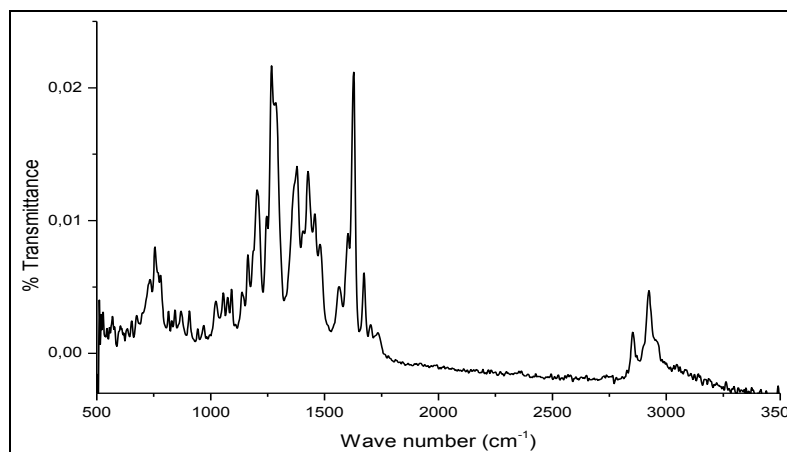
The analogy of these features with the spectral NMR data of the related metabolites previously reported, suggested the structure the compound **3** as chrysophanol linked to another moiety of chrysophanol [5-6].

All the chemical shifts of the NMR analysis (^1H , ^{13}C , HSQC and HMBC) of compound **3** are summarized in the following table (**Table IV.8**).

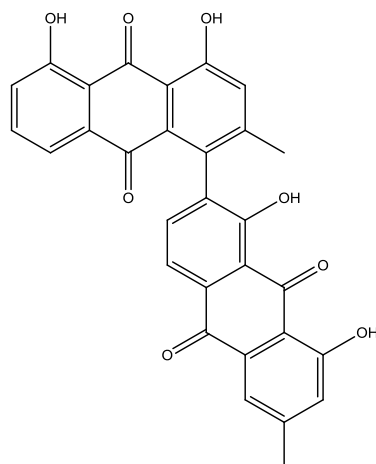
Table IV.8. ^1H , ^{13}C and HMBC-NMR data (400 MHz) of compound **3** (CD_3COCD_3).

Positions	δ_{C} (ppm)	δ_{H} (ppm), <i>mult.</i> , <i>J</i> (Hz)	HMBC
1	164.7	-	-
2	126.1	7.47 (<i>s</i> , 1H)	C-11, C-4, C-1, C-9a
3	150.7	-	-
4	131.6	-	-
5	120.1	7.58 (<i>d</i> , 1H, <i>J</i> =7.4 Hz)	C-7, C-10, C-8a
6	138.3	7.82 (<i>t</i> , 1H, <i>J</i> =7.9 Hz)	C-8, C-5a
7	124.5	7.40 (<i>d</i> , 1H, <i>J</i> =7.4 Hz)	C-8a, C-5
8	163.1	-	-
9	188.1	-	-
10	183.2	-	-
1'	161.1	-	-
2'	138.6	-	-
3'	137.4	7.64 (<i>d</i> , 1H, <i>J</i> =7.6 Hz)	C-1', C-4, C-4'a
4'	120.6	7.96 (<i>d</i> , 1H, <i>J</i> =7.6 Hz)	C-2', C-10', C-9'a
5'	122.0	7.76 (<i>s</i> , 1H)	C-11', C-8'a, C-7', C-10'
6'	151.0	-	-
7'	125.1	7.28 (<i>s</i> , 1H)	C-11', C-8'a, C-5'
8'	168.0	-	-
9'	188.0	-	-
10'	182.6	-	-
4a	135.6	-	-
5a	135.6	-	-
8a	116.9	-	-
9a	116.0	-	-
4'a	134.0	-	-
5'a	134.4	-	-
8'a	115.1	-	-
9'a	116.8	-	-
11	21.3	2.24 (<i>s</i> , 3H)	C-2, C-3, C-4
11'	22.1	2.59 (<i>s</i> , 3H)	C-5', C-6', C-7'

The IR spectrum of this compound **3** showed absorption bands for chelated carbonyls and for hydroxyl groups at 1627 and 2976 cm^{-1} , respectively (**Fig. IV.35**).

**Figure IV.35.** IR Spectrum of compound **3**.

Based on all the above data, compound **3** was identified as **1', 4, 5, 8'-tetrahydroxy-2, 6'-dimethyl-[1,2'-bianthracene]-9, 9', 10, 10'-tetraone (Asphodeline)**, the structure was confirmed by comparison of its physical properties and proton and carbon NMR data to literature [6-7-16]. This structure was reported previously from the *Asphodelus* genus [16].



1',4,5,8'-tetrahydroxy-2,6'-dimethyl-[1,2'-bianthracene]-9,9',10,10'-tetraone
(Asphodeline)

IV.5.4. Identification of compound 4

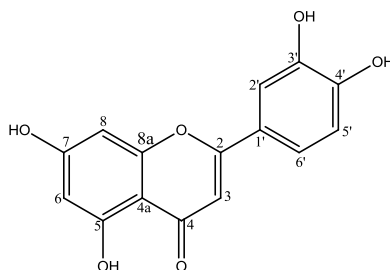


Figure IV.36. Structure of **compound 4**

Compound 4 was obtained as brown powder. The ESI-MS recorded on negative mode (**Fig. IV.37**) gave an $[M-H]^-$ ion at $m/z = 284.9$ consistent with the molecular formula of $C_{15}H_{10}O_6$ with 11 unsaturations.

The violet black fluorescence under Wood's UV light was characteristic of a flavone or a flavonol substituted on position 3.

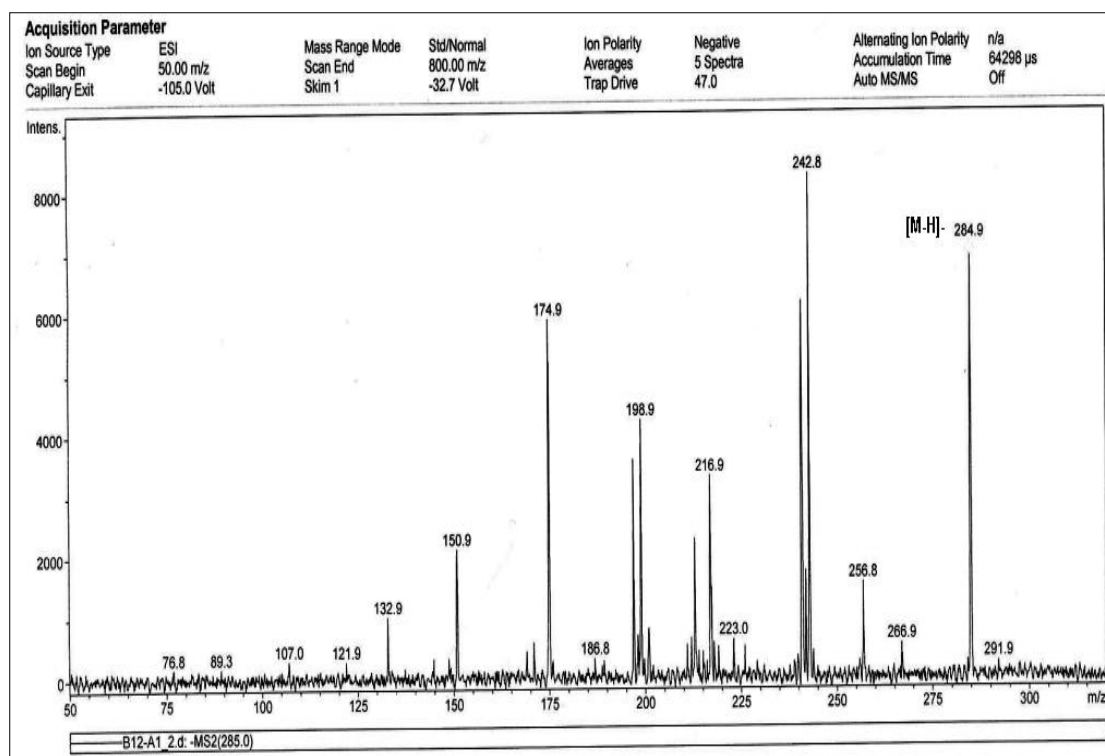


Figure IV.37. ESI-MS spectrum in negative ion mode of compound **4**.

The UV spectrum (**Fig. IV.38**), recorded in Methanol, gives two absorption bands, the first band (I) at 347 nm and other band (II) at 255 nm indicating a skeleton of flavone type for this compound. A bathochromic effect, observed after the addition of NaOH ($\Delta\lambda = +45$ nm) with increase in intensity, indicates the presence of a free OH in position 4'. The appearance of a new band in the same spectrum at 328 nm suggest the presence of a free OH at position 7.

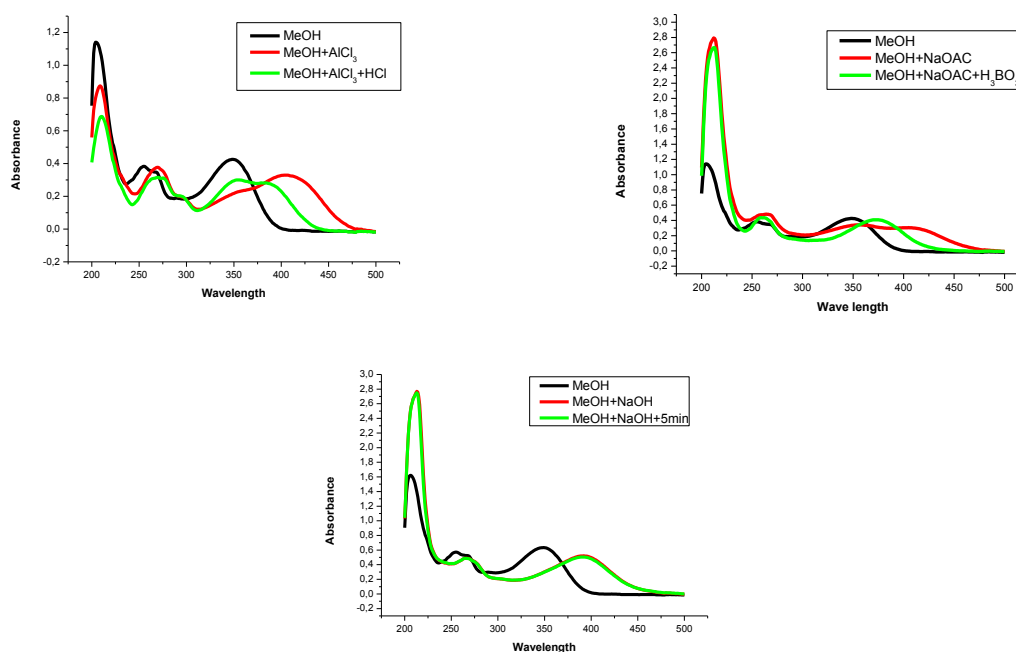


Figure IV.38. UV analysis spectrums of compound **4**.

The addition of (NaOAc) to the methanolic solution induced the bathochromic effect of 16 nm for the band II, confirming the presence of a free OH at position 7. The addition of (H_3BO_3) to the (MeOH+NaOAc) solution caused a bathochromic effect of the band I ($\Delta\lambda = +24$ nm), indicating the presence of a 3', 4'- *ortho* di-OH system on cycle B, this was confirmed by the hypsochromic displacement of the band I ($\Delta\lambda = -31$ nm) induced after the addition of (HCl) to the (MeOH+ $AlCl_3$) solution. The bathochromic effect of the band I ($\Delta\lambda = +73$ nm) observed on the spectrum recorded in MeOH+ $AlCl_3$ compared to the spectrum recorded in MeOH indicated the presence of a free OH group at position 5.

Table IV.9. UV-Visible data of compound 4.

<i>Solvents</i>	<i>Band I (λ_{max} nm)</i>	<i>Band II (λ_{max} nm)</i>	<i>Other bands</i>
MeOH	347	255	-
+ NaOH	392	268	328
+ NaOAc	356	262	-
+ NaOAc + H_3BO_3	380	260	-
+ $AlCl_3$	420	267	-
+ $AlCl_3$ + HCl	389	272	-

All these UV-Visible spectral data are in agreement with those reported previously in the literature for the luteolin [17].

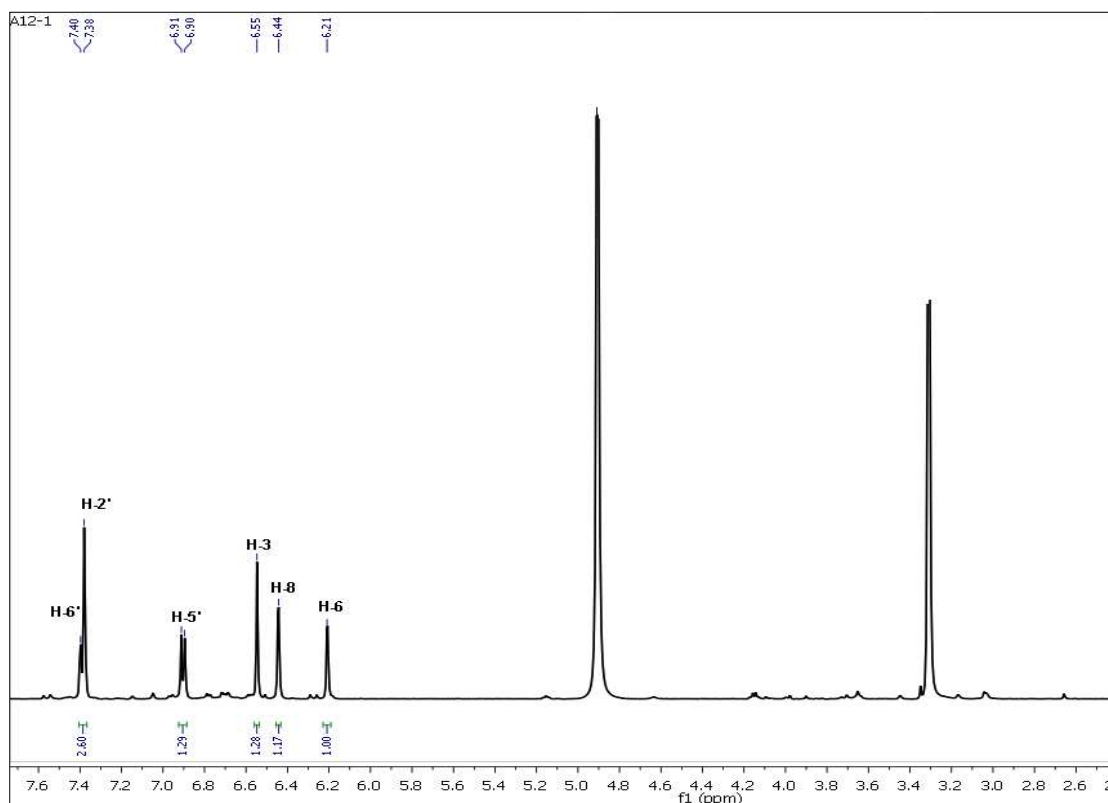


Figure IV.39. 1H -NMR Spectrum (600 MHz, CD_3OD) of compound 4.

The examination of the $^1\text{H-NMR}$ spectrum recorded in MeOH (**Fig. IV.39**) confirm the skeleton of a Luteolin structure [4] characterized by:

- A singlet of 1H integration at δ_{H} 6.55 ppm attributable to the proton H-3.
- Two doublets of 1H integration for each at δ_{H} 6.21 ppm and δ_{H} = 6.44 ppm with a coupling constant ($J = 2.0$ Hz) attributable to the protons H-6 and H-8 respectively, thus confirming the hydroxylation of positions 5 and 7 of ring A.
- A signal at δ_{H} 7.40 ppm of 2H integration attributable to H-2' and H-6', this signal corresponds in fact to two superimposed signals: one in the form of a double doublet ($J = 8.4 - 2.0$ Hz) characterizing H-6' and the other in the form of a doublet ($J = 2.0$ Hz) characterizing H-2', this signal confirm the hydroxylation of the positions 3' and 4' of cycle B. Moreover, the signal in the form of a doublet which appears at δ_{H} 6.90 ppm ($J = 8.9$ Hz) is attributable to H-5'.

The examination of the HSQC and the HMBC spectrums recorded in CD_3OD (**Fig. IV.33**, **Fig. IV.34**) confirm too the skeleton of Luteolin by the presence of correlations identified as follow:

- For HSQC spectrum (**Fig. IV.33**):
 - ✓ The proton H-6' showed a correlation with the carbon C-6' at δ_{C} 119.6 ppm.
 - ✓ The proton H-2' showed a correlation with the carbon C-2' at δ_{C} 113.9 ppm.
 - ✓ The proton H-5' showed a correlation with the carbon C-5' at δ_{C} 116.2 ppm.
 - ✓ The proton H-3 showed a correlation with the carbon C-3 at δ_{C} 103.7 ppm.
 - ✓ The proton H-8 showed a correlation with the carbon C-8 at δ_{C} 95.4 ppm.
 - ✓ The proton H-6 showed a correlation with the carbon C-6 at δ_{C} 100.4 ppm.

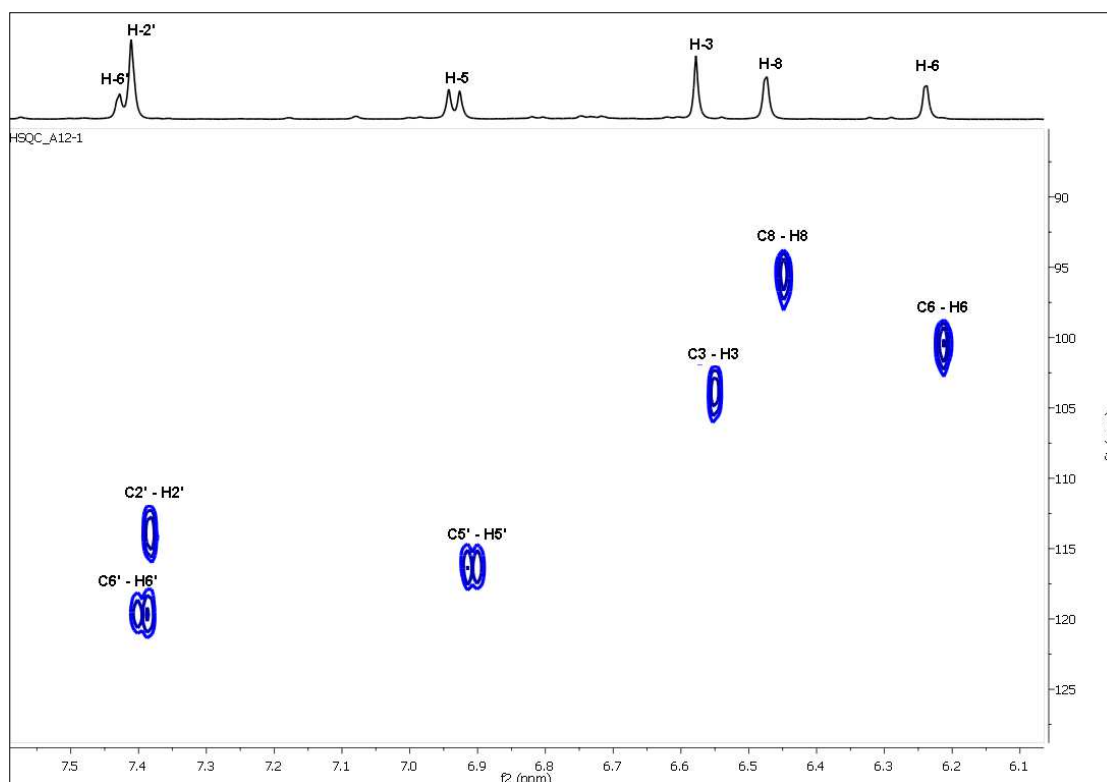


Figure IV.40. HSQC-NMR Spectrum (600 MHz, CD_3OD) of compound **4**.

- For HMBC spectrum (**Fig. IV.41**):
 - ✓ The H-6 proton showed four (4) correlations: The first with a carbon at δ_C 104.4 ppm, this carbon showed two other correlations with the protons H-3 and the proton H-8, this carbon can be only quaternary C-4a, the second correlation with a carbon at δ_C 95.4 ppm attributable to C-8, the third and the fourth correlations with carbons at δ_C 161.1 ppm and δ_C 164.2 ppm attributable to C-5 and C-7, respectively.
 - ✓ The H-8 proton showed four (4) correlations: The first with a quaternary carbon at δ_C 104.4 ppm, attributable to C-4a, the second correlation with a carbon at δ_C 100.4 ppm attributable to C-6, the third with a carbon at δ_C 164.2 ppm attributable to C-7. The last correlation with a carbon at δ_C 158.6 ppm attributable to quaternary carbon C-8a.
 - ✓ The H-3 proton showed four (4) correlations: The first with a quaternary carbon at δ_C 104.4 ppm, attributable to C-4a, the second correlation with a carbon at δ_C 121.9 ppm attributable to C-1', the third and the fourth correlations with carbon at δ_C 162.8 and δ_C 182.2 ppm attributable to C-2 and C-4, respectively.
 - ✓ The H-2' proton showed four (4) correlations: The first with a carbon at δ_C 119.6 ppm, attributable to C-6', the second correlation with a carbon at δ_C 149.8 ppm attributable to C-4', the third with a carbon at δ_C 162.8 ppm attributable to C-2. The last correlation with a carbon at δ_C 146.3 ppm attributable to the carbon C-3'.

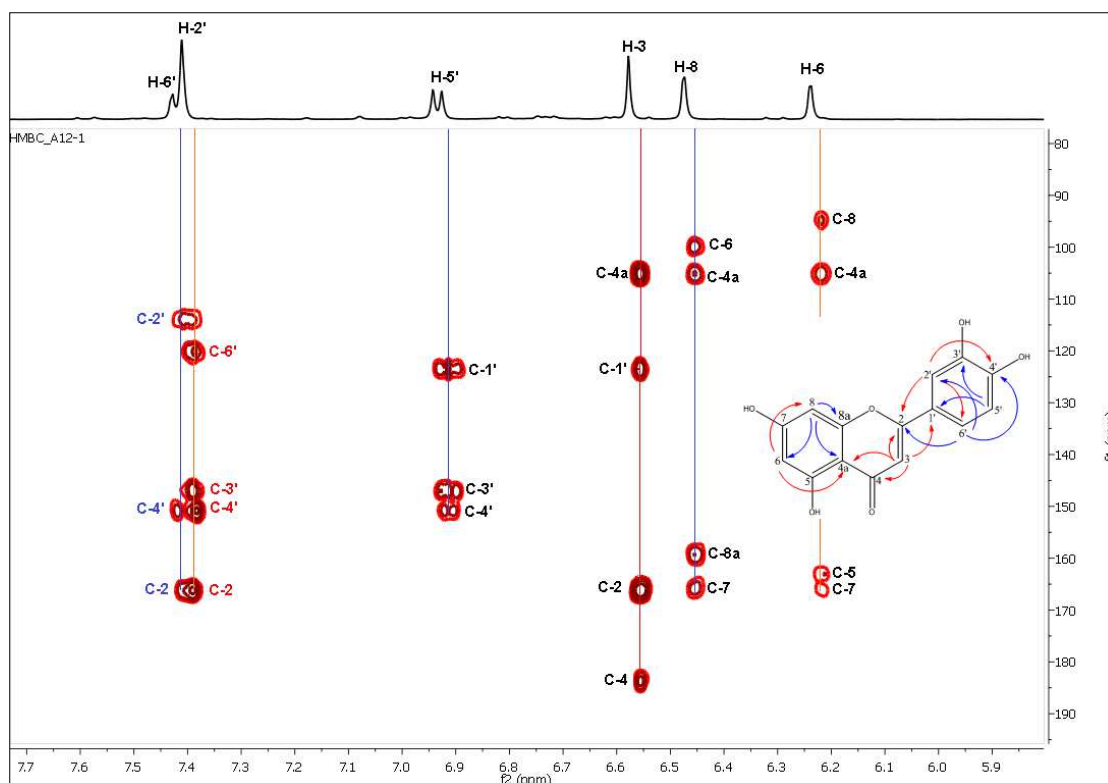


Figure IV.41. HMBC-NMR Spectrum (600 MHz, CD₃OD) of compound **4**.

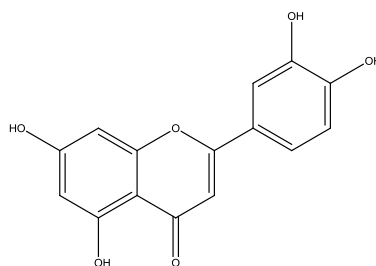
- ✓ The H-6' proton showed three (3) correlations: The first with a carbon at δ_C 149.8 ppm, attributable to C-4', the second correlation with a carbon at δ_C 113.9 ppm attributable to C-2', the last with a carbon at δ_C 162.8 attributable to C-2.
- ✓ The H-5' proton showed three (3) correlations: The first with a carbon at δ_C 149.8 ppm, attributable to C-4', the second correlation with a carbon at δ_C 146.3 ppm attributable to C-3', the last with a carbon at δ_C 121.9 attributable to C-1'.

All the chemical shifts of the NMR analysis (^1H , ^{13}C , HSQC and HMBC) of compound **4** are summarized in the following table: (Table IV.10)

Table IV.10. ^1H , ^{13}C and HMBC-NMR data (600 MHz) of compound **4** (CD_3OD).

Positions	δ_C (ppm)	δ_H (ppm), <i>mult.</i> , <i>J</i> (Hz)	HMBC
1	-	-	-
2	162.8	-	-
3	103.7	6.55 (<i>s</i> , 1H)	C-4a, C-1', C-2, C-4
4	182.2	-	-
5	161.1	-	-
6	100.4	6.21 (<i>d</i> , 1H, <i>J</i> =2.0 Hz)	C-8, C-4a, C-5, C-7
7	164.2	-	-
8	95.4	6.44 (<i>d</i> , 1H, <i>J</i> =2.0 Hz)	C-6, C-4a, C-7, C-8a
4a	104.4	-	-
8a	158.6	-	-
1'	121.9	-	-
2'	113.9	7.38 (<i>d</i> , 1H, <i>J</i> =2.0 Hz)	C-6', C-4', C-3', C-2
3'	146.3	-	-
4'	149.8	-	-
5'	116.2	6.90 (<i>d</i> , 1H, <i>J</i> =8.0 Hz)	C-1', C-3', C-4'
6'	119.6	7.40 (<i>dd</i> , 1H, <i>J</i> =8.4-2.0 Hz)	C-4', C-2', C-2

All these spectroscopic data and the comparison with those of the literature confirm the structure of the compound **4** which was a **5, 7-dihydroxy-2-(3, 4-dihydroxyphenyl)-chromèn-4-one (Luteolin)** [4], as well as it was reported previously from the *Asphodelus* genus [3].



Luteolin

IV.5.5. Identification of compound 5

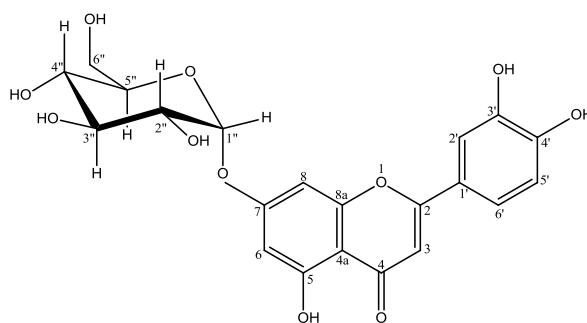


Figure IV.42. Structure of compound 5.

Compound 5 was obtained as an orange powder. The ESI-MS (**Fig. IV.44**) recorded on negative mode gave an $[M-H]^-$ ion at $m/z = 447.0$ suggesting a mass of 448 uma consistent with the molecular formula of $C_{21}H_{20}O_{11}$ with 12 unsaturations which gave a possibility to have a skeleton of a glycosylated flavonoid. This spectrum showed also a signal at $m/z = 285.0$ $[M-H-162]^-$ may corresponding to a skeleton of a flavonoid of formula $C_{15}H_{10}O_6$ after the loss of a hexose unit.

The UV-Visible analysis (**Fig. IV.43**), recorded in Methanol, gave two absorption bands, the first band (I) at 345 nm and other band (II) at 252 nm indicating a skeleton of flavone type for this compound. A bathochromic effect, observed after the addition of NaOH ($\Delta\lambda = +45\text{nm}$) with increase in intensity, indicated the presence of a free OH in position 4'.

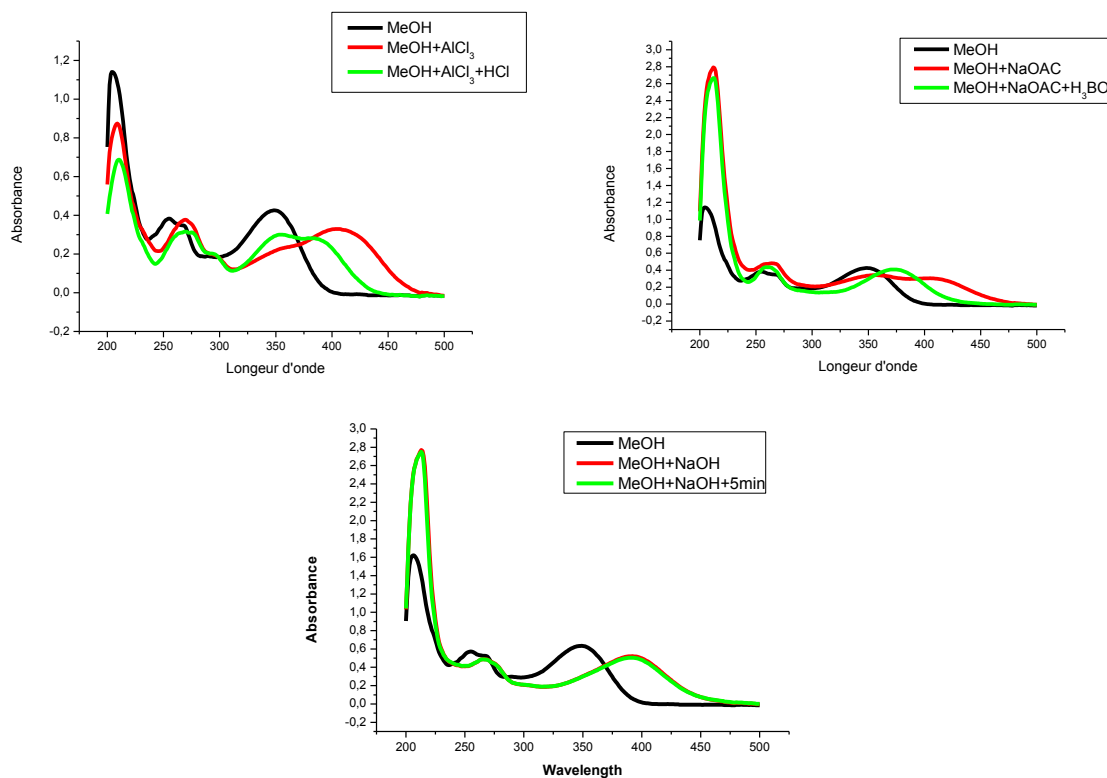


Figure IV.43. UV-Visible analysis spectrums of compound 5.

The addition of (H_3BO_3) to the ($\text{MeOH}+\text{NaOAc}$) solution causes a bathochromic effect of the band I ($\Delta\lambda=+23$ nm), indicating the presence of a 3', 4'- *ortho* di-OH system on cycle B, this was confirmed by the hypsochromic displacement of the band I ($\Delta\lambda= -30$ nm) induced after the addition of (HCl) to the ($\text{MeOH}+\text{AlCl}_3$) solution. The bathochromic effect of the band I ($\Delta\lambda = +76$ nm) observed on the spectrum recorded in $\text{MeOH}+\text{AlCl}_3$ compared to the spectrum recorded in MeOH indicates the presence of a free OH group at position 5.

Table IV.11. UV data of compound 5

Solvents	Band I (λ_{max} nm)	Band II (λ_{max} nm)
MeOH	345	252
+ NaOH	390	266
+ NaOAc	354	262
+ NaOAc + H_3BO_3	377	260
+ AlCl_3	421	268
+ AlCl_3 + HCl	390	271

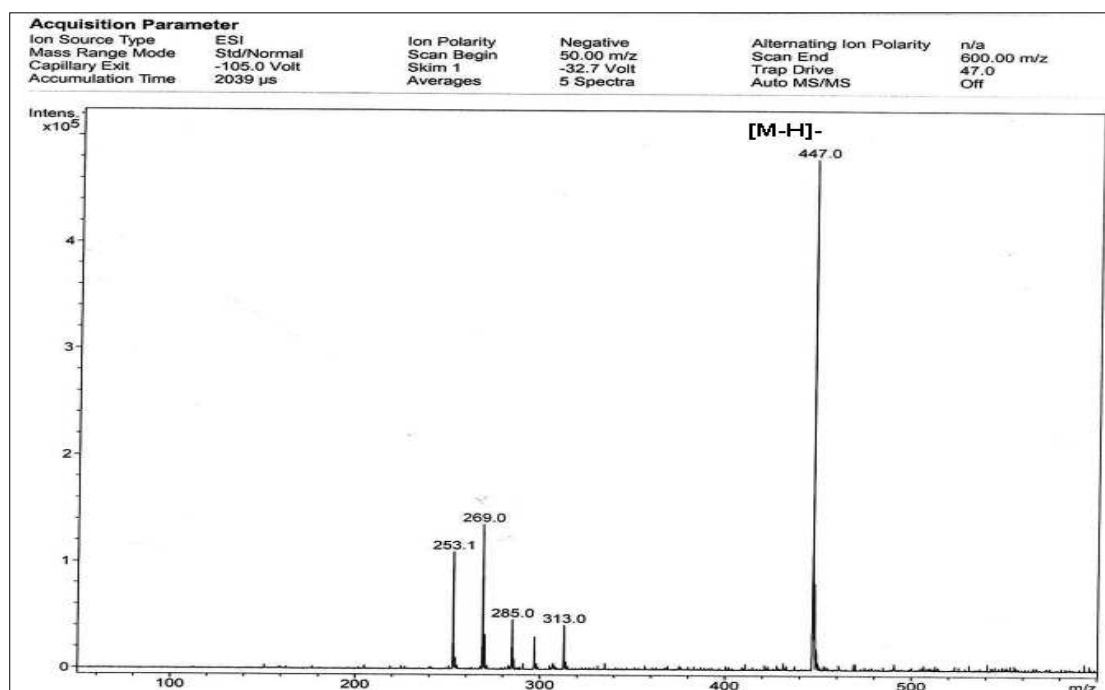


Figure IV.44. ESI-MS spectrum in negative ion mode of compound 5.

The analysis of the ^1H NMR spectrum and its spread (**Fig. IV.45**, **Fig. IV.46** and **Fig. IV.47**) indicated that this compound could be a glycosylated flavone, explained by the presence of:

- A doublet of 1H intensity at δ_{H} 5.06 ppm ($J=7.3\text{Hz}$) typical of an H-1'' anomeric proton.
- Signals between δ_{H} 3.22 ppm and δ_{H} 3.45 ppm integrating for 6H relative to the osidic protons of a hexose unit.

- Two doublets of 1H intensity for each at δ_H 6.77 ppm ($J = 1.6$ Hz) and δ_H 6.42 ppm ($J = 1.6$ Hz), respectively characteristic of the protons H-8 and H-6 of the cycle A.
- A singlet of 1H intensity at δ_H 6.72 ppm attributable to H-3.
- Highly deshielded singlet at δ_H 12.96 ppm due to the presence of one chelated hydroxyl group.
- For the cycle B, the $^1\text{H-NMR}$ spectrum had three signals resonate as an ABX system at δ_H 7.40 ppm (1H, s), δ_H 7.42 ppm (1H, dd, $J = 8.2, 2.0$ Hz) and δ_H 6.69 ppm (1H, d, $J = 8.2$ Hz) attributable respectively to the protons H-2', H-6' and H-5' indicating the presence of a 1', 3', 4'-trisubstitution on cycle B.

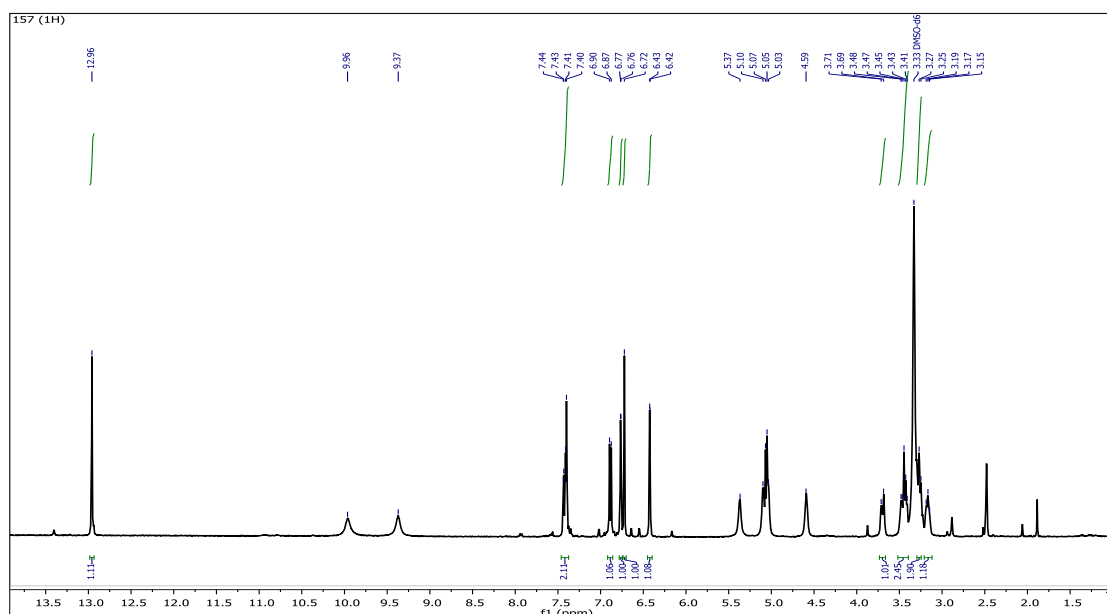


Figure IV.45. $^1\text{H-NMR}$ Spectrum (400 MHz, $\text{DMSO-}d_6$) of compound 5.

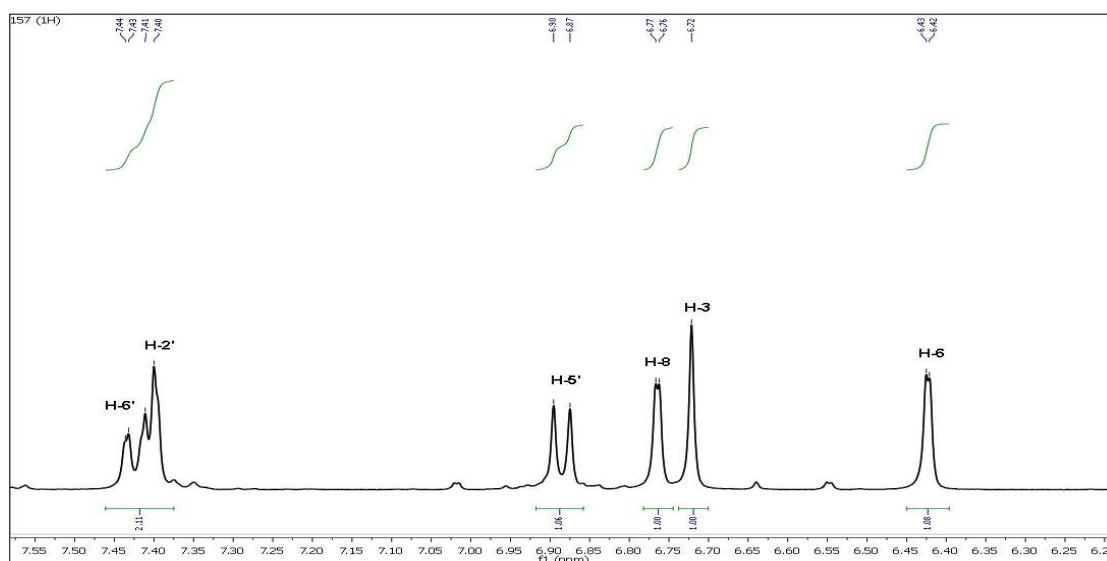


Figure IV.46. $^1\text{H-NMR}$ Spectrum (400 MHz, $\text{DMSO-}d_6$) of compound 5. (From 6.20 ppm to 7.50 ppm).

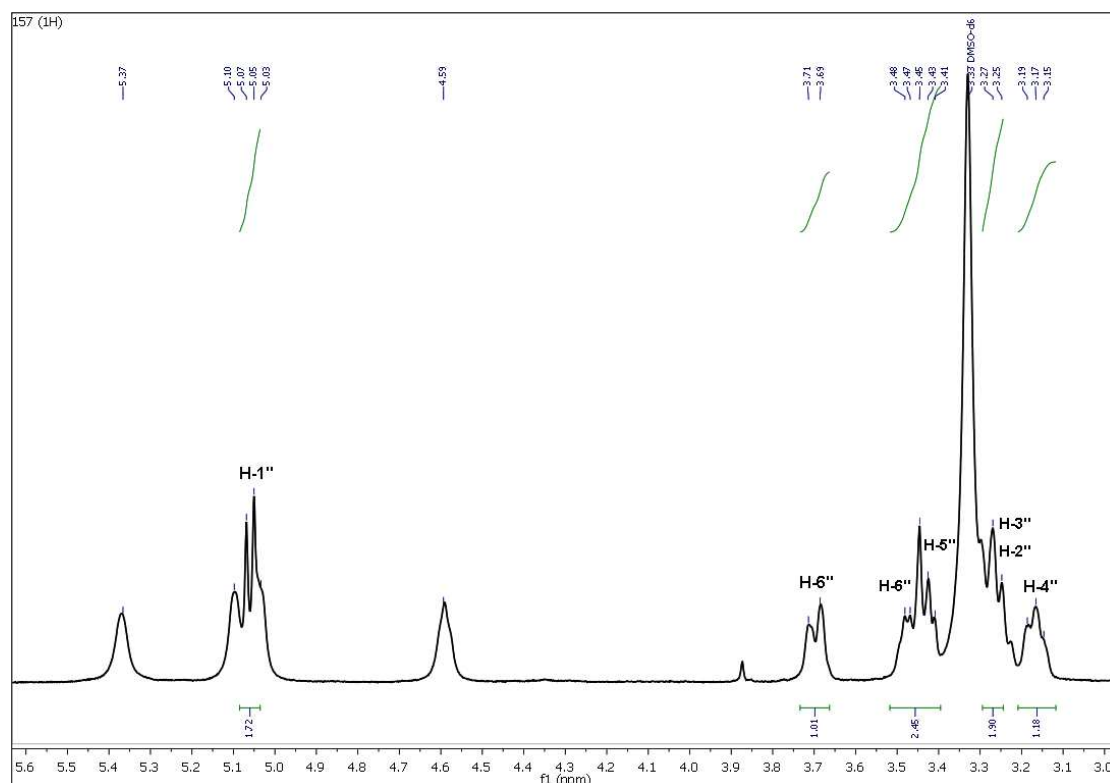


Figure IV.47. $^1\text{H-NMR}$ Spectrum (400 MHz, DMSO- d_6) of compound **5**.
(From 3.00 ppm to 5.50 ppm).

The examination of the HSQC spectrum (**Fig. IV.48**) recorded in DMSO- d_6 showed the presence of correlations identified as follow:

- ✓ The proton H-6' showed a correlation with the carbon C-6' at δ_{C} 119.6 ppm.
- ✓ The proton H-2' showed a correlation with the carbon C-2' at δ_{C} 113.5 ppm.
- ✓ The proton H-5' showed a correlation with the carbon C-5' at δ_{C} 116.2 ppm.
- ✓ The proton H-8 showed a correlation with the carbon C-8 at δ_{C} 95.0 ppm.
- ✓ The proton H-3 showed a correlation with the carbon C-3 at δ_{C} 103.4 ppm.
- ✓ The proton H-6 showed a correlation with the carbon C-6 at δ_{C} 99.5 ppm.
- ✓ The proton H-1'' showed a correlation with the carbon C-1'' at δ_{C} 100.5 ppm.
- ✓ The proton H-6''*a* and H-6''*b* showed correlations with the carbon C-6'' at δ_{C} 60.5 ppm.
- ✓ The proton H-5'' showed a correlation with the carbon C-5'' at δ_{C} 77.2 ppm.
- ✓ The proton H-3'' showed a correlation with the carbon C-3'' at δ_{C} 77.1 ppm.
- ✓ The proton H-2'' showed a correlation with the carbon C-2'' at δ_{C} 70.3 ppm.
- ✓ The proton H-4'' showed a correlation with the carbon C-4'' at δ_{C} 72.0 ppm.
- ✓ No correlation was observed for the proton of the proposed chelated hydroxyl groups at δ_{H} 12.96 ppm which confirm our proposition.

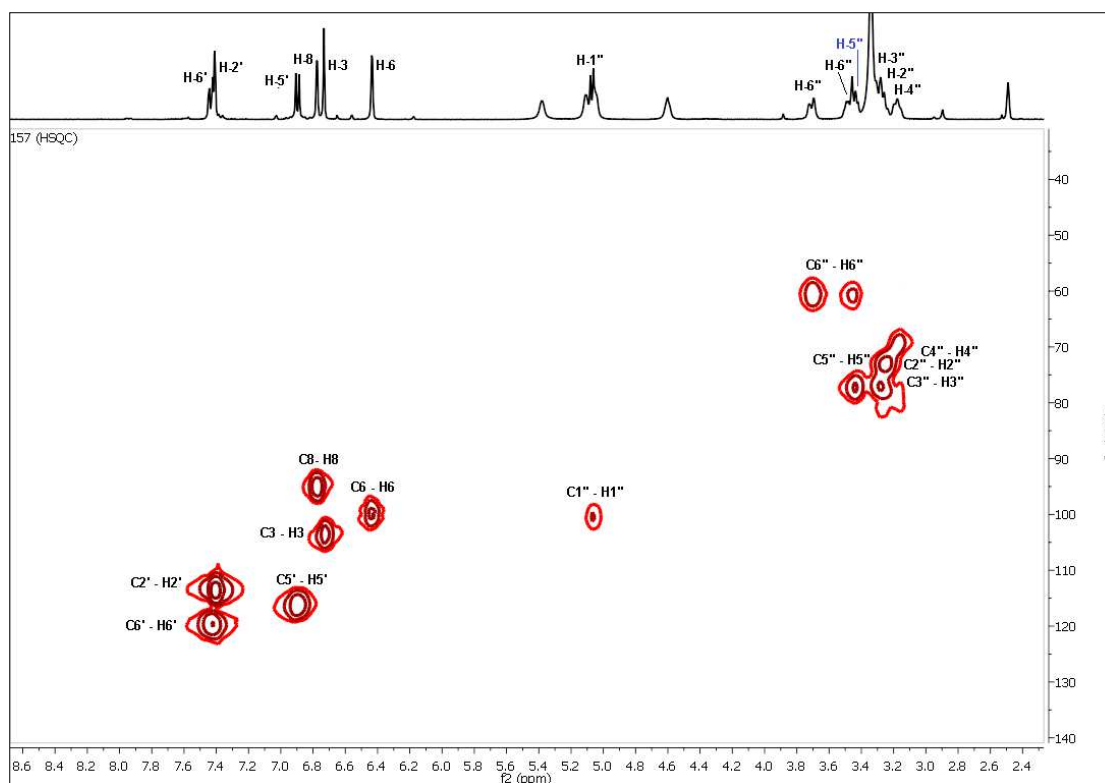


Figure IV.48. HSQC-NMR Spectrum (400 MHz, DMSO-*d*₆) of compound **5**.

According to the literature, these chemical shifts obtained are characteristic of glucose carbons C-1'', C-2'', C-3'', C-4'', C-5'' and C-6'' glucose. This proposal was confirmed by an acid hydrolysis and by comparison of this obtained sugar by a co-chromatography with other authentic controls. The ¹³C-NMR data from the HSQC correlations (**Fig. IV.48**) were in good agreement with those reported previously for an Isoorientin [18-19].

The examination of the HMBC spectrum (**Fig. IV.49** and **Fig. IV.50**) recorded in DMSO-*d*₆ of the aromatic region of the spectrum confirm the proposal structure of this compound by the presence of some correlations identified as follow:

- ✓ The proton of the hydroxyl group linked to C-5 (5-OH) showed four (4) clear correlations confirming its position: The first with a carbon at δ_C 99.5 ppm, attributable to C-6, the second correlation with a carbon at δ_C 105.8 ppm attributable to C-4a, the third with a carbon at δ_C 182.3 attributable to the carbonyl group on C-4. The last correlation with a carbon at δ_C 163.2 attributable to the carbon C-7.

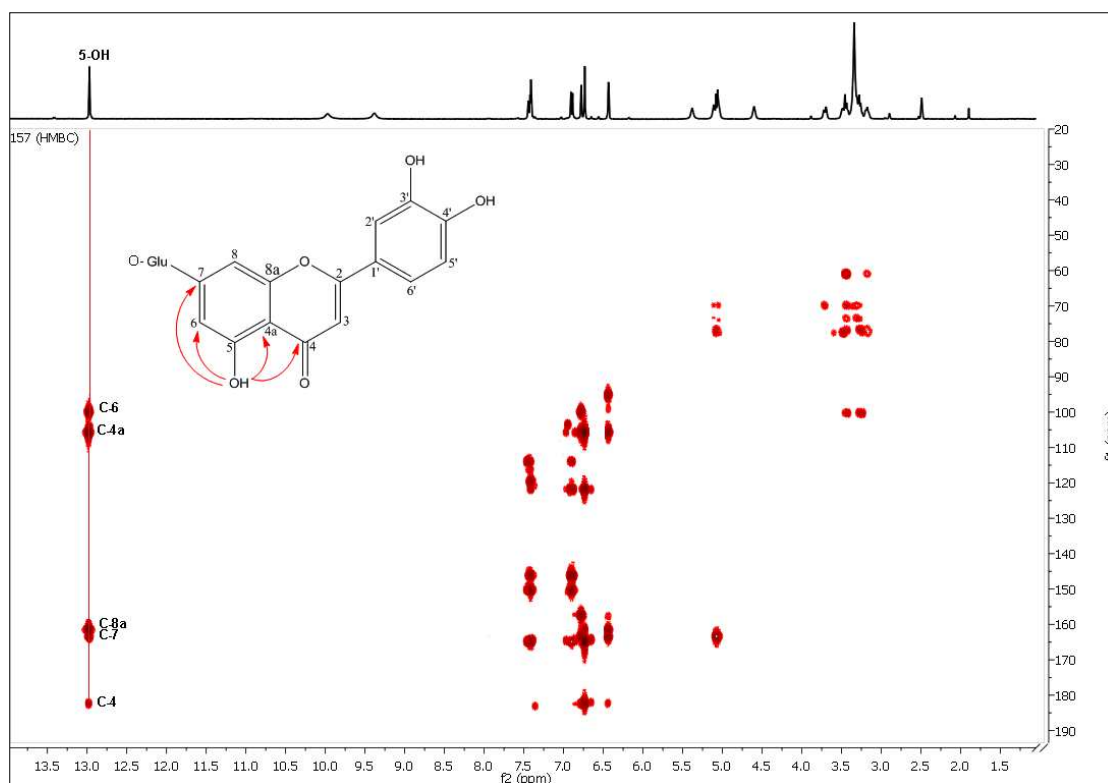


Figure IV.49. HMBC-NMR Spectrum (400 MHz, DMSO-*d*₆) of compound **5**.

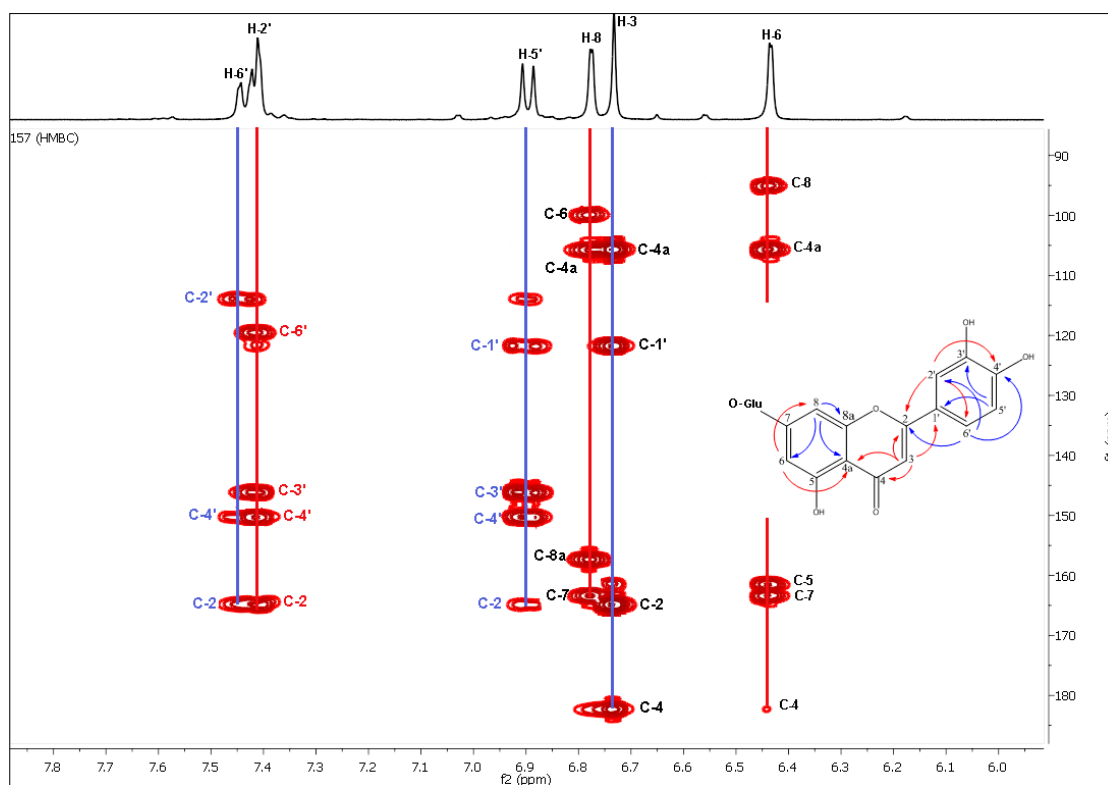


Figure IV.50. HMBC-NMR Spectrum (400 MHz, DMSO-*d*₆) of compound **5**.
(From 6.00 ppm to 7.80 ppm).

- ✓ The H-6' proton showed three (3) correlations: The first with a carbon at δ_C 113.5 ppm, attributable to C-2', the second correlation with a carbon at δ_C 149.8 ppm attributable to C-4', and with a carbon at δ_C 164.9 ppm attributable to C-2.
- ✓ The H-2' proton showed four (4) correlations: with a carbon at δ_C 119.6 ppm, attributable to C-6', the second correlation with a carbon at δ_C 149.8 ppm attributable to C-4', the third with a carbon at δ_C 164.9 ppm attributable to C-2, this last correlation confirm the attachment of the aromatic cycle with the B cycle on carbon C-2. The last correlation with a carbon at δ_C 146.1 ppm attributable to the carbon C-3'.
- ✓ The H-5' proton showed three (3) correlations: firstly with a carbon at δ_C 121.6 ppm, attributable to C-1', secondly correlation with a carbon at δ_C 146.1 ppm attributable to C-3', the third with a carbon at δ_C 149.8 ppm attributable to C-4'.
- ✓ The H-8 proton showed four (4) correlations: The first with a carbon at δ_C 99.5 ppm, attributable to C-6, the second correlation with a carbon at δ_C 105.8 ppm attributable to the quaternary carbon C-4'a, the third with a carbon at δ_C 163.2 ppm attributable to C-7. The last correlation with a carbon at δ_C 157.4 ppm attributable to the carbon C-8a.
- ✓ The H-3 proton showed four (4) correlations with a carbon at δ_C 105.8 ppm, attributable to C-4a, the second correlation with a carbon at δ_C 121.6 ppm attributable to C-1', this correlation confirm the attachment of the B cycle with the aromatic cycle on carbon C-1'. The third with a carbon at δ_C 182.3 ppm attributable to the carbonyl group on C-4. The last correlation with a carbon at δ_C 164.9 ppm attributable to the carbon C-2.
- ✓ The H-6 proton showed four (4) correlations: The first with a carbon at δ_C 95.0 ppm, attributable to C-8, the second correlation with a carbon at δ_C 105.8 ppm attributable to C-4a, the third with a carbon at δ_C 161.3 ppm attributable to the carbon on C-5. The last correlation with a carbon at δ_C 163.2 ppm attributable to the carbon C-7.

All these HMBC correlations confirm the structure of the aglycon part of this compound as a Luteolin.

The examination of the HMBC spectrum of the sugar region (upfield region) (**Fig. IV.51**) of the spectrum showed other correlations tasks identified as follows:

- ✓ The anomeric proton H-1'' showed three (3) correlations: The first with a carbon at δ_C 163.2 ppm, attributable to C-7 confirm the attachment of the sugar moiety with the aglycon on C-7, the second correlation with a carbon at δ_C 77.1 ppm attributable to C-3'', and with a carbon at δ_C 77.2 ppm attributable to C-5''.
- ✓ The two protons H-6''a and H-6''b on C-6'' showed the only possible correlation with a carbon at 77.2 ppm attributable to C-5''.
- ✓ The proton H-5'' showed three (3) correlations: The first with the carbon at δ_C 100.5 ppm attributable to C-1'' of the anomeric proton, the second correlation with a carbon at δ_C 77.1 ppm attributable to C-3'', and a correlation with a carbon at δ_C 60.5 ppm attributable to C-6''.

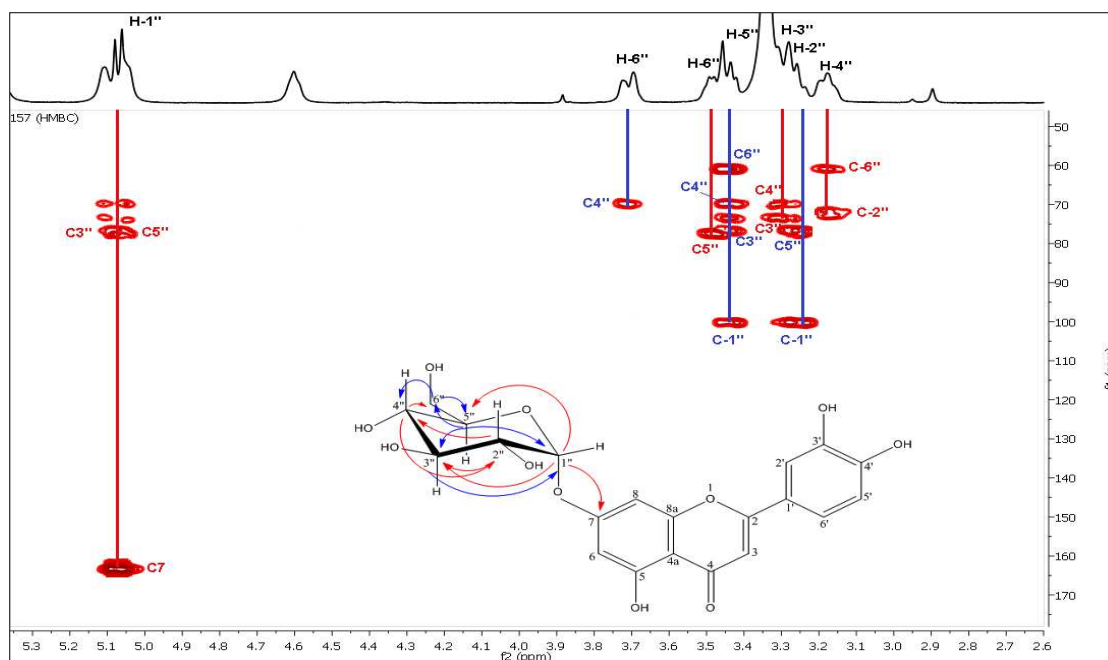


Figure IV.51. HMBC-NMR Spectrum (400 MHz, DMSO-*d*₆) of compound **5**.
(From 2.60 ppm to 5.30 ppm).

- ✓ The proton H-3'' showed two (2) correlations: The first with the carbon at δ_C 100.5 ppm attributable to C-1'' of the anomeric proton, the second correlation with a carbon at δ_C 77.2 ppm attributable to C-5''.
- ✓ The proton H-2'' showed the only possible correlation with a carbon at 72.0 ppm attributable to C-4''.
- ✓ The proton H-4'' showed two (2) correlations: The first with the carbon at δ_C 73.0 ppm attributable to C-2'' and a second with a carbon at δ_C 60.5 ppm attributable to C-6''.

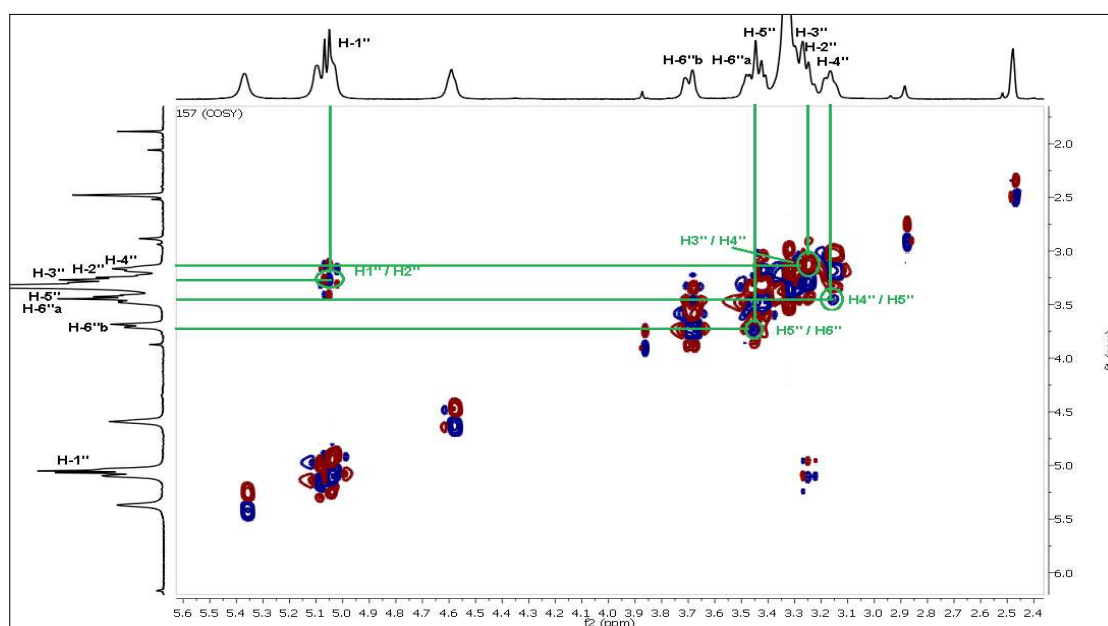


Figure IV.52. ¹H-¹H COSY-NMR Spectrum (400 MHz, DMSO-*d*₆) of compound **5**

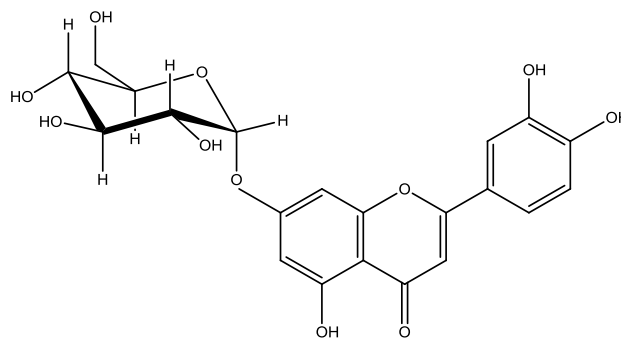
The interpretation of the correlations observed on the ^1H - ^1H COSY spectrum (Fig. IV.52) between the anomeric H-1'' at δ_{H} 5.06 ppm (*d*, $J=7.3$ Hz) and the proton at δ_{H} 3.25 ppm (*m*), allowed to identify the proton H-2'', as well as the identification of the other osidic protons H-3'', H-4'', H-5'', H-6''*a* and H-6''*b*.

All the chemical shifts of the NMR analysis (^1H , ^{13}C , HSQC and HMBC) of compound **5** are summarized in the following table (Table IV.12).

Table IV.12. ^1H , ^{13}C and HMBC NMR data (400 MHz) of compound **5** (DMSO-*d*₆).

Positions	δ_{C} (ppm)	δ_{H} (ppm), <i>mult.</i> , J (Hz)	HMBC
1	-	-	-
2	164.9	-	-
3	103.4	6.72 (<i>s</i> , 1H)	C-4a, C-1', C-4, C-2
4	182.3	-	-
5	161.3	-	-
6	99.5	6.42 (<i>d</i> , 1H, $J=1.6$ Hz)	C-8, C-4a, C-5, C-7
7	163.2	-	-
8	95.0	6.77 (<i>d</i> , 1H, $J=1.6$ Hz)	C-6, C-4a, C-7, C-8a
4a	105.8	-	-
8a	157.4	-	-
1'	121.6	-	-
2'	113.5	7.40 (<i>s</i> , 1H)	C-6', C-4', C-3', C-2
3'	146.1	-	-
4'	149.8	-	-
5'	116.2	6.89 (<i>d</i> , 1H, $J=8.2$ Hz)	C-1', C-3', C-4'
6'	119.6	7.42 (<i>dd</i> , 1H, $J=8.2-2.0$ Hz)	C-4', C-2', C-2
1''	100.5	5.06 (<i>d</i> , 1H, $J=7.3$ Hz)	C-3'', C-5'', C-7
2''	73.0	3.25 (<i>m</i> , 1H)	C-4''
3''	77.1	3.28 (<i>m</i> , 1H)	C-1'', C-5''
4''	72.0	3.22 (<i>m</i> , 1H)	C-2'', C-6''
5''	77.2	3.44 (<i>m</i> , 1H)	C-1'', C-3'', C-6''
6''<i>a</i>	60.5	3.45 (<i>m</i> , 1H)	C-5''
6''<i>b</i>	60.5	3.70 (<i>m</i> , 1H)	C-4''
5-OH	-	12.96 (<i>s</i> , 1H)	C-6, C-4a, C-4, C-7

All these ESI-MS, UV-Visible and NMR data confirm the structure of the compound **5** as a **3', 4', 5, tetrahydroxy 7-O-glucosyl flavone** known as: **luteolin-7-O-glucosyl**. [10].



Luteolin-7-o-glucosyl

IV.5.6. Identification of compound 6

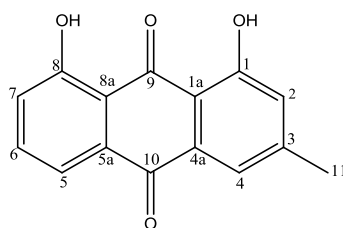


Figure IV.53. Structure of compound 6

Compound 6 was obtained as an orange powder. The UV-Visible spectrum showed a maximal absorption at 224, 250, 280 and 410 nm, suggestive of an anthraquinone structure [20]. The ESI-MS recorded on positive mode (**Fig. IV.54**) gave an $[M+H]^+$ ion at $m/z = 255.0$ consistent with the molecular formula of $C_{15}H_{10}O_4$ with 11 unsaturations.

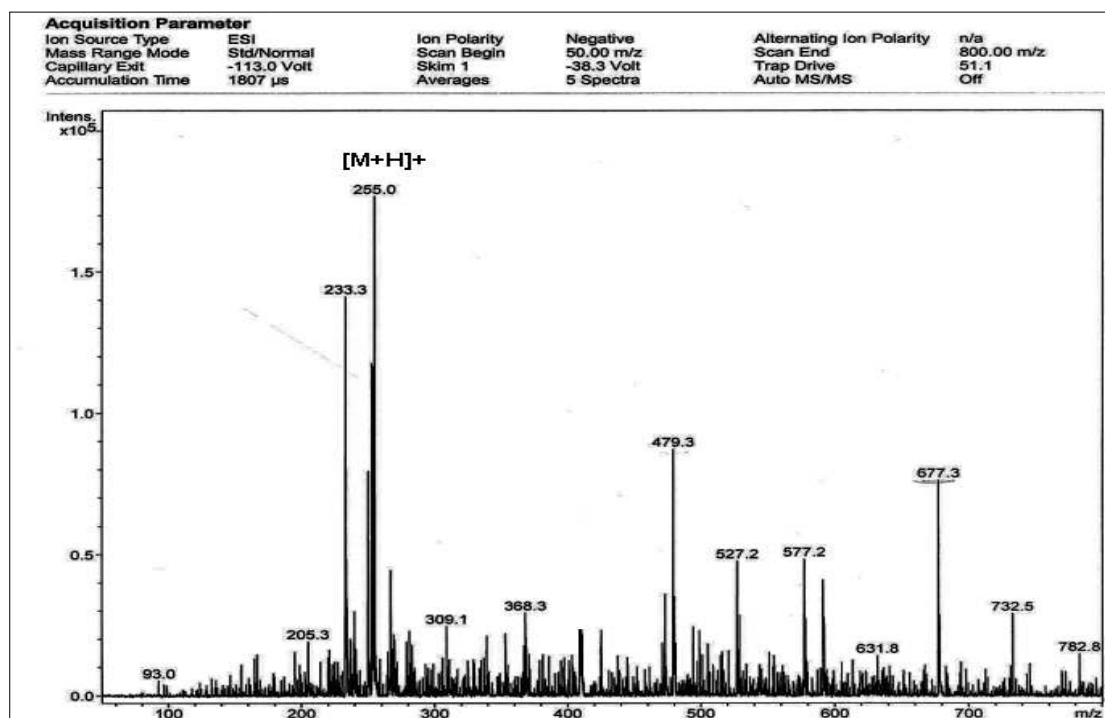


Figure IV.54. ESI-MS spectrum in negative ion mode of compound 6.

The 1H -NMR spectrum of Compound 6 (**Fig. IV.55** and **Fig. IV.56**) showed two highly deshielded singlets at δ_H 12.02 ppm and δ_H 12.13 ppm which can correspond to the two chelated hydroxyl groups. The position of these two chelated hydroxyl groups will be demonstrated later with the analysis of the HMBC spectrum. The 1H -NMR spectrum showed also a pair of *meta*-coupled protons at δ_H 7.11 ppm (1H, *s*, H-2) and δ_H 7.66 ppm (1H, *d*, $J = 2.2$ Hz, H-4) with the C-3 attached methyl at δ_H 2.47 ppm (3H, *s*). In addition to an ABX spin system was observed at δ_H

7.83 ppm (1H, *d*, $J = 7.3$ Hz, H-5), δ_{H} 7.69 ppm (1H, *t*, $J = 9.5$ Hz, H-6) and δ_{H} 7.30 ppm (1H, *d*, $J = 8.6$ Hz, H-7).

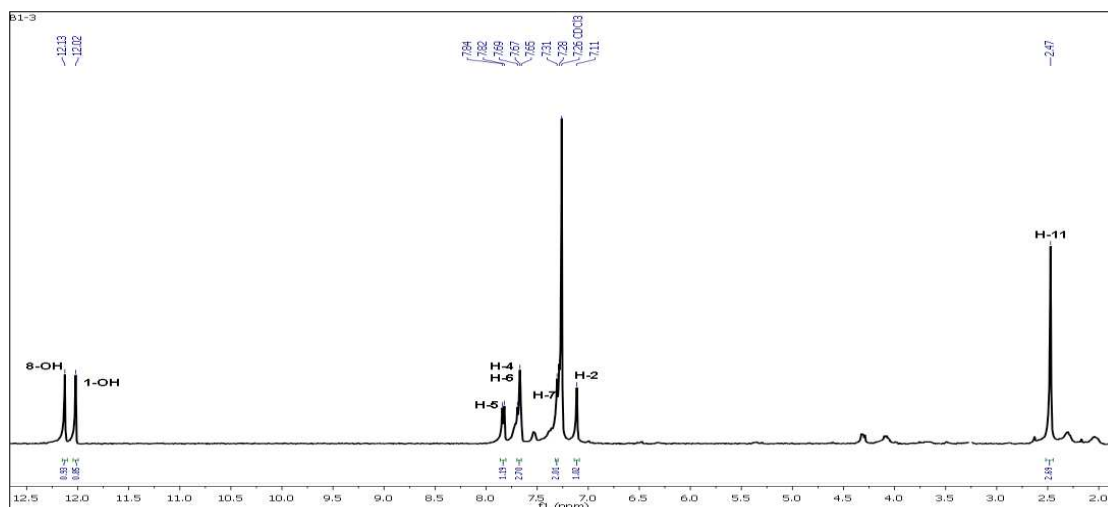


Figure IV.55. ¹H-NMR Spectrum (400 MHz, CDCl₃) of compound 6.

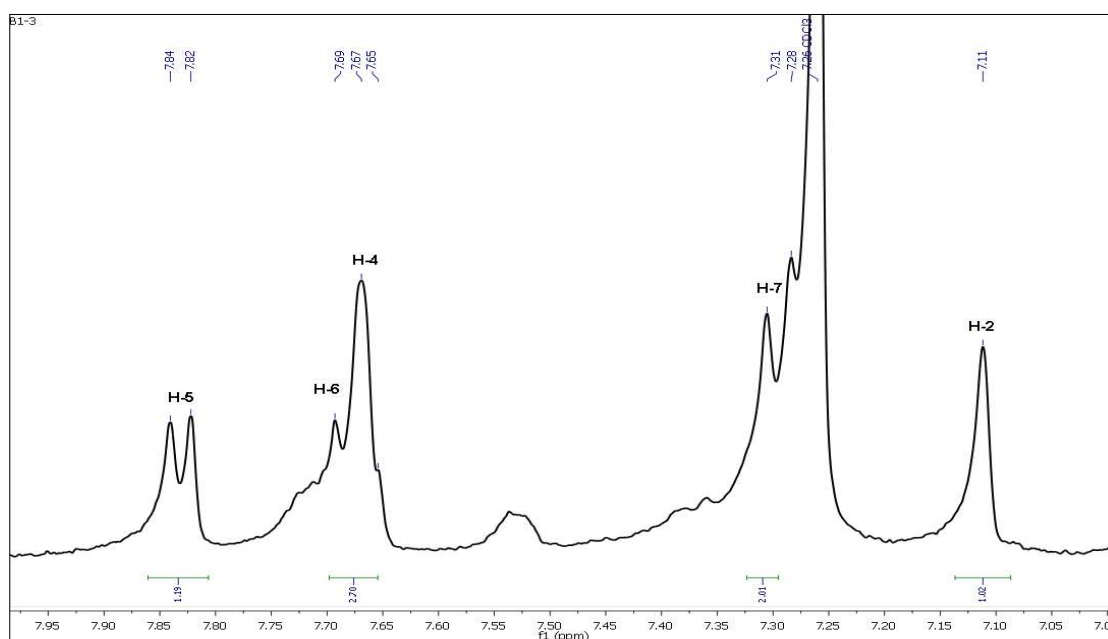


Figure IV.56. ¹H-NMR Spectrum (400 MHz, CDCl₃) of compound 6.
(From 7.00 ppm to 8.00 ppm).

The examination of the HSQC spectrum (**Fig. IV.57**) recorded in CDCl₃ showed the presence of some correlations identified as follow:

- ✓ The proton H-2 showed a correlation with the carbon C-2 at δ_{C} 124.4 ppm.
- ✓ The proton H-4 showed a correlation with the carbon C-4 at δ_{C} 121.2 ppm.
- ✓ The proton H-7 showed a correlation with the carbon C-4 at δ_{C} 124.4 ppm.
- ✓ The proton H-6 showed a correlation with the carbon C-4 at δ_{C} 138.7 ppm.

- ✓ The proton H-5 showed a correlation with the carbon C-4 at δ_C 119.9 ppm.
- ✓ The protons of the methyl group 11-CH₃ showed a correlation with the carbon C-11 at δ_C 22.4 ppm.
- ✓ No correlations were observed for the protons of the proposed chelated hydroxyl groups at δ_H 12.03 ppm and δ_H 12.13 ppm which confirm that are two hydroxyl groups [15].

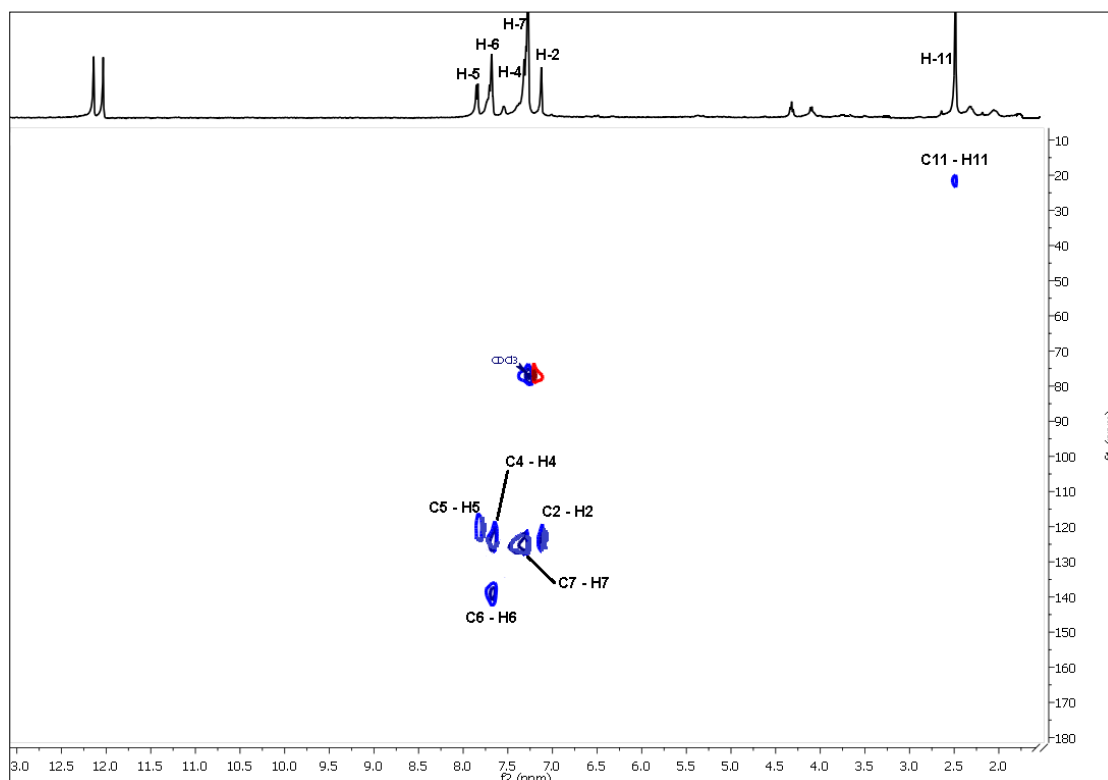


Figure IV.57. HSQC-NMR Spectrum (400 MHz, CDCl₃) of compound **6**.

The examination of the HMBC spectrum (**Fig. IV.58** and **Fig. IV.59**) recorded in CDCl₃ showed the presence of many correlations identified as follow:

- ✓ The methyl group (CH₃) at δ_H 2.47 ppm showed three (3) correlations: the first with a carbon at δ_C 124.4 ppm attributable to C-2, the second with a carbon at δ_C 121.2 ppm attributable to C-4 and a third correlation with a carbon at δ_C 149.3 ppm attributable to C-3, this correlation confirm the position of the methyl group on the carbon C-3 of the aromatic ring.
- ✓ The hydroxyl group (OH) at δ_H 12.03 ppm showed three (3) correlations: the first with the carbon at δ_C 162.7 ppm (Carbonyl group) attributable to C-1, the second with the carbon at δ_C 124.4 ppm attributable to C-2 and the third with a carbon at 113.8 ppm attributable to the quaternary carbon C-1a. These correlations confirm the position on the hydroxyl group at the carbon C-1.
- ✓ The second hydroxyl group (OH) at δ_H 12.13 ppm showed three (3) correlations: the first with the carbon at δ_C 162.4 ppm (carbonyl group) attributable to C-8, the second with the carbon at δ_C 124.4 ppm attributable to C-7 and the third with a carbon at 115.9 ppm attributable to the quaternary carbon C-

8a. These correlations confirm the position on the second hydroxyl group at the carbon C-8.

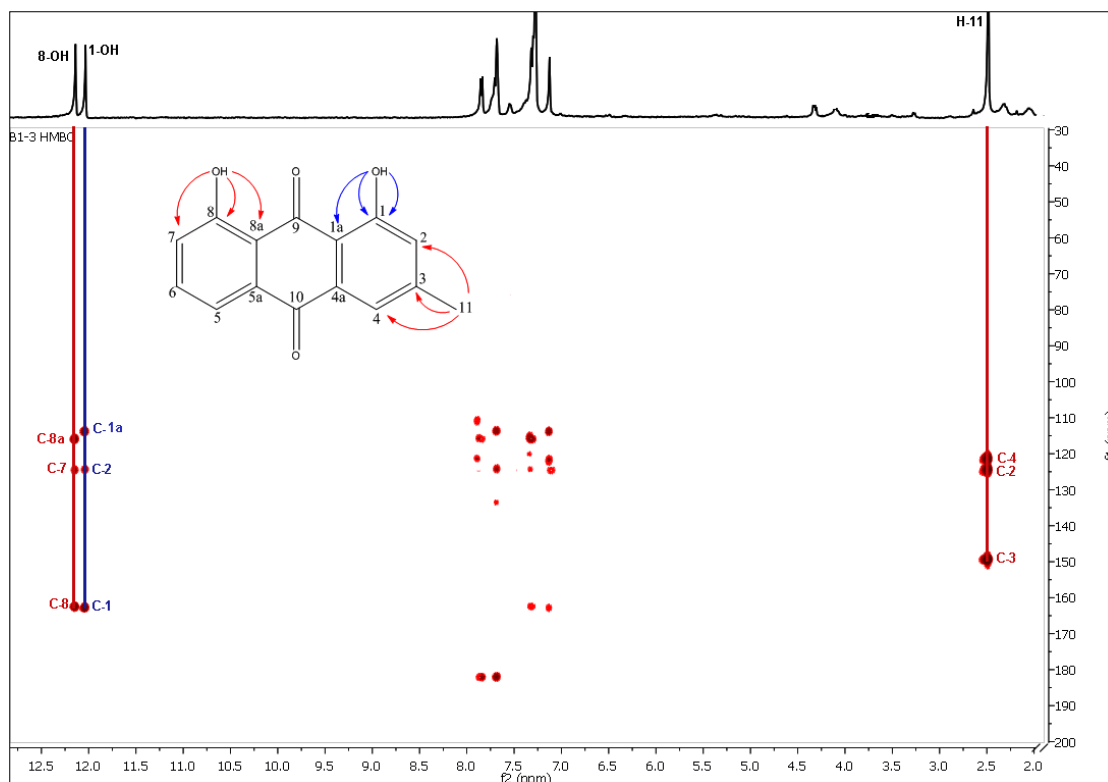


Figure IV.58. HMBC-NMR Spectrum (400 MHz, CDCl_3) of compound **6**.

- ✓ The H-2 proton showed four (4) correlations: The first with a carbon at δ_{C} 113.8 ppm, this carbon showed two other correlations with the protons H-4 and the hydroxyl group 1-OH, so this carbon can be only quaternary C-1a, the second correlation with a carbon at δ_{C} 162.9 ppm attributable to C-1, the third with a carbon at δ_{C} 121.2 ppm attributable to C-4 and the fourth with a carbon at δ_{C} 22.4 ppm, attributable to the methyl group 11- CH_3 .
- ✓ The H-7 proton showed three (3) correlations: The first with a carbon at δ_{C} 115.9 ppm, this carbon showed two other correlation tasks with the protons H-5 and the hydroxyl group 8-OH, so this carbon can be only quaternary C-8a, the second correlation with a carbon at δ_{C} 162.4 ppm attributable to C-8 and the third with a carbon at δ_{C} 119.9 ppm attributable to C-5.
- ✓ The H-4 proton showed three (3) correlations: The first with a quaternary carbon at δ_{C} 113.8 ppm attributable to C-1a, the second correlation with a carbon at δ_{C} 124.4 ppm attributable to C-2 and the third with a carbon of the carbonyl group at δ_{C} 182.2 ppm attributable to C-10.
- ✓ The H-6 proton showed only one (1) correlation with a carbon at δ_{C} 133.7 ppm attributable to the quaternary carbon C-5a.
- ✓ The H-5 proton showed three (3) correlations with a quaternary carbon at δ_{C} 115.9 ppm attributable to C-8a, the second correlation with a carbon at δ_{C} 124.4

ppm attributable to C-7 and the third with a carbon of the carbonyl group at δ_C 182.2 ppm attributable to C-10.

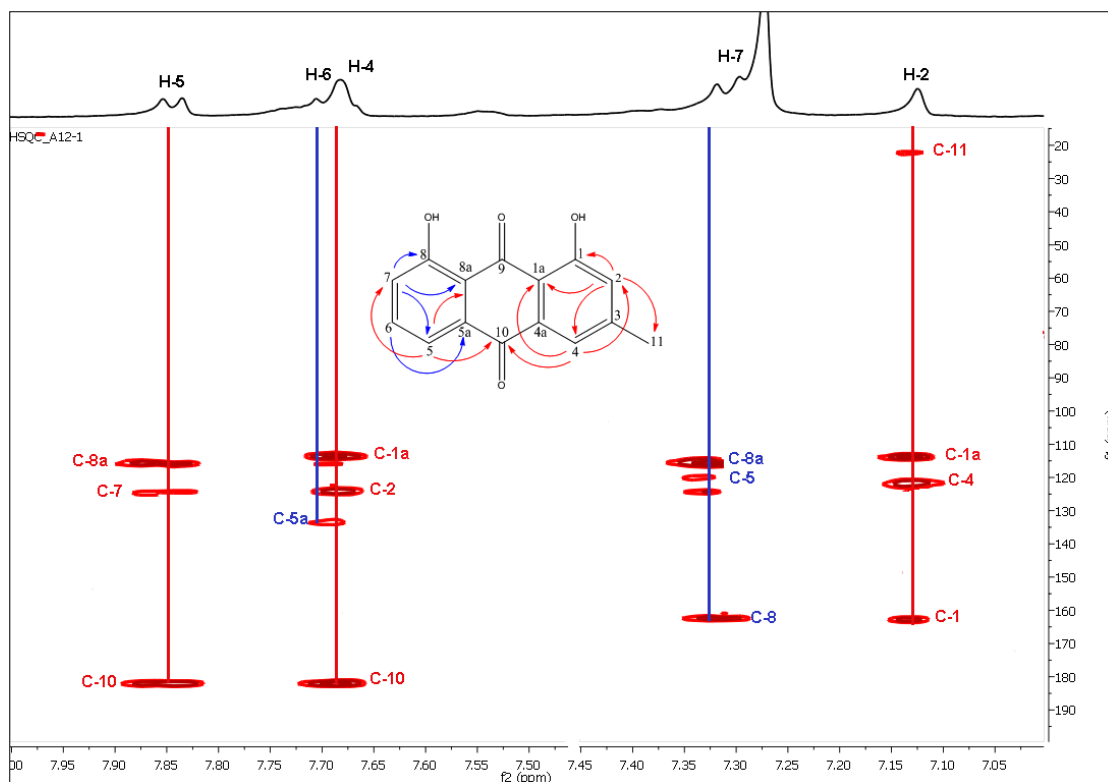


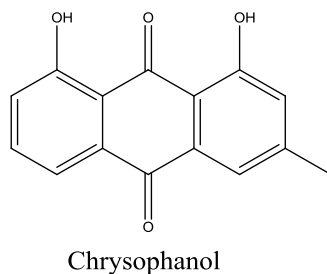
Figure IV.59. HMBC-NMR Spectrum (400 MHz, CDCl_3) of compound **6**.
(From 7.00 ppm to 8.00 ppm).

All the chemical shifts of the ^1H , ^{13}C , HSQC and HMBC NMR data of compound **6** are summarized in the following table (**Table IV.13**).

Table IV.13. ^1H NMR, ^{13}C and HMBC data (600 MHz) of compound **6** (CDCl_3).

Positions	δ_C (ppm)	δ_H (ppm), mult., J (Hz)	HMBC
1	162.7	-	-
2	124.4	7.11 (s, 1H)	C-1, C-1a, C-4, C-11
3	149.3	-	-
4	121.2	7.66 (d, 1H, $J=2.2$ Hz)	C-1a, C-2, C-10
5	119.9	7.83 (d, 1H, $J=7.3$ Hz)	C-8a, C-7, C-2
6	138.7	7.69 (t, 1H, $J=9.5$ Hz)	C-5a
7	124.4	7.30 (d, 1H, $J=8.6$ Hz)	C-8a, C-5, C-8
8	162.4	-	-
9	183.0	-	-
10	182.2	-	-
4a	133.0	-	-
5a	133.7	-	-
8a	115.9	-	-
1a	113.8	-	-
11	22.4	2.47 (s, 3H)	C-2, C-4, C-3
1-OH	-	12.02 (s, 1H)	C-1, C-2, C-1a
8-OH	-	12.13 (s, 1H)	C-8, C-7, C-8a

The HMBC correlations of this compound were confirmed the structure determination. Accordingly, compound **6** was identified as **1, 8-dihydroxy-3-methylantracene-9, 10-dione** or **Chrysophanol**, its spectral data were in very good agreement with the reported literatures [21] as well as reported previously from the *Asphodelus* genus [22].



IV.5.7. Identification of compound 7

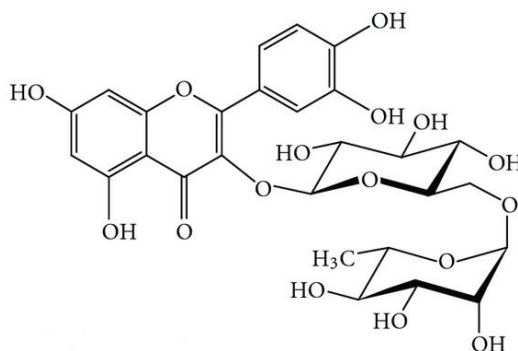


Figure IV.60. Structure of **compound 7**

Compound 7 was isolated as a yellow powder. It gave a visible spot on TLC on both 254 and 366 nm wavelengths and a yellow color after being sprayed by sulfuric acid and heated at 100°C. The mass experiment was carried out using ESI-MS in positif mode (**Fig. IV.61**) reveals a pseudo-molecular ion peak at $m/z = 611.15$ $[M+H]^+$ indicating a molecular weight of 610 uma corresponding to the molecular formula $C_{21}H_{20}O_{11}$ with 12 unsaturations.

The presence of a Quercetin aglycone for this compound is clearly deduced from the 1H and ^{13}C -NMR spectra analysis (**Fig. IV.62** and **Fig. IV.63**). The 1H -NMR spectrum showed the presence of the characteristic protons of a Quercetin skeleton: H-6 (δ_H 6.21 ppm, *d*, $J = 2.1$ Hz), H-8 (δ_H 6.39 ppm, *d*, $J = 2.1$ Hz), H-10 (δ_H 7.71 ppm, *d*, $J = 2.1$ Hz), H-13 (δ_H 6.91 ppm, *d*, $J = 8.4$ Hz) and H-14 (δ_H 7.65 ppm, *d*, $J = 8.3$ Hz).

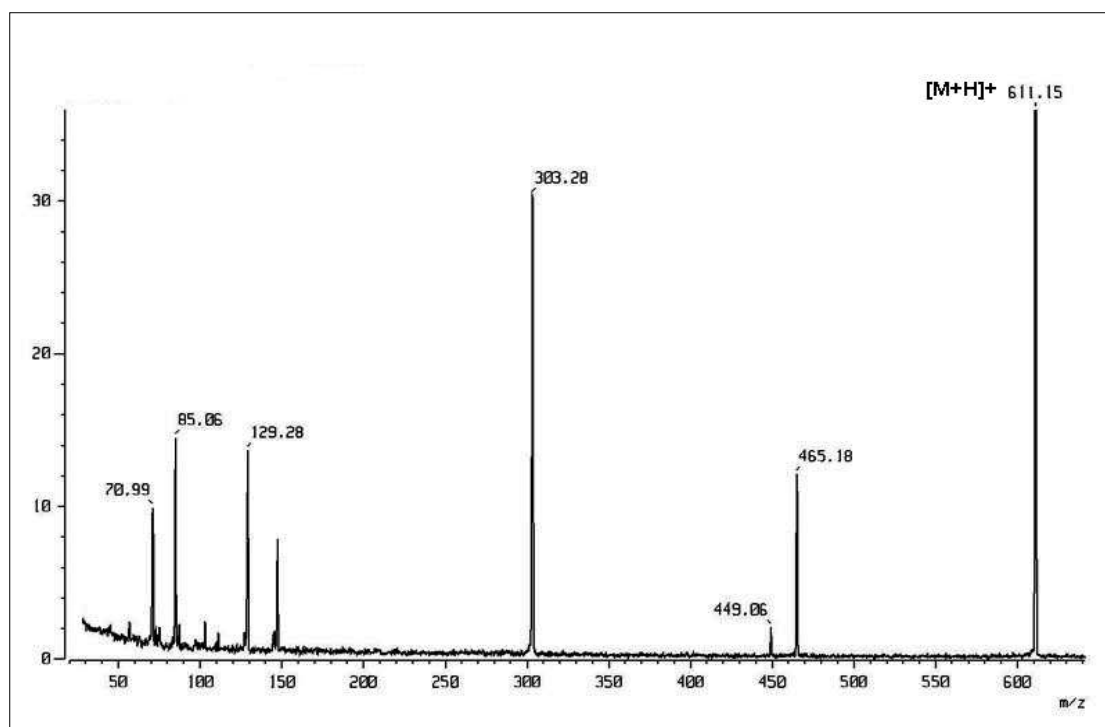


Figure IV.61. ESI-MS data in positive ion mode of **compound 7**

The osidic zone of the ^1H and ^{13}C -NMR spectrums (**Fig. IV.62** and **Fig. IV.63**) of this compound showed 10 oxymethoxy groups, one oxymethylene group and a methyl group, thus suggesting the presence of two hexose units having protons and carbons anomeric signals at $[\text{H}-1']$ (δ_{H} 5.11 ppm, d , $J = 7.7$ Hz) / (δ_{C} 104.4 ppm) and $[\text{H}-1'']$ (δ_{H} 4.42 ppm, d , $J = 1.6$ Hz) / (δ_{C} 102.1 ppm)].

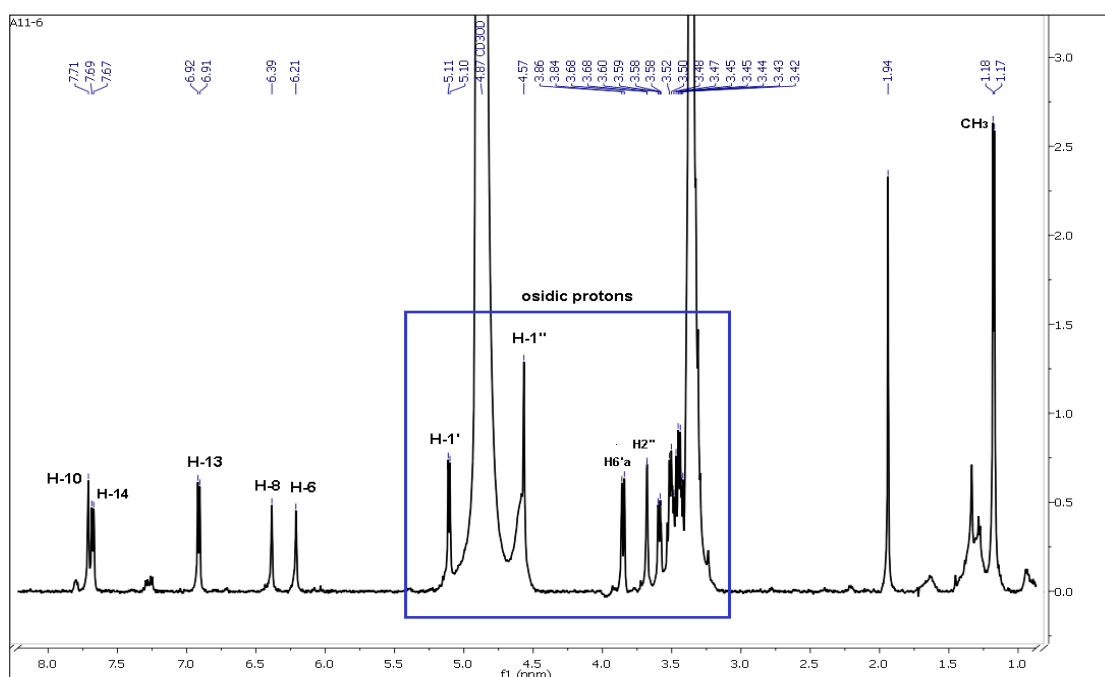


Figure IV.62. ^1H -NMR Spectrum (600 MHz, CD_3OD) of **compound 7**.

The presence of a possible hexose unit (glucose) was demonstrated by the observed correlations on the ^1H - ^1H COSY spectrum (Fig. IV.65) between the H-1' anomeric proton (δ_{H} 5.11 ppm, *d*, $J = 7.7$ Hz) and the H-2' proton (δ_{H} 3.49 ppm, *dd*, $J = 8.4$ - 7.7 Hz), as well as between the protons H-2'/ H-3' (δ_{H} 3.43 ppm, *m*) / H-4' (δ_{H} 3.29 ppm, *m*) / H-5' (δ_{H} 3.41 ppm, *m*) / H-6'a (δ_{H} 3.82 ppm, *dd*, $J = 10.7$ - 4.9 Hz) and H-6'b (δ_{H} 3.40 ppm, *dd*, $J = 10.7$ - 5.0 Hz) of the same system of spins. The large values of the coupling constants of these protons confirm our suggestions for the presence of a glucose. The coupling of protons H-1' and H-2' with $J=7.7$ Hz assign for this glucose a β configuration (β -D-glucose).

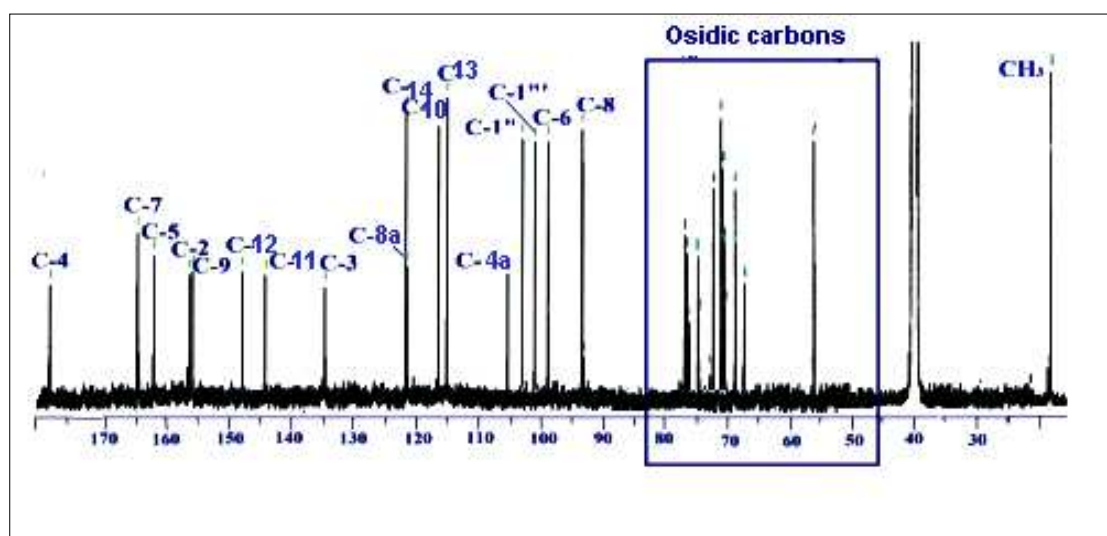


Figure IV.63. ^{13}C -NMR Spectrum (600 MHz, CD_3OD) of compound 7.

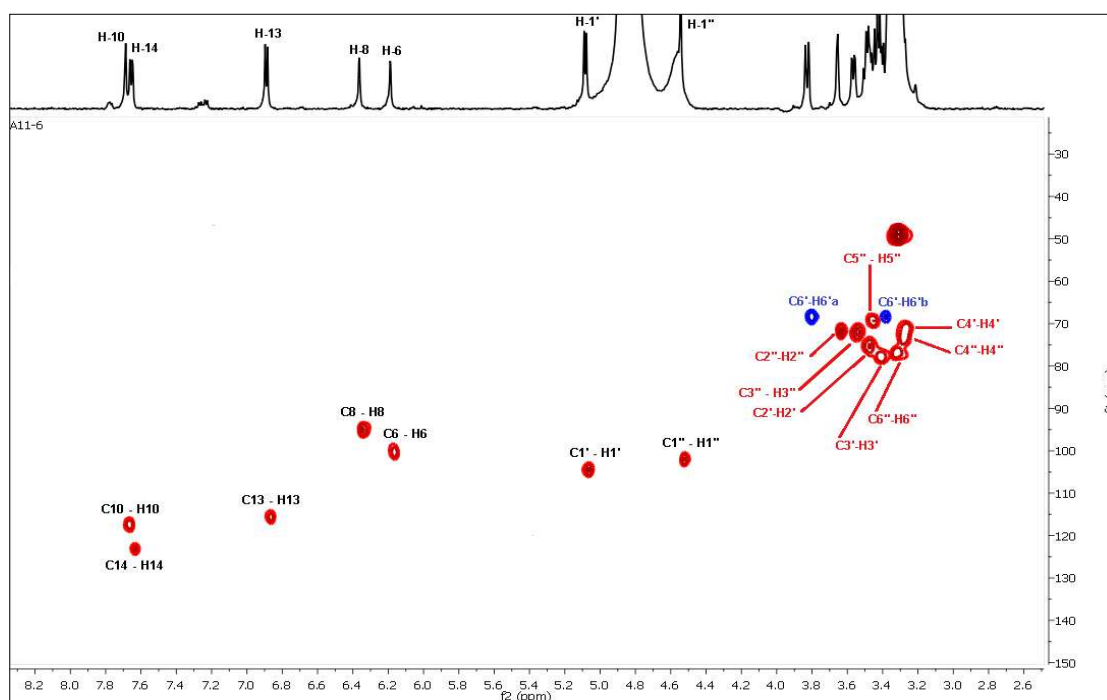


Figure IV.64. HSQC-NMR Spectrum (600 MHz, CD_3OD) of compound 7.

Thus, the presence of a possible rhamnose unit was evidenced following to the analysis of the correlations observed on the COSY spectrum (**Fig. IV.65**) of the remaining osidic protons starting from the second anomeric proton H-1'' (δ_{H} 4.57 ppm, *d*, $J = 1.6$ Hz). These correlations make it possible to identify the sequence H-1''/ H-2'' (δ_{H} 3.68 ppm, *d*, $J = 3.2$ Hz) / H-3'' (δ_{H} 3.55 ppm, *dd*, $J = 9.4-3.2$ Hz) / H-4'' (δ_{H} 3.30 ppm, *m*) / H-5'' (δ_{H} 3.47 ppm, *m*) / H-6'' (δ_{H} 3.34 ppm, *d*, $J = 6.2$ Hz). The values of coupling constants indicate an equatorial orientation for the protons H-1'' and H-2'' and an axial arrangement for the protons H-3'', H-4'' and H-5'' confirming the existence of the osidic unit α -L-rhamnose.

The osidic chain was determined to be a rutinoside imply a junction (1 \rightarrow 6) glucose-rhamnose, due firstly, to the deshielding of the carbon C-6' (δ_{C} 68.3 ppm) of the glucose compared with C-6' terminal glucose (δ_{C} 61.1 ppm) and secondly, to the chemical shift value of the C-1'' anomeric carbon (δ_{C} 101.9 ppm) of rhamnose.

The interglycosidic bond was confirmed by the correlation spot observed on the HMBC spectrum (**Fig. IV.66**) between the anomeric proton H-1'' and the carbons C-6 constituting the rutinoside unit. The correlation of the anomeric proton H-1'' with the C-3 carbon of the aglycone reveals the point of attachment of the rutinoside unit to the aglycone quercetin.

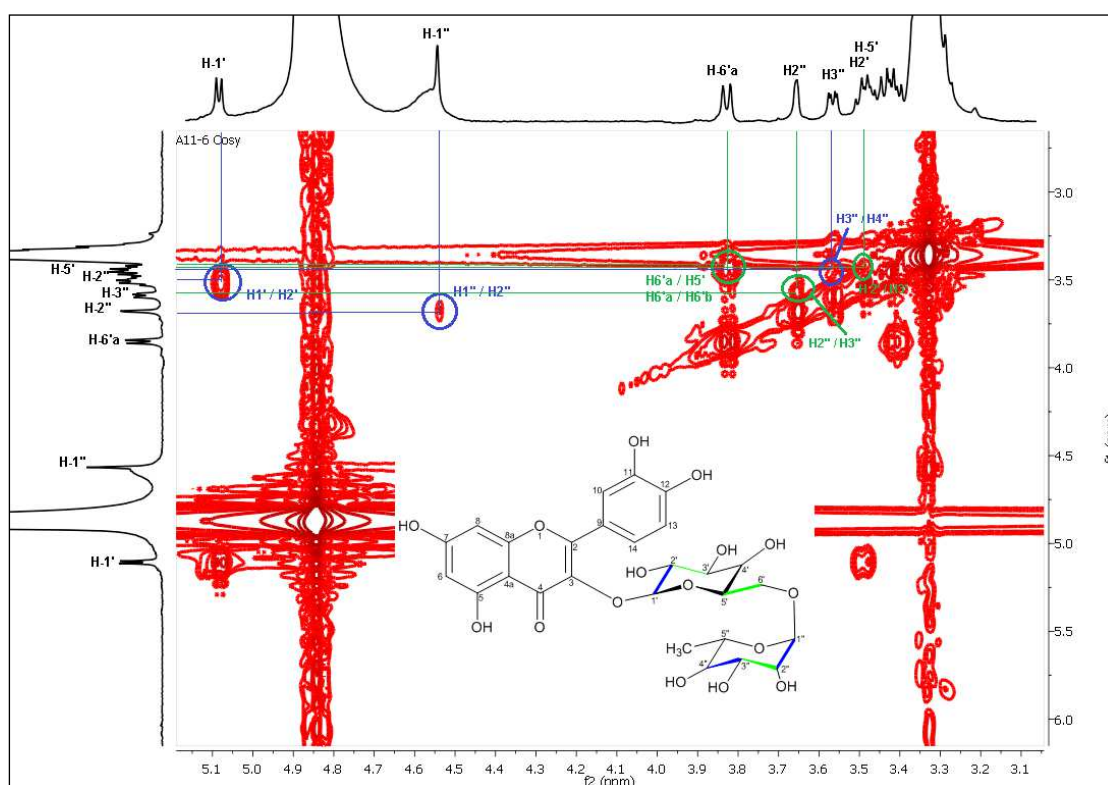


Figure IV.65. ^1H - ^1H COSY-NMR Spectrum (600 MHz, CD_3OD) of compound **7**. (From 3.00 ppm to 5.10 ppm).

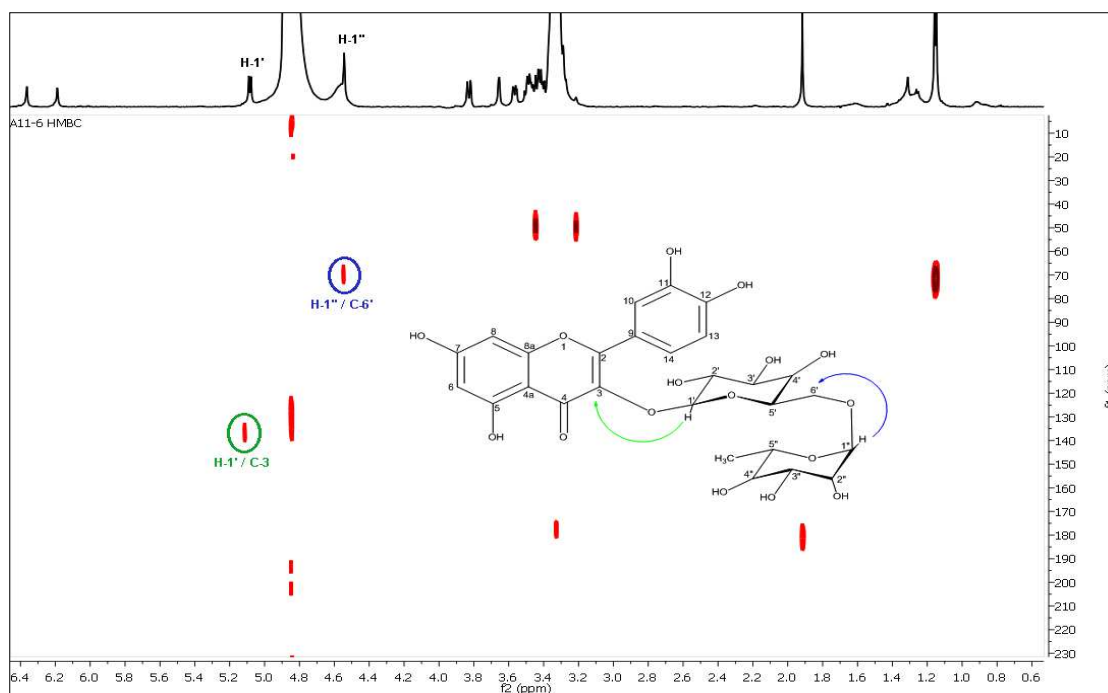


Figure IV.66. HMBC-NMR Spectrum (600 MHz, CD₃OD) of compound **7**.
(From 0.50 ppm to 6.50 ppm).

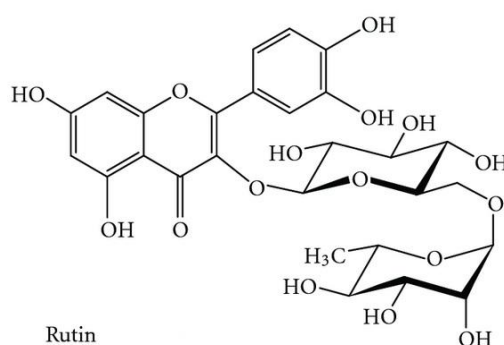
All the chemical shifts of the NMR proton and carbon data of compound **7** are summarized in the (Table IV.14).

Table IV.14. ¹H-NMR and ¹³C data (600 MHz) of compound **7** (CD₃OD).

Positions	δ_C (ppm)	δ_H (ppm), <i>mult.</i> , <i>J</i> (Hz)
1	-	-
2	158.9	-
3	135.3	-
4	178.2	-
5	162.5	-
6	100.3	6.21 (<i>d</i> , 1H, <i>J</i> =2.1 Hz)
7	165.6	-
8	95.0	6.39 (<i>d</i> , 1H, <i>J</i> =2.1 Hz)
9	158.1	-
10	117.4	7.71 (<i>d</i> , 1H, <i>J</i> =2.1 Hz)
11	145.3	-
12	149.1	-
13	115.6	6.91 (<i>d</i> , 1H, <i>J</i> =8.4 Hz)
14	123.2	7.65 (<i>d</i> , 1H, <i>J</i> =8.3 Hz)
1'	104.2	5.11 (<i>d</i> , 1H, <i>J</i> =7.7 Hz)
2'	75.3	3.49 (<i>dd</i> , 1H, <i>J</i> =8.4-7.7 Hz)
3'	77.9	3.43 (<i>m</i> , 1H)
4'	71.2	3.29 (<i>m</i> , 1H)
5'	77.8	3.41 (<i>m</i> , 1H)
6'a	68.3	3.82 (<i>dd</i> , 1H, <i>J</i> =10.7-4.9 Hz)
6'b	68.3	3.40 (<i>dd</i> , 1H, <i>J</i> =10.7-5.0 Hz)
1''	101.9	4.57 (<i>d</i> , 1H, <i>J</i> =1.6 Hz)

2''	71.8	3.68 (<i>d</i> , 1H, <i>J</i> =3.2 Hz)
3''	71.9	3.55 (<i>dd</i> , 1H, <i>J</i> =9.4-3.2 Hz)
4''	73.3	3.30 (<i>m</i> , 1H)
5''	69.3	3.47 (<i>m</i> , 1H)
CH ₃	17.6	1.15 (<i>d</i> , 3H)

All these spectroscopic data and the comparison with those of the literature [23] make it possible to assign the structure for compound **7** as **Quercetin-3-O-rutinoside (Rutin)**. This compound was previously isolated from many species [24] [25], as well as from the *Asphodelus* genus [26].



IV.5.8. Identification of compound **8**

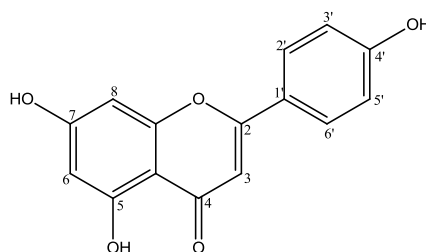


Figure IV.67. Structure of compound **8**.

Compound 8 was isolated as a yellow powder. It has shown a visible black-violet spot on 366 nm wavelengths. The ESI-MS on negative ion mode gave an ion peak at $m/z = 269$ attributable to pseudomolecular anion $[M-H]^-$ in agreement with a molecular formula of $C_{15}H_{10}O_5$ with 11 unsaturations.

The examination of the 1H -NMR spectrum (**Fig. IV.68** and **Fig. IV.69**) showed the possibility to have a flavonoid skeleton (flavone type). In more details, the 1H NMR spectrum of this compound **8** exhibited two doublets of *meta* coupled aromatic protons at δ_H 6.19 ppm (1H, *d*, *J* = 2.1 Hz) and δ_H 6.48 ppm (1H, *d*, *J* = 2.0 Hz) attributed to protons H-6 and H-8 respectively, of A ring of a flavones moiety. Signals of two vicinal *ortho* coupled aromatic protons at δ_H 7.92 ppm (2H, *d*, *J* = 8.8 Hz) and δ_H 6.92 ppm (2H, *d*, *J* = 8.8 Hz) were assigned to H2'/6' and H3'/5' respectively, of

the B ring. Additionally, the singlet appearing at δ_{H} 6.78 ppm was ascribed to vinyl proton H-3 belonging to C-ring.

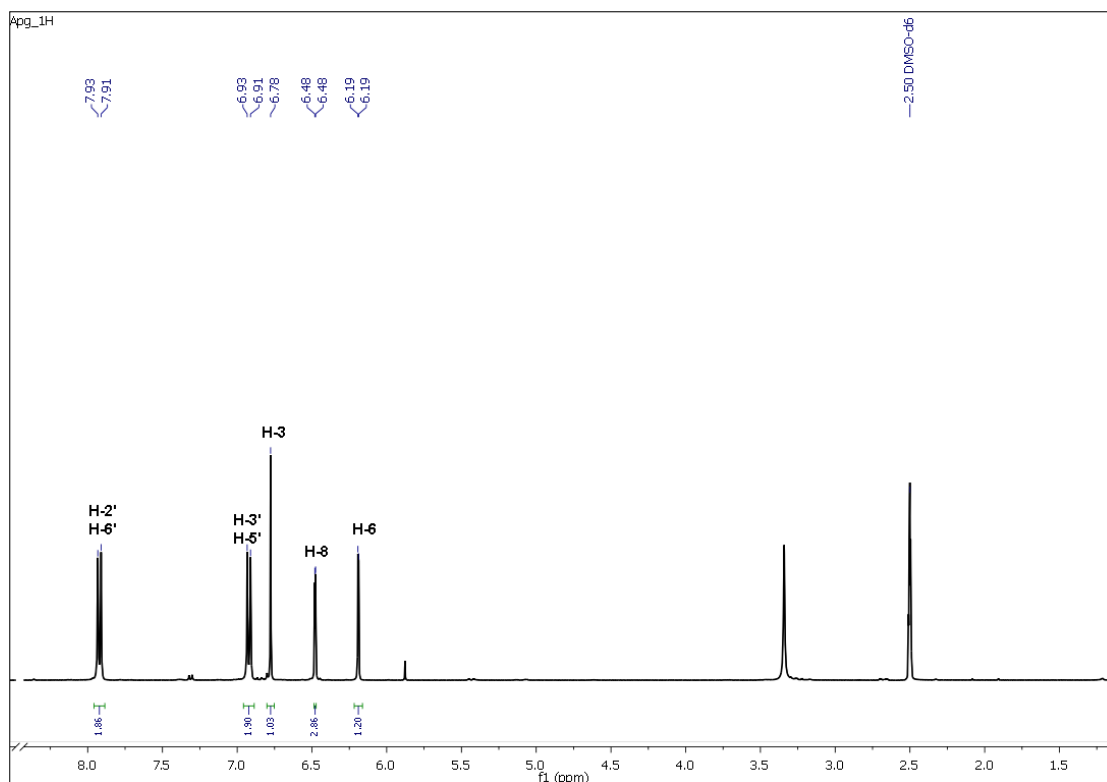


Figure IV.68. $^1\text{H-NMR}$ Spectrum (400 MHz, DMSO-*d*₆) of compound 8.

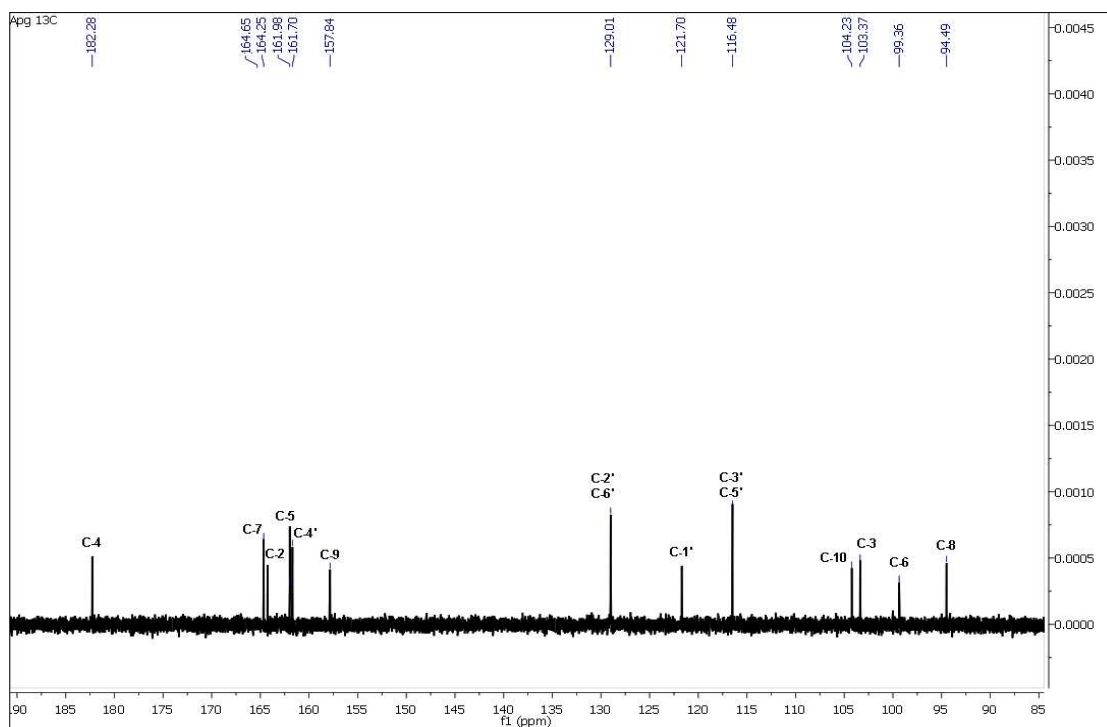


Figure IV.69. $^{13}\text{C-NMR}$ Spectrum (100 MHz, DMSO-*d*₆) of compound 8.

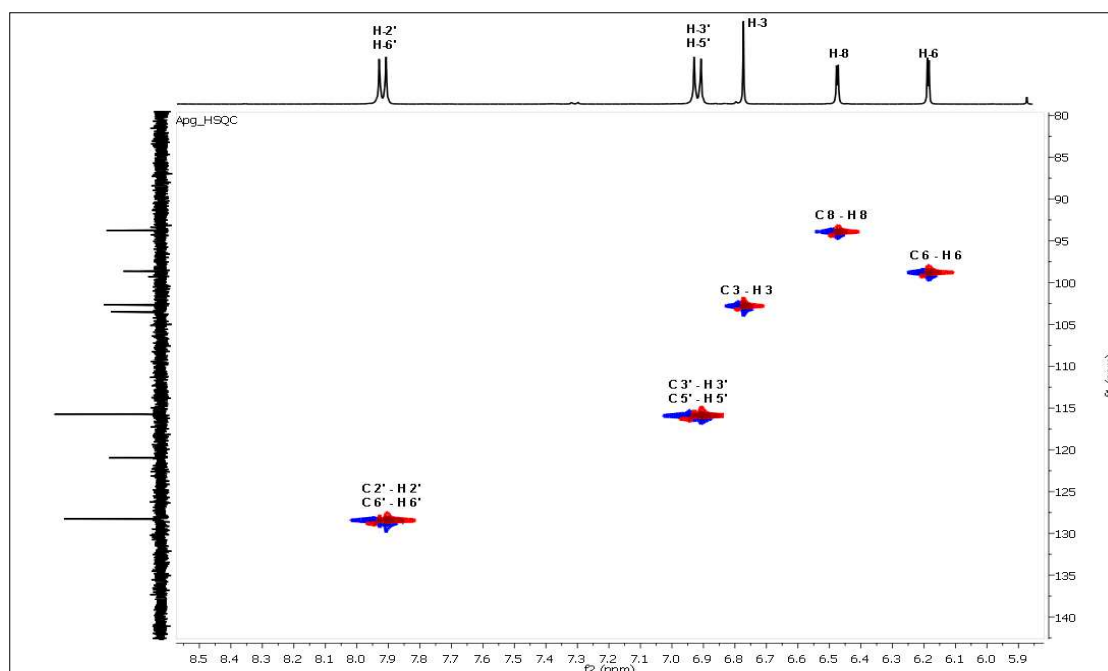


Figure IV.70. HSQC-NMR Spectrum (400 MHz, DMSO-*d*₆) of compound **8**.

The examination of the HSQC spectrum (**Fig. IV.70**) recorded in DMSO-*d*₆ showed the presence of many correlations identified as follow:

- ✓ The protons H-2' and H-6' showed a correlation with the carbons C-2' and C-6' respectively, at δ_C 129.0 ppm.
- ✓ The protons H-3' and H-5' showed a correlation with the carbons C-3' and C-5' respectively at δ_C 116.4 ppm.
- ✓ The protons H-3, H-8 and H-6 correlate with the carbons C-3, C-8 and C-6 at δ_C 103.3, 94.4 and 99.3 ppm, respectively.

Examination of the HMBC spectrum (**Fig. IV.71**) recorded in DMSO-*d*₆ showed the presence of many correlations identified as follow:

- ✓ The H-6 proton showed four (4) correlations: The first with a quaternary carbon at δ_C 104.2 ppm, this carbon shows two other correlation tasks with the protons H-8 and H-3, so this carbon can be only C-4a, the second with a carbon at δ_C 161.9 ppm, the absence of a correlation of this latter with H-8, confirm that this carbon is C-5, the third with a carbon at δ_C 164.6 ppm, attributable to C-7. The fourth with a carbon at δ_C 94.4 ppm, attributable to C-8.
- ✓ The H-8 proton showed four (4) correlations: with the quaternary carbon C-4a at δ_C 104.2 ppm, the second with another quaternary carbon at δ_C 157.8 ppm attributable to C-8a, the third with C-7 at δ_C 164.6 ppm, and the fourth with a carbon at δ_C 99.3 ppm, attributable to C-6.
- ✓ The H-3 proton showed four (4) correlations: the first with C-4a at δ_C 104.2 ppm, the second and third are with two quaternary carbons at δ_C 121.1 and 164.2 ppm, attributable to carbons C-1' and C-2, respectively. The last with carbon at δ_C 182.2 ppm, which can only be C-4.

- ✓ The H-3' and H-5' protons showed two (2) correlation, with C-1' at δ_C 121.7 ppm and the second with C-4' at δ_C 161.7 ppm.
- ✓ The H-2' and H-6' protons showed three (3) correlations, the first with C-3' at δ_C 116.4 ppm, the second at δ_C 161.7 ppm attributable to carbon C-4'. The last with carbon at δ_C 164.2 ppm, attributable to carbons C-2.

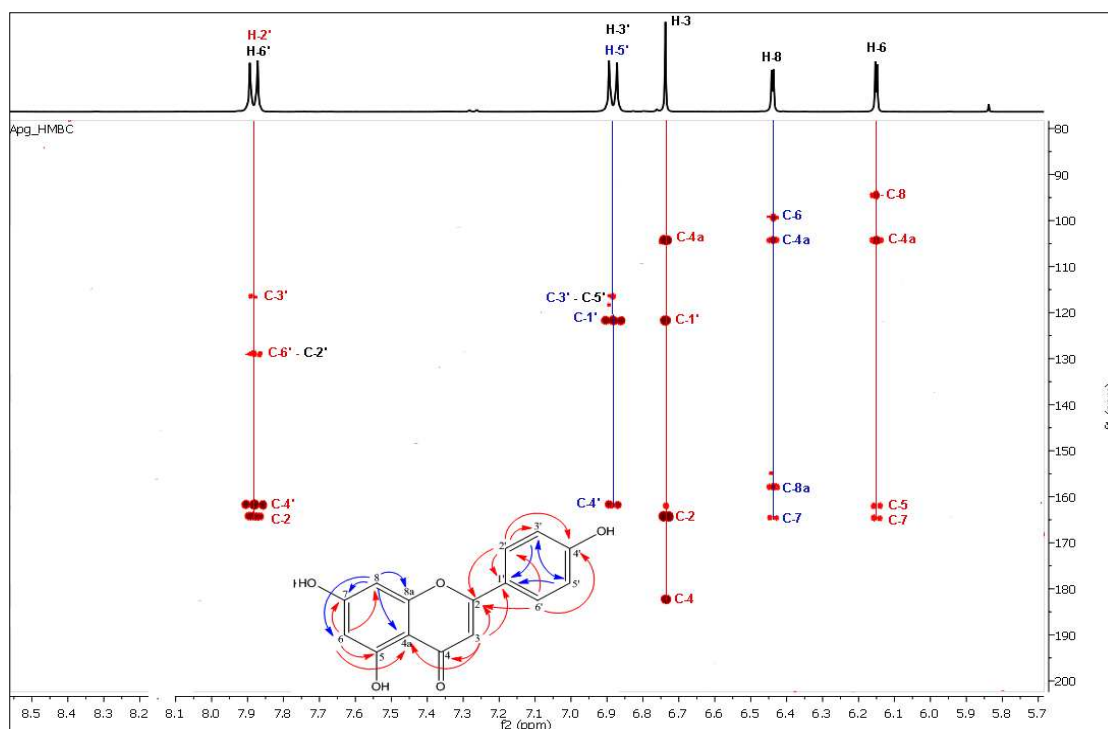


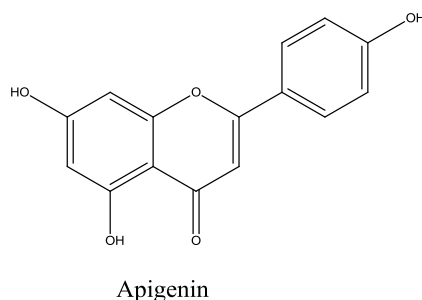
Figure IV.71. HMBC-NMR Spectrum (400 MHz, DMSO- d_6) of compound **8**.

All the chemical shifts of the NMR protons, carbons and HMBC correlations of compound **8** are summarized in the following table (**Table IV.15**).

Table IV.15. ^1H , ^{13}C and HMBC NMR data (400MHz) of compound **8** (DMSO- d_6).

Positions	δ_C (ppm)	δ_H (ppm), mult., J (Hz)	HMBC
1	-	-	-
2	164.2	-	-
3	103.3	6.78 (<i>s</i>)	C-1', C-4a, C-4, C-2
4	182.2	-	-
5	161.9	-	-
6	99.3	6.19 (<i>d</i> , 1H, $J=2.1$ Hz)	C-4a, C-8, C-7, C-5
7	164.6	-	-
8	94.4	6.48 (<i>d</i> , 1H, $J=2.0$ Hz)	C-4a, C-8a, C-7, C-6
4a	104.2	-	-
8a	157.8	-	-
1'	121.7	-	-
2'	129.0	7.92 (<i>d</i> , 1H, $J=8.8$ Hz)	C-3', C-1', C-4', C-2
3'	116.4	6.92 (<i>d</i> , 1H, $J=8.8$ Hz)	C-5', C-1', C-4'
4'	161.7	-	-
5'	116.4	6.92 (<i>d</i> , 1H, $J=8.8$ Hz)	C-3', C-1', C-4'
6'	129.0	7.92 (<i>d</i> , 1H, $J=8.8$ Hz)	C-5', C-1', C-4', C-2

Comparison of these ESI-MS, ^1H , ^{13}C , HMBC and HSQC NMR data with those of the literature [2] allowed us to assign the structure of **5, 7, 4'-trihydroxyflavone (Apigenin)** to compound **8**.



4.5.9. Identification of compound **9**

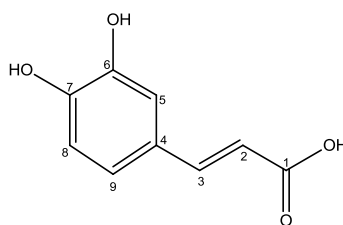


Figure IV.72. Structure of compound **9**

Compound 9 was isolated as a yellow amorphous powder. It showed a visible spot on TLC on both 254 and 366 nm wavelengths.

The examination of the ^1H -NMR spectrums (**Fig. IV.73** and **Fig. IV.74**) showed that it could be an aromatic compound while the benzene ring was characterized by:

- Two doublets with δ_{H} 7.34 ppm and δ_{H} 8.65 ppm with the same coupling constant $J=15.9$ Hz attributable to two vicinal protons of a double bond. The value of the coupling constant indicates the *trans* configuration of these two protons.
- A doublet at δ_{H} 7.90 ppm which can only be attributed to proton H-8 because the value of the coupling constant $J = 8.2$ Hz indicates the presence of a proton in an *ortho* position.
- A doublet of doublet with δ_{H} 8.03 ppm ($J = 8.2-1.9$ Hz) attributable to proton H-9.
- A doublet at δ_{H} 8.14 ppm giving *meta* coupling with $J = 1.9$ Hz attributable to the H-5 proton.

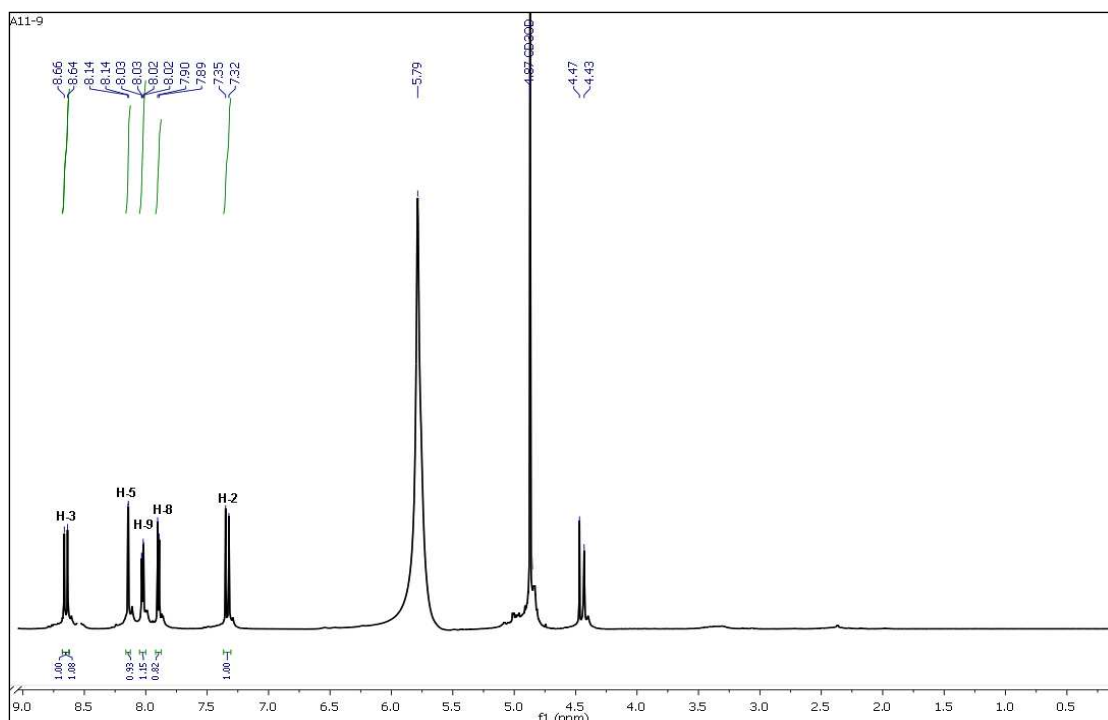


Figure IV.73. $^1\text{H-NMR}$ Spectrum (600 MHz, CD_3OD) of compound **9**.

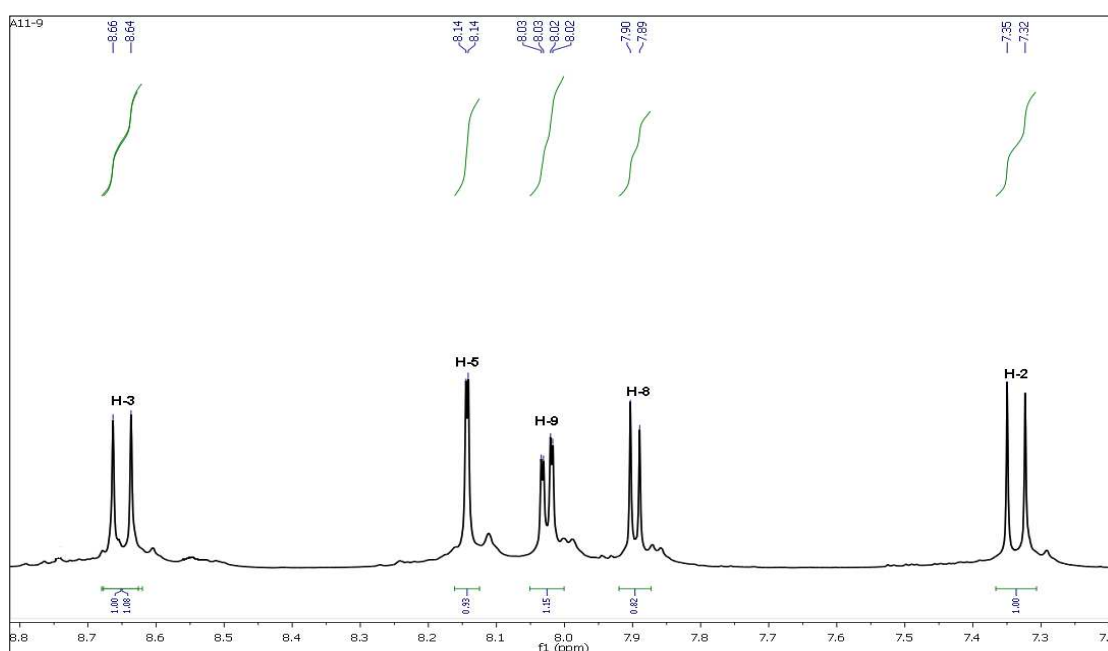


Figure IV.74. $^1\text{H-NMR}$ Spectrum (600 MHz, CD_3OD) of compound **9**.
(From 7.20 ppm to 8.80 ppm).

The $^{13}\text{C-NMR}$ spectrum of this compound (**Fig. IV.75**) indicated the presence of 9 carbon signals, including a carbonyl function carbon signal at δ_{C} 166.3 ppm, two olefinic carbons at δ_{C} 143.7 and δ_{C} 111.5 ppm for a possible $\text{C}_3=\text{C}_2$ double bond, respectively and six (6) aromatic carbons signals at δ_{C} 124.1 ppm, 111.9 ppm, 145.7 ppm, 144.1 ppm, 113.0 ppm and 119.6 ppm, respectively.

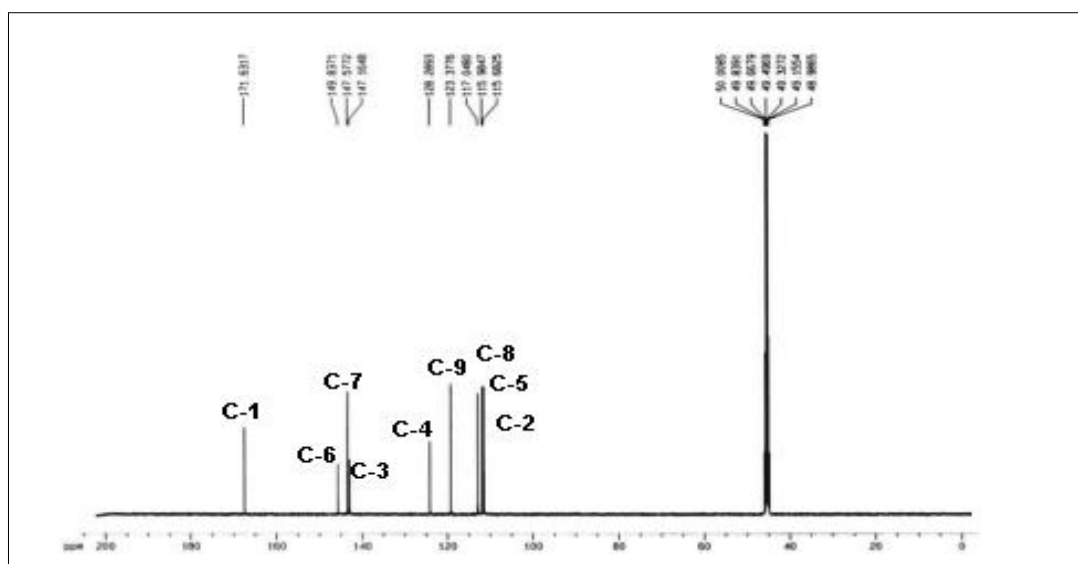


Figure IV.75. ^{13}C -NMR Spectrum (150 MHz, CD_3OD) of compound **9**.

The examination of the HSQC spectrum (**Fig. IV.69**) recorded in CD_3OD showed the presence of many correlations identified as follow:

- ✓ The proton H-3 showed a correlation with the carbon at δ_{C} 143.3 ppm attributable to carbon C-3.
- ✓ The proton H-5 showed a correlation with the carbon at δ_{C} 111.9 ppm attributable to carbon C-3.
- ✓ The proton H-9 showed a correlation with the carbon at δ_{C} 119.6 ppm attributable to carbon C-9.
- ✓ The protons H-8 and H-2 showed correlations with the carbons at δ_{C} 113.0 and 111.5 ppm attributable to the carbons C-8 and C-2, respectively.

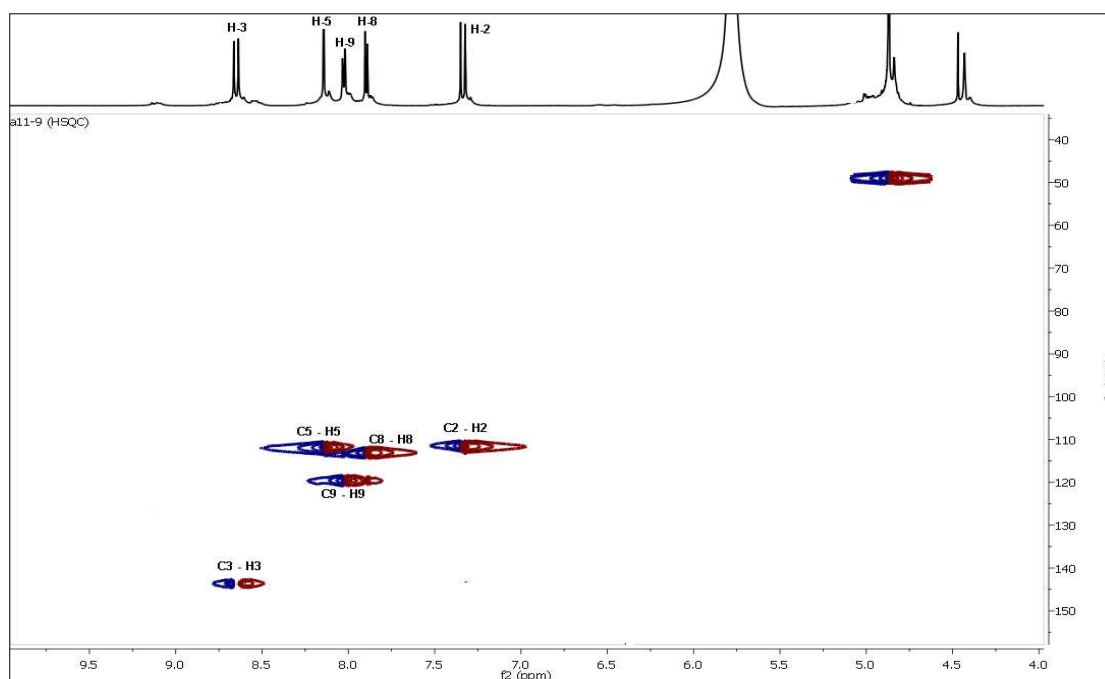


Figure IV.76. HSQC-NMR Spectrum (600 MHz, CD_3OD) of compound **9**.

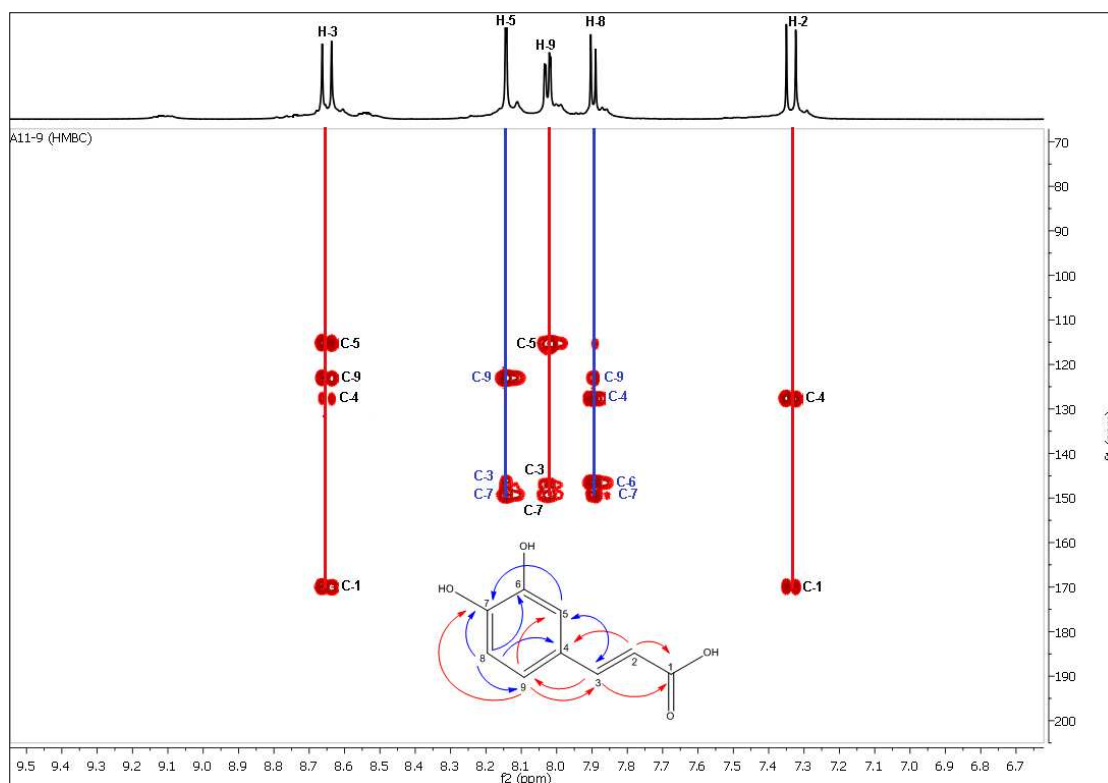


Figure IV.77. HMBC-NMR Spectrum (600 MHz, CD₃OD) of compound **9**.

The examination of the HMBC spectrum (**Fig. IV.77**) recorded in CD₃OD showed the presence of many correlations identified as follow:

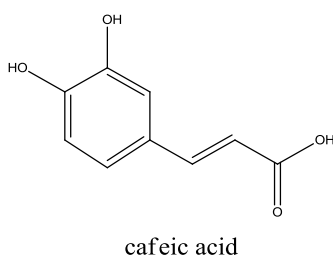
- ✓ The H-3 proton showed four (4) correlations: The first with the carbon at δ_C 111.9 ppm attributable to C-5, the second correlation with the carbon at δ_C 119.6 ppm, this carbon is C-9, the third with the carbon at δ_C 124.1 ppm, attributable to C-4. The last correlation with a carbon at δ_C 166.3 ppm, attributable to C-1 (the carbon of the carboxylic function).
- ✓ The H-5 proton showed three (3) correlations at δ_C 119.6, 143.7 and 144.1 ppm attributable to the carbons C-9, C-3 and C-7 respectively.
- ✓ The H-9 proton showed also three (3) correlation spots at δ_C 111.9, 143.7 and 144.1 ppm attributable to the carbons C-5, C-3 and C-7 respectively.
- ✓ The H-8 proton showed four (4) correlation spots: The first with the carbon at δ_C 119.6 ppm attributable to C-9, the second correlation with the carbon at δ_C 124.1 ppm attributable to C-4, the third with the carbon at δ_C 145.7 ppm, attributable to C-6 and a last correlation with a carbon at δ_C 144.1 ppm, attributable to C-7.
- ✓ The H-2 proton showed two (2) correlation spots at δ_C 124.1 and 166.3 ppm attributable to the carbons C-4 and C-1 respectively.

All the chemical shifts of the NMR protons, carbons, HSQC and HMBC correlations of compound **9** are summarized in the following table (**Table IV.16**).

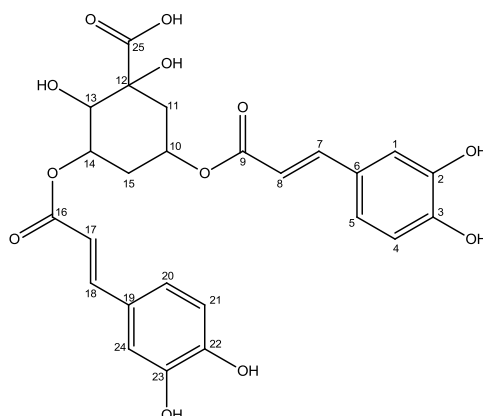
Table IV.16. ^1H , ^{13}C and HMBC-NMR data (600 MHz) of compound **9** (CD_3OD).

Positions	δ_{C} (ppm)	δ_{H} (ppm), <i>mult.</i> , <i>J</i> (Hz)	HMBC
1	166.3	-	-
2	111.5	7.34 (<i>d</i> , 1H, <i>J</i> =15.9 Hz)	C-4, C-1
3	143.7	8.65 (<i>d</i> , 1H, <i>J</i> =15.9 Hz)	C-5, C-9, C-4, C-1
4	124.1	-	-
5	111.9	8.14 (<i>d</i> , 1H, <i>J</i> =1.9 Hz)	C-9, C-3, C-7
6	145.7	-	-
7	144.1	-	-
8	113.0	7.90 (<i>d</i> , 1H, <i>J</i> =8.2 Hz)	C-9, C-4, C-6, C-7
9	119.6	8.03 (<i>dd</i> , 1H, <i>J</i> =8.2 - 1.9 Hz)	C-5, C-3, C-7

The comparison of these data with those reported in the literature [2] allowed us to assign and confirm the structure of a **Caffeic acid** to compound **9**. All the spectral data of the isolated Caffeic acid were in good agreement with the published values of standards [27].



IV.5.10. Identification of compound **10**

**Figure IV.78.** Structure of compound **10**

Compound 10 was obtained as a yellowish amorphous solid, its molecular weight was determined to be 516 by ESI-MS ion peaks at m/z 516.8 $[\text{M}+\text{H}]^+$ and m/z 515.2 $[\text{M}-\text{H}]^-$ (**Fig. IV.79**), corresponding to the molecular formula $\text{C}_{25}\text{H}_{24}\text{O}_{12}$ with 14 unsaturations.

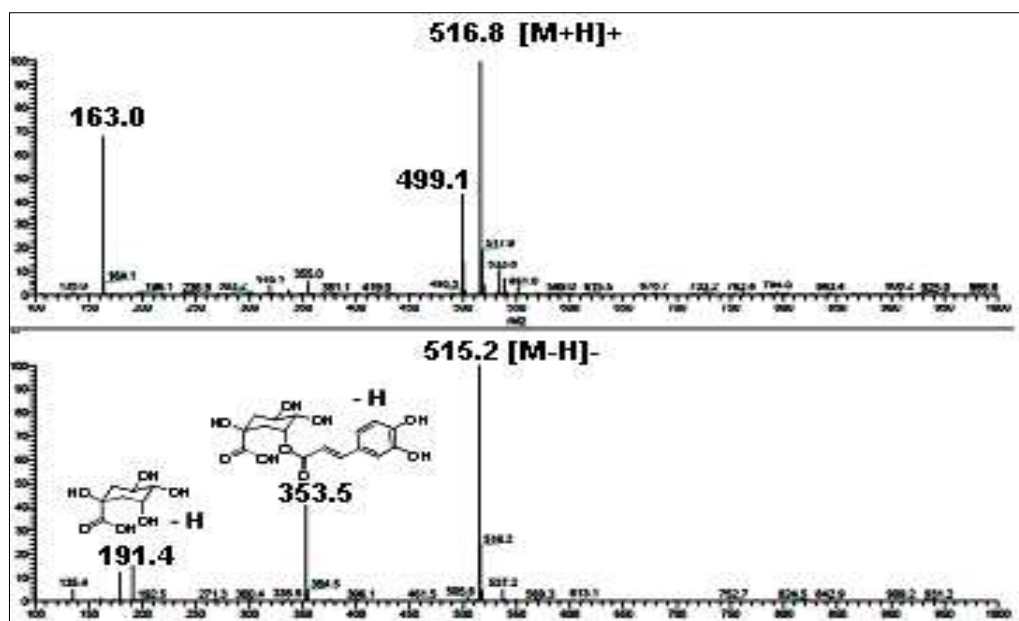


Figure IV.79. ESI-MS (+) and (-) ion mode of compound 10.

The ^1H and ^{13}C -NMR spectra of compound 10 (Fig. IV.80 and Fig. IV.81) showed two methylenes, three oxygenated protons and a carbonyl carbon at δ_{C} 177.3 ppm, which were assigned for a quinic acid unit. In addition, the presence of two *trans*-caffeoyl groups was indicated by two ABX systems and two *trans*-olefinic protons.

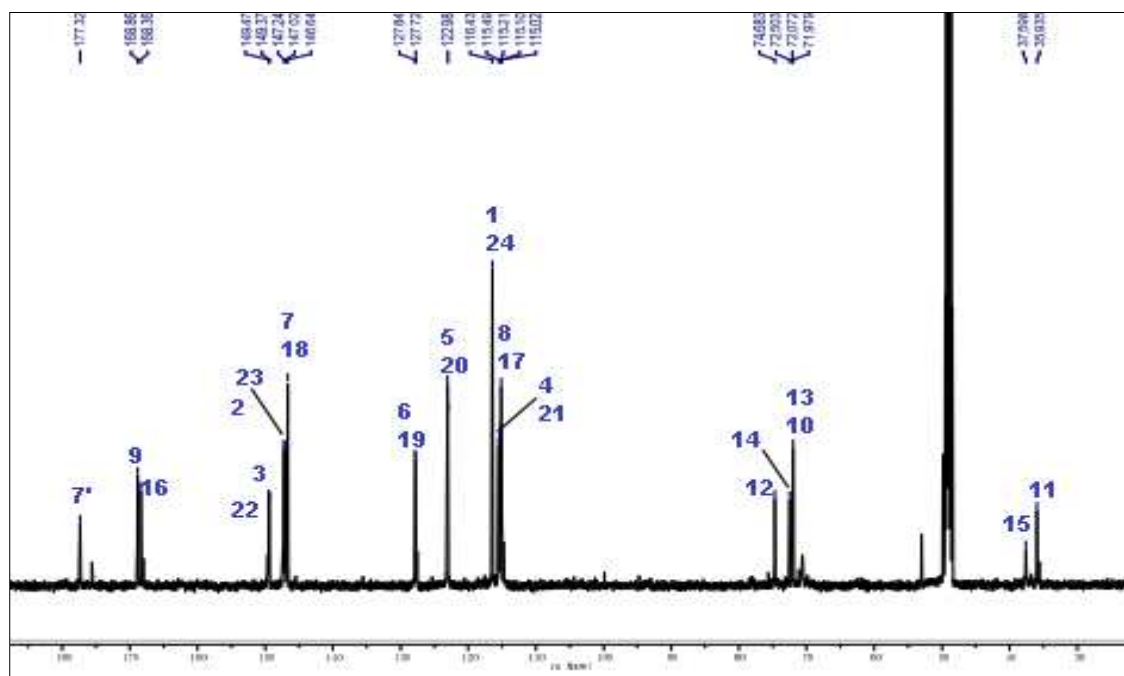


Figure IV.80. ^{13}C -NMR spectrum (600 MHz, CD_3OD) of compound 10.

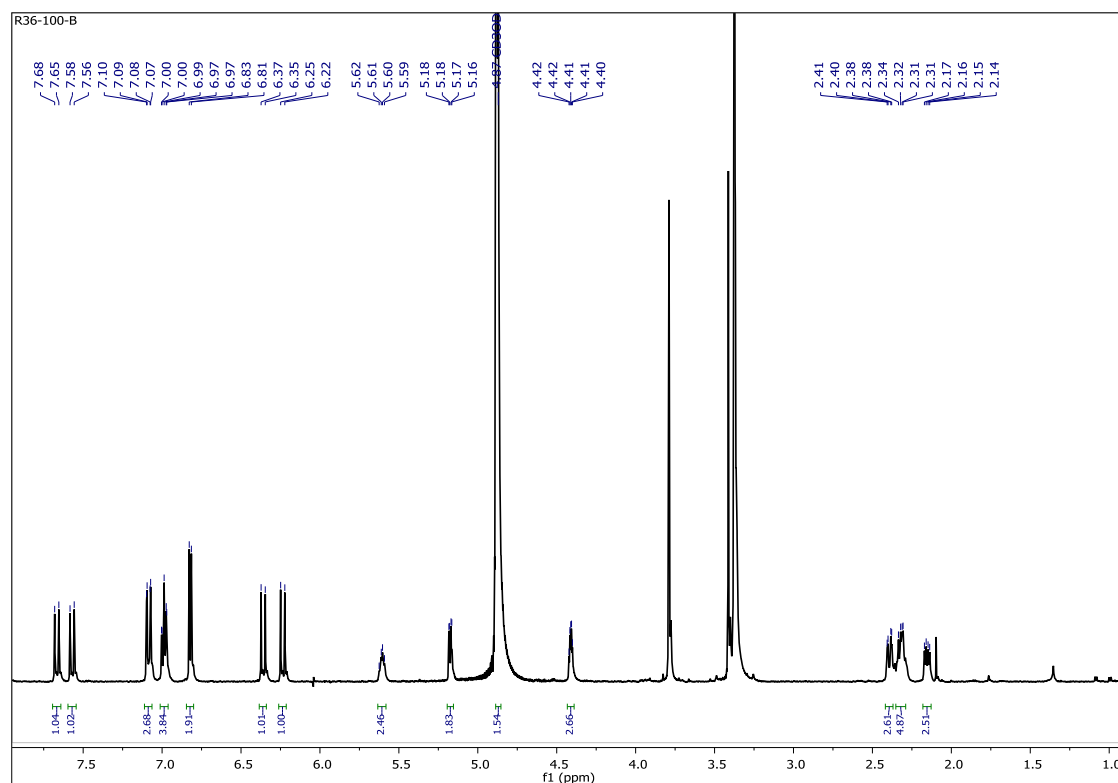


Figure IV.81. ¹H-NMR Spectrum (600 MHz, CD₃OD) of compound 10.

The ¹H-NMR spectrum (**Fig. IV.82**) showed two pairs of doublets with coupling constants of 15.9 Hz indicative of *trans* olefinic protons found in hydroxy cinnamic acids. In the aromatic region, resonances for two ABX systems [δ_{H} 7.07 ppm (*d*, $J=1.9$ Hz), 6.81 ppm (*d*, $J=8.1$ Hz) and 6.97 ppm (*dd*, $J=8.1, 2.0$ Hz); and δ_{H} 7.09 ppm (*d*, $J=1.9$ Hz), 6.83 ppm (*d*, $J=8.1$ Hz) and 6.99 (*dd*, $J=8.2, 2.0$ Hz)] were observed, which were assigned to two 1, 3, 4-trisubstituted phenyl units. From these observations, along with the analysis of the ¹³C-NMR data, two caffeic acid moieties were inferred to be present.

The presence of the quinic acid moiety was indicated by ¹H-NMR resonances (**Fig. IV.83**) of three oxymethine protons at δ_{H} 5.61 ppm (*q*, $J = 8.1-7.3$ Hz), 5.17 ppm (*dd*, $J = 8.0-3.0$ Hz) and 4.41 ppm (*ddd*, $J = 6.4-3.3-3.3$ Hz), together with two pairs of sp³ methylene protons at δ_{H} 2.32 / 2.30 ppm and δ_{H} 2.39 / 2.15 ppm for H₂-15 and H₂-11, respectively. All of the latter are characteristic of a quinic acid unit, with regard to their multiplicity and coupling patterns.

The deshielded resonances of two oxymethine protons in the quinic acid nucleus at δ_{H} 5.61 ppm (H-10) and δ_{H} 4.41 ppm (H-14) implied acylation of the hydroxyl group at these positions as earlier reported for other naturally occurring quinic acid derivatives [28-29].

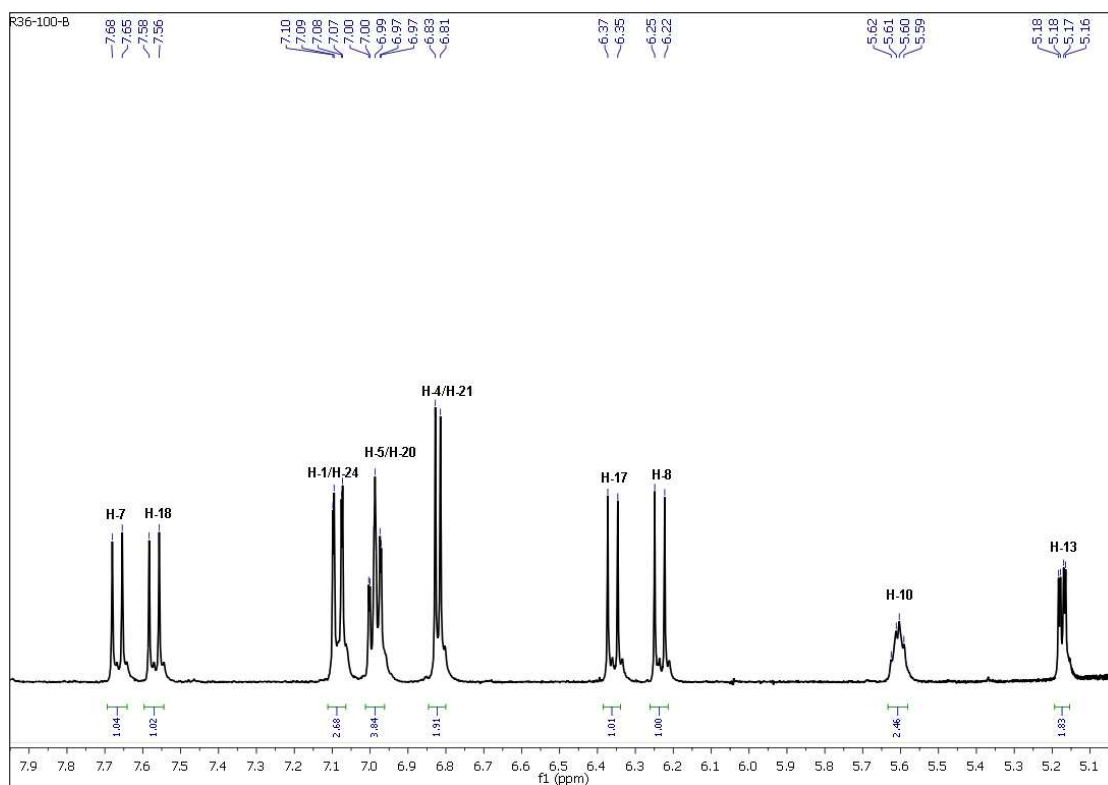


Figure IV.82. $^1\text{H-NMR}$ Spectrum (600 MHz, CD_3OD) of compound 10.
(From 5.00 ppm to 7.90 ppm)

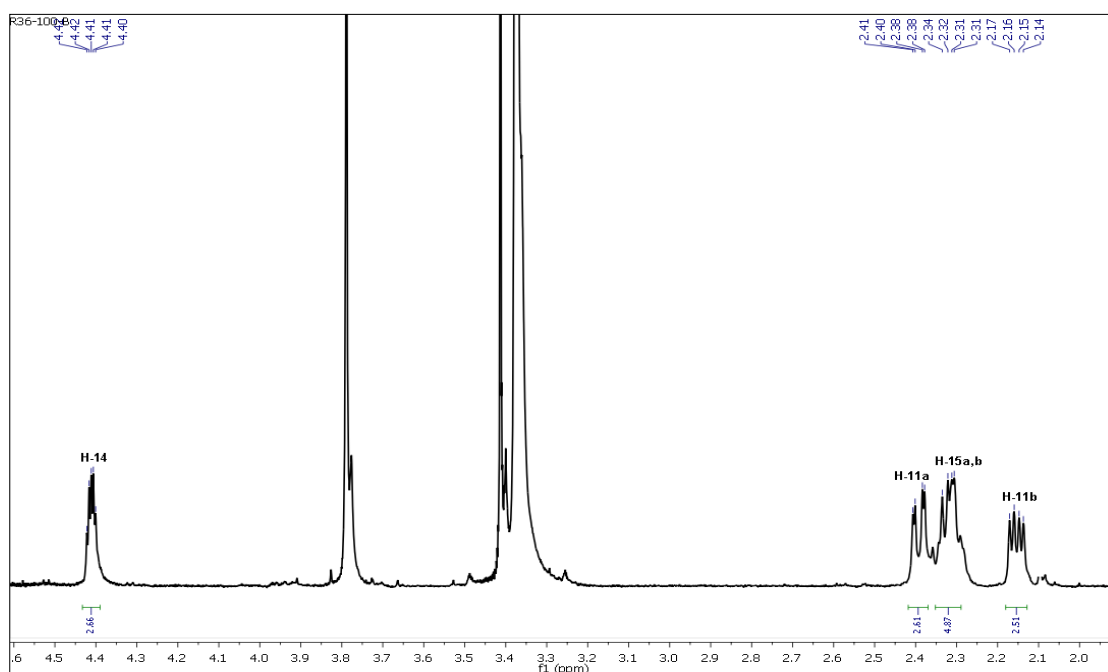


Figure IV.83. $^1\text{H-NMR}$ Spectrum (600 MHz, CD_3OD) of compound 10.
(From 2.00 ppm to 4.50 ppm).

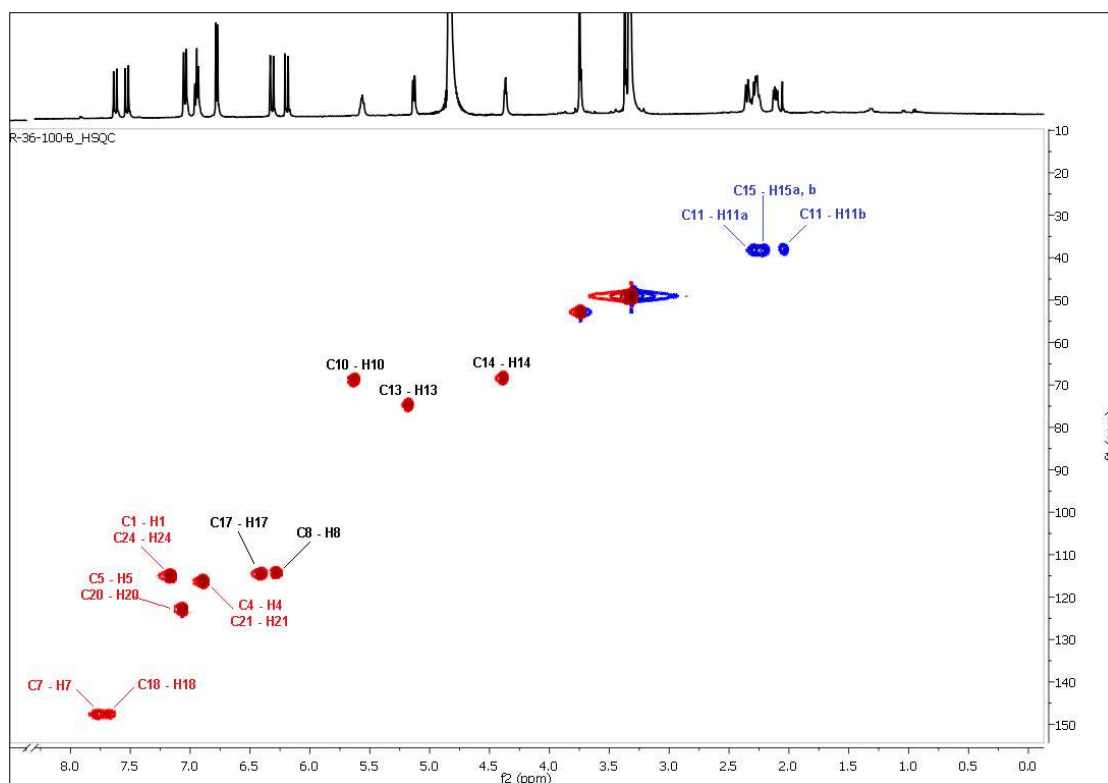


Figure IV.84. HSQC-NMR Spectrum (600 MHz, CD₃OD) of compound **10**.

The examination of HSQC spectrum (**Fig. IV.84**) recorded in CD₃OD showed the presence of correlations give more details about the assignment of this compound structure identified as follow:

- ✓ The protons H-7 and H-18 showed a correlation with the carbon C-7 and C-18, respectively, at δ_C 147.6 ppm.
- ✓ The protons H-1 and H-24 showed a correlation with the carbon C-1 and C-24, respectively, at δ_C 115.0 ppm.
- ✓ The protons H-5 and H-20 showed a correlation with the carbon C-5 and C-20, respectively, at δ_C 123.2 ppm.
- ✓ The protons H-4 and H-21 showed a correlation with the carbon C-4 and C-21, respectively, at δ_C 116.4 ppm.
- ✓ The protons H-17 and H-8 showed a correlation with the carbon C-17 and C-8, respectively, at δ_C 114.5 ppm.
- ✓ The proton H-10 showed a correlation with the carbon C-10 at δ_C 68.9 ppm.
- ✓ The proton H-13 showed a correlation with the carbon C-13 at δ_C 74.5 ppm.
- ✓ The proton H-14 showed a correlation with the carbon C-14 at δ_C 68.3 ppm.
- ✓ The protons H-11a and H-11b showed a correlation with the carbon C-11 at δ_C 38.2 ppm.
- ✓ The protons H-15a and H-15b showed a correlation with the carbon C-15 at δ_C 38.3 ppm.

The assignments of the protons of the quinic acid nucleus were corroborated by analysis of the ¹H-¹H COSY spectra (**Fig. IV.85**).

The attachments of the two caffeoyl moieties at C-10 and C-14 of quinic acid part were deduced from the HMBC correlation of H-10 and H-14, respectively, (**Fig. IV.87** and **Fig.IV.88**) with their ester carbonyl carbons (C-9 and C-16) at δ_C 168.4 ppm and δ_C 167.8 ppm, respectively.

- ✓ The H-14 proton showed four (4) correlations: The first with the carbon at δ_C 68.9 ppm attributable to C-10, the second correlation with the carbon at δ_C 75.5 ppm attributable to C-12, the third with the carbon at δ_C 38.3 ppm, attributable to C-15 and a last correlation with a carbon at δ_C 167.8 ppm, attributable to C-16 which confirm the attachment point of the caffeoyl moiety.
- ✓ The H-10 proton showed two (2) correlations: The first with the carbon at δ_C 75.5 ppm attributable to C-12, and a second correlation with a carbon at δ_C 168.4 ppm, attributable to the ester carbonyl carbon C-9 which confirms also the attachment point of the caffeoyl moiety at C-10.

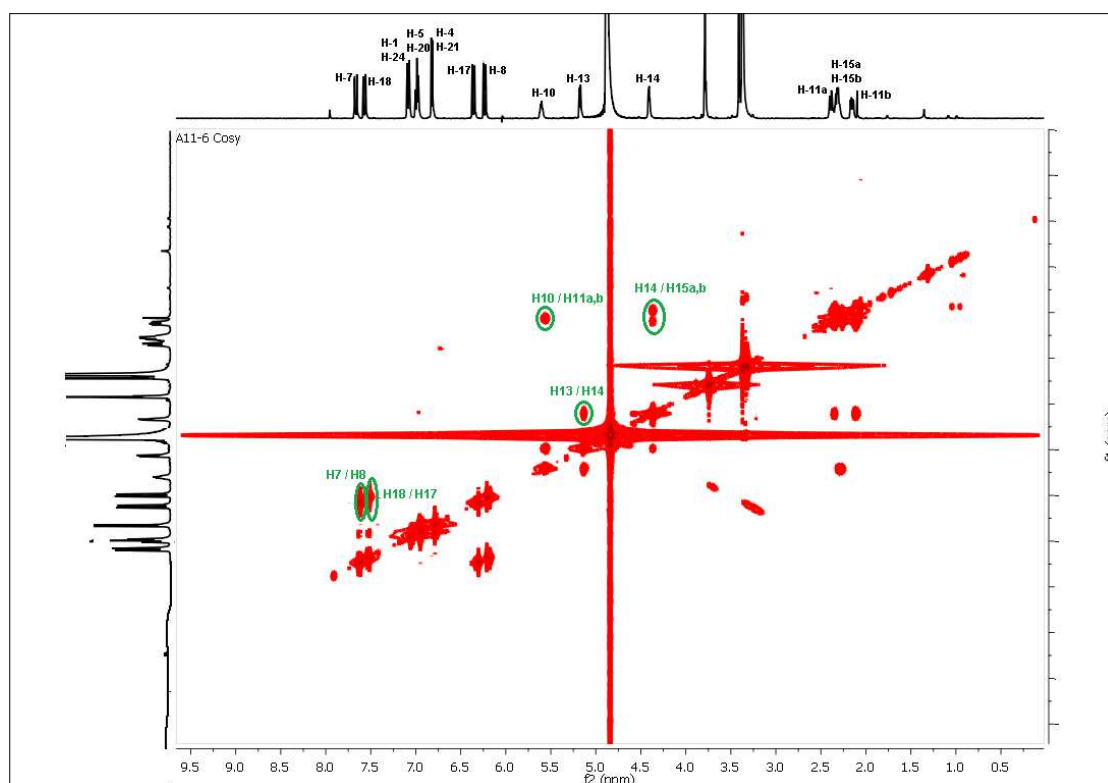


Figure IV.85. ^1H - ^1H COSY-NMR Spectrum (600 MHz, CD_3OD) of compound **10**

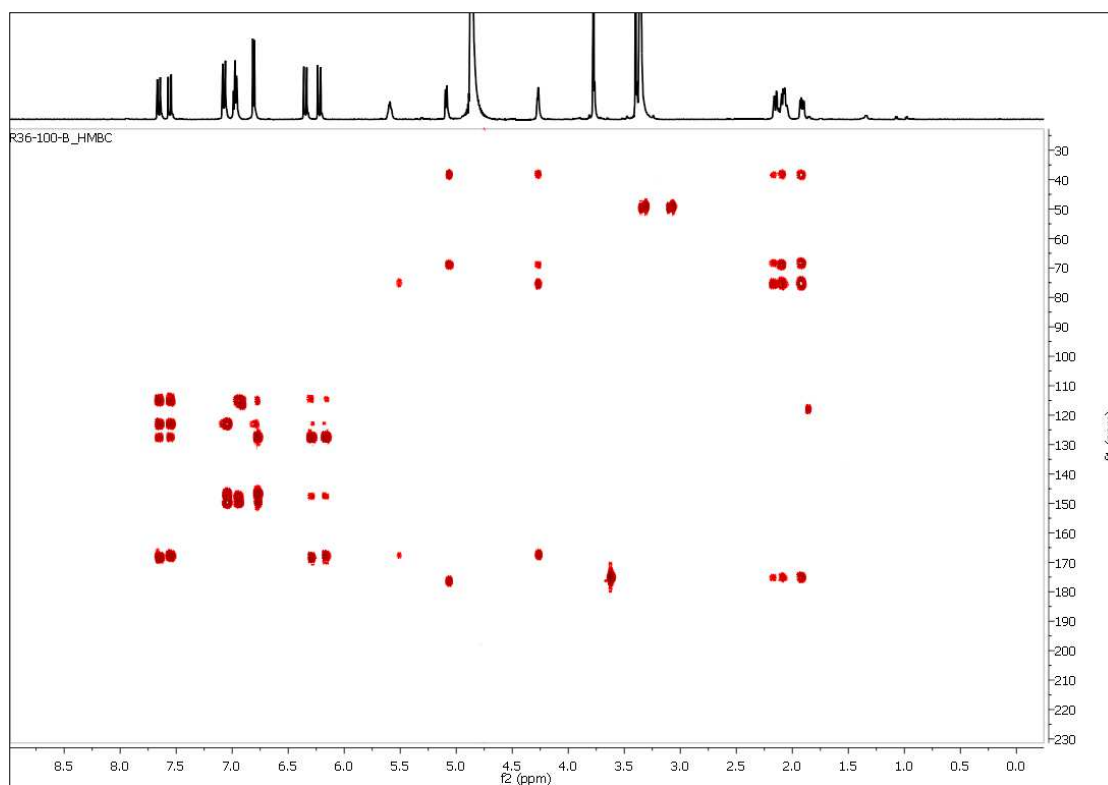


Figure IV.86. HMBC-NMR Spectrum (600 MHz, CD₃OD) of compound 10.

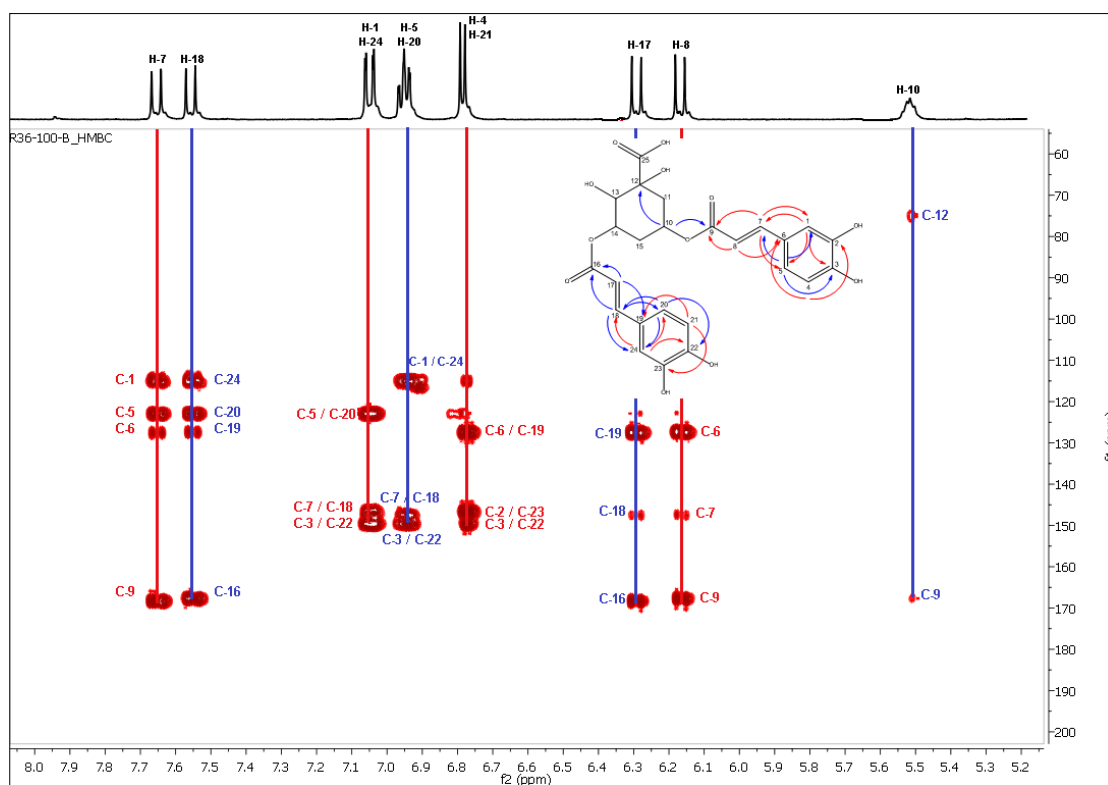


Figure IV.87. HMBC-NMR Spectrum (600 MHz, CD₃OD) of compound 10.
(From 5.00 ppm to 8.00 ppm).

The examination of the entire HMBC spectrum (**Fig. IV.87 and Fig.IV.88**) recorded in CD₃OD showed the presence of other correlations identified as follow:

- ✓ Both H-7 and H-18 protons showed four (4) correlations: The first with the carbon at δ_C 115.0 ppm attributable to C-1 and C-24, the second with the carbon at δ_C 123.2 ppm attributable to C-5 and C-20, the third with the carbon at δ_C 127.7 ppm and δ_C 127. ppm attributable to C-6 and C-19, respectively, the last correlation with the carbon at δ_C 168.4 ppm and δ_C 167.8 ppm, attributable to both ester carbonyl carbons C-9 and C-16, respectively.
- ✓ Both H-1 and H-24 protons showed three (3) correlations: The first with the carbon at δ_C 123.2 ppm attributable to C-5 and C-20, the second correlation with the carbon at δ_C 147.6 ppm attributable to C-7 and C-18, the third with the carbon at δ_C 149.6 ppm attributable to C-3 and C-22.
- ✓ Both H-5 and H-20 protons showed three (3) correlations: The first with the carbon at δ_C 115.0 ppm attributable to C-1 and C-24, the second correlation with the carbon at δ_C 147.6 ppm attributable to C-7 and C-18, the third with the carbon at δ_C 149.6 ppm attributable to C-3 and C-22.
- ✓ Both H-4 and H-21 protons showed three (3) correlations: The first with carbons at δ_C 127.7 and 127.3 ppm attributable to C-6 and C-19, respectively, the second correlation with the carbon at δ_C 146.2 and 146.8 ppm attributable to C-2 and C-23, respectively, the third correlation with the carbon at δ_C 149.6 ppm attributable to C-3 and C-22.
- ✓ Both H-8 and H-17 proton showed three (3) correlations: The first with carbons at δ_C 127.7 and 127.3 ppm attributable to C-6 and C-19, respectively, the second correlation with the carbon at δ_C 147.6 ppm attributable to C-7 and C-18, the last correlation with carbons at δ_C 168.4.6 and 167.8 ppm attributable to C-9 and C-16, respectively.
- ✓ The proton H-10 showed (2) correlations at δ_C 75.5 ppm and δ_C 168.4 ppm attributable to C-12 and C-9, respectively.
- ✓ The proton H-13 showed four (4) correlations: The first with the carbon at δ_C 38.2 ppm attributable to C-11, the second correlation with the carbon at δ_C 38.3 ppm attributable to C-15, the third with the carbon at δ_C 68.3 ppm attributable to C-14, the last correlation with the carbon at δ_C 175.7 ppm, attributable to the carboxylic function carbon C-25.
- ✓ The proton H-14 showed also four (4) correlations: with the carbon at δ_C 38.3 ppm attributable to C-15, with the carbon at δ_C 68.9 ppm attributable to C-10, with the carbon at δ_C 75.5 ppm attributable to C-12, the last with the carbon at δ_C 167.8 ppm, attributable to the ester carbonyl carbons C-16.
- ✓ The protons H-11a and H-11b showed together four (4) correlation: with the carbon at δ_C 38.3 ppm attributable to C-15, with the carbon at δ_C 68.9 ppm attributable to C-10, with the carbon at δ_C 74.5 ppm attributable to C-13, the last with the carbon at δ_C 175.5 ppm, attributable to the ester carbonyl carbons C-25.

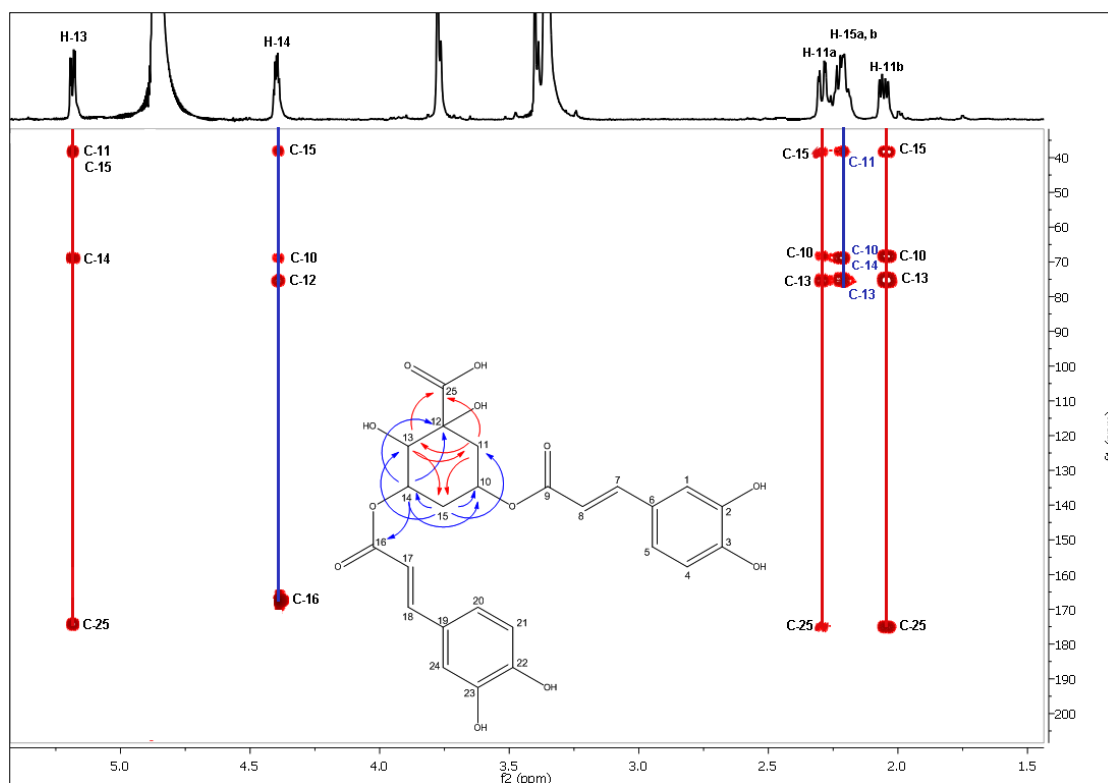


Figure IV.88. HMBC-NMR Spectrum (600 MHz, CD₃OD) of compound **10**.
(From 1.50 ppm to 5.50 ppm).

- ✓ The protons H-15a and H-15b showed together four (4) correlations: with the carbon at δ_C 38.2 ppm attributable to C-11, with the carbon at δ_C 68.9 ppm attributable to C-10, with the carbon at δ_C 68.3 ppm attributable to C-14, the last with the carbon at δ_C 74.5 ppm, attributable to the ester carbonyl carbons C-13.

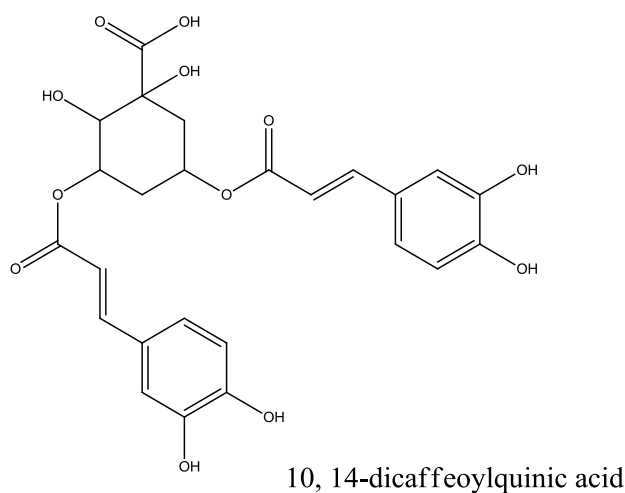
All the chemical shifts of the NMR protons, carbons, HSQC and HMBC correlations of compound **10** are summarized in the following table (**Table IV.17**).

Table IV.17. ¹H, ¹³C and HMBC NMR data (600 MHz) of compound **10** (CD₃OD).

Positions	δ_C (ppm)	δ_H (ppm), mult., J (Hz)	HMBC
1	115.0	7.09 (d, 1H, J=1.9 Hz)	C-5, C-7, C-3
2	146.2	-	-
3	149.6	-	-
4	116.4	6.83 (d, 1H, J=8.1 Hz)	C-6, C-2, C-3
5	123.2	6.99 (dd, 1H, J=8.2-2.0 Hz)	C-1, C-3, C-7
6	127.7	-	-
7	147.6	7.67 (d, 1H, J=15.8 Hz)	C-1, C-5, C-6, C-9
8	114.5	7.57 (d, 1H, J=15.8 Hz)	C-6, C-9, C-7
9	168.4	-	-
10	68.9	5.61 (q, 1H, J=8.1-7.3Hz)	C-12, C-9
11a	38.2	2.39 (dd, 1H, J=13.8-3.2 Hz)	C-15, C-13, C-9, C-10
11b	38.2	2.15 (dd, 1H, J=13.6-4.6 Hz)	C-15, C-13, C-9, C-10
12	75.5	-	-
13	74.5	5.17 (dd, 1H, J=8.0-3.0 Hz)	C-11, C-15, C-14, C-16

14	68.3	4.41 (<i>m</i> , 1H)	C-10, C-12, C-15, C-16
15a	38.3	2.32 (<i>dd</i> , 2H, <i>J</i> =11.8-5.8 Hz)	C-11, C-13
15b	38.3	2.30 (<i>dd</i> , 2H, <i>J</i> =11.8-5.8 Hz)	C-11, C-13
16	167.8	-	-
17	114.5	6.36 (<i>d</i> , 1H, <i>J</i> =15.8 Hz)	C-19, C-16, C-18
18	147.6	7.57 (<i>d</i> , 1H, <i>J</i> =15.8 Hz)	C-24, C-20, C-16, C-19
19	127.3	-	-
20	123.2	6.97 (<i>dd</i> , 1H, <i>J</i> =8.2-2.0 Hz)	C-24, C-18, C-22
21	116.4	6.82 (<i>d</i> , 1H, <i>J</i> =8.1 Hz)	C-19, C-23, C-22
22	149.6	-	-
23	146.8	-	-
24	115.0	7.07 (<i>d</i> , 1H, <i>J</i> =1.9 Hz)	C-20, C-18, C-22
25	175.5	-	-

All the above spectral data were consistent with those of 3, 5-dicaffeoylquinic acid [28-30]. Thus, compound **10** was concluded to be **10, 14-dicaffeoylquinic acid**.



IV.5.11. Identification of compounds 11. (New Compound)

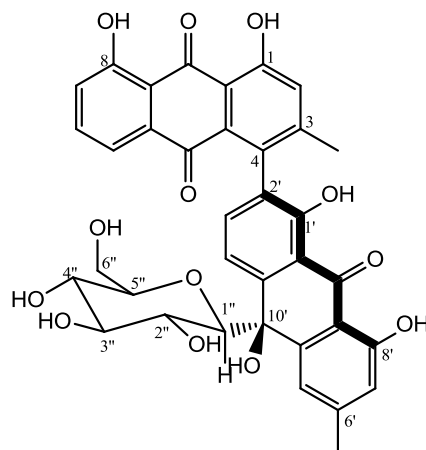


Figure IV.89. Structure of compound **11**.

Compound 11 was obtained as a yellowish amorphous powder. Its HRESI-MS analysis (**Fig. IV.90**) gave an $[M-H]^-$ ion at $m/z = 669.16353$ (calculated for $C_{36}H_{29}O_{13}$, 669.16081), consistent with the molecular formula $C_{36}H_{30}O_{13}$, indicating 22 degrees of unsaturation in the structure.

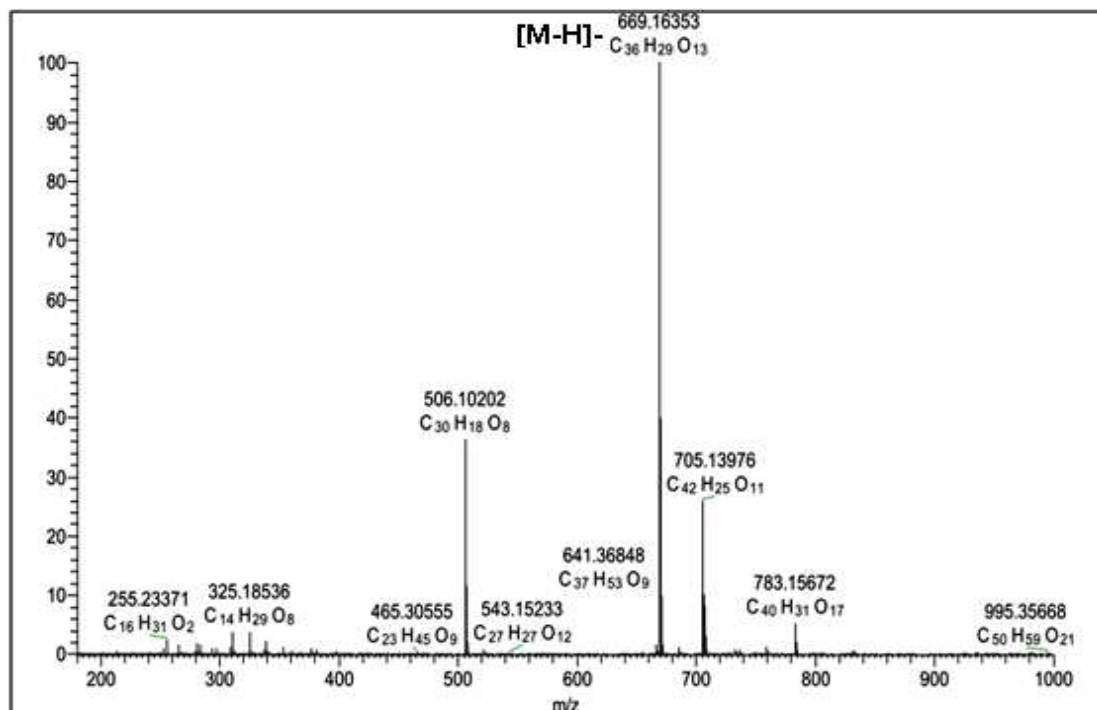


Figure IV.90. HR-ESIMS spectrum in negative ion mode of compound **11**.

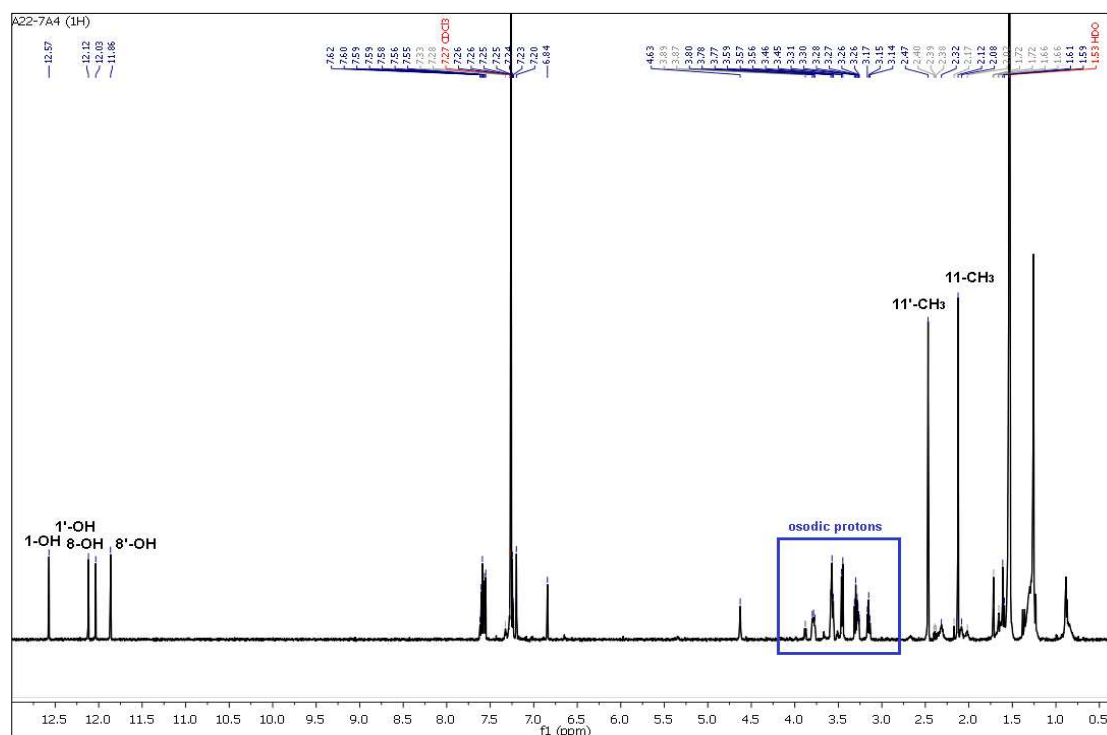


Figure IV.91. 1H -NMR Spectrum (600 MHz, $CDCl_3$) of compound **11**.

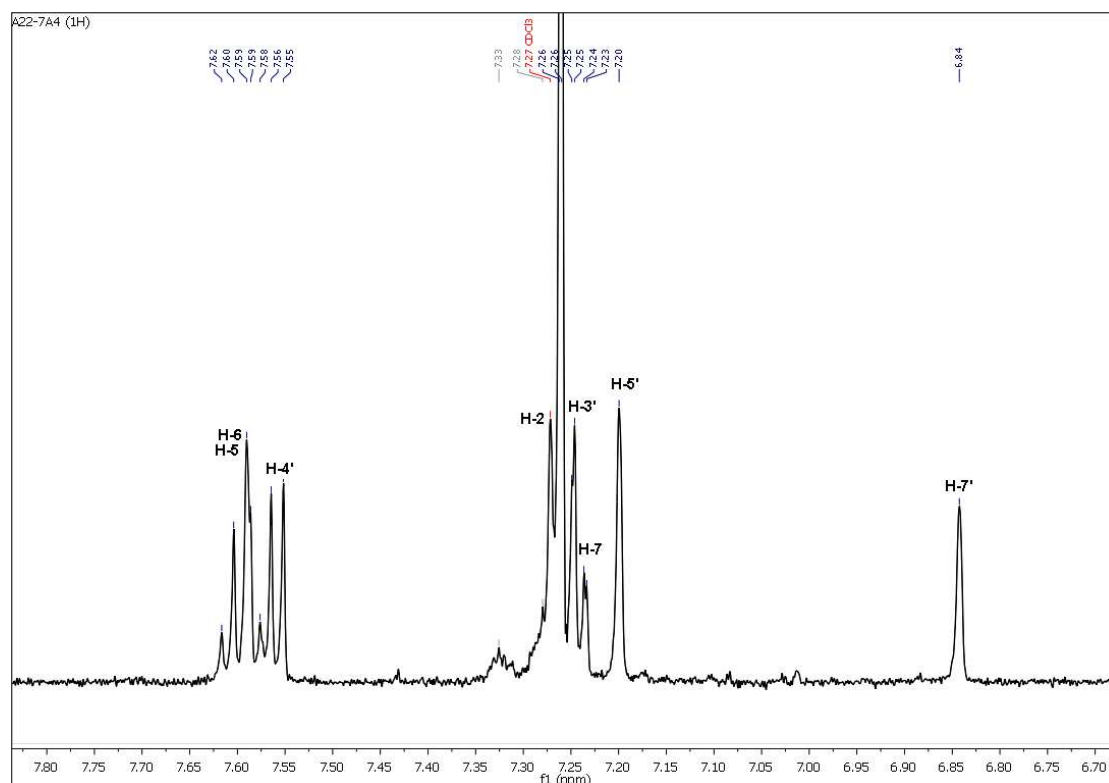


Figure IV.92. ^1H -NMR Spectrum (600 MHz, CDCl_3) of compound **11**.
(From 6.70 ppm to 7.70 ppm).

The full structure was elucidated by extensive NMR analysis including ^1H (**Fig. IV.91**, **Fig. IV.92**, **Fig. IV.93**), HMBC (**Fig. IV.97**) and HSQC (**Fig. IV.94**) experiments. In more details, assignment of ^{13}C resonances performed by HSQC and HMBC analysis of this compound showed 36 carbon resonances, including two methyl groups (δ_{C} 21.9 ppm and δ_{C} 22.9 ppm), one oxymethylene (δ_{C} 62.9 ppm), eight aromatic methines, five sp^3 oxymethines, 12 quaternary carbons, four oxygenated sp^2 tertiary carbons, three carbonyl carbons (δ_{C} 194.5 ppm, 182.6 ppm and 193.4 ppm) and one oxygenated sp^3 tertiary carbon.

The ^1H -NMR spectrum (**Fig. IV.91**) showed eight downfield resonances attributable to eight aromatic protons, two singlets at δ_{H} 2.13 ppm and δ_{H} 2.47 ppm assigned to two aromatic methyl groups (CH_3). The spectrum showed also the presence of an hexose unit characterized by five oxymethine protons at δ_{H} 3.45 ppm (*d*, $J = 9.3$ Hz), δ_{H} 3.30 ppm (*t*, $J = 9.3$ -9.3 Hz), δ_{H} 3.57 ppm (*t*, $J = 9.3$ -9.3 Hz), δ_{H} 3.15 ppm (*t*, $J = 9.3$ -9.3 Hz), δ_{H} 3.27 ppm (*m*) and one oxymethylene at δ_{H} 3.57 ppm. δ_{H} 3.77 ppm (*m*) coupled to their neighbors in this order based essentially on ^1H - ^1H COSY experiment (**Fig. IV.101**), confirming with the presence of this hexose unit.

In addition, the ^1H -NMR spectrum (**Fig. IV.91**) showed four highly deshielded singlets at δ_{H} 11.87 ppm, 12.03 ppm, 12.12 ppm and 12.58 ppm, indicative of exchangeable hydrogens bond to oxygen, and assigned, in particular to four phenolic OH groups (δ_{C} 162.9 ppm, 162.2 ppm, 159.3 ppm and 162.7 ppm) [31].

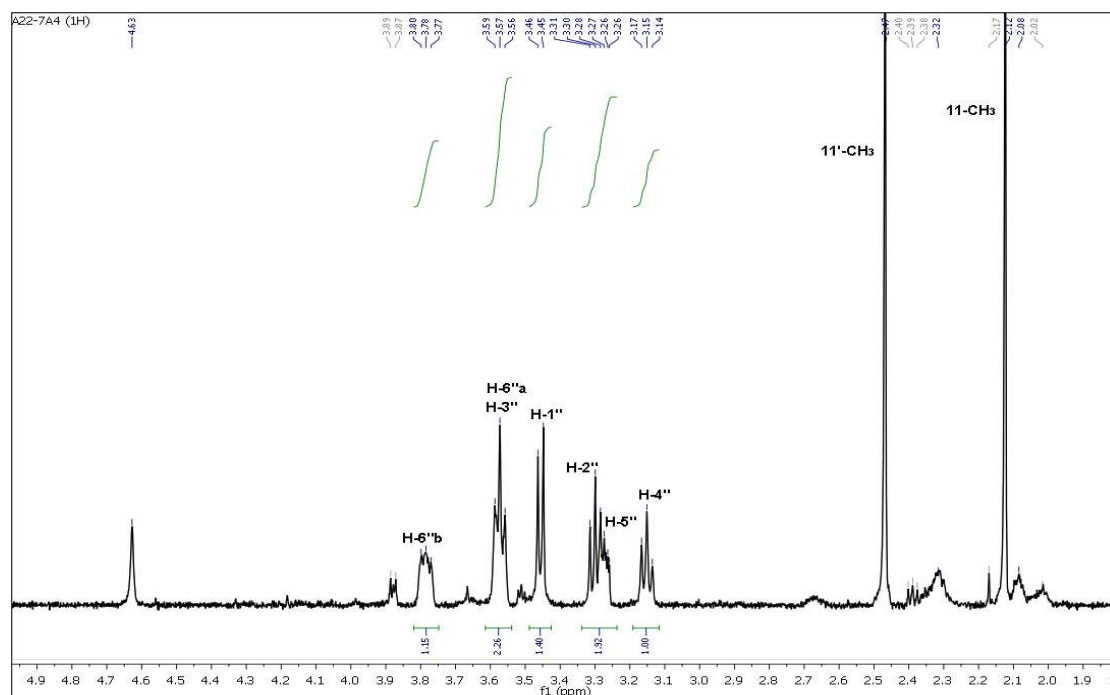


Figure IV.93. ^1H -NMR Spectrum (600 MHz, CDCl_3) of compound **11**.
(From 2.90 ppm to 4.30 ppm).

The full assignment of C/H resonances, accomplished also by a careful analysis of HMBC correlations, allowed confirming this hypothesis. In more details very diagnostic were correlations of the methyl group ($\delta_{\text{H/C}}$ 2.13 / 21.9 ppm) with C-2, C-3 and C-4 and with the singlet at δ_{H} 7.27 ppm (H-2) (**Fig. IV.98**).

Moreover, an ABX spin system for three aromatic protons at δ_{H} 7.59 ppm (1H, *d*, $J = 8.2$ Hz, H-5), δ_{H} 7.60 ppm (1H, *t*, $J = 8.2$ Hz, H-6) and δ_{H} 7.24 ppm (1H, *d*, $J = 8.2$ Hz, H-7) and their long range H/C correlation pattern H-5/C-10, H-7/C-8a, allowed to identify a chrysophanol (1,8-dihydroxy-3-methylanthraquinone, $\text{C}_{15}\text{H}_{10}\text{O}_4$) moiety leaving C-4 (δ_{C} 131.5 ppm) as the point of attachment to an oxoanthrone structure [31], identified analyzing the remaining the $^1\text{H} / ^{13}\text{C}$ resonances.

In more details, the C-6' location of the other methyl group ($\delta_{\text{H/C}}$ 2.47 / 22.9 ppm) was supported by HMBC correlations with C-5', C-6' and C-7' and with the singlet at δ_{H} 7.20 ppm (H-5'). Moreover, the presence of a pair of deshielded *ortho*-coupled protons with an AX pattern at δ_{H} 7.25 ppm (1H, *d*, $J = 8.2$ Hz, H-3') and δ_{H} 7.55 ppm (1H, *d*, $J = 8.2$ Hz, H-4') and two *meta*-coupled protons, at δ_{H} 7.20 ppm (1H, *s*, H-5') and δ_{H} 6.84 ppm (1H, *s*, H-7'), separated by the CH_3 -11' methyl group (HMBC correlations in (**Fig. IV.112** and **Fig. IV.113**)), suggested the point of attachment in this portion of molecule at C-2' (δ_{C} 129.6 ppm) [31]. Finally, particularly valuable were the correlation found for the quaternary carbinol at δ_{C} 77.3 ppm (C-10') with the proton at position H-4' and H-5', the former belonging to the AX system, the latter belonging to one of the two *meta*-proton system.

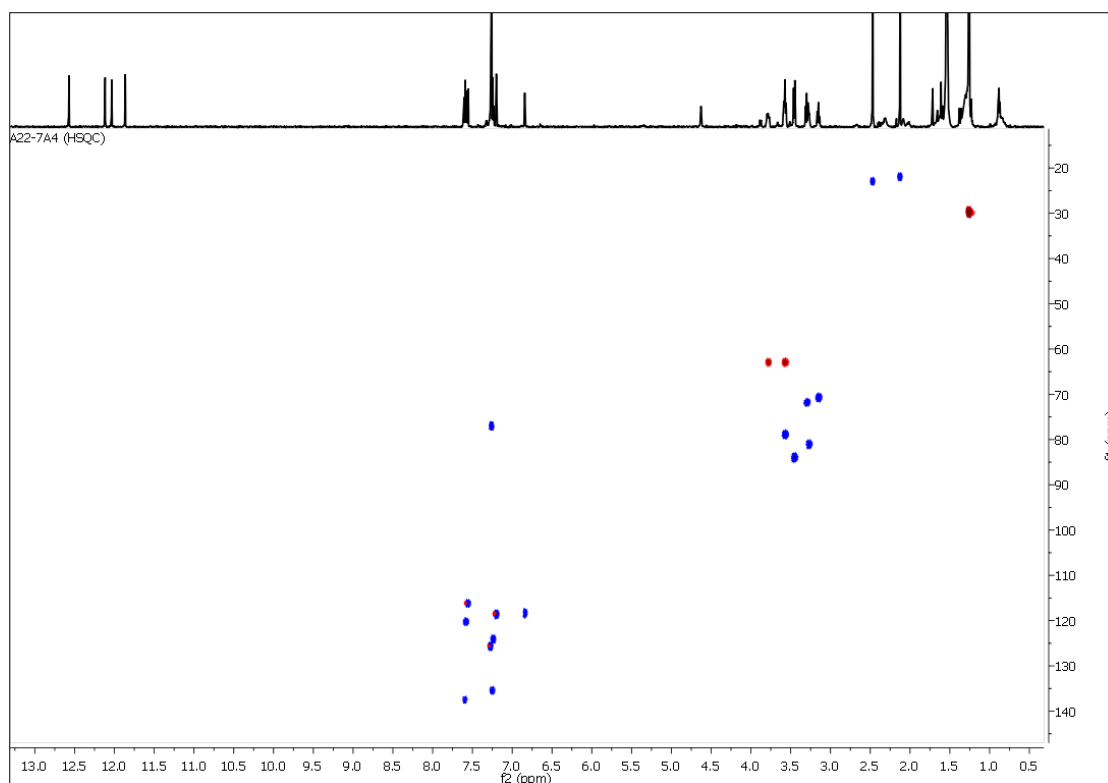


Figure IV.94. HSQC-NMR Spectrum (600 MHz, CDCl_3) of compound **11**.

All the above data, compared with those with the present compounds present in literature, suggested that compound **11** was strictly related to asphodosides A, and anthraquinone-oxanthrone C-glycoside [31], with an hexose unit linked at C-10' position of aglycone portion instead of pentose, as deduced by comparison of ESI-MS spectra and by ^1H and ^{13}C resonances. In particular, C-glycoside oxanthrone structure for compound **11** was supported by upfield shift of the anomeric carbon signals at δ_{C} 83.8 ppm (C-1''), and the HMBC correlation of H-1'' to C-10' (**Fig. IV.98**), providing full evidence of the exact location of the sugar moiety. The presence of a C- β -glucopyranosyl unit in compound **11** was supported by several evidences:

- i) The presence in ESI-MS spectrum of a signal at $m/z = 506$, due to the loss of a hexose unit from $[\text{M} - \text{H} - 162]^-$,
- ii) The multiplicity of the sugar signals and the $J_{\text{H-H}}$ values were in good agreement with those reported for other β -glucopyranosyl moieties [5-32] in accordance with all these data the structure **11**.

The IR indications on the presence of carbonyl groups (1604 cm^{-1}), hydroxyl groups (3405 cm^{-1}) and aromatic rings (1423 cm^{-1}) further supported the anthraquinone type structure (**Fig. IV.100**).

To confirm all the previous data, the examination of the HSQC spectrums (**Fig. IV.94**, **Fig. IV.95** and **Fig. IV.96**) recorded in CDCl_3 of the aromatic region showed the presence of many correlations giving more details about the assignment of compound structure identified as follow:

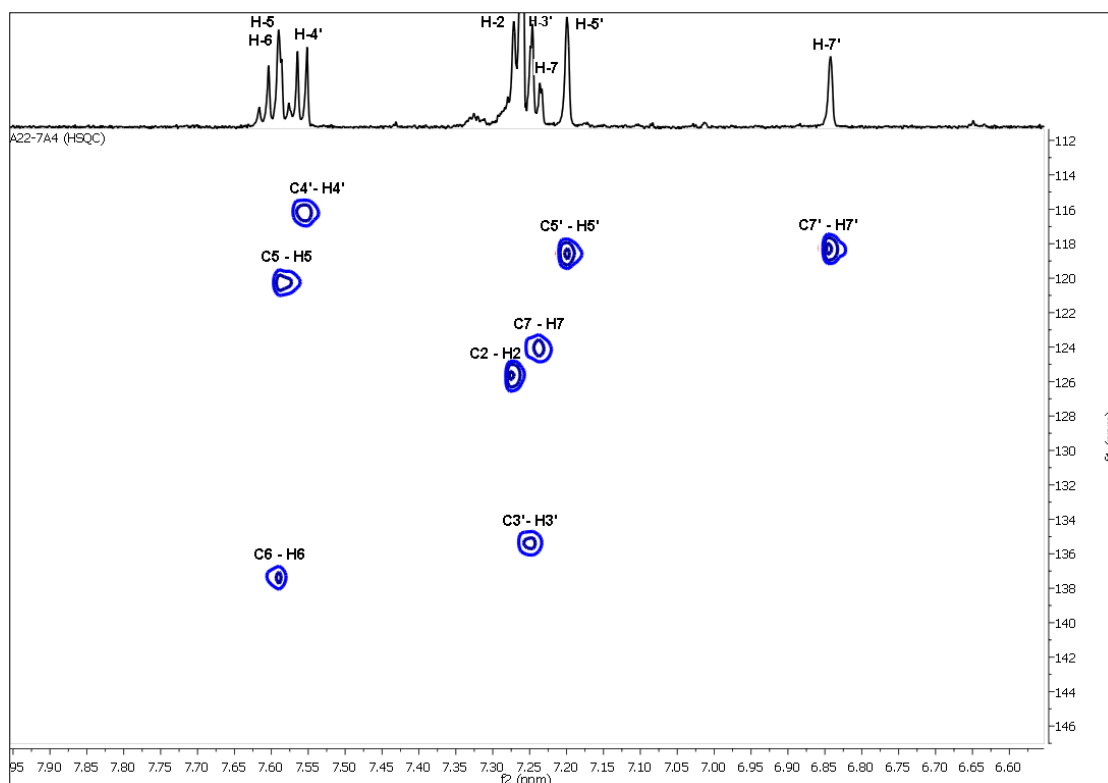


Figure IV.95. HSQC-NMR Spectrum (600 MHz, CDCl_3) of compound **11**.
(From 6.75 ppm to 7.75 ppm)

The proton H-4' showed a correlation with the carbon C-4' at δ_{C} 116.2 ppm.

- ✓ The proton H-6 showed a correlation with the carbon C-6 at δ_{C} 137.4 ppm.
- ✓ The proton H-5 showed a correlation with the carbon C-5 at δ_{C} 120.5 ppm.
- ✓ The proton H-2 showed a correlation with the carbon C-2 at δ_{C} 125.6 ppm.
- ✓ The proton H-3' showed a correlation with the carbon C-3' at δ_{C} 135.4 ppm.
- ✓ The proton H-7 showed a correlation with the carbon C-7 at δ_{C} 124.2 ppm.
- ✓ The proton H-5' showed a correlation with the carbon C-5' at δ_{C} 118.5 ppm.
- ✓ The proton H-7' showed a correlation with the carbon C-7' at δ_{C} 118.3 ppm.

For the osidic region, the HSQC spectrum showed also correlations identified as follow:

- ✓ Both H-6''*a*, H-6''*b* showed correlation with the carbon C-6'' at δ_{C} 62.9 ppm.
- ✓ The proton H-3'' showed a correlation with the carbon C-3'' at δ_{C} 78.8 ppm.
- ✓ The proton H-1'' showed a correlation with the carbon C-1'' at δ_{C} 83.8 ppm.
- ✓ The proton H-2'' showed a correlation with the carbon C-2'' at δ_{C} 71.7 ppm.
- ✓ The proton H-4'' showed a correlation with the carbon C-4'' at δ_{C} 70.7 ppm.
- ✓ The proton H-5'' showed a correlation with the carbon C-5'' at δ_{C} 81.0 ppm.
- ✓ The two methyl groups protons at 11'- CH_3 and 11- CH_3 showed correlation with the carbons at δ_{C} 22.9 ppm and δ_{C} 21.9 ppm, respectively.

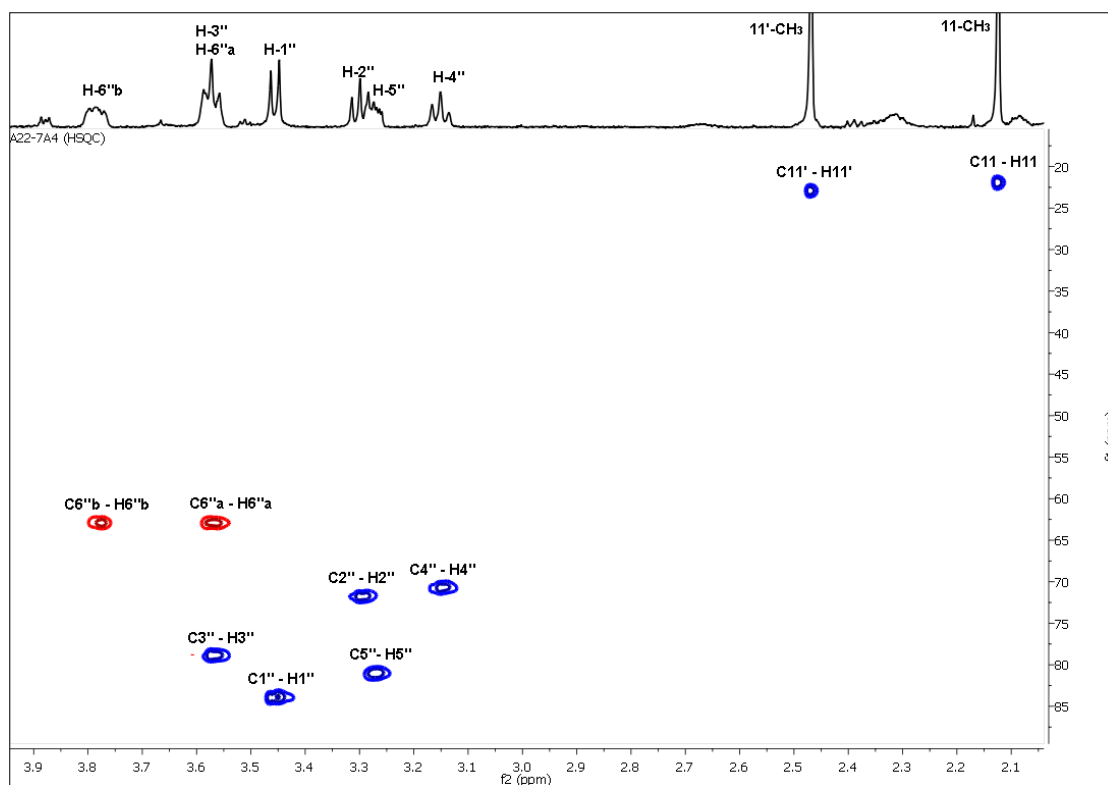


Figure IV.96. HSQC-NMR Spectrum (600 MHz, CDCl₃) of compound **11**.
(From 1.90 ppm to 3.80 ppm).

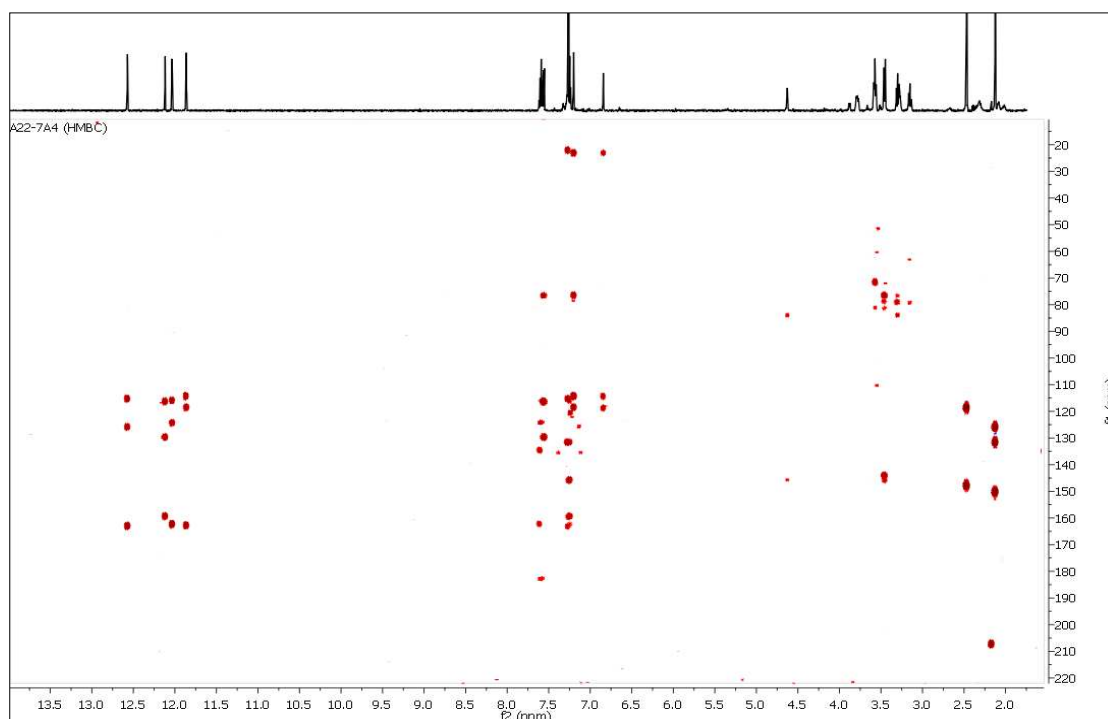


Figure IV.97. HMBC-NMR Spectrum (600 MHz, CDCl₃) of compound **11**

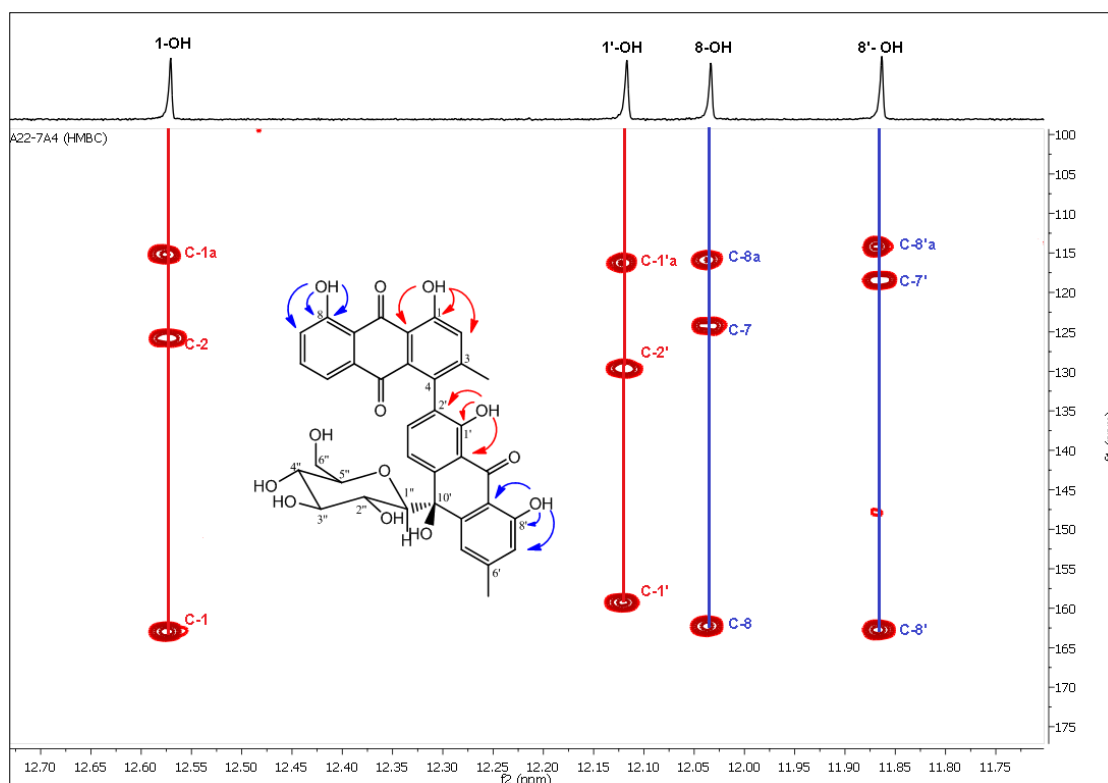


Figure IV.98. HMBC-NMR Spectrum (600 MHz, CDCl_3) of compound **11**.
(From 11.55 ppm to 12.75 ppm).

The HMBC correlations reported in (**Fig. IV.98**) showed the cross peaks from the phenolic OH groups at δ_{H} 12.58, 12.03, 12.12 and 11.87 ppm with C-1; C-2 and C-1a, with C-8; C-7 and C-8a, with C-1'; C-2' and C-1'a, and with C-8'; C-7' and C-8'a, respectively. All these data suggested that the four phenolic OH groups should be located at C-1, C-8, C-1' and C-8', respectively. All these data were suggestive of the presence of a glycosyl bianthrone structure [33-31].

All the other HMBC correlations for the aromatic region (downfield region) were clearly observed in (**Fig. IV.99**), the same thing for the upfield region where all the possible correlations were observed (**Fig. IV.100**).

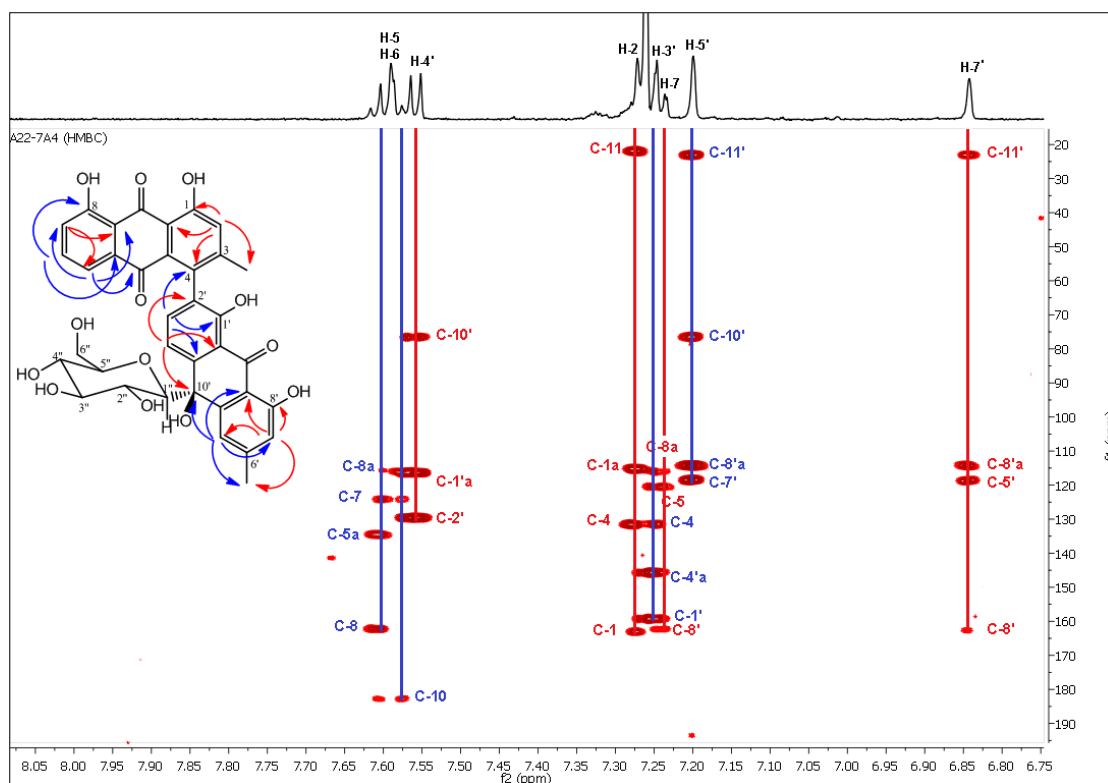


Figure IV.99. HMBC-NMR Spectrum (600 MHz, CDCl₃) of compound 11.
(From 6.00 ppm to 7.70 ppm).

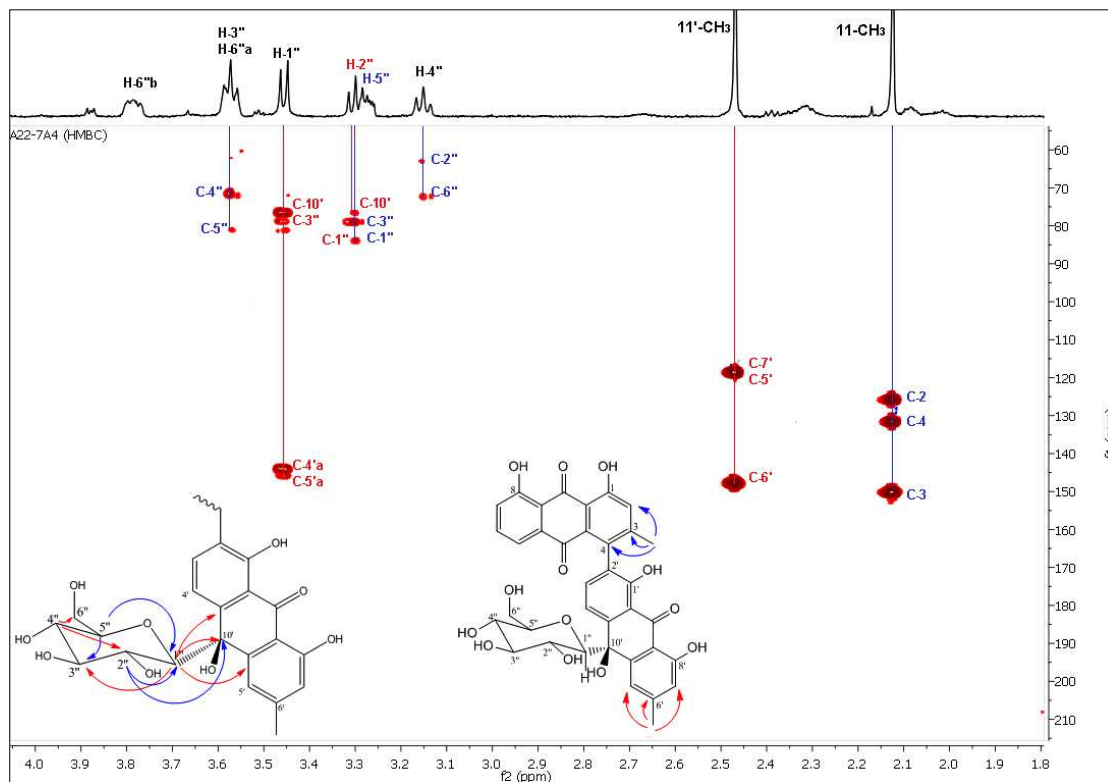


Figure IV.100. HMBC-NMR Spectrum (600 MHz, CDCl₃) of compound 11.
(From 0.50 ppm to 4.30 ppm).

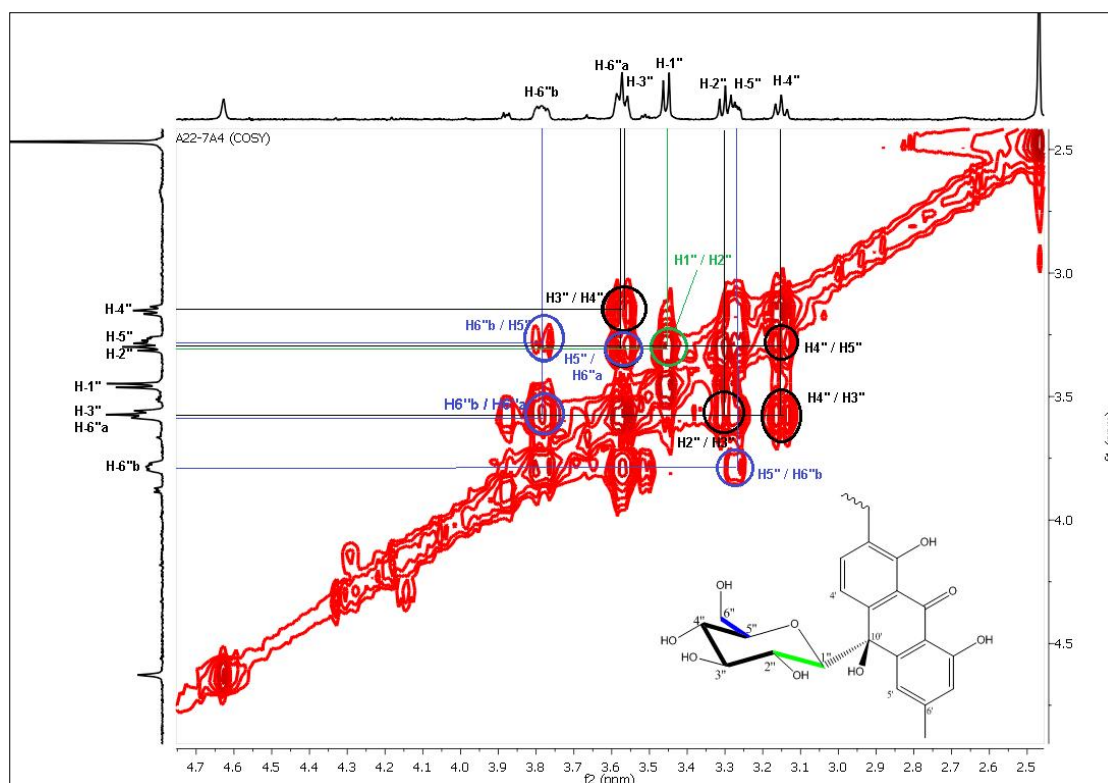


Figure IV.101. ^1H - ^1H COSY NMR Spectrum (600 MHz, CDCl_3) of compound **11**.
(From 2.50 ppm 4.70 ppm).

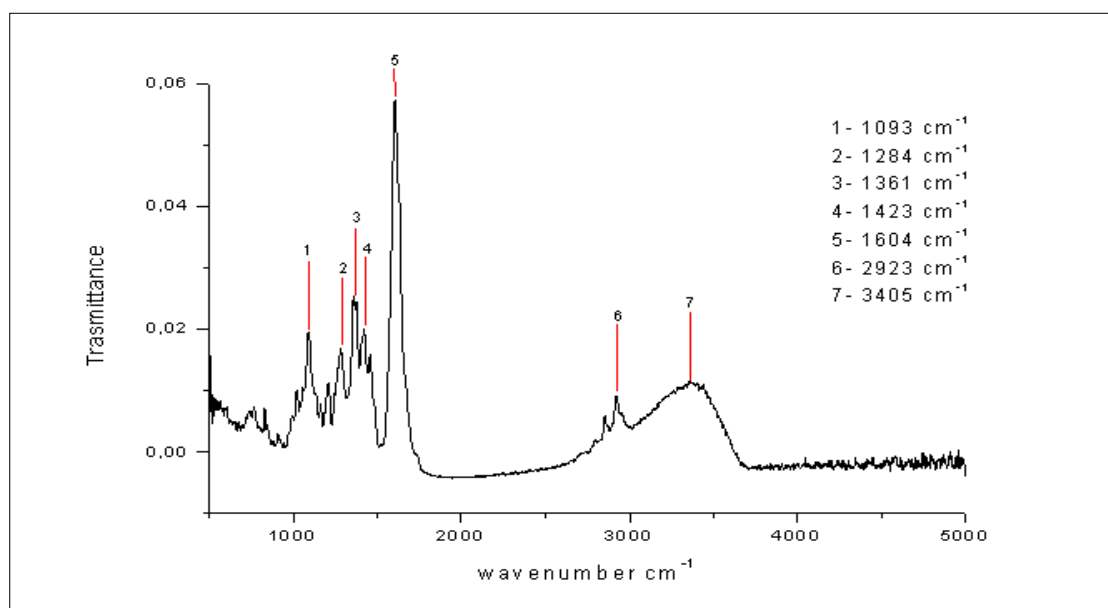


Figure IV.102. IR Spectrum of compound **11**.

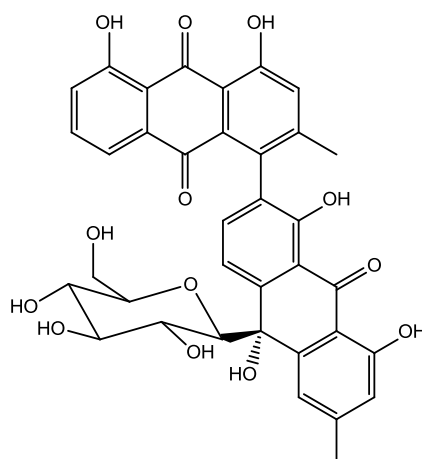
All the chemical shifts of the NMR ^1H , ^{13}C , HSQC and HMBC correlations of compound **11** are summarized in the following table (**Table IV.18**).

Table IV.18. ^1H , ^{13}C and HMBC NMR data of compound **11** (CDCl_3).

Positions	δ_{C} (ppm)	δ_{H} (ppm), <i>mult.</i> , <i>J</i> (Hz)	HMBC
1	162.9	-	-
2	125.6	7.27 (<i>s</i> , 1H)	C-11, C-1a, C-4, C-1
3	150.4	-	-
4	131.5	-	-
5	120.5	7.59 (<i>d</i> , 1H, 8.2 Hz)	C-10, C-7
6	137.4	7.60 (<i>t</i> , 1H, 8.2 Hz)	C-5a, C-8
7	124.2	7.24 (<i>d</i> , 1H, 8.2 Hz)	C-8a, C-5
8	162.2	-	-
9	194.5	-	-
10	182.6	-	-
1a	115.0	-	-
4a	131.5	-	-
5a	134.5	-	-
8a	116.3	-	-
1'	159.3	-	-
2'	129.6	-	-
3'	135.4	7.25 (<i>d</i> , 1H, 8.2 Hz)	C-4, C-4'a, C-1'
4'	116.2	7.55 (<i>d</i> , 1H, 8.2 Hz)	C-10', C-2', C-1'a
5'	118.5	7.20 (<i>s</i> , 1H)	C-11', C-8'a, C-7', C-10'
6'	147.9	-	-
7'	118.3	6.84 (<i>s</i> , 1H)	C-11', C-8'a, C-5', C-8'
8'	162.7	-	-
9'	193.4	-	-
10'	77.3	-	-
1'a	116.3	-	-
4'a	145.7	-	-
5'a	146.7	-	-
8'a	114.2	-	-
1''	83.8	3.45 (<i>d</i> , 1H, 9.3 Hz)	C-10'', C-4'a, C-5'a, C-3''
2''	71.7	3.30 (<i>t</i> , 1H, 9.3 Hz)	C-10'', C-1'', C-3''
3''	78.8	3.57 (<i>t</i> , 1H, 9.3 Hz)	C-2'', C-4'', C-5''
4''	70.7	3.15 (<i>t</i> , 1H, 9.3 Hz)	C-3'', C-5'', C-6''
5''	81.0	3.27 (<i>m</i> , 1H)	C-3'', C-1''
6''	62.9	3.57, 3.77 (<i>m</i> , 1H)	C-4''
11	21.9	2.13 (<i>s</i> , 3H)	C-3, C-2, C-4
11'	22.9	2.47 (<i>s</i> , 3H)	C-6', C-5', C-7'
1-OH	-	12.58 (<i>s</i> , 1H)	C-1, C-2, C-1a
8-OH	-	12.03 (<i>s</i> , 1H)	C-8, C-7, C-8a
1'-OH	-	12.12 (<i>s</i> , 1H)	C-1', C-2', C-1'a
8'-OH	-	11.87 (<i>s</i> , 1H)	C-8', C-7', C-8'a

Based on these full spectroscopic studies, the new planar structure of **10'-oxanthrone-(10'S)- β -glucopyranosyl asphodelin** could be attributed to compound **11**.

This compound was isolated for the first time and never mentioned in literature previously.



IV.5.12. Identification of compound 12. (New compound)

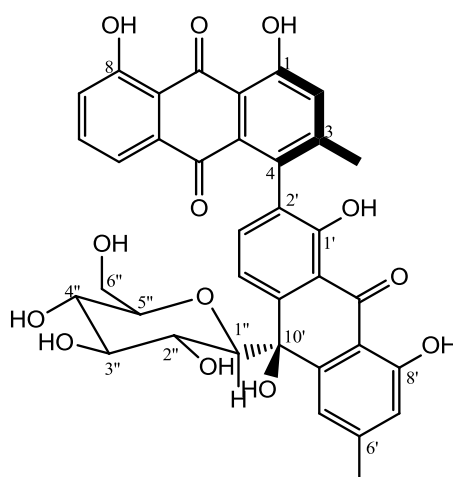


Figure IV.103. Structure of compound 12.

Compound 12 was obtained as a yellowish amorphous powder. Its HRESI-MS analysis (**Fig. IV.104**) gave an $[M-H]^-$ ion at m/z 669.16345 (calculated for $C_{36}H_{29}O_{13}$, 669.16081), consistent with the molecular formula $C_{36}H_{30}O_{13}$, indicating 22 degrees of unsaturation in the structure similar to the previous compound (**11**) molecular formula.

The structure was elucidated by NMR analysis including 1H (**Fig. IV.105**, **Fig. IV.106**, **Fig. IV.107**), HMBC (**Fig. IV.111**), and HSQC data (**Fig. IV.108**). Similar to the previous compound **11**, the ^{13}C -NMR spectrum of compound **12** showed also 36 carbon resonances, including two methyl groups (δ_C 21.5 ppm and δ_C 23.0 ppm), an oxymethylene (δ_C 62.9 ppm), eight aromatic methines, five sp^3 oxymethines, 12 quaternary carbons, four oxygenated sp^2 tertiary carbons, three carbonyl carbons (δ_C 194.1 ppm, 183.7 ppm, and 192.8 ppm), and one oxygenated sp^3 tertiary carbon.

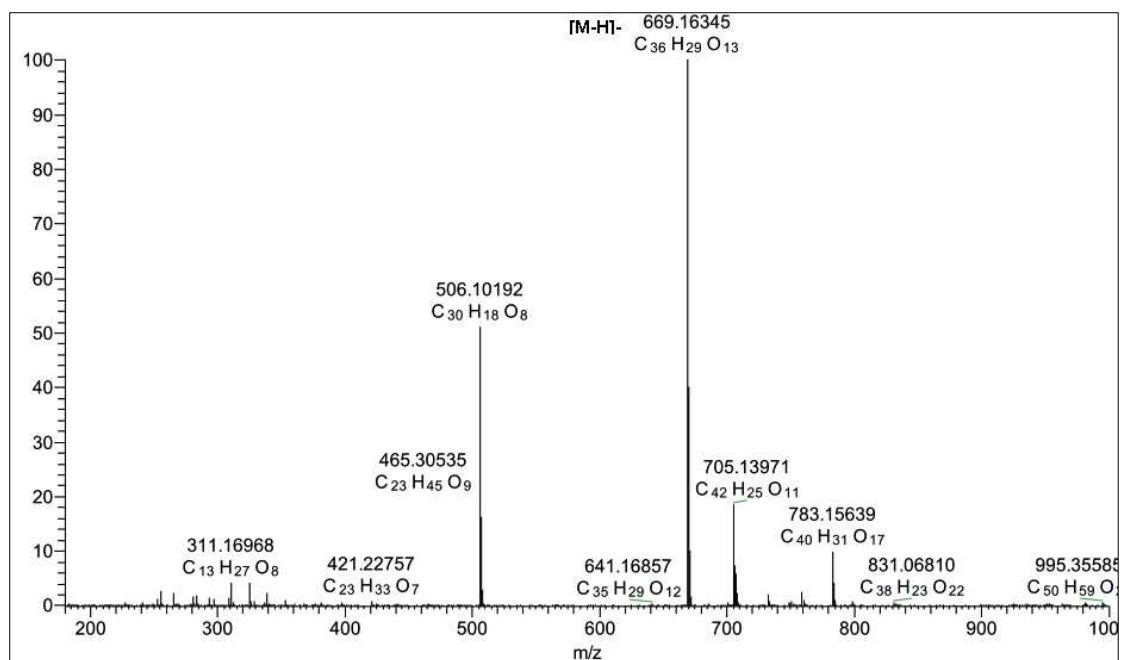


Figure IV.104. HRESI-MS spectrum in negative ion mode of compound **12**.

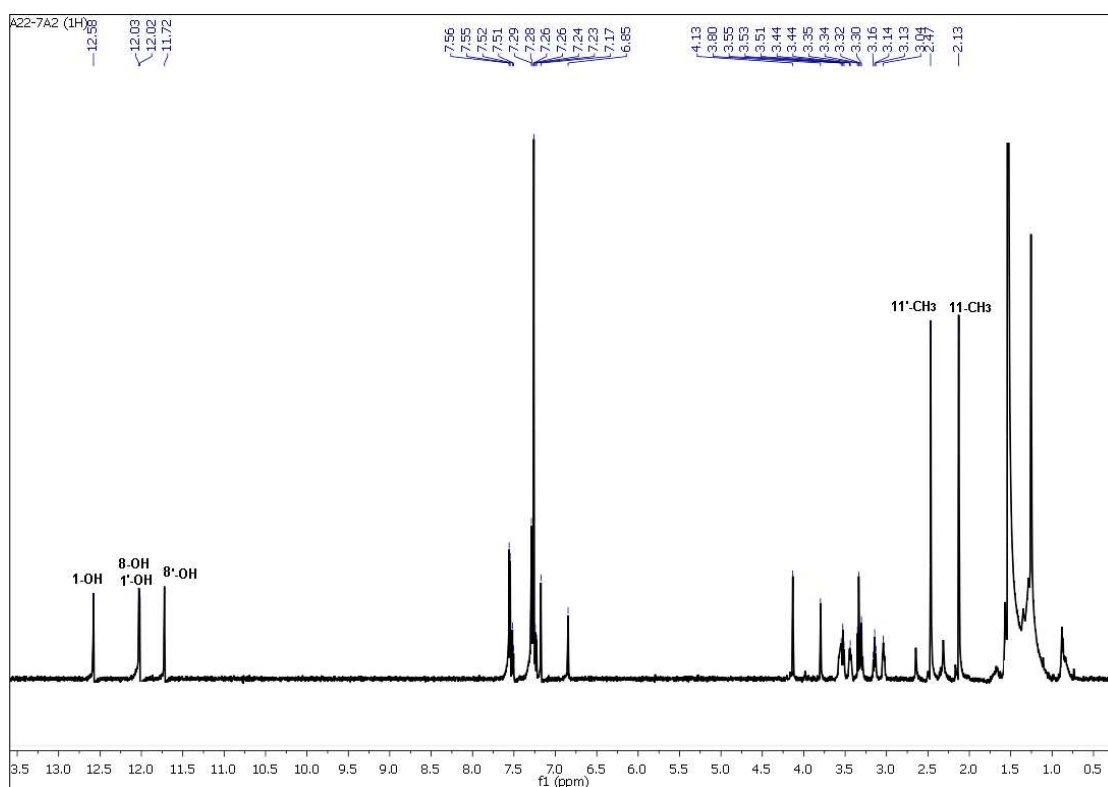


Figure IV.105. ¹H-NMR Spectrum (600 MHz, CDCl₃) of compound **12**.

The ¹H-NMR spectrum showed as the previous compound **11** eight deshielded resonances ascribable to eight aromatic protons (Fig. IV.106), and two singlets at δ_{H} 2.13 ppm and δ_{H} 2.47 ppm assigned to two aromatic methyl groups (Fig. IV.105).

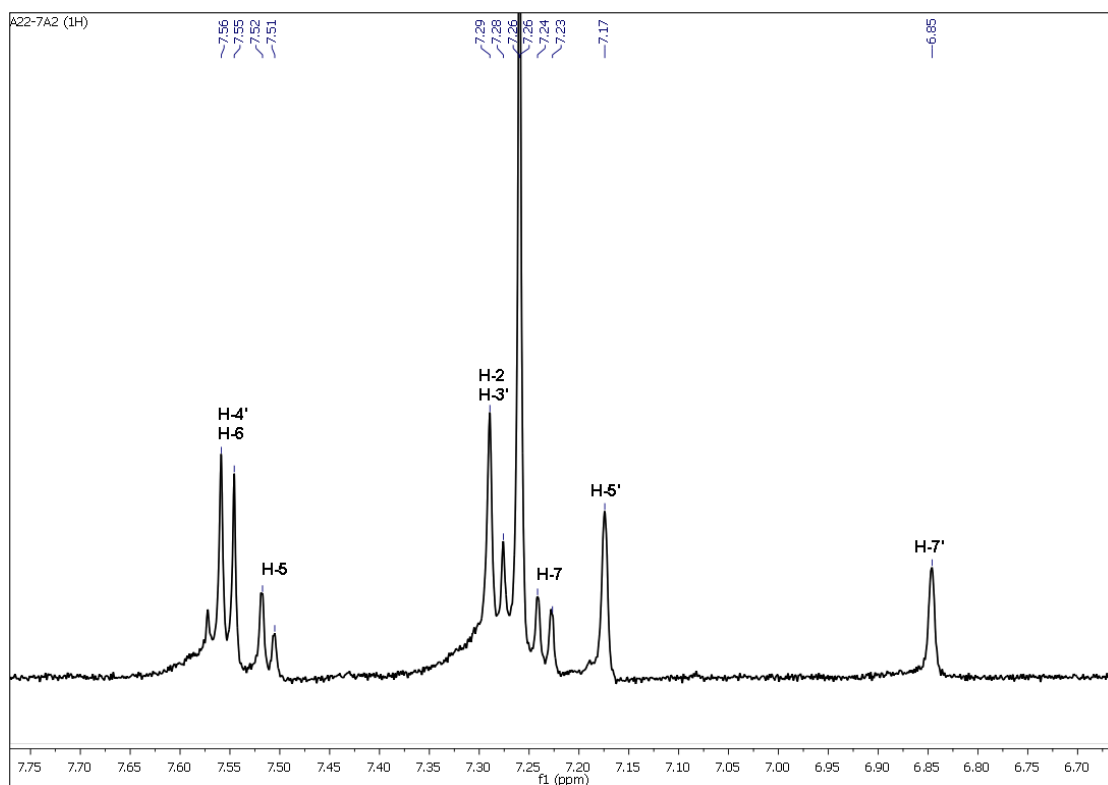


Figure IV.106. $^1\text{H-NMR}$ Spectrum (600 MHz, CDCl_3) of compound **12**.
(From 6.70 ppm to 7.80 ppm)

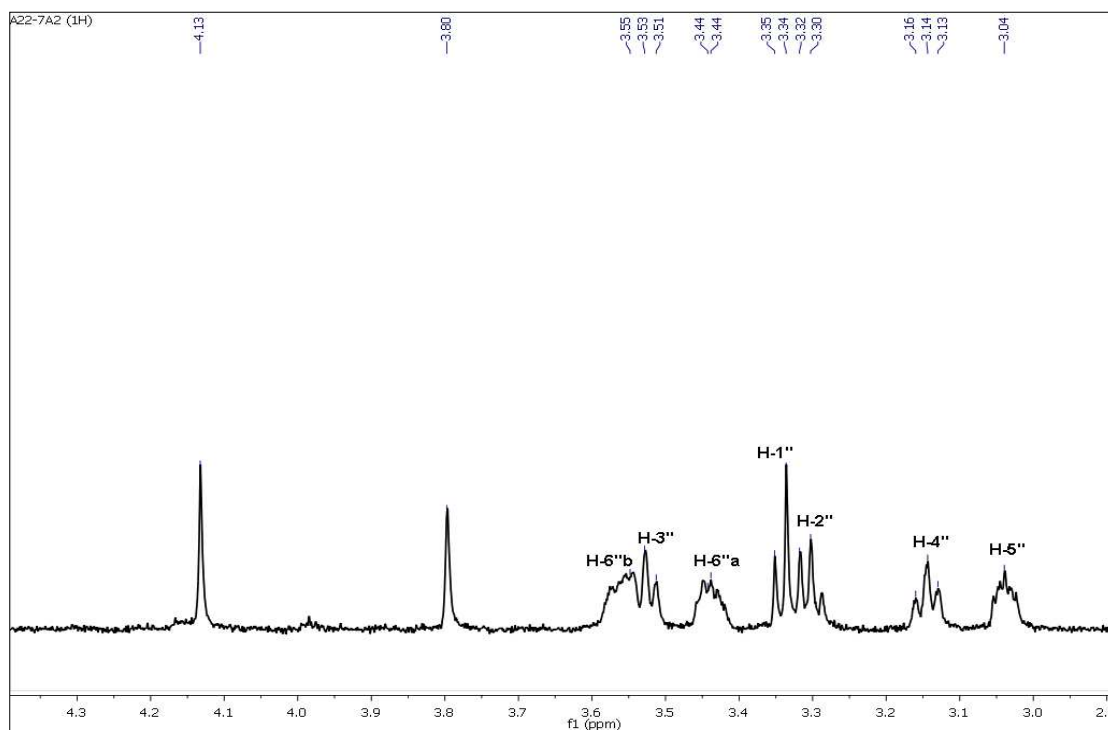


Figure IV.107. $^1\text{H-NMR}$ Spectrum (600 MHz, CDCl_3) of compound **12**.
(From 2.90 ppm to 4.30 ppm).

The $^1\text{H-NMR}$ spectrum showed also the presence of a hexose unit characterized by five oxymethine protons (**Fig. IV.107**) at δ_{H} 3.34 ppm (*d*, 9.3 Hz), δ_{H} 3.30 ppm (*t*, 9.3 Hz), δ_{H} 3.53 ppm (*t*, 9.3 Hz), δ_{H} 3.15 ppm (*t*, 9.3 Hz), and δ_{H} 3.04 ppm (*m*) and an oxymethylene at δ_{H} 3.44 ppm (*m*) and δ_{H} 3.56 ppm (*m*), coupled to their neighbors in this order, as suggested by the COSY experiment (**Fig. IV.115**). In addition, the $^1\text{H-NMR}$ spectrum showed four highly deshielded singlets at δ_{H} 11.72 ppm, 12.03 ppm, 12.02 ppm, and 12.58 ppm (**Fig. IV.105**), indicative of four exchangeable hydrogens bound to oxygen, and assigned to four phenolic groups (δ_{C} 164.1 ppm, 163.2 ppm, 159.4 ppm and 163.5 ppm) [31].

The HMBC correlations shown in (**Fig. IV.112**) was similar to the previous compound **11** which indicate the cross-peaks between each phenolic group and their respective neighboring carbons, thus permitting their placement at C-1, C-8, C-1' and C-8'. The arrangement of the aromatic protons, as deduced by COSY and HMBC correlations (**Fig. IV.113**), indicated the presence of an ABX spin system at δ_{H} 7.52 ppm (*d*, 8.1 Hz, H-5), δ_{H} 7.56 ppm (*t*, 8.1 Hz, H-6), and δ_{H} 7.23 ppm (*d*, 8.2 Hz, H-7), an AX pattern at δ_{H} 7.28 ppm (*d*, 8.1 Hz, H-3') and δ_{H} 7.55 ppm (*d*, 8.1 Hz, H-4'), two *meta*-coupled protons at δ_{H} 7.17 ppm (*s*, H-5') and δ_{H} 6.85 (*s*, H-7'), separated by the CH_3 -11' methyl group (**Fig. IV.113**), and an isolated singlet at δ_{H} 7.29 ppm (*s*, H-2) showing correlation with the methyl protons at δ_{C} 21.5 ppm (C-11). Comparison of the NMR data of compound **12** with those of reported compounds suggested that it was closely related as the previous compound **11** to asphodoside A [31].

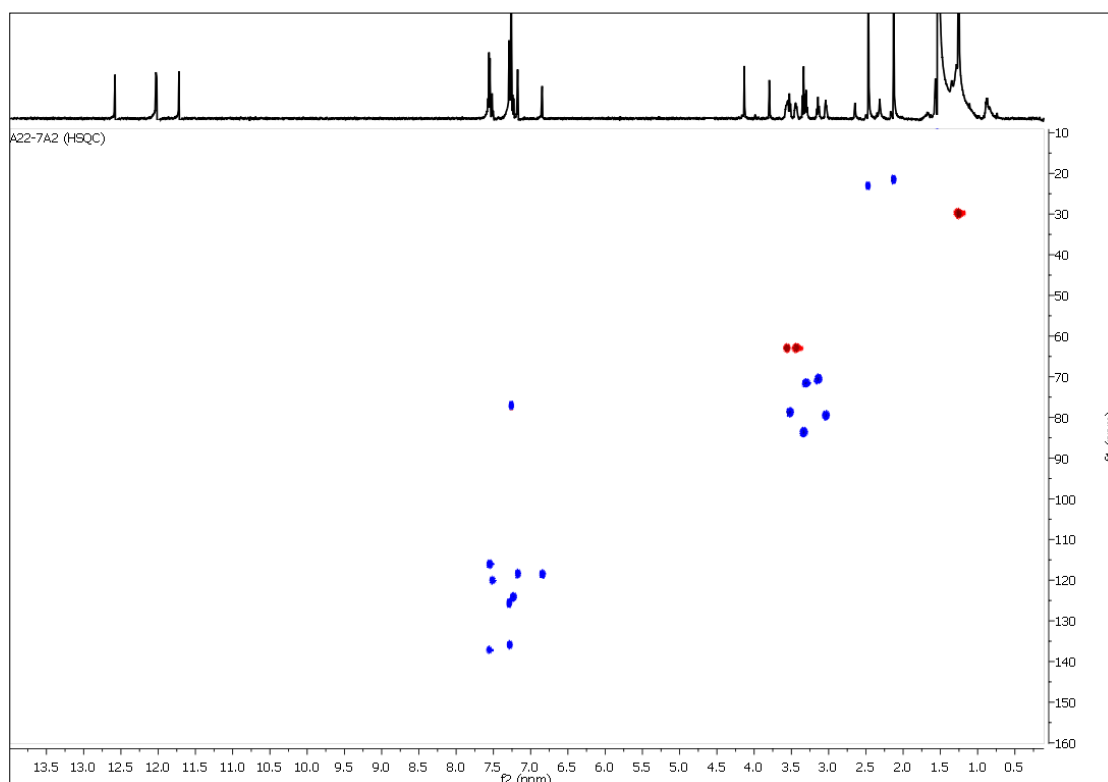


Figure IV.108. HSQC-NMR Spectrum (600 MHz, CDCl_3) of compound **12**.

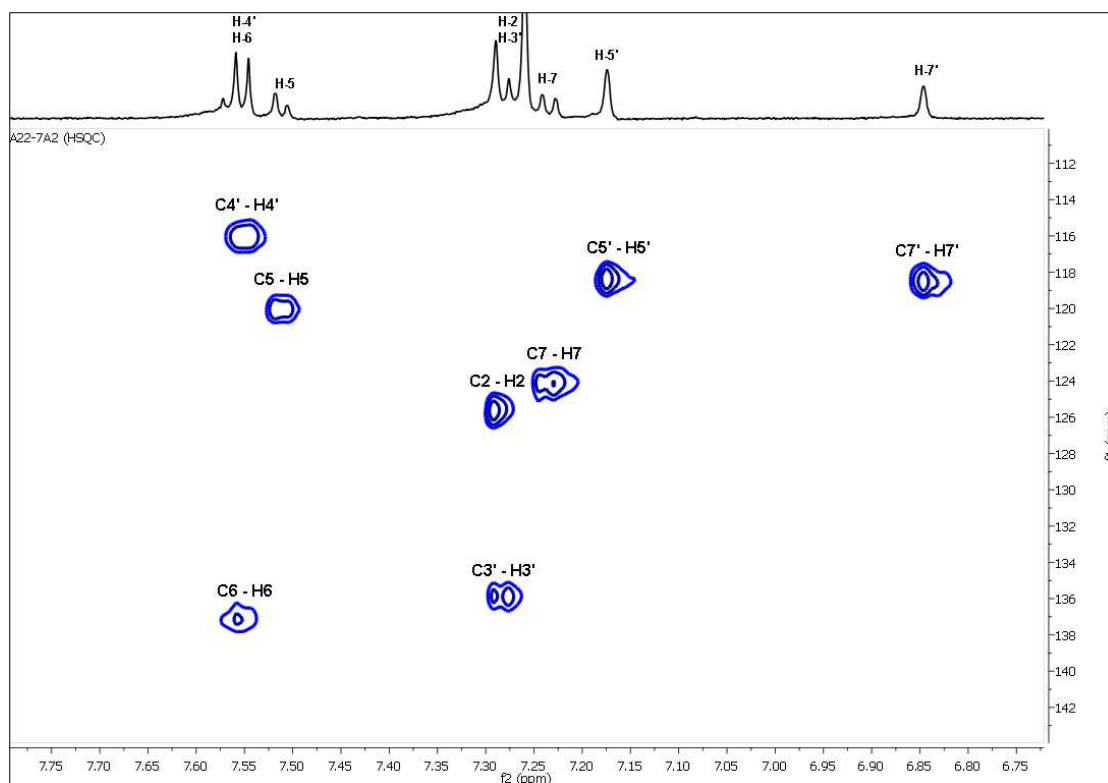


Figure IV.109. HSQC-NMR Spectrum (600 MHz, CDCl₃) of compound **12**.
(From 6.60 ppm to 7.90 ppm).

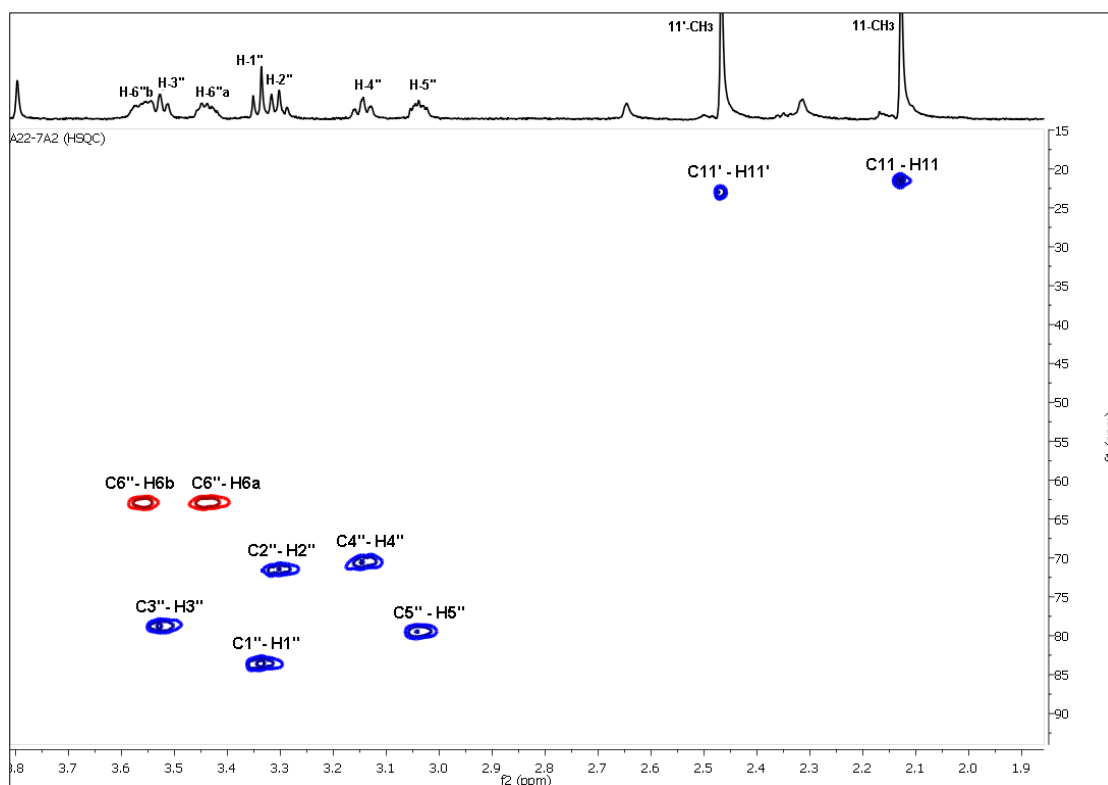


Figure IV.110. HSQC-NMR Spectrum (600 MHz, CDCl₃) of compound **12**.
(From 2.10 ppm to 3.90 ppm).

A xylopyranosylbianthrone containing a pentose unit linked at C-10' instead of the hexose moiety revealed and deduced by comparison of the ESI-MS and NMR data of compound **12**. The aromatic singlet at δ_{H} 7.29 ppm (H-2) with the biosynthetically anticipated methyl signal at δ_{C} 21.5 ppm (C-11), as well as the ABX spin system, was assigned to the anthraquinone substructure and was supported by the long-range H-C correlation patterns (H-5/C-10, H-7/C-8a, H-2/C-1a) (**Fig. IV.113**).

The remaining $^1\text{H}/^{13}\text{C}$ resonances and in particular the AX system (H-3' and H-4') and the pair of *meta*-coupled protons, separated by the 11'-methyl group, were attributed to the oxanthrone substructure. The correlations between the tertiary carbinol at δ_{C} 77.9 ppm (C-10') and H-4' and H-5' were diagnostic for this assignment. The presence of a β -glucopyranosyl unit in compound **12** was supported as with compound **11** by: (i) the presence in the ESIMS data of an ion at $m/z = 506$, due to the loss of a hexosyl unit from $[\text{M}-\text{H}-162]^-$, and (ii) the multiplicity of the sugar signals and the $J_{\text{H-H}}$ values were in good agreement with those reported for other β -glucopyranosyl moieties.

Analysis of the long-range C / H correlations established the link between the anthraquinone, oxanthrone, and β -glucopyranosyl moieties. In particular, the correlation between C-4 (δ_{C} 132.5 ppm) and H-3' (δ_{H} 7.28 ppm) defined the linkage between the anthraquinone and oxanthrone substructures (C-4/C-2'), while the correlation between C-10' (δ_{C} 77.9 ppm) and the anomeric proton provided evidence of the location of the sugar moiety as well as the type of glucosidic linkage, as supported by the shielded anomeric carbon resonance at δ_{C} 83.5 ppm (C-1'').

The examination of the HSQC spectrum (**Fig. IV.109**) recorded in CDCl_3 of the aromatic region showed similar to the previous compound **11** correlations giving more details about the assignment of this compound structure identified as follow:

- ✓ The proton H-4' showed a correlation with the carbon C-4' at δ_{C} 116.0 ppm.
- ✓ The proton H-6 showed a correlation with the carbon C-6 at δ_{C} 137.1 ppm.
- ✓ The proton H-5 showed a correlation with the carbon C-5 at δ_{C} 120.0 ppm.
- ✓ The proton H-2 showed a correlation with the carbon C-2 at δ_{C} 125.6 ppm.
- ✓ The proton H-3' showed a correlation with the carbon C-3' at δ_{C} 135.9 ppm.
- ✓ The proton H-7 showed a correlation with the carbon C-7 at δ_{C} 124.1 ppm.
- ✓ The proton H-5' showed a correlation with the carbon C-5' at δ_{C} 119.3 ppm.
- ✓ The proton H-7' showed a correlation with the carbon C-7' at δ_{C} 118.5 ppm.

For the osidic region, the HSQC spectrum (**Fig. IV.110**) showed also other correlations identified as follow:

- ✓ Both H-6''*a*, H-6''*b* showed correlation with the carbon C-6'' at δ_{C} 62.9 ppm.
- ✓ The proton H-3'' showed a correlation with the carbon C-3'' at δ_{C} 78.7 ppm.
- ✓ The proton H-1'' showed a correlation with the carbon C-1'' at δ_{C} 83.5 ppm.
- ✓ The proton H-2'' showed a correlation with the carbon C-2'' at δ_{C} 71.4 ppm.
- ✓ The proton H-4'' showed a correlation with the carbon C-4'' at δ_{C} 70.5 ppm.
- ✓ The proton H-5'' showed a correlation with the carbon C-5'' at δ_{C} 79.4 ppm.

- ✓ The two methyl groups protons at 11'-CH₃ and 11-CH₃ showed correlation with the carbons at δ_C 23.0 ppm and δ_C 21.5 ppm, respectively.

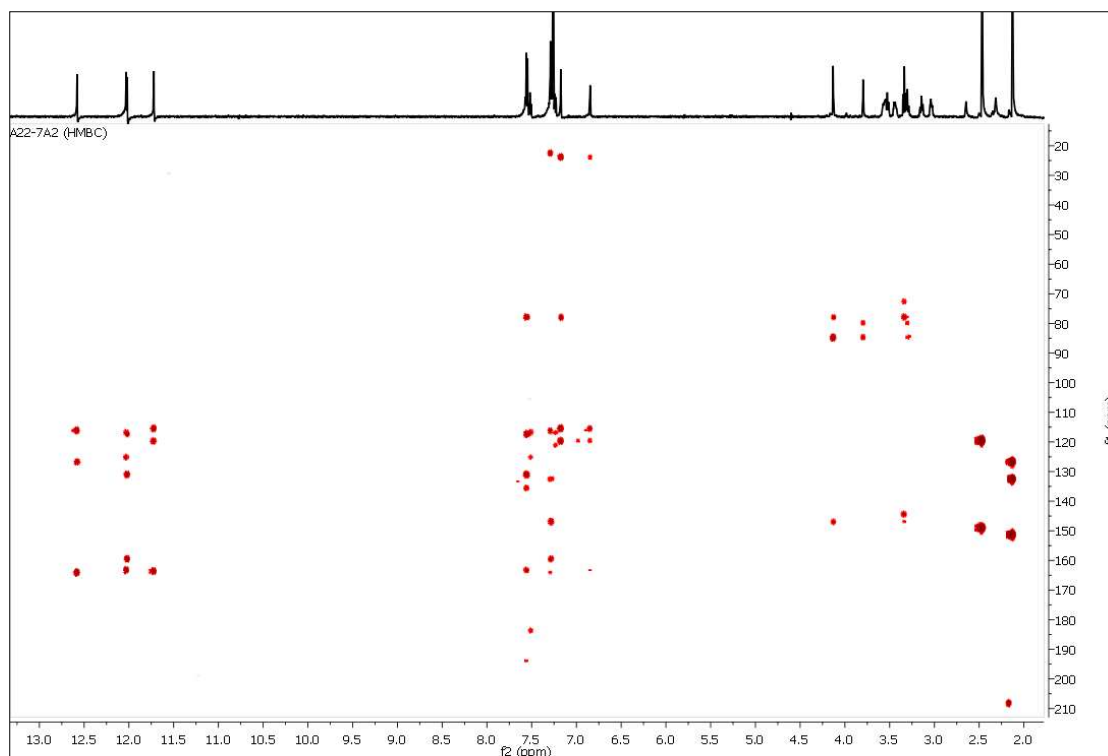


Figure IV.111. HMBC-NMR Spectrum (600 MHz, CDCl₃) of compound 12.

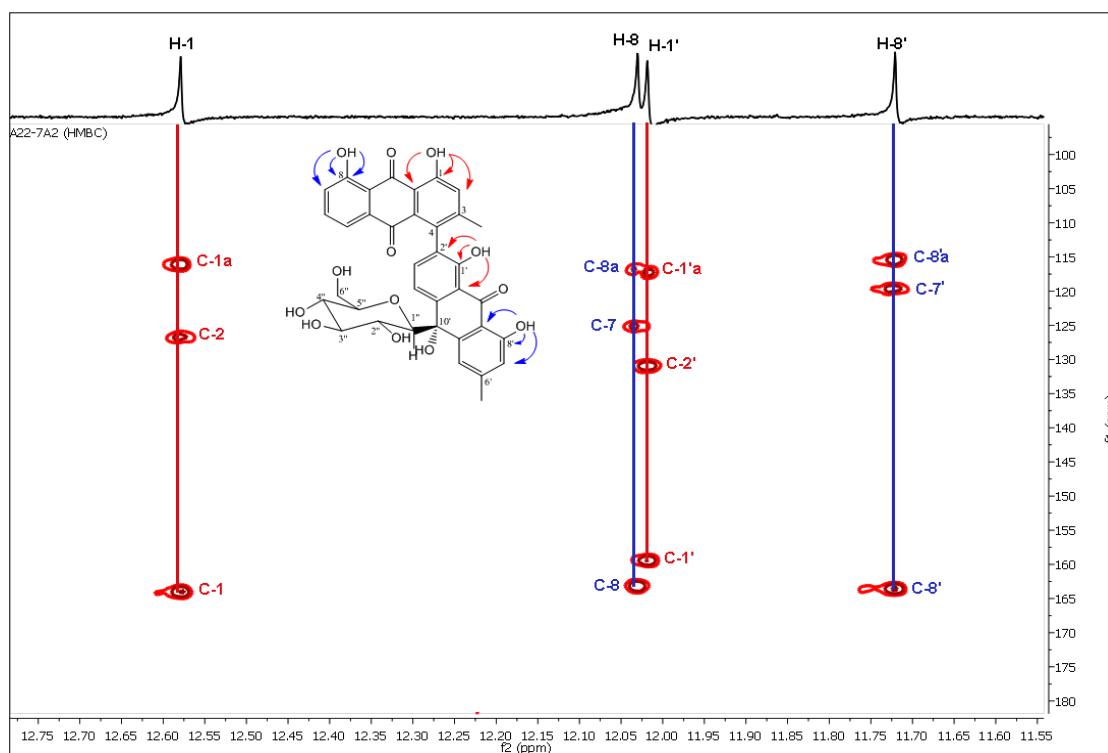


Figure IV.112. HMBC-NMR Spectrum (600 MHz, CDCl₃) of compound 12. (From 11.75 ppm to 12.70 ppm).

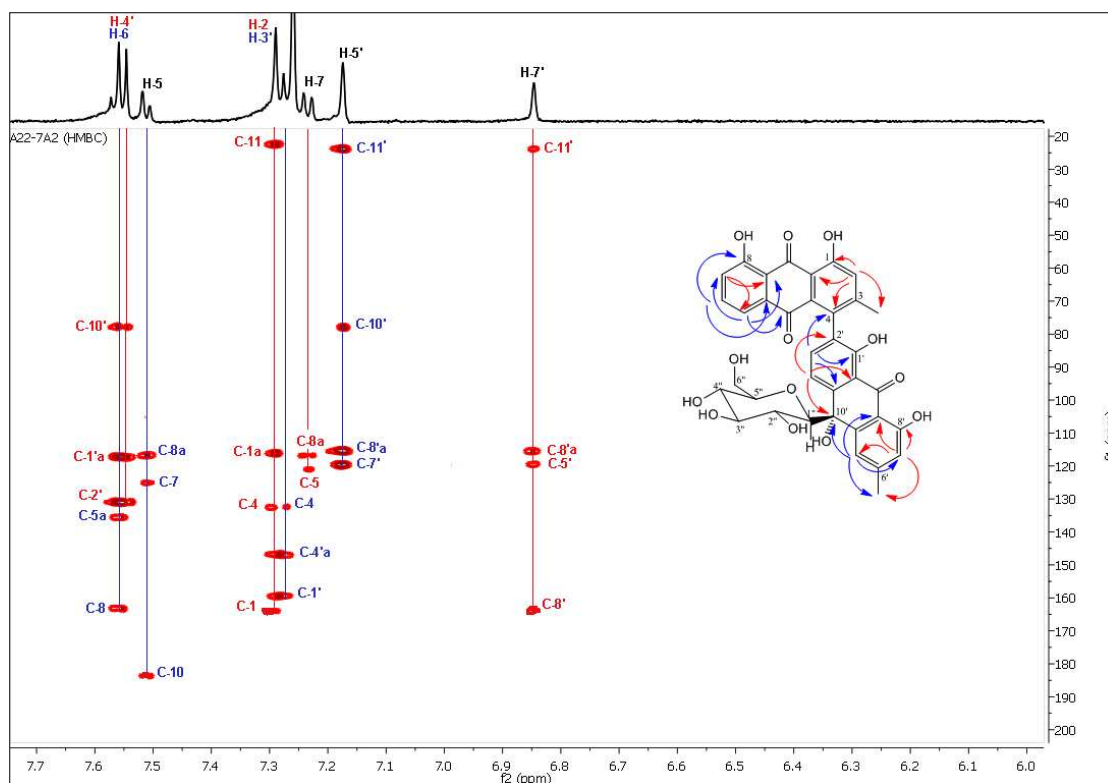


Figure IV.113. HMBC-NMR Spectrum (600 MHz, CDCl_3) of compound **12**.
(From 6.75 ppm to 7.70 ppm).

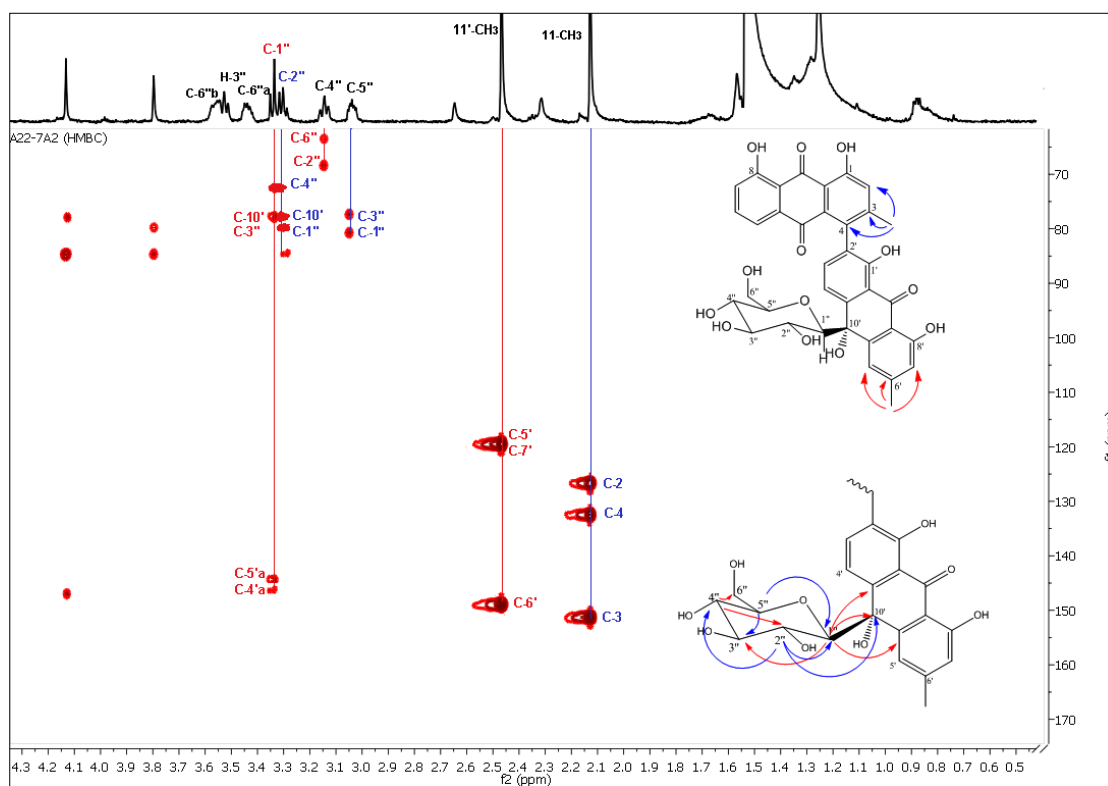


Figure IV.114. HMBC-NMR Spectrum (600 MHz, CDCl_3) of compound **12**.
(From 1.80 ppm 4.00 ppm).

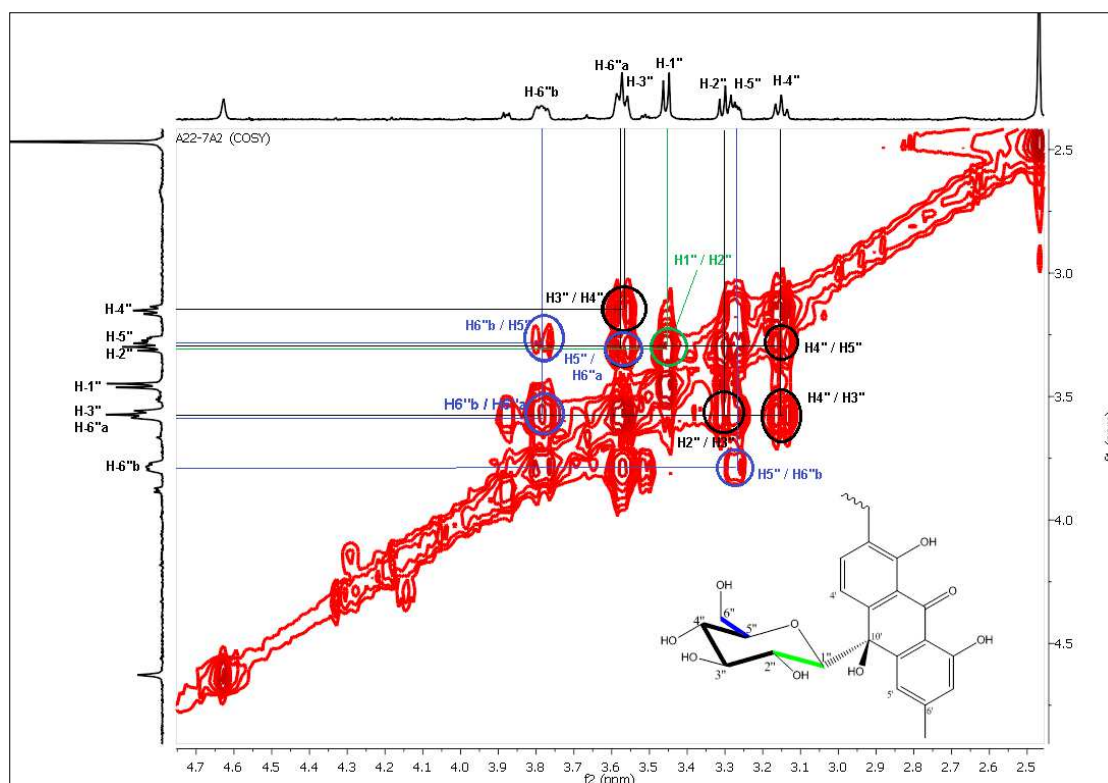


Figure IV.115. ^1H - ^1H COSY NMR Spectrum (600 MHz, CDCl_3) of compound **12**. (From 2.50 ppm 4.70 ppm).

All the chemical shifts of the NMR ^1H , ^{13}C , HSQC and HMBC correlations of compound **12** are summarized in the following table (**Table IV.19**).

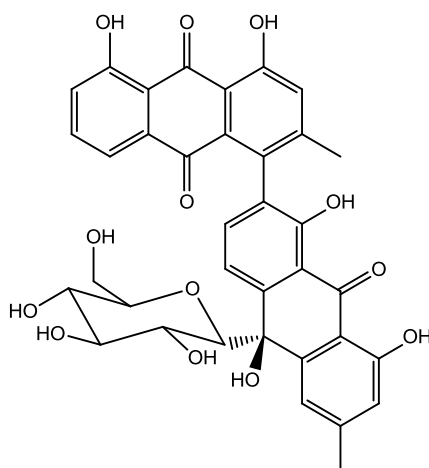
Table IV.19. ^1H , ^{13}C and HMBC NMR data of compound **12** (CDCl_3).

Positions	δ_{C} (ppm)	δ_{H} (ppm), <i>mult.</i> , <i>J</i> (Hz)	HMBC
1	164.1	-	-
2	125.6	7.29 (<i>s</i> , 1H)	C-11, C-1a, C-4, C-1
3	151.2	-	-
4	132.5	-	-
5	120.0	7.52 (<i>d</i> , 1H, 8.1 Hz)	C-8a, C-7, C-10
6	137.1	7.56 (<i>t</i> , 1H, 8.1 Hz)	C-5a, C-8
7	124.1	7.23 (<i>d</i> , 1H, 8.1 Hz)	C-8a, C-5
8	163.2	-	-
9	194.1	-	-
10	183.7	-	-
1a	116.1	-	-
4a	132.5	-	-
5a	135.5	-	-
8a	116.8	-	-
1'	159.4	-	-
2'	130.9	-	-
3'	135.9	7.28 (<i>d</i> , 1H, 8.1 Hz)	C-4, C-4'a, C-1'
4'	116.0	7.55 (<i>d</i> , 1H, 8.1 Hz)	C-10', C-1'a, C-2'
5'	118.3	7.17 (<i>s</i> , 1H)	C-11', C-10', C-8'a,
6'	148.9	-	-

7'	118.5	6.85 (<i>s</i> , 1H)	C-11', C-8'a, C-5', C-8'
8'	163.5	-	-
9'	192.8	-	-
10'	77.9	-	-
1'a	117.2	-	-
4'a	146.8	-	-
5'a	144.4	-	-
8'a	115.3	-	-
1''	83.5	3.34 (<i>d</i> , 1H, 9.3 Hz)	C-10'', C-3'', C-5'a, C-4'a
2''	71.4	3.30 (<i>t</i> , 1H, 9.3 Hz)	C-4'', C-10'', C-1''
3''	78.7	3.53 (<i>t</i> , 1H, 9.3 Hz)	
4''	70.5	3.15 (<i>t</i> , 1H, 9.3 Hz)	C-6'', C-2''
5''	79.4	3.04 (<i>m</i> , 1H)	C-3'', C-1''
6''	62.9	3.44, 3.56 (<i>m</i> , 1H)	
11	21.5	2.13 (<i>s</i> , 3H)	C-2, C-4, C-3
11'	23.0	2.47 (<i>s</i> , 3H)	C-5', C-7', C-6'
1-OH	-	12.58 (<i>s</i> , 1H)	C-1a, C-2, C-1
8-OH	-	12.03 (<i>s</i> , 1H)	C-8a, C-7, C-8
1'-OH	-	12.02 (<i>s</i> , 1H)	C-1'a, C-2', C-1'
8'-OH	-	11.72 (<i>s</i> , 1H)	C-8'a, C-7', C-8'

Based on these full spectroscopic studies, the new planar structure of **10'-oxanthrone-(10'S)- β -glucopyranosyl asphodelin** could be attributed to compound **12**.

After a careful examination of all the 1D data and 2D NMR correlations, we can find and confirm the same planar structure for both compounds **11** and **12**.



After the determination of the planar structure of these two metabolites and assuming the presence of D-glucose, to establish the correct stereo-assignment of both compounds **11** and **12**, two main issues were considered: the possible atropisomerism around the biaryl axis and the different configuration at **C-10'** (**11a**, **11b**, **12a** and **12b**).

Firstly, an extensive conformational search related to all the possible diastereoisomers of compounds **11** and **12** (**11a**, **11b**, **12a** and **12b**, (**Fig. IV.116**)), required for the subsequent phases of computation of the ECD spectra and NMR parameters, was performed at the empirical level (Molecular Mechanics, MM), combining Monte Carlo Molecular Mechanics (MCMM), Low-Mode Conformational Sampling (LMCS), and Molecular Dynamics (MD) simulations.

In addition, to corroborate the hypothesized atropisomerism due to the hindered rotation along the disubstituted biaryl axis [34-35], the molecular mechanics (MM) sampled conformers of the possible atropisomers for each diastereoisomer were subsequently submitted to geometry and energy optimization steps at MPW1PW91/6-31G(d) density functional level of theory (DFT). After the optimization of the geometries, the conformers were visually inspected in order to avoid further possible redundant conformers. DFT calculations were employed for predicting the rotational energy barrier related to the interconversion between the atropisomers, specifically considering the configuration at C-10'*R* as a representative system for the investigated compounds.

In more details, this parameter was calculated for the *M*, 10'*R* (**11b**) and *P*, 10'*R* (**12b**) atropisomers, obtaining $\Delta G^\ddagger = 24.0$ kcal/mol and $\Delta G^\ddagger = 21.53$ kcal/mol, referred to difference between the most stable conformers of **11b** and **12b** and the related energy of the transition state, respectively. In particular, the high rotational barrier calculated for **11b** ($\Delta G^\ddagger = 24.0$ kcal/mol) indicated the hindered rotation about the biaryl bond [33], corroborating the presence of atropisomerism and the related hindered interconversion.

In the second phase, we compared the calculated and experimental ECD spectra to predict the atropisomeric forms of compounds **11** and **12**. Starting from the selected conformers related to diastereoisomers (**11a**, **11b**, **12a** and **12b**, (**Fig. IV.116**)), featuring both the configurations *R* and *S* at the stereogenic center (C-10') and at the biaryl axis (*M* / *P* atropisomeric forms), we have calculated the TDDFT-predicted curves (MPW1PW91/6-31G (d, p) functional/basis set) in EtOH IEFPCM to reproduce the effect of the solvent [36].

Interestingly, the comparison of the two experimental ECD curves of compounds **11** and **12** (**Fig. IV.117**) with the ECD calculated curves, showed that the atropisomeric forms *M* (**11a** and **11b**) are similar to ECD of compound **11** while the atropisomeric forms *P* (**12a** and **12b**) are superimposable to experimental ECD of compound **12**, regardless the relative configuration at C-10'

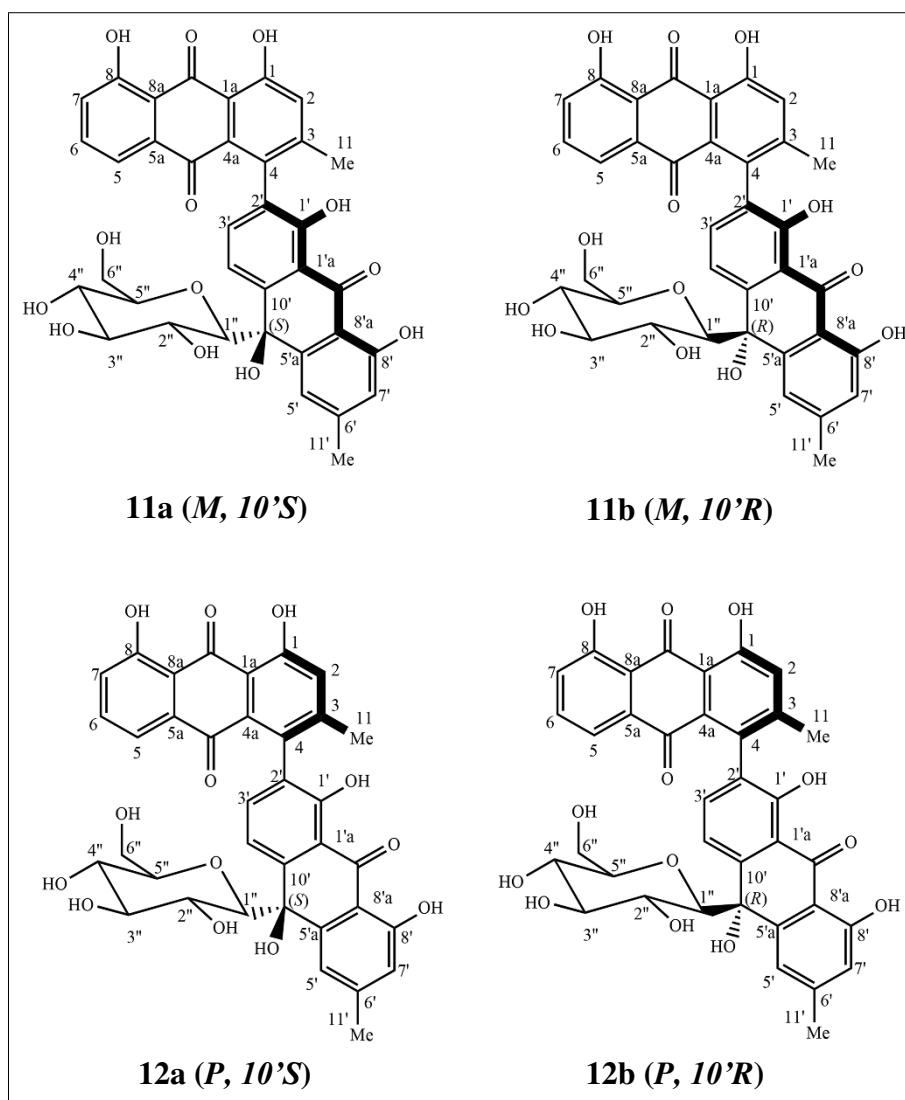


Figure IV.116. Proposed stereo-assignment of compounds **11** and **12**.

Therefore, these results suggest that the Cotton effects are not influenced by the three dimensional arrangement at C-10', further supporting the hindered rotation on the biaryl bond. These results highlighted a first important result in the stereo-assignment process: the real structure of compound **11** was restricted among those of **11a** and **11b** and, consistently, compound **12** will correspond to **12a** or **12b**. Consequently, in order to propose the configuration assignment at C-10', we have applied a DFT/NMR approach which have been successfully used in the characterization of unknown stereostructures by us [37-38] and by other research groups [39].

In (**Fig. IV.117**), we reported the region of interest (350 to 500 nm) as reported for other known similar C- glucosyl anthraquinones [31-32-40].

The results highlighted the better accordance with the experimental data of **11a** (^{13}C MAE= 2.78 ppm) versus **11b** (^{13}C MAE= 4.95 ppm), and of **12a** (^{13}C MAE= 2.13 ppm) versus **12b** (^{13}C MAE= 4.49 ppm), suggesting the absolute configuration *S* at

position 10' for both the atropisomers. Accordingly, we confirm the structure of compounds **11** as (*M*,10' *S*)-1',4,5,8',10'-Pentahydroxy-2,6'-dimethyl-10'- β -glucopyranosyl-[1,2'-bianthracene]-9,9',10(10'H)-trione and compound **12** as (*P*,10' *S*)-1',4,5,8',10'-Pentahydroxy-2,6'-dimethyl-10'- β -gluco-pyranosyl-[1,2'-anthracene]-9,9',10(10'H)-trione as shown in (Fig. IV.118).

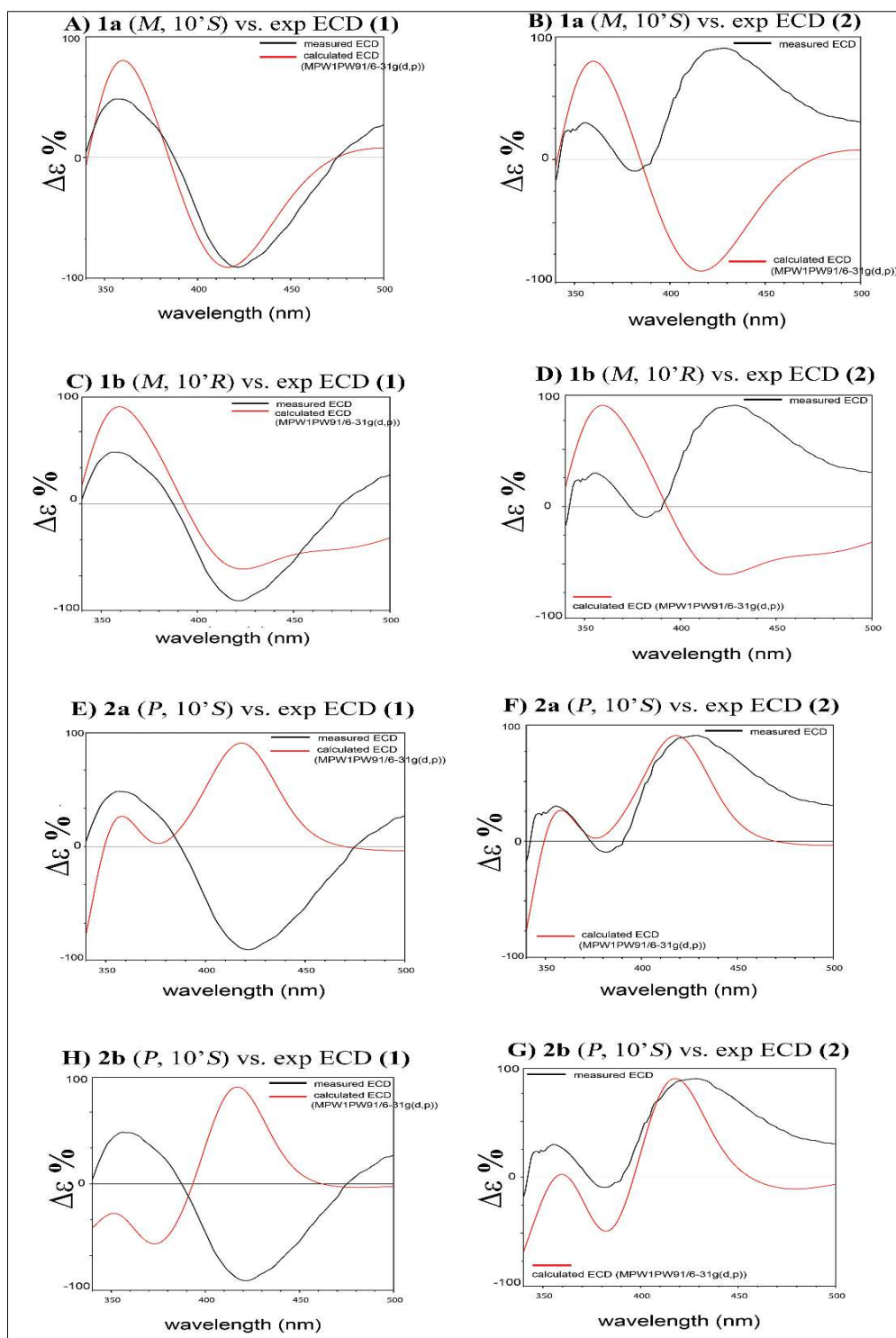


Figure IV.117. Comparison of the experimental ECD spectra of compounds **11** and **12** with the TDDFT-predicted curves of compounds **11a**, **11b**, **12a** and **12b**.

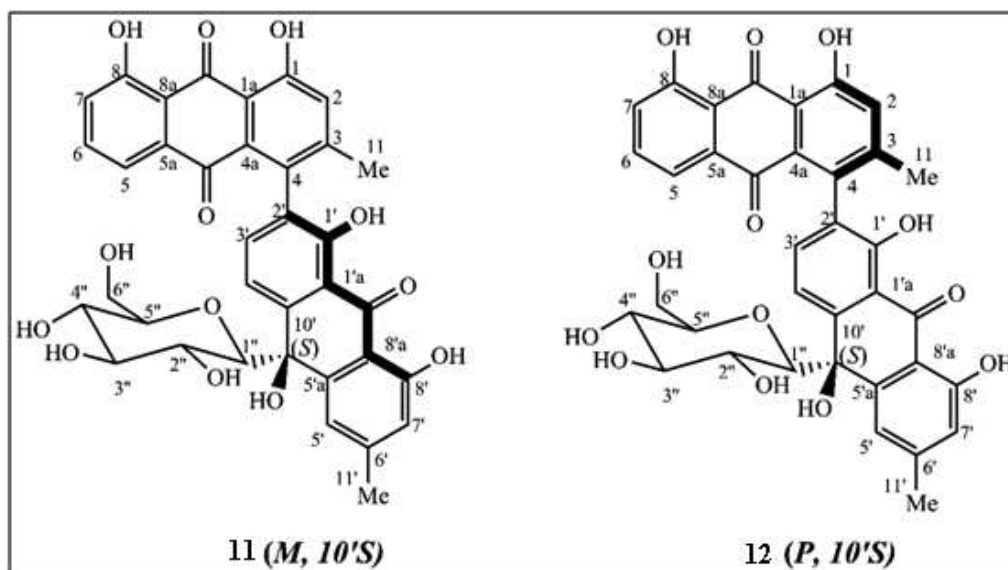


Figure IV.118. Final Structures of compounds 11 and 12.

IV.5.13. Identification of compound 13

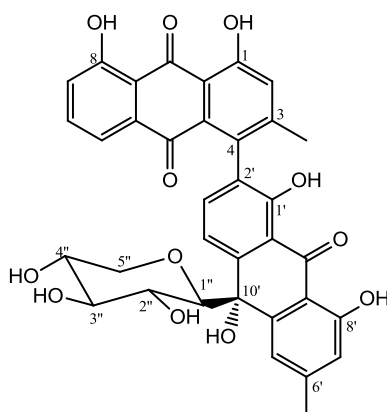


Figure IV.119. Structure of compound 13.

Compound 13 was obtained as a yellowish amorphous powder. The ESI-MS (**Fig. IV.120**) gave an $[M-H]^-$ ion at $m/z = 639.1$ consistent with the molecular formula of $C_{35}H_{28}O_{12}$ indicating 22 degrees of unsaturation.

The 1H -NMR spectrum (**Fig. IV.121**) showed four highly deshielded singlets at δ_H 12.52 ppm, 11.98 ppm, 12.10 ppm and δ_H 11.89 ppm indicative of exchangeable hydrogens bond to oxygen, assigned later, in particular to four phenolic OH groups (δ_C 161.7 ppm, 162.2 ppm, 158.4 ppm and 162.1 ppm).

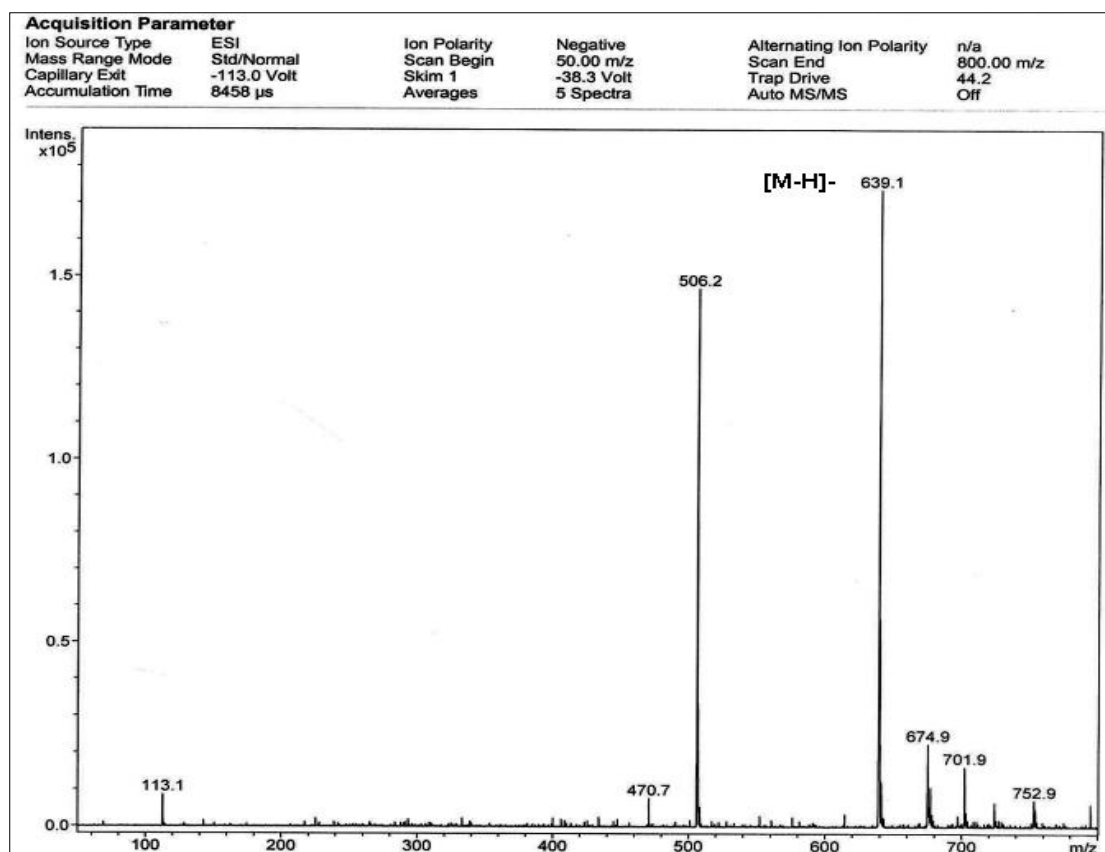


Figure IV.120. ESI-MS spectrum in negative ion mode of compound 13.

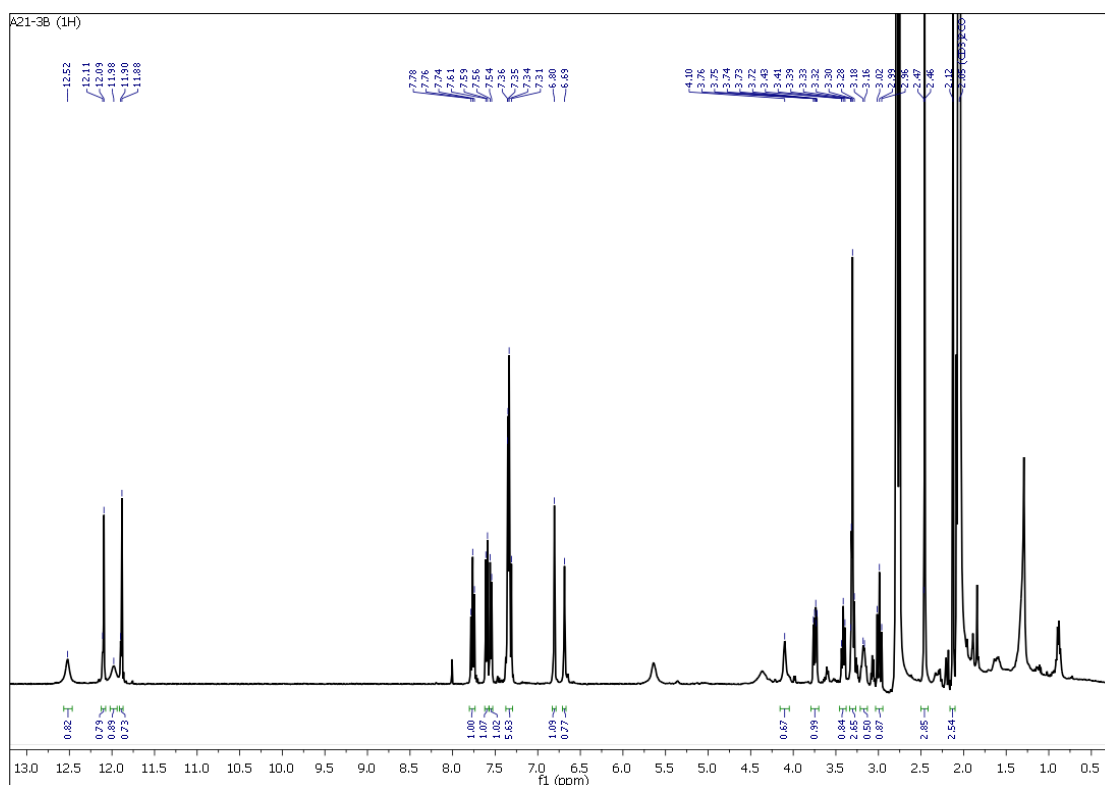


Figure IV.121. $^1\text{H-NMR}$ Spectrum (400 MHz, CD_3COCD_3) of compound 13.

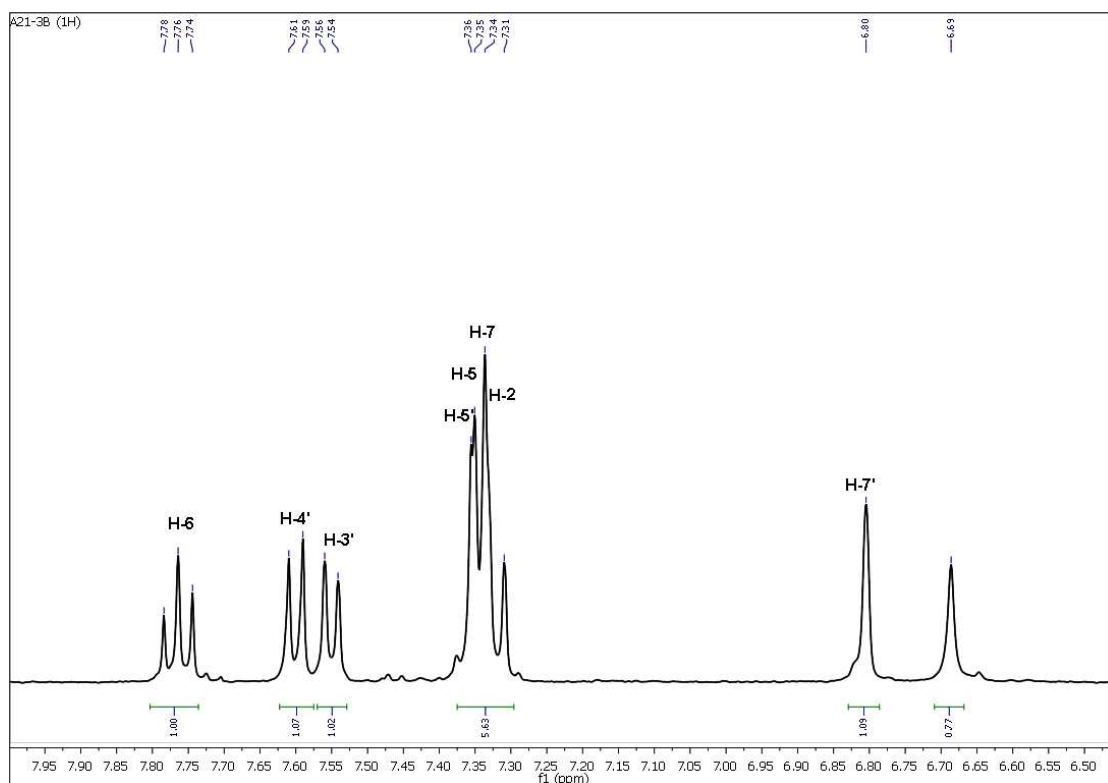


Figure IV.122. $^1\text{H-NMR}$ Spectrum (400 MHz, CD_3COCD_3) of compound **13**.
(From 6.50 ppm to 8.00 ppm).

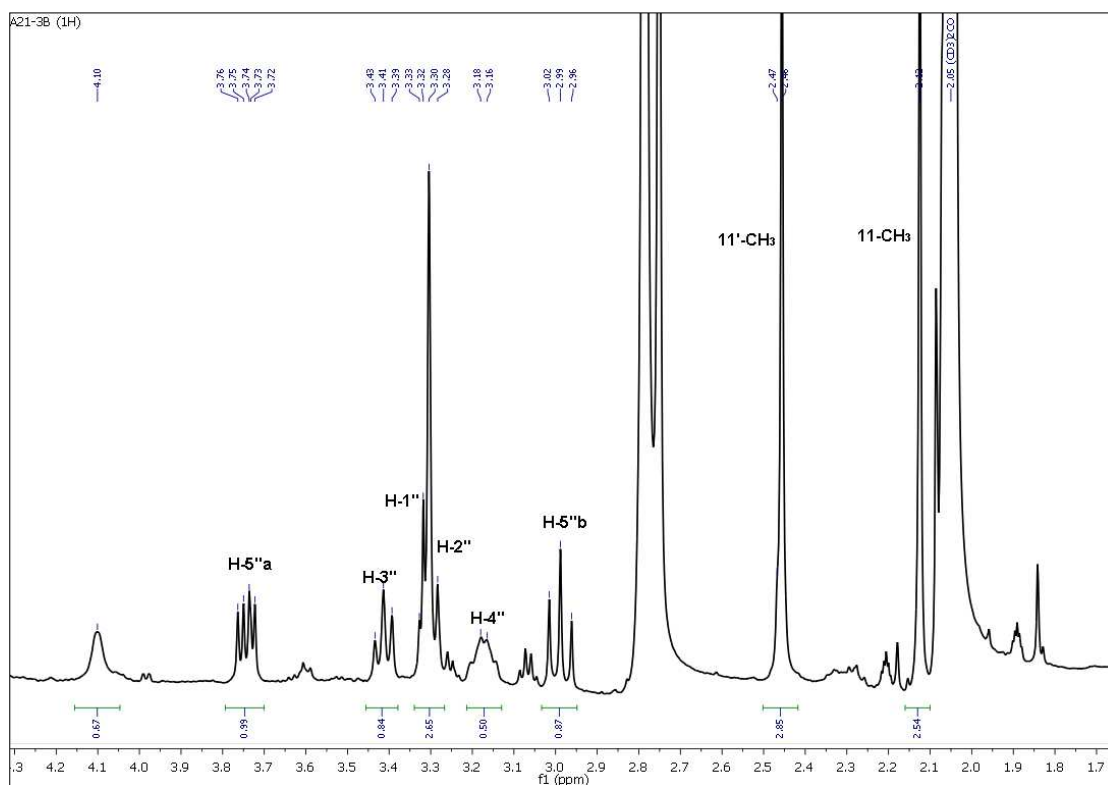


Figure IV.123. $^1\text{H-NMR}$ Spectrum (400 MHz, CD_3COCD_3) of compound **13**.
(From 1.70 ppm to 4.20 ppm).

The ^{13}C (Fig. IV.124) and HSQC (Fig. IV.125) NMR spectrums displayed 35 carbon signals, including two methyl groups at δ_{C} 20.4 ppm (C-11) and δ_{C} 21.6 ppm (C-11') as well as three carbonyl carbons at δ_{C} 194.5 ppm, 182.6 ppm and 193.4 ppm; these data supported the interpretation that this compound was an anthraquinone-oxoanthrone derivative [33]. Its anthraquinone structure showed a singlet at δ_{H} 7.31 ppm (*s*, H-2), with the biogenetically expected methyl signal at δ_{C} 20.4 ppm (C-11). In addition, an ABX spin system was observed for three aromatic protons of the chrysophanol moiety which resonated at δ_{H} 7.63 ppm (1H, *d*, $J = 7.9$ Hz, H-5), δ_{H} 7.76 ppm (1H, *t*, $J = 7.9$ Hz, H-6) and δ_{H} 7.34 ppm (1H, *d*, $J = 7.9$ Hz, H-7), leaving C-4 at δ_{C} 131.8 ppm as the point of attachment to the oxoanthrone structure. The ^1H -NMR spectroscopic pattern of the other half of the molecule showed a chrysophanol moiety, where the ABX pattern was replaced by a pair of deshielded *ortho*-coupled protons [33] with an AX pattern at δ_{H} 7.55 ppm (1H, *d*, $J = 7.4$ Hz, H-3') and δ_{H} 7.60 ppm (1H, *d*, $J = 7.8$ Hz, H-4'), respectively.

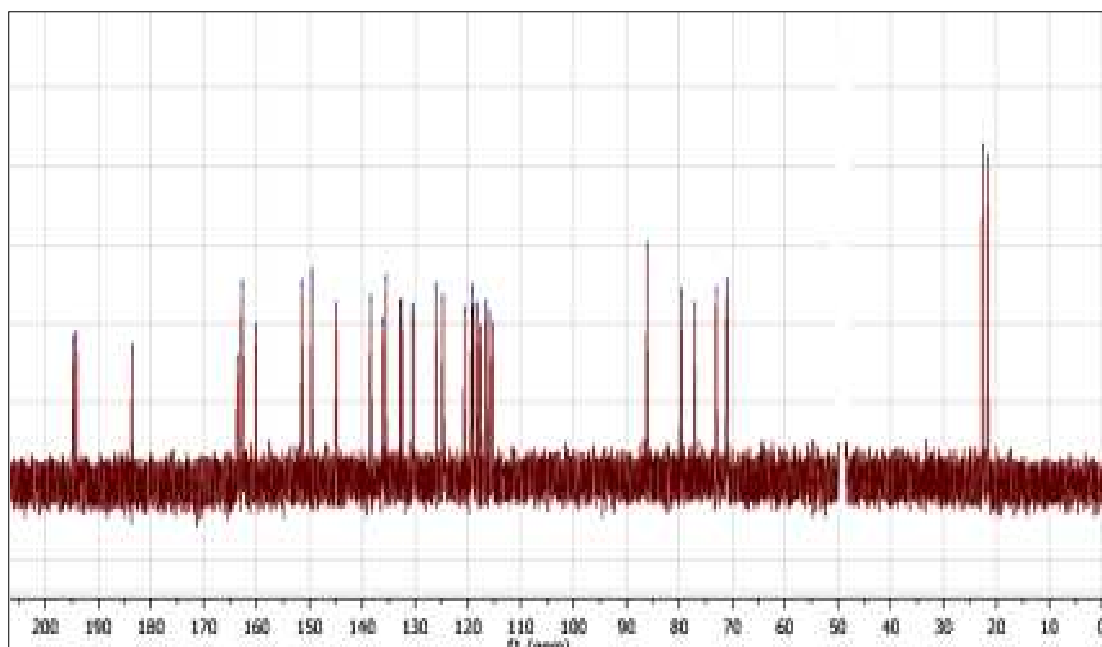


Figure IV.124. ^{13}C -NMR Spectrum (400 MHz, CD_3COCD_3) of compound **13**.

The examination of the HSQC spectrum (Fig. IV.126 and Fig. IV.127) recorded in CD_3COCD_3 of the aromatic region showed correlations giving more details about the assignment of this compound structure identified as follow:

- ✓ The proton H-6 showed a correlation with the carbon C-6' at δ_{C} 135.6 ppm.
- ✓ The proton H-4' showed a correlation with the carbon C-4' at δ_{C} 116.7 ppm.
- ✓ The proton H-3' showed a correlation with the carbon C-3' at δ_{C} 120.0 ppm.
- ✓ The proton H-5' showed a correlation with the carbon C-5' at δ_{C} 119.3 ppm.
- ✓ The proton H-5 showed a correlation with the carbon C-5 at δ_{C} 137.2 ppm.
- ✓ The proton H-2 showed a correlation with the carbon C-2 at δ_{C} 123.8 ppm.
- ✓ The proton H-7 showed a correlation with the carbon C-7 at δ_{C} 123.8 ppm.
- ✓ The proton H-7' showed a correlation with the carbon C-7' at δ_{C} 117.2 ppm.

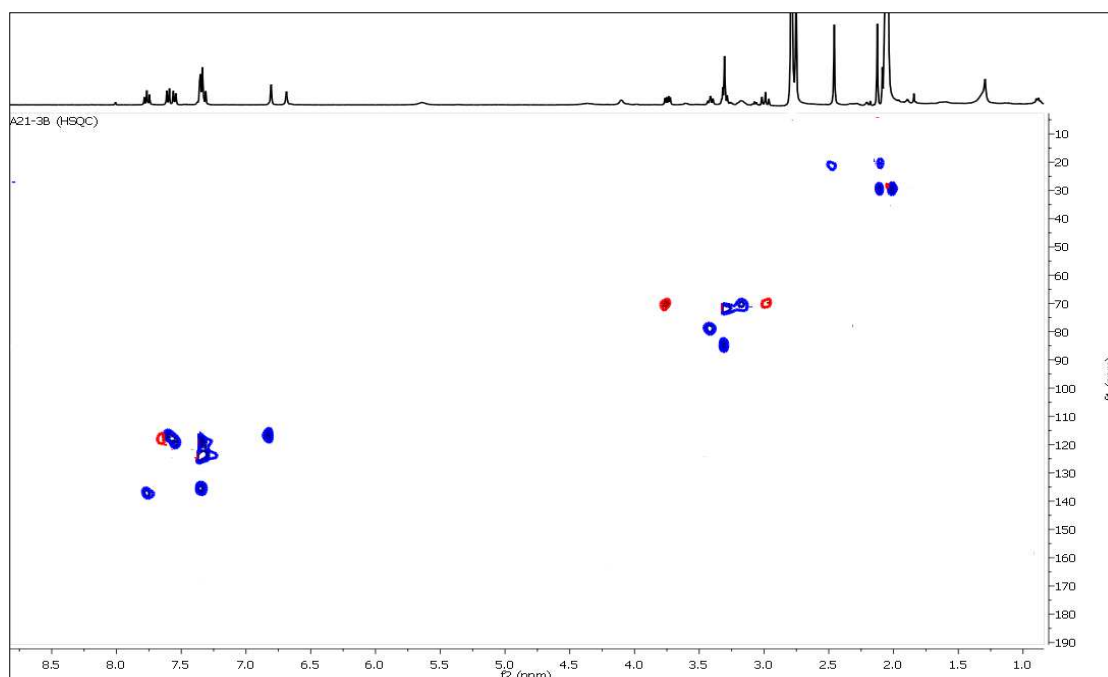


Figure IV.125. HSQC-NMR Spectrum (400 MHz, CD_3COCD_3) of compound **13**.

For the upfield region, the HSQC spectrum showed also correlations identified as follow:

- ✓ Both H-5''*a*, H-5''*b* showed correlation with the carbon C-5'' at δ_{C} 70.3 ppm.
- ✓ The proton H-3'' showed a correlation with the carbon C-3'' at δ_{C} 79.1 ppm.
- ✓ The proton H-1'' showed a correlation with the carbon C-1'' at δ_{C} 84.8 ppm.
- ✓ The proton H-2'' showed a correlation with the carbon C-2'' at δ_{C} 72.1 ppm.
- ✓ The proton H-4'' showed a correlation with the carbon C-4'' at δ_{C} 70.1 ppm.

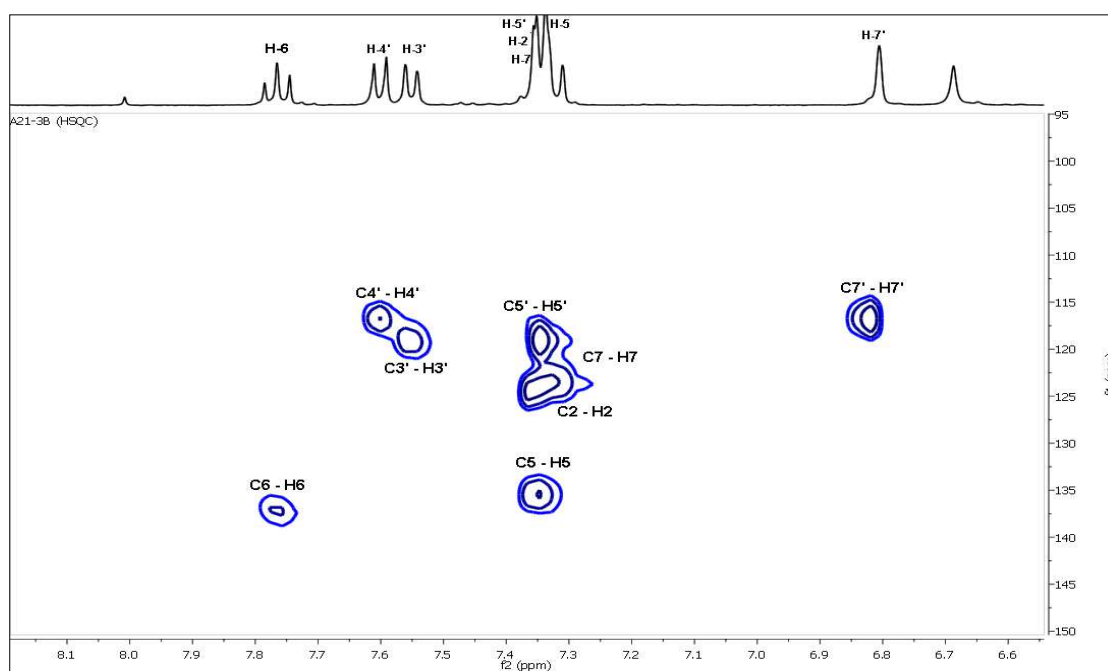


Figure IV.126. HSQC-NMR Spectrum (400 MHz, CD_3COCD_3) of compound **13**.
(From 6.60 ppm to 8.10 ppm).

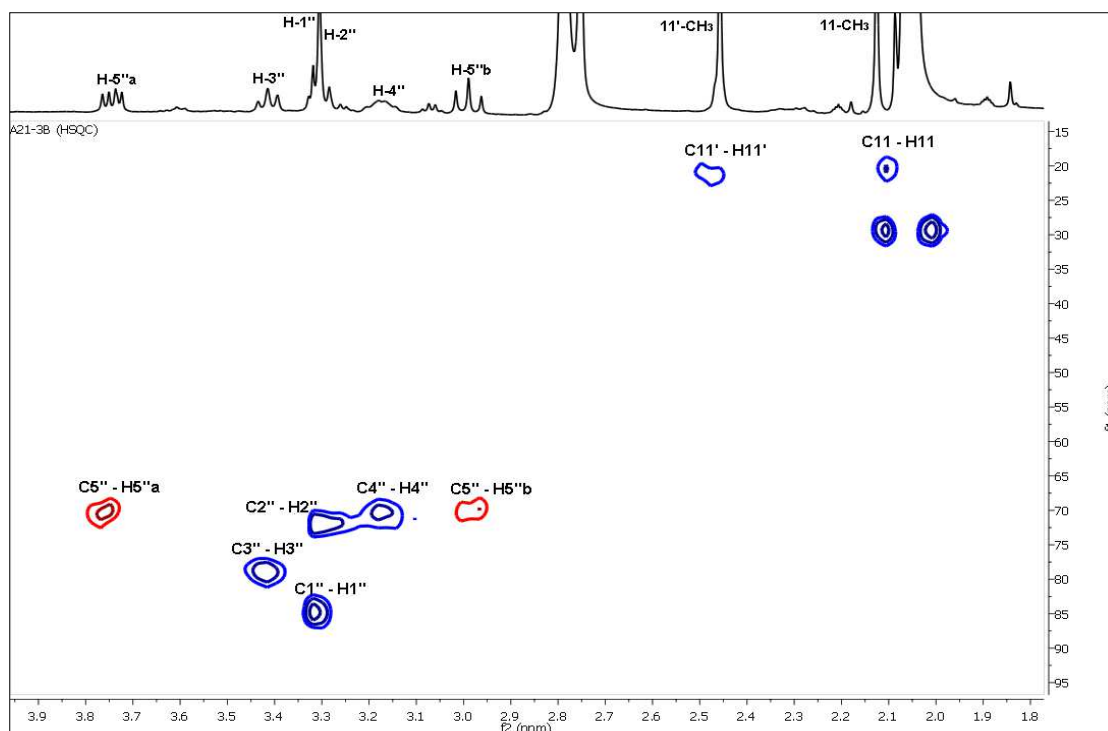


Figure IV.127. HSQC-NMR Spectrum (400 MHz, CD_3COCD_3) of compound **13**. (From 1.80 ppm to 3.90 ppm).

The entire chemical shifts of the NMR ^1H , ^{13}C , HSQC and HMBC correlations of compound **13** are summarized in the following table (**Table IV.20**).

Table IV.20. ^1H , ^{13}C and HMBC NMR data of compound **13** (CD_3COCD_3).

Positions	δ_{C} (ppm)	δ_{H} (ppm), <i>mult.</i> , <i>J</i> (Hz)	HMBC
1	161.7	-	-
2	123.8	7.31 (<i>s</i> , 1H)	C-11, C-1a, C-4, C-1
3	150.5	-	-
4	131.8	-	-
5	137.2	7.63 (<i>d</i> , 1H, 7.9 Hz)	C-10, C-7
6	135.6	7.76 (<i>t</i> , 1H, 7.9 Hz)	C-5a, C-8
7	123.8	7.34 (<i>d</i> , 1H, 7.9 Hz)	C-8a, C-5
8	162.2	-	-
9	194.5	-	-
10	182.6	-	-
1a	115.5	-	-
4a	131.5	-	-
5a	134.6	-	-
8a	116.0	-	-
1'	158.4	-	-
2'	128.4	-	-
3'	120.0	7.55 (<i>d</i> , 1H, 7.4 Hz)	C-4, C-4'a, C-1'
4'	116.7	7.60 (<i>d</i> , 1H, 7.8 Hz)	C-10', C-2', C-1'a
5'	119.3	7.35 (<i>d</i> , 1H, 1.8 Hz)	C-11', C-8'a, C-7', C-10'
6'	147.1	-	-
7'	117.2	6.80 (<i>s</i> , 1H)	C-11', C-8'a, C-5'
8'	162.1	-	-

9'	193.4	-	-
10'	75.7	-	-
1'a	116.0	-	-
4'a	145.8	-	-
5'a	146.7	-	-
8'a	114.2	-	-
1''	84.8	3.31 (<i>d</i> , 1H, 8.5 Hz)	C-10', C-4'a, C-5'a, C-3''
2''	72.1	3.30 (<i>m</i> , 1H)	C-10', C-1'', C-3''
3''	79.1	3.41 (<i>t</i> , 1H, 8.2 Hz)	C-2'', C-4'', C-5''
4''	70.1	3.17 (<i>t</i> , 1H, 9.3 Hz)	C-3'', C-5'', C-6''
5''a	70.3	3.74 (<i>m</i> , 1H)	C-3'', C-1''
5''b	70.3	2.99 (<i>t</i> , 1H, 10.8 Hz)	
11	20.4	2.11 (<i>s</i> , 3H)	C-3, C-2, C-4
11'	21.6	2.47 (<i>s</i> , 3H)	C-6', C-5', C-7'
1-OH	-	12.52 (<i>s</i> , 1H)	
8-OH	-	11.98 (<i>s</i> , 1H)	
1'-OH	-	12.10 (<i>s</i> , 1H)	C-1', C-2', C-1'a
8'-OH	-	11.89 (<i>s</i> , 1H)	C-8', C-7', C-8'a

This indicated that the point of attachment in this molecule is at C-2' (δ_C 128.4 ppm). In the $^1\text{H-NMR}$ spectrum, the anomeric proton appeared at δ_H 3.31 ppm (1H, *d*, $J=8.52$ Hz, H-1'') suggesting a β configuration [32]. The upfield shift of the anomeric carbon resonancel at δ_C 84.8 ppm (C-1'') in the $^{13}\text{C-NMR}$ spectrum (**Table IV.15**) and the HMBC correlations from H-13 to C-10' provided evidence that the sugar moiety was connected to the aglycone at C-10'' to form an oxanthrone C-glycoside.

The HMBC spectrum exhibited cross-peaks from: H-2 to C-4 (δ_C 131.8 ppm), C-1a (δ_C 115.5 ppm), C-1 (δ_C 161.7 ppm) and C-11 (δ_C 20.4 ppm); from the methyl protons to C-2 (δ_C 123.8 ppm), C-3 (δ_C 150.5 ppm) and C-4 (δ_C 131.8 ppm); from H-5 to C-7 (δ_C 123.8 ppm), C-8a (δ_C 116.0 ppm) and C-10 (δ_C 182.6 ppm); from H-6 to C-5a (δ_C 134.6 ppm) and C-8 (δ_C 162.2 ppm); from H-7 to C-5 (δ_C 137.2 ppm) and C-8a (δ_C 116.0 ppm); from H-3' to C-1' (δ_C 158.4 ppm), C-4'a (δ_C 145.8 ppm) and C-4, (δ_C 131.8 ppm) confirming the point of attachment, from H-5' to C-7' (δ_C 117.2 ppm), C-8'a (δ_C 114.2 ppm), C-10' (δ_C 75.7 ppm) and from the C-11' methyl protons to C-5' (δ_C 119.3 ppm), C-6' (δ_C 147.1 ppm) and C-7' (δ_C 117.2 ppm), respectively.

To determine the absolute configuration of the stereogenic center at C-10', its ECD spectrum was measured and compared to calculated values for the R enantiomer. The experimental ECD spectrum showed a positive Cotton effect at 422 nm and a negative Cotton effect at 391 nm (**Fig. IV.128**). The CAM-B3LYP simulated ECD spectrum [41], generated from 40 excited states using Gaussian band shapes for the peaks, had peaks at 391 and 422 nm, similar to the experimental data. The calculated ECD of the R enantiomer showed excellent agreement with the experimental data. Therefore, structure of compound **13** is **Asphodelin-10'-oxanthrone-(10'R)- β -D-xylopyranoside**. These spectral data were in good agreement with the reported literatures [31].

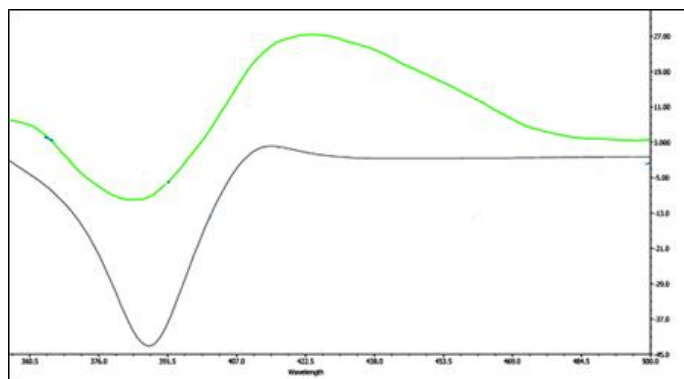
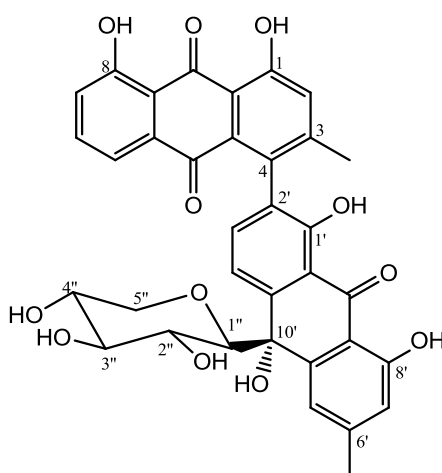


Figure IV.128. Experimental (**Green** for compound **13**) spectrum compared to the calculated (**black**) ECD spectrum of compound **13**.



asphodelin-10'-oxanthrone-(10'R)-B- D - xylopyranoside

IV.5.14. Identification of compound 14

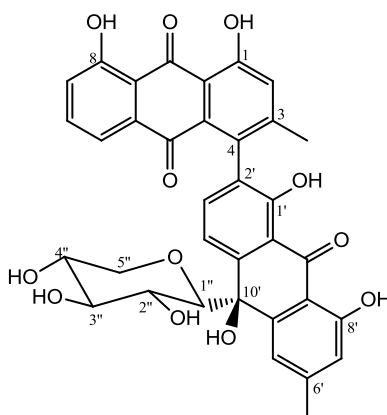


Figure IV.129. Structure of compound **14**

Compound 14 was obtained as a yellowish amorphous powder. Its ESI-MS (**Fig. IV.124**) gave an $[M-H]^-$ ion at $m/z = 639.0$, consistent with the molecular formula of $C_{35}H_{28}O_{12}$.

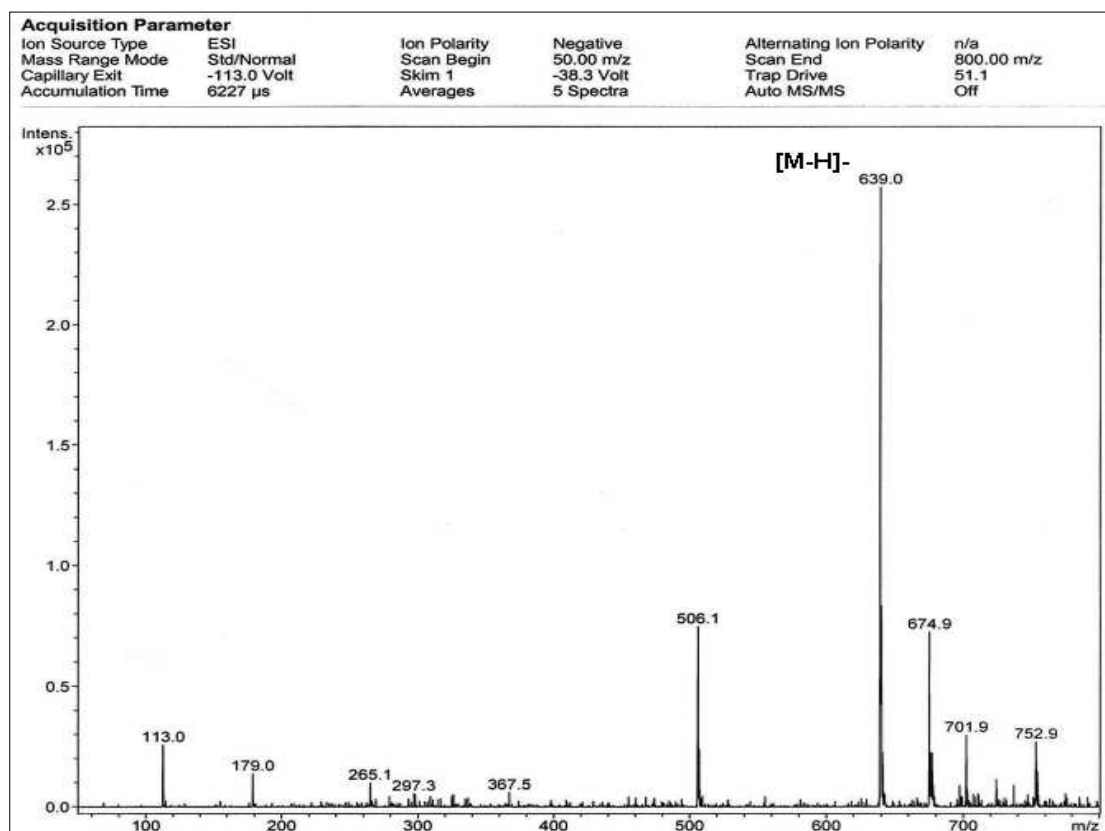


Figure IV.130. ESI-MS spectrum in negative ion mode of **compound 14**.

The 1H -NMR spectrum (**Fig. IV.131**) showed two chelated phenolic proton signals at δ_H 11.91 ppm, 12.18 ppm, 12.04 ppm and 12.59 ppm attributed to OH-8', OH-1', OH-8 and OH-1 respectively [42]. The 1H -NMR spectrum showed one-half of the molecule; one signal at δ_H 7.29 ppm (1H, *s*, H-2), with the C-3 attached methyl δ_C 22.1 ppm (3H, *s*), indicating C-4 is the site of attachment to the other half of the molecule. In addition, an ABX spin system was observed for three aromatic protons which resonated at δ_H 7.51 ppm (1H, *d*, $J = 8.2$ Hz, H-5), δ_H 7.57 ppm (1H, *t*, $J = 8.2$ Hz, H-6), and δ_H 7.23 ppm (1H, *d*, $J = 6.1$ Hz, H-7) of the chrysofanol moiety.

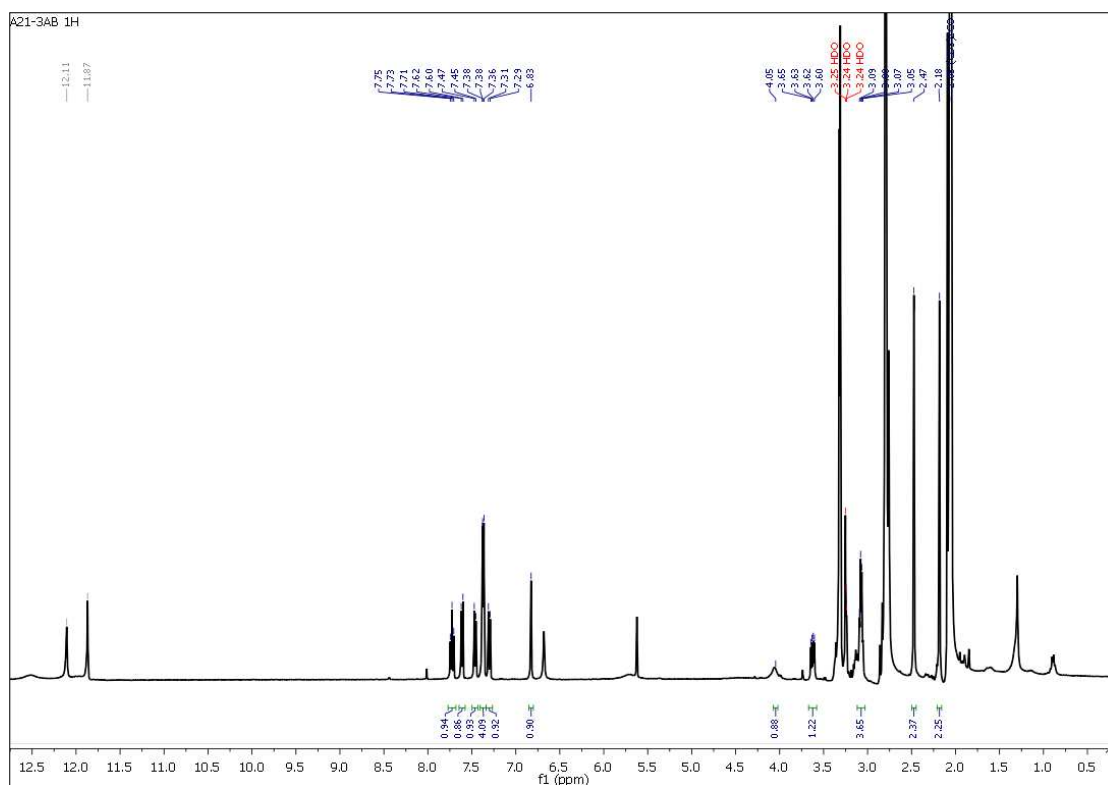


Figure IV.131. $^1\text{H-NMR}$ Spectrum (400 MHz, CD_3COCD_3) of compound 14.

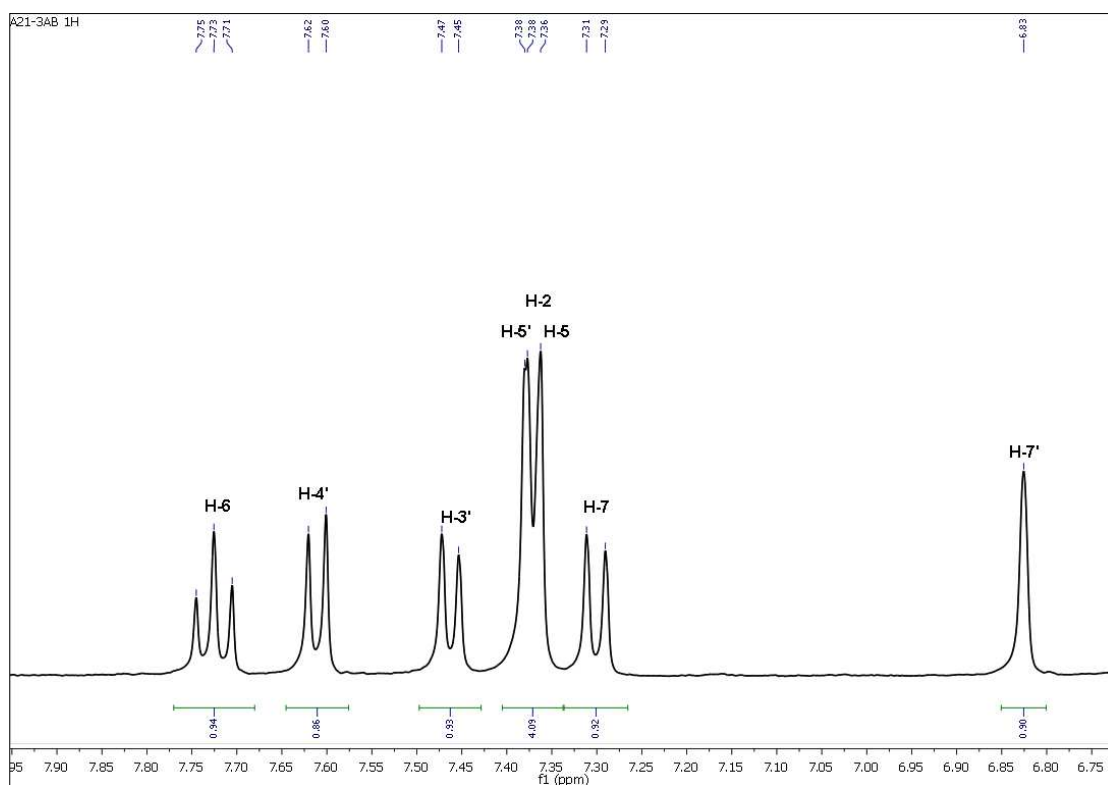


Figure IV.132. $^1\text{H-NMR}$ Spectrum (400 MHz, CD_3COCD_3) of compound 14.
(From 6.70 ppm to 7.90 ppm).

The $^1\text{H-NMR}$ spectral data of the other half of the molecule showed that, it's a chrysophanol oxanthrone moiety, and the ABX pattern in the chrysophanol was replaced by a pair of deshielded *ortho*-coupled protons with AX spin system at δ_{H} 7.28 ppm (1H, *d*, $J = 8.2$ Hz, H-3') and δ 7.53 ppm (1H, *d*, $J = 7.8$ Hz, H-4'). This indicated that C-2' (δ 129.5 ppm) was the point of attachment in this half. In the ^1H NMR spectrum the anomeric proton appeared at δ_{H} 3.28 ppm (1H, *d*, H-1'', $J = 9.3$ Hz) indicating the $-\beta$ - configuration of the anomeric proton at C-1''.

The $^{13}\text{C-NMR}$, HSQC and HMBC spectr of compound 14 displayed 35 carbon signals, 5 signals were assigned to the sugar moiety and 30 signals were assigned to the aglycone including two methyl groups at δ_{C} 22.1 ppm (CH₃-11) and δ_{C} 24.0 ppm (CH₃-11') as well as three carbonyl carbons at δ_{C} 194.0 ppm (C-9), δ_{C} 182.4 ppm (C-10) and δ_{C} 191.76 ppm (C-9'), supported that the compound was a dimeric derivative.

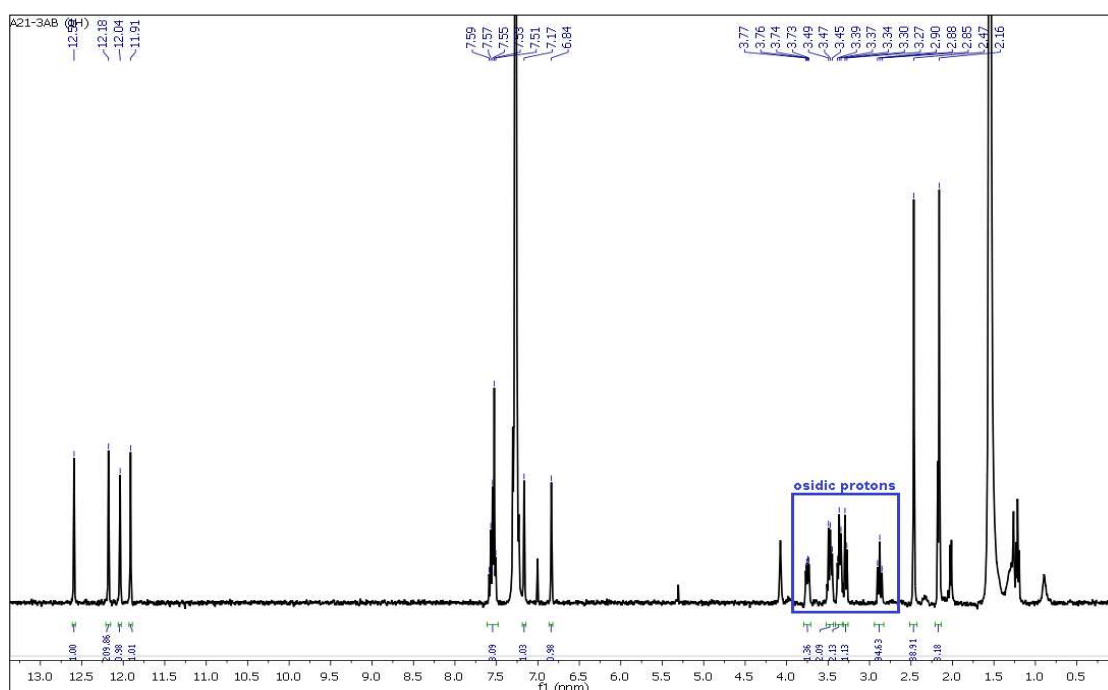


Figure IV.133. $^1\text{H-NMR}$ Spectrum (400 MHz, CDCl_3) of compound 14.

The examination of the HSQC spectrum (**Fig. IV.136**) recorded in CDCl_3 of the aromatic region showed correlations spots giving more details about the assignment of this compound structure identified as follows:

- ✓ The proton H-6' showed a correlation with the carbon C-6' at δ_{C} 147.4 ppm.
- ✓ The proton H-4' showed a correlation with the carbon C-4' at δ_{C} 116.9 ppm.
- ✓ The proton H-3' showed a correlation with the carbon C-3' at δ_{C} 136.1 ppm.
- ✓ The proton H-5' showed a correlation with the carbon C-5' at δ_{C} 119.0 ppm.
- ✓ The proton H-5 showed a correlation with the carbon C-5 at δ_{C} 120.5 ppm.
- ✓ The proton H-2 showed a correlation with the carbon C-2 at δ_{C} 126.1 ppm.
- ✓ The proton H-7 showed a correlation with the carbon C-7 at δ_{C} 124.6 ppm.
- ✓ The proton H-7' showed a correlation with the carbon C-7' at δ_{C} 118.9 ppm.

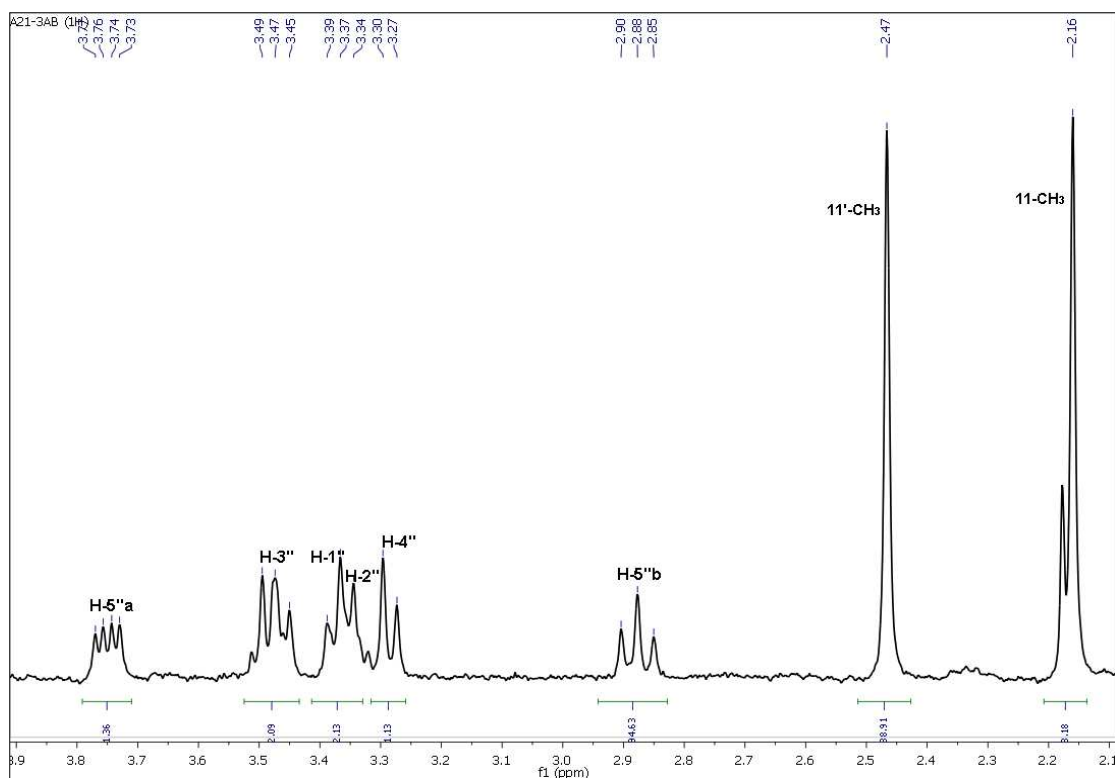


Figure IV.134. $^1\text{H-NMR}$ Spectrum (400 MHz, CDCl_3) of compound 14.
(From 2.10 ppm to 3.90 ppm).

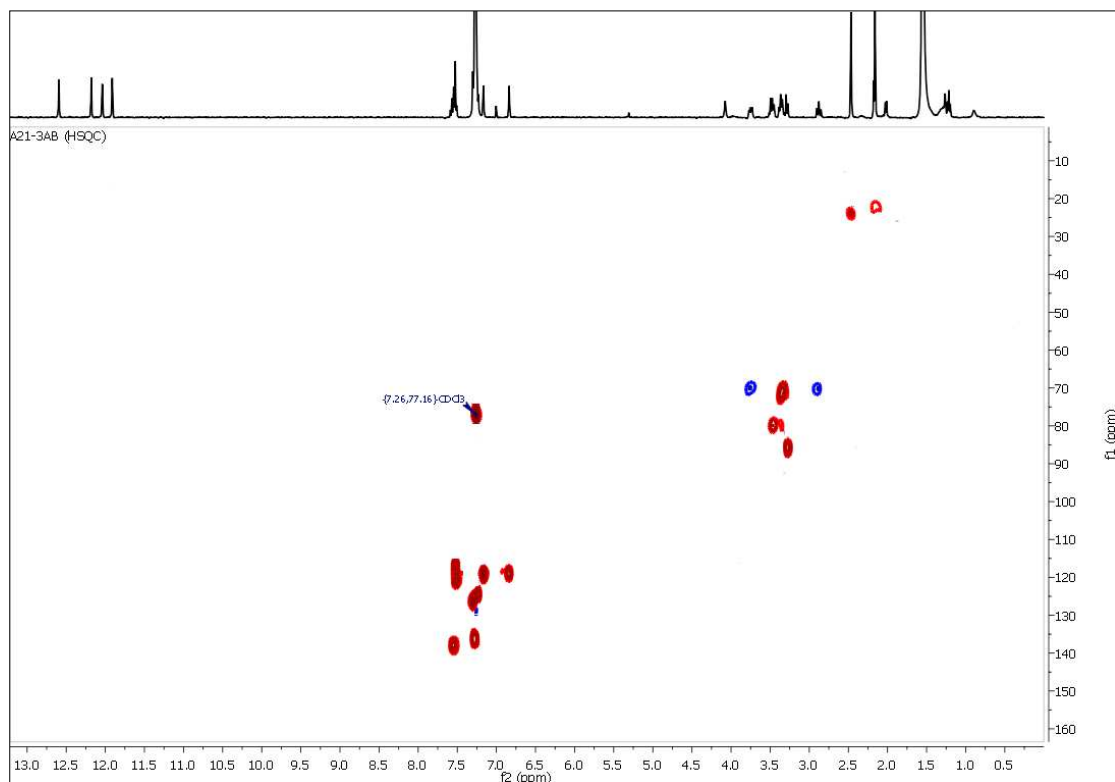


Figure IV.135. HSQC-NMR Spectrum (400 MHz, CDCl_3) of compound 14.

For the upfield region, the HSQC spectrum showed also correlations identified as follow:

- ✓ Both H-5''*a*, H-5''*b* showed correlation with the carbon C-5'' at δ_C 70.1 ppm.
- ✓ The proton H-3'' showed a correlation with the carbon C-3'' at δ_C 79.3 ppm.
- ✓ The proton H-1'' showed a correlation with the carbon C-1'' at δ_C 85.9 ppm.
- ✓ The proton H-2'' showed a correlation with the carbon C-2'' at δ_C 71.1 ppm.
- ✓ The proton H-4'' showed a correlation with the carbon C-4'' at δ_C 79.8 ppm.

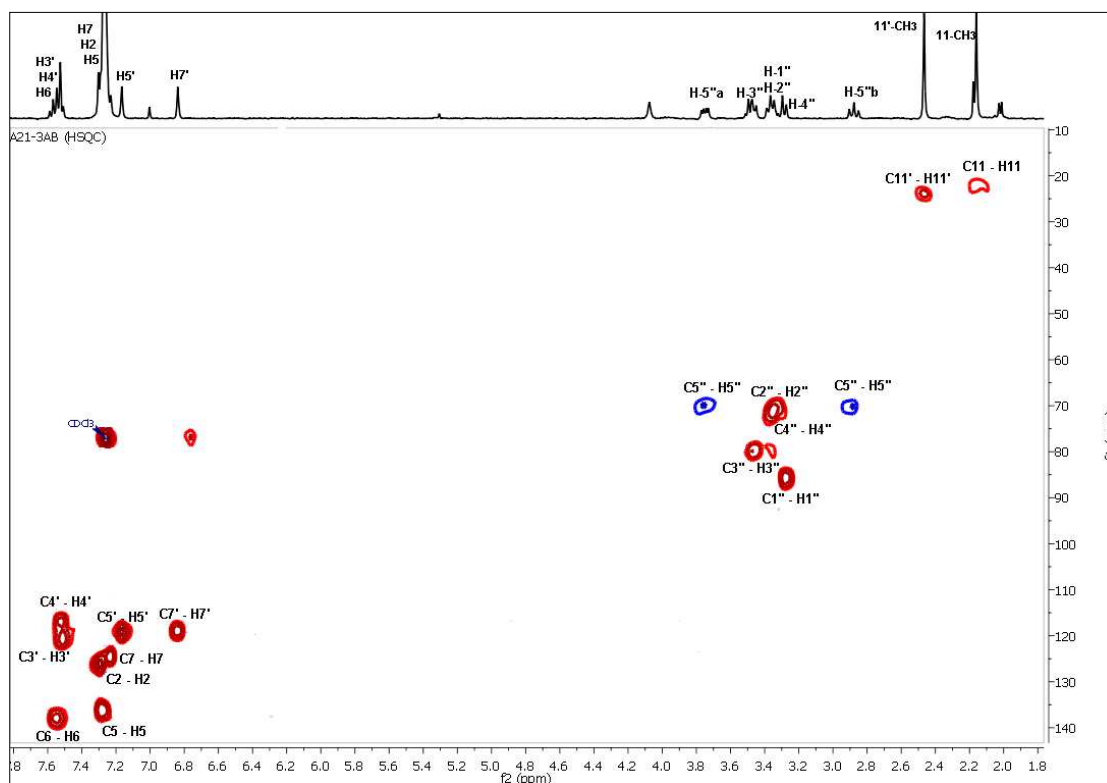


Figure IV.136. HSQC-NMR Spectrum (400 MHz, CDCl_3) of compound **14**.

The HMBC spectrum (**Fig. IV.139**) showed a cross-peak between H-3' and C-4, confirming the point of attachment of chrysophanol moiety to chrysophanol oxanthrone moiety was C-2 and C-4', respectively. The linked site of the sugar unit to C-10' position was determined by the HMBC experiment (**Fig. IV.138**) where a correlation was observed between arabinose H-1'' (δ_H 3.28 ppm) and C-10' (δ_C 78.3 ppm) of the aglycone.

The HMBC spectrum exhibited also cross-peaks from: H-2 to C-4 (δ_C 131.3 ppm), C-1a (δ_C 114.9 ppm), C-1 (δ_C 162.8 ppm) and C-11 (δ_C 22.1 ppm); from the methyl protons to C-2 (δ_C 126.1 ppm), C-3 (δ_C 150.0 ppm) and C-4 (δ_C 131.3 ppm); from H-5 to C-7 (δ_C 124.6 ppm), C-8a (δ_C 116.0 ppm) and C-10 (δ_C 182.4 ppm); from H-6 to C-5a (δ_C 134.5 ppm) and C-8 (δ_C 162.0 ppm); from H-7 to C-5 (δ_C 120.5 ppm) and C-8a (δ_C 116.0 ppm); from H-3' to C-1' (δ_C 162.2 ppm), C-4'a (δ_C 143.3 ppm) and C-4, (δ_C 131.3 ppm) confirming the point of attachment, from H-5' to C-7' (δ_C 118.9 ppm), C-8'a (δ_C 114.2 ppm), C-10' (δ_C 78.3 ppm) and from the C-11' methyl protons to C-5' (δ_C 119.0 ppm), C-6' (δ_C 147.4 ppm) and C-7' (δ_C 118.9 ppm), respectively.

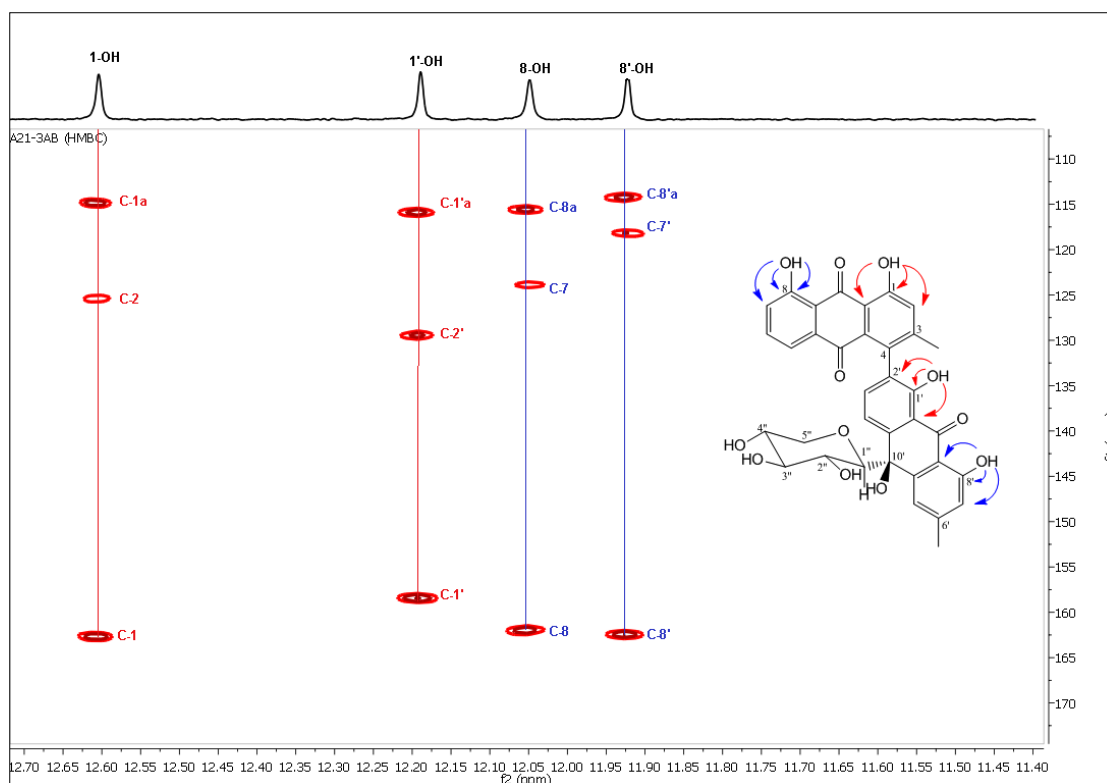


Figure IV.137. HMBC-NMR Spectrum (400 MHz, CDCl_3) of compound **14**.
(From 11.40 ppm to 12.70 ppm).

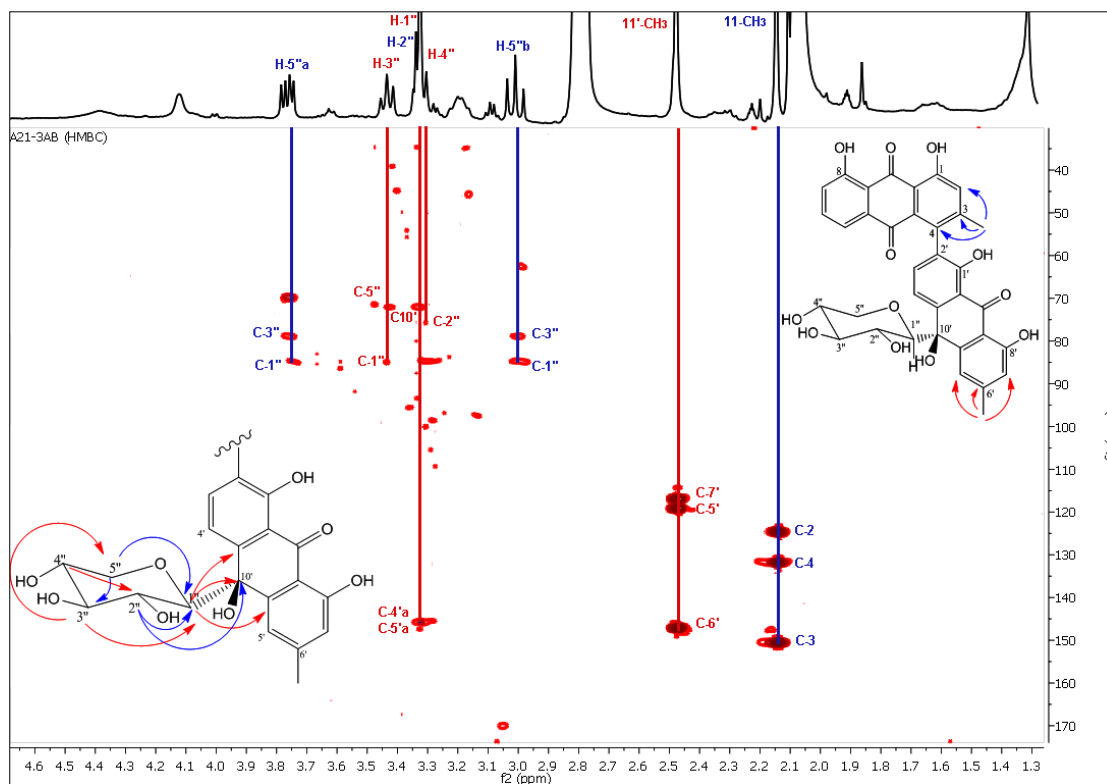


Figure IV.138. HMBC-NMR Spectrum (400 MHz, CDCl_3) of compound **14**.
(From 1.30 ppm to 4.60 ppm).

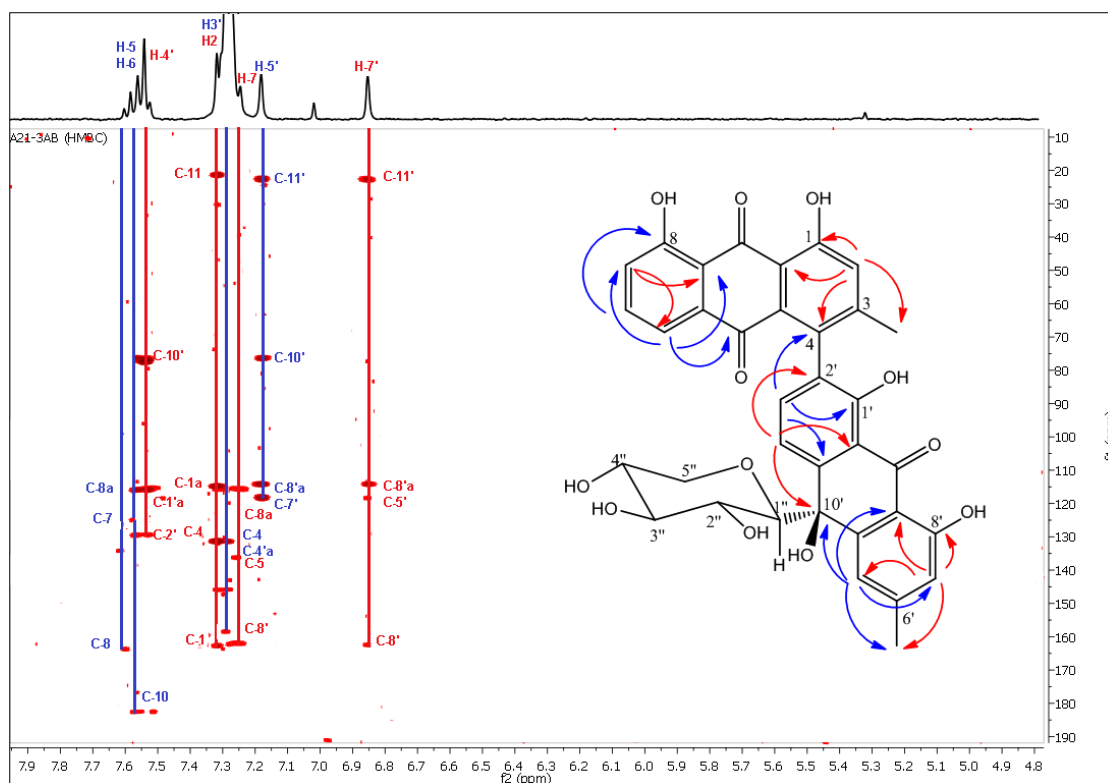


Figure IV.139. HMBC-NMR Spectrum (400 MHz, CDCl_3) of compound **14**.
(From 4.80 ppm to 7.90 ppm).

All the chemical shifts of the NMR ^1H , ^{13}C , HSQC and HMBC correlations of compound **14** are summarized in the following table (**Table IV.21**).

Table IV.21. ^1H , ^{13}C and HMBC NMR data of compound **14** (CDCl_3).

Positions	δ_{C} (ppm)	δ_{H} (ppm), M., J (Hz)	HMBC
1	162.8	-	-
2	126.1	7.29 (s, 1H)	C-11, C-1a, C-4, C-1
3	150.0	-	-
4	131.3	-	-
5	120.5	7.51 (d, 1H, 8.2)	C-10, C-7
6	138.0	7.57 (t, 1H, 8.2)	C-8
7	124.6	7.23 (d, 1H, 6.1)	C-8a, C-5
8	162.0	-	-
9	194.0	-	-
10	182.4	-	-
1a	114.9	-	-
4a	131.5	-	-
5a	134.5	-	-
8a	116.0	-	-
1'	162.2	-	-
2'	129.5	-	-
3'	136.1	7.28 (d, 1H, 8.2)	C-4, C-4'a, C-1'
4'	116.9	7.53 (d, 1H, 7.8)	C-10', C-2', C-1'a
5'	119.0	7.17 (s, 1H)	C-11', C-8'a, C-7', C-10'

6'	147.4	-	-
7'	118.9	6.84 (<i>s</i> , 1H)	C-11', C-8'a, C-5', C-8'
8'	162.2	-	-
9'	193.1	-	-
10'	78.3	-	-
1'a	115.9	-	-
4'a	143.3	-	-
5'a	146.0	-	-
8'a	114.2	-	-
1''	85.9	3.28 (<i>d</i> , 1H, 9.3 Hz)	C-10', C-4'a, C-5'a
2''	71.1	3.35 (<i>m</i> , 1H, 9.0 Hz)	C-10', C-1''
3''	79.9	3.47 (<i>m</i> , 1H, 8.6 Hz)	C-1'', C-5''
4''	79.8	3.37 (<i>d</i> , 1H, 9.3 Hz)	C-2''
5''a	70.1	2.88 (<i>m</i> , 1H)	C-3'', C-1''
5''b	70.1	3.75 (<i>m</i> , 1H)	C-3'', C-1''
1	22.1	2.16 (<i>s</i> , 3H)	C-3, C-2, C-4
11'	24.0	2.46 (<i>s</i> , 3H)	C-6', C-5', C-7'
1-OH	-	12.59 (<i>s</i> , 1H)	C-1, C-2, C-1a
8-OH	-	12.04 (<i>s</i> , 1H)	C-8, C-7, C-8a
1'-OH	-	12.18 (<i>s</i> , 1H)	C-1', C-2', C-1'a
8'-OH	-	11.91 (<i>s</i> , 1H)	C-8', C-7', C-8'a

The ^1H , ^{13}C , HSQC and HMBC NMR spectroscopic data of compounds **14** and **13** were similar (Table IV.20 and IV.21), but gave an opposite CD spectra suggesting a difference in configuration at C-10'. The CD spectrum of compound **14** (Fig. IV. 140) showed a Cotton effect opposite to that of compound **13**.

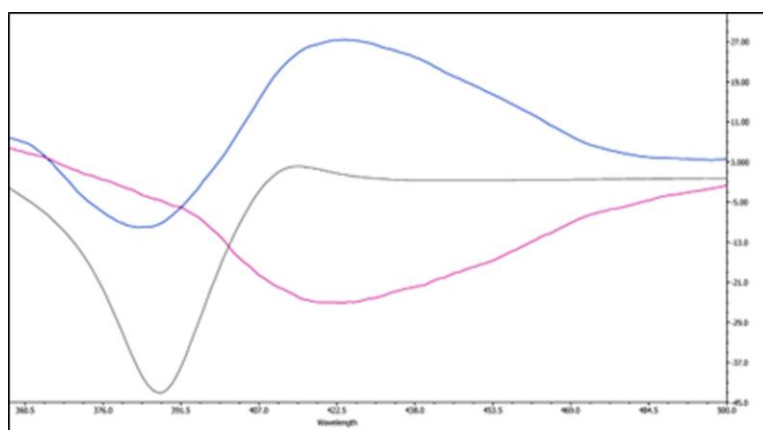
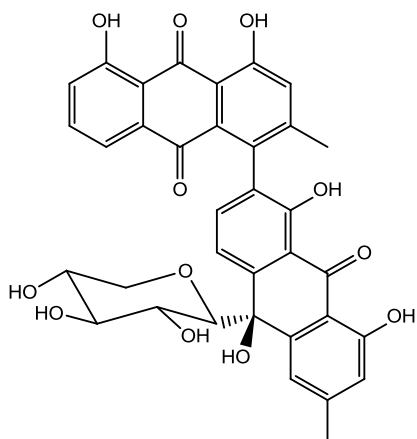


Figure IV.140. Experimental (Blue for compound **13** and Pink for compound **14**) spectrum compared to the calculated (black) ECD spectrum of compound **13**.

Accordingly compound **14** was assigned as **asphodelin-10'-oxanthrone-(10'S)- β -D-xylopyranoside**.



asphodelin-10'-oxanthrone-(10' S)-B-D-xylopyranoside.

REFERENCES

- [1] Kahkonen, M. P., Hopia, A. I., Vuorela, H. J., Rauha, J. P., Pihlaja, K., Kujala, T. S., Heinonen, M., *J. Agric. Food Chem.*, **1999**, *47*, 3954-3962.
- [2] Ersoz, T., Harput, U. S., Saracoglu, I., Calis, I., *Turk. J. Chem.*, **2002**, *26*, 581-588.
- [3] Faidi, K., Hammami, S., Bensalem, A., El Mokni, R., Garrab, M., Mastouri, M., Gorcii, M., Trabelsi Ayedi, M., Taglialatela-Scafati, O., Mighri, Z., *J. Med. Plant Res.* **2014**, *8*, 550-557.
- [4] Harborne, J. B., *The flavonoids Advances in research since 1986. Éditions Chapman & Hall. Cambridge*, **1994**.
- [5] Adinolfi, M., Corsaro, M. M., Lanzetta, R., Parrilli, M., Scopa, A., *Phytochemistry*, **1989**, *28*, 284-288.
- [6] Lanzetta, R., Parrilli, M., Adinolfi, M., Aquila, T., Corsaro, M. M., *Tetrahedron*, **1990**, *46*, 1287-1294.
- [7] Li, C., Shi, J. G., Zhang, Y. P., Zhang, C. Z., *J. Nat. Prod.*, **2000**, *63*, 653-656.
- [8] Park, J. B., *J. Agr. Food Chem.*, **2009**, *57*, 8868-8872.
- [9] Al Taweel, A. M., Perveen, S., El-Shafae, A. M., Fawzy, G. A., Malik, A., Afza, N., Iqbal, L., Latif, M., *Molecules*, **2012**, *17*, 2675-2682.
- [10] Ihsan, C. S., Serap, B., Hasan, K., Bernhard, P., Jorg, H., *Z. Naturforsch.*, **2006**, *61b*, 1304-1310.
- [11] Habib, M. R., Nikkon, F., Rahman, M., Haque, M. E., Karim, M. R., *Pakistan Journal of Biological Sciences*, **2007**, *10*, 4174-4176.
- [12] Jamal, A. K., Yaacob, W. A., Din, L. B., *European Journal of Scientific Research*, **2009**, *28*, 76-81.
- [13] Sai, V., Chaturvedula, P., Prakash, I., *International current pharmaceutical journal*, **2012**, *1*, 239-242.
- [14] Safder, M., Riaz, N., Irman, M., Nawaz, H., Malik, A., Jabran, A., *J. Chem. Soc. Pak.*, **2009**, *31*, 122-125.
- [15] Hernandez-Medel M. D. R., Ramirez-Corzas, C. O., Rivera-Dominguez, M. N., Ramirez-Mendez, J., Santillan, R., RojasLima, S., *Phytochemistry*, **1991**, *50*, 1379-1383.
- [16] El-Sayed, M. E. G., *Journal of Pharmacognosy and Phytochemistry*, **2017**, *6*, 259-264.
- [17] Jay, M., Gonnet, J. F., *Biochemical Systematics and Ecology*, **1974**, *2*, 47-51.
- [18] Markham, K. R., Chari, V. M., **1982**, *The Flavonoids: Advances in Research, Chapman and Hall, London*. p. 19.
- [19] Peng, J., Fan, G., Hong, Z., Chai, Y., Wu, Y., *J. of Chromatography A*, **2005**, *1074*, 111-115.
- [20] Thomson, R. H., *Naturally Occurring Quinones. London, New York, Chapman and Hall*, **1971**.
- [21] Zhang, H., Guo, Z., Wu, N., Xu, W., Han, L., Li, N., Han, Y., *Molecules*, **2012**, *17*, 843- 850.
- [22] Bonsignore, L., Cottiglia, F., Loy, G., Begala, M., Sanna, L., Scordo, F., Serpi, M., *Chim. Farm.*, **1998**, *137*, 186-190.

- [23] Ishii, H., Kitagawa, I., Matsushita, K., Shirakawa, K., Tori, K., Tozyo, T., Yoshikawa, M., Yoshimura, Y., *Tetrahedron Letters*, **1981**, 22, 1529-1532.
- [24] Lorente, F. T., Garcia-Grau, M. M., Nieto, J. L., Barberan, F. A. T., *Phytochemistry*, **1992**, 31, 2027-2029.
- [25] Riehle, P., Vollmer, M., Rohn, S., **2013**, *Food Research International*, 53, 891-899.
- [26] Eddine, L. S., Segni, L., Ridha, O. M., *Int. J. Pharm. Clin. Res.*, **2015**, 7, 119-125.
- [27] Lim, E. K., Higin, G. S., Li, Y., Bowles, J., *Biochem. J.*, **2001**, 373, 987-992.
- [28] Pauli, G. F., Poetsch, F., Nahrstedt, A., *Phytochem. Analysis*, **1998**, 9, 177-185.
- [29] Lin, L. C., Kuo, Y. C. Chou, C. J., *J. Nat. Prod.*, **1999**, 62, 405-408.
- [30] Wald, B., Wray, V., Galensa, R. Herrmann, K., *Phytochemistry*, **1989**, 28, 663-664.
- [31] Ghoneim, M. M., Elokely, K. M., ElHela, A. A., Mohammad, A. E., Jacob, M., Radwan, M. M., Doerksen, R. J., Cutler, S. J., Ross, S. A., *Phytochemistry*, **2014**, 105, 79-84.
- [32] Yang, Y., Yan, Y. M., Wei, W., Luo, J., Zhang, L. S., Zhou, X. J., Wang, P. C., Yang, Y. X., Cheng, Y. X., *Bioorg. Med. Chem. Lett.* **2013**, 23, 3905-3909.
- [33] VanWyk, B. E., Yenesew, A., Dagne, E., *Biochem. Syst. Ecol.* **1995**, 23, 277-281.
- [34] Bringmann, G., Price Mortimer, A. J., Keller, P. A., Gresser, M. J., Garner, J., Breuning, M., *Angew. Chem. Int. Ed. Engl.*, **2005**, 44, 5384-5427.
- [35] Smyth, J. E., Butler, N. M., Keller, P. A., *Nat. Prod. Rep.*, **2015**, 32, 1562-1583.
- [36] Tomasi, J., Mennucci, B., Cammi, R., *Chem. Rev.*, **2005**, 105, 2999-3093.
- [37] Chini, M. G., Malafrente, N., Vaccaro, M. C., Gualtieri, M. J.; Vassallo, A., Vasaturo, M., Castellano, S., Milite, C., Leone, A., Bifulco, G., De Tommasi, N., Dal Piaz, F., *Chem. Eur. J.*, **2016**, 22, 13236-13250.
- [38] Masullo, M., Cantone, V., Cerulli, A., Lauro, G., Messano, F., Russo, G. L., Pizza, C., Bifulco, G., Piacente, S., *J. Nat. Prod.*, **2015**, 78, 2975-2982.
- [39] Willoughby, P. H., Jansma, M. J., Hoyer, T. R., *Nat. Protoc.*, **2014**, 9, 643-660
- [40] Zhu, J. J., Zhang, C. F., Zhang, M., Bligh, S. W., Yang, L., Wang, Z. M., Wang, Z. T., *J. Chromatogr. A*, **2010**, 1217, 5384-5388.
- [41] Sang, Y. M., Yan, L. K., Wang, J. P., Su, Z. M., *J. Phys. Chem. A*, **2012**, 116, 4152-4158.
- [42] Yagi, A., Makino, K., Nishioka, I., *Chem. Pharm. Bull.*, **1978**, 28, 1111-1116.

CHAPTER V

EVALUATION OF BIOLOGICAL ACTIVITIES ON *A. TENUIFOLIUS*

V.1. Antioxidant activities

Plants and their products are rich sources of phytochemicals, they possess a variety of biological activities including antioxidant potential. Natural antioxidants are in high demand for applications, such as nutraceuticals, bio-pharmaceuticals, as well as food additive because of consumer preference [1]. In order to protect foods and human beings against oxidative damage caused by free radicals, synthetic antioxidants such as butylated hydroxyanisole (BHA), butylated hydroxytoluene (BHT), tertiary-butylhydroquinone (TBHQ) are used [2-3-4]. However, many researchers reported the adverse effects of synthetic antioxidants such as toxicity, carcinogenicity and potential health hazards. Therefore, naturally occurring nutritive and non-nutritive antioxidants have recently become a major area of scientific research due to safety and limitation of synthetic antioxidant usage [5-6]. Plants, including herbs and spices have many phytochemicals which are potential sources of natural antioxidants, like, phenolic diterpenes, flavonoids, tannins and phenolic acids. Many studies have reported that extracts from natural products such as fruits, vegetables and medicinal herbs, have positive effects against cancer, the intake of plant flavonoids has been shown to be inversely related to the risk of cardiovascular disease [7-8].

Several antioxidant methods have been proposed to evaluate the antioxidant characteristics and to explain antioxidants mechanisms and actions. Of these, free synthetic radical scavenging like DPPH[•] and β -Carotene bleaching test are most commonly used for the evaluation of the total antioxidant behavior of the different extracts [9-10]. Numerous studies have demonstrated that the antioxidant activity measured depends substantially on the test system used [11-12] and recommended to base any conclusions on at least two different test systems [13].

V.1.1. DPPH radical scavenging assay

This is the simplest and most widely reported method for screening antioxidant activity in foods and many plant drugs [14-15].

DPPH (2, 2-diphenyl-1-picryl-hydrazyl-hydrate) free radical method is an antioxidant assay based on electron-transfer that produces a violet solution in ethanol [16]. This free radical, stable at room temperature, is reduced in the presence of an antioxidant molecule, giving rise to colorless ethanol solution. The use of the DPPH assay provides an easy and rapid way to evaluate antioxidants by spectrophotometry [17], so it can be useful to assess various products at a time. DPPH is very popular for the study of natural antioxidants [18].



Figure V.1. Structure of DPPH[•] radical and its reduction by an antioxidant (AO-H). (Adapted from [19]).

The effect of the various tested extracts of *A. tenuifolius* on DPPH[•] degradation was estimated according to the method described by Hanato *et al.*, 1988 [18] and Espin *et al.*, 2000 [20] with small modifications. The different dried plant extracts were diluted in pure methanol at different concentrations, and then 2 ml were added to 0.5 ml of a 0.2 mM DPPH[•] methanolic solution. The mixture was shaken vigorously and left standing at room temperature for 30 min. The absorbance of the resulting solution was then measured at 517 nm measured after 30 min. The antiradical activity (three replicates per treatment) was expressed as IC₅₀ (μg.ml⁻¹), the antiradical dose required to cause a 50% inhibition. A lower IC₅₀ value corresponds to a higher antioxidant activity [21].

The ability to scavenge the DPPH[•] radical was calculated using the following equation:

$$\text{DPPH scavenging effect (\%)} = [(A_0 - A_1) \times 100] / A_0$$

Where A_0 is the absorbance of the control at 30 min, and A_1 is the absorbance of the sample at 30 min.

V.1.1.1. Results & Discussion

The antioxidant activity of the different extracts of *A. tenuifolius* was evaluated firstly by the capacity to eliminate free radical DPPH. This parameter is significant for the evaluation of the therapeutic value of the plant. Free radical-scavenging activities of these different extracts were measured in DPPH assay and the reaction followed a concentration-dependent pattern. There were three concentrations in each of the extracts and four for the crude extract. Free radical scavenging increases with increasing of all extracts concentrations (**Fig. V.2**). The radical scavenging ability of *A. tenuifolius* extracts was measured spectrophotometrically. The Inhibition Percentages (IP %) of DPPH scavenging capacity are presented in (**Table V.1**).

Table V.1. Antioxidant activity (%) of the various extracts of *A. Tenuifolius* measured by the scavenging of DPPH radicals. * Values are expressed as mean \pm SD

AcOEt Extract						
Control A ₀	0,387					
	R1	R2	R3	Average	DPPH scavenging activity (%)	IC ₅₀ + SD (ug.ml ⁻¹)
50	0,342	0,349	0,350	0,347	10,335	
100	0,170	0,168	0,169	0,169	56,330	92 \pm 4.05 *
150	0,093	0,090	0,080	0,087	77,347	
Chloroform Extract						
Control A ₀	0,387					
	R1	R2	R3	Average	DPPH scavenging activity (%)	IC ₅₀ + SD (ug.ml ⁻¹)
0,5	0,348	0,346	0,330	0,341	11,800	
10	0,292	0,292	0,291	0,291	24,633	25 \pm 4.36 *
50	0,021	0,025	0,026	0,024	93,798	
Butanol Extract						
Control A ₀	0,387					
	R1	R2	R3	Average	DPPH scavenging activity (%)	IC ₅₀ + SD (ug.ml ⁻¹)
0,5	0,350	0,347	0,348	0,348	9,991	
10	0,335	0,338	0,331	0,334	13,522	45 \pm 2.88 *
50	0,178	0,173	0,171	0,174	55,038	
Crude Extract						
Control A ₀	0,387					
	R1	R2	R3	Average	DPPH scavenging activity (%)	IC ₅₀ + SD (ug.ml ⁻¹)
0,5	0,344	0,348	0,346	0,346	10,594	
5	0,335	0,330	0,34	0,335	13,436	55 \pm 4.15 *
50	0,212	0,205	0,200	0,205	46,856	
100	0,102	0,095	0,100	0,099	74,418	
BHT						73.10 \pm 1.70 [22]

On the basis of these results, we can conclude that employing the DPPH technique, the different extracts showed a various antioxidant activity with an IC₅₀ value ranged from 25 to 92 μ g/ml. BHT used as positive control exhibited an antioxidative effect (IC₅₀ = 73.10 μ g. ml⁻¹) [22]. A higher DPPH radical scavenging activity is associated with a lower IC₅₀ value.

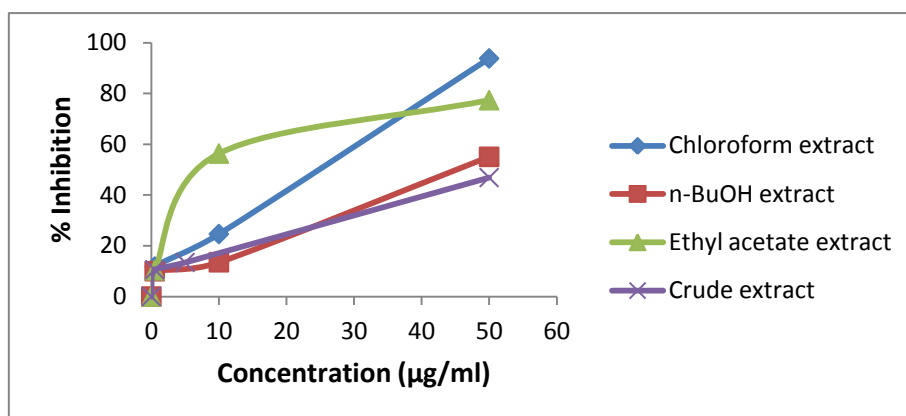


Figure V.2. Scavenging effect of different extracts of *A. tenuifolius* on DPPH radical (%) versus concentration ($\mu\text{g/ml}$).

All the extracts showed an antiradical activity by inhibiting DPPH radical in a concentration-dependent manner. The free radical scavenging activity of the Chloroform extract was higher than Butanol, crude extract and Ethyl acetate extracts at all concentrations with a lowest IC_{50} value at 25 ± 4.36 . The Ethyl acetate extract exhibited a poor activity with an IC_{50} value at 92 ± 4.05 . The Chloroform extract showed an inhibition of 93.798% at a concentration of 0.05 mg. ml^{-1} .

The IC_{50} value of Ethyl acetate extract ($92 \pm 4.05 \text{ mg / ml}$) was higher than those of crude extract ($55 \pm 4.15 \mu\text{g. ml}^{-1}$) and of the Butanol extract ($45 \pm 2.88 \mu\text{g. ml}^{-1}$). It was evident that the extracts show the hydrogen donating ability to act as antioxidants.

The order of antioxidant activity of different extracts of *A. tenuifolius* based on DPPH method was: Ethyl acetate extract < BTH < Crude extract < Butanol extract < Chloroform extract. This difference is strongly related to the phenolic content and also to the type of the active compound present in each variety.

V.1.2. β -Carotene Bleaching assay:

β -Carotene is a naturally occurring orange-colored carbon-hydrogen carotenoid, abundant in yellow-orange fruits and vegetables and in dark green, leafy vegetables [23]. It is also the most widely distributed carotenoid in foods [24].

The β -carotene Bleaching (BCB) method is based on the loss of the yellow color of β -carotene due to its reaction with radicals which are formed by linoleic acid oxidation in an emulsion. The antioxidant activity of the different extracts of *A. tenuifolius* was evaluated secondly by the β -carotene - linoleic acid bleaching method (BCB) [25].

β -Carotene solution (0.2 mg of β -carotene dissolved in 0.2 ml of Chloroform), linoleic acid (20 mg) and Tween 20 (200 mg) were mixed. Chloroform was removed by using a rotary evaporator at 50°C . Distilled water (50 ml) was added. Four milliliters (4 ml) of the emulsion were transferred into several tubes containing 0.2 ml of the different

extracts of *A. Tenuifolius* (5000 ppm in Ethanol) or Ethanol as control. BHT was used as positive control. The tubes were placed at 50°C for 3 hours. The absorbance was measured at 470 nm. Results were expressed as percent of β -carotene bleaching inhibition (AA %) and calculated as follows:

$$AA \% = (A_{\beta\text{-carotene after 180 min}} / A_{\text{initial } \beta\text{-carotene}}) \times 100$$

V.1.2.1. Results & Discussion

The comparable β -carotene bleaching (BCB) rates of the control BHT (as a standard) and the different extracts of *A. tenuifolius* are shown in (Fig. V.4.). The β -carotene bleaching method is one of the most frequently applied methods for determining the total antioxidant property of the plants extracts. In the BCB assay, linoleic acid produces hydroperoxides as free radicals during incubation at 50°C and attacks the β -Carotene molecules that cause reduction in the absorbance at 470 nm. β -Carotene in the systems undergoes rapid discoloration in the absence of antioxidant and vice versa in its presence. The presence of different antioxidants can delay the extent of β -carotene bleaching by neutralizing the linoleate free radical and other free radicals formed in the system [26]. Thus, the degradation rate of β -carotene - linoleate depends on the antioxidant activity of the extracts.

Table V.2. showed the mean antioxidant activity based on the β -carotene bleaching rate of the various extracts of the studied plant. The extract with the lowest β -Carotene degradation rate exhibit the highest antioxidant activity. All extracts had higher antioxidant activities than had the BHT standard.

Table V.2. Antioxidant activity of the different extracts of *A. tenuifolius* and standard assayed by β -Carotene linoleate bleaching. * Values are expressed as mean \pm SD

Extracts	T ₀	T ₁₈₀	Antioxydant Activity (%)	
CHCl₃ Extract			(Average)	
	0,510	0,529	103,725 \pm 0.013	95,692% \pm 0.027
	0,580	0,530	91,379 \pm 0.035	
	0,573	0,527	91,972 \pm 0.032	
BuOH Extract				
	0,466	0,447	95,923 \pm 0.013	97,775% \pm 0.007
	0,461	0,458	99,349 \pm 0.002	
	0,462	0,453	98,052 \pm 0.006	
AcOEt Extract				
	0,470	0,347	73,830 \pm 0.086	73,581% \pm 0.087
	0,470	0,341	72,553 \pm 0.091	
	0,468	0,348	74,359 \pm 0.084	
Crude Extract				
	0,498	0,477	95,783 \pm 0.014	96,582% \pm 0.012
	0,497	0,482	96,982 \pm 0.010	
	0,497	0,482	96,982 \pm 0.010	

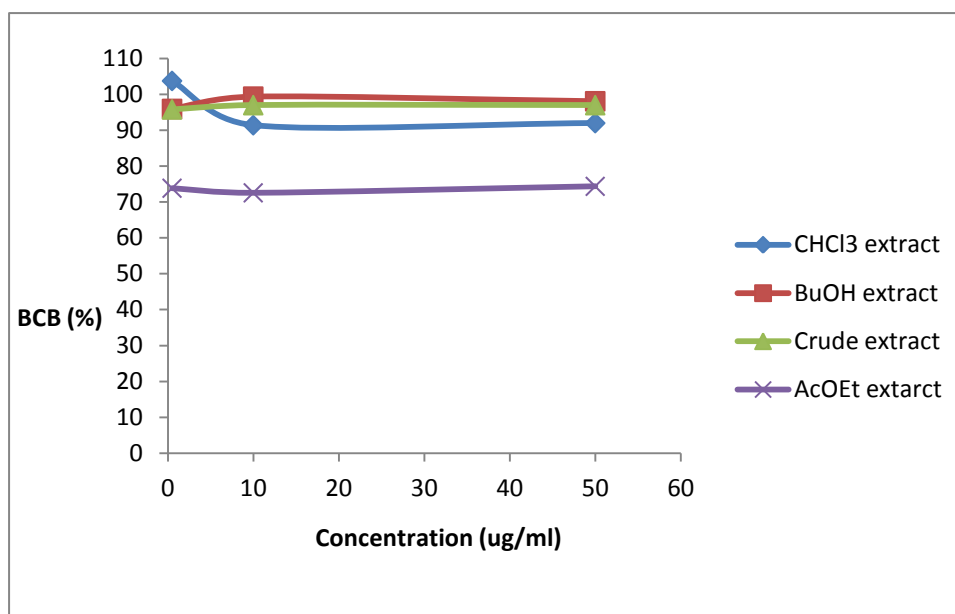


Figure V.3. Scavenging effect of different extracts of *A. tenuifolius* on β -Carotene bleaching (BCB).

The highest antioxidant activity among the samples was observed in Butanol extract whereas Ethyl acetate extract had the lowest antioxidant activity. Results showed that there was considerably variation in the antioxidant activities where it ranges from the lowest of 73.581% to the highest of 97.775% where the orders of the antioxidant activity are as follow: Butanol extract (97.775%) > Crude extract (96,582%) > Chloroform extract (95,692%) > Ethyl Acetate extract (73.581%).

V.1.3. Conclusion

The antioxidant activity of the chloroform extract and other extracts of *A. tenuifolius* was determined by the DPPH and β -Carotene bleaching tests, all the extracts confirmed their free scavenger potency. This activity is largely related to the composition of the extracts and their richness in phenolic compounds as mentioned previously in both TPC and TFC studies suggesting that phenolic compounds are the major contributors to the antioxidant activity of *A. tenuifolius*.

V.2. Antibacterial and antifungal activities

Bacterial infections are among the important infectious diseases. Hence, over 50 years of extensive researches have been launched for achieving new antimicrobial medicines isolated from different sources. Despite progress in development of antibacterial agents, there are still special needs to find new antibacterial agents due to development of multidrug resistant bacteria [27].

Systematic studies among various pharmacological compounds have revealed that any drug may have the possibility of possessing diverse functions and thus may have

useful activity in completely different spheres of medicine. Drugs derived from natural sources play a significant role in the prevention and treatment of human diseases. In many developing countries, traditional medicine is one of the primary health care systems [28-29]. Herbs are widely exploited in the traditional medicine and their curative potentials are well documented [30].

Natural products from plants may give a new source of antimicrobial agents with possibly novel mechanisms of action [31-32]. The effects of plant extracts on bacteria have been studied by a very large number of researchers in different parts of the world [33].

Recently, many phytochemicals, including antibacterial agents, have been clarified from edible plants [34-35]

In this study, the antibacterial and antifungal potential of *A. tenuifolius* extracts has been evaluated using both disk diffusion assays and the microdilution assays.

V.2.1. Disk diffusion assay

Antimicrobial and antifungal activities of the four extracts were evaluated against 8 strains generally recognized as the most important pathogens affecting food dishes: *Escherichia coli* (ATCC 35218), *Vibrio parahaemolyticus* (ATCC 17802), *Staphylococcus aureus* (ATCC 25923), *Salmonella typhimurium* (DT 104), *Staphylococcus epidermidis* (CIP 106510), *Salmonella typhimurium* (ATCC 1408), *Bacillus cereus* (ATCC 11778), *Listeria monocytogenes* (ATCC 19115) and against 4 yeasts belonging to the *Candida* genus: *C. tropicalis* (06-085), *C. parapsilosis* (ATCC 22019), *C. krusei* (ATCC 6258), *C. albicans* (ATCC 2019). The assay was done using the agar disk diffusion method [36-37].

All bacteria were grown on Mueller–Hinton broth supplemented with 1% NaCl at 37°C for 18 to 24 hours prior to inoculation onto the nutrient agar. A loop of bacteria from the agar slant stock was cultivated in nutrient broth overnight and spread with a sterile cotton swab into Petri plates containing 10 ml of API suspension medium and adjusted to the 0.5 McFarland turbidity standards with a Densimat (BioMérieux, France). Sterile filter paper discs (6 mm in diameter, Biolife, Italy) were impregnated with 10 µl of each extract at three different concentrations (10, 30, and 50 mg/ml), then placed on the cultured plates and allowed to dry. After 1 hour at 4°C, the treated Petri dishes were incubated at 37°C for 24 hours.

The same technique was used to evaluate the antifungal activity of all the extracts against four fungal species. All strains were grown on Sabouraud Chloramphenicol agar plate at 30°C for 48 hours. Several colonies of similar morphology were transferred into API suspension medium and adjusted to 2 McFarland turbidity standards with a Densimat (BioMérieux, France). The inocula of the respective yeast were streaked onto Sabouraud chloramphenicol agar plates at 30°C using a sterile swab and then dried. Sterile papers dishes were impregnated with the same extract concentrations as for bacteria. Ampicillin (10 mg/ml) and Amphotericin B (10 mg/ml) were used as a positive control.

The antimicrobial activities were evaluated by measuring the diameter of the growth inhibition zone around the discs. All tests were performed in triplicate and the mean diameter of the inhibition zone was calculated. The results were expressed in terms of zone of inhibition (ZI) of growth around each disc in millimeters as low activity (1 to 6 mm), moderate activity (7 to 10 mm), high activity (11 to 15 mm), very high activity (16 to 20 mm) [38].

V.2.2. Microdilution assay: MICs and MBCs determinations

The Minimal Inhibitory Concentration (MIC) and the Minimal Bactericidal Concentration (MBC) were determined according to the method described by Gomez *et al.*, 2015 [39]. The MIC is the lowest concentration of substance at which it plays to inhibit the growth of target microorganisms. The MBC was interpreted as the highest dilution (lowest concentration) of the sample which showed clear fluid with no development of turbidity and without visible growth. Each extract was first dissolved in 10% dimethylsulfoxide (DMSO), then diluted to the highest concentration in 5 ml sterile glass test tubes, and then serial two-fold dilutions were made to obtain a concentration range from 0.146 to 150 mg/mL. In each 96-well plates, we added 95 μ l of Mueller-Hinton broth (for bacteria) or 95 μ l of Sabouraud Chloramphenicol broth (for yeast strains), and 5 μ l of the correspondent inoculums strain. 100 μ l from the stock solution and its serial dilutions were transferred into eleven consecutive wells. The last well containing 195 μ l of the correspondent nutrient broth without extract and 5 μ l of the inoculums on each strip was used as the negative control. The final volume in each well was 200 μ l. Plates were incubated at 37°C for 24 hours.

V.2.3. Results & Discussion

The different extracts obtained from the aerial part of *A. tenuifolius* were tested using the disc diffusion assay at three different concentrations against a set of Gram positive and Gram negative bacteria. The results of the antibacterial activities acquired from the paper disc method are presented in **Table V.3.**, indicated that the Chloroform extract showed an antibacterial activity against the majority of the tested bacteria with a dose- activity relationship, as evident from the diameters of the inhibition zone (**Table V.3.**).

In fact, the highest inhibition was registered for all extracts with inhibition zone diameter mean values ranging from 8.67 mm to 19.30 mm diameter of zone inhibition for the Chloroform extract, from 9.67 mm to 10.70 mm diameter of zone inhibition for the butanol extract. No inhibition was registered for the Ethyl acetate and the crude extracts with all the tested bacteria.

The growth inhibition zone measured ranged from 9.67 to 19.30 mm for all the sensitive bacteria, and null for all the fungal strains for the different extracts.

The inhibitory effect of the Chloroform extract against *S. epidermidis* was 13 mm diameter of zone inhibition, against *S. aureus* was 9.67 mm, against *V.*

parahaemolyticus was 8.67 mm, against *S. typhimurium* was 19.30 mm diameter of zone inhibition and no inhibitory effect was observed against *E. coli*, *S. typhimurium* ATCC 1408, *B. cereus* and *L. monocytogenes*.

For the Butanol extract, no inhibitory effect was observed against all the tested bacteria only with *S. aureus* with 9.67 mm and against *S. typhimurium* DT104 with 10.70 mm diameter of inhibition zone.

We found that the chloroform extract showed comparatively better antibacterial activity against the gram-positive bacteria and the gram-negative bacteria.

As positive control, Ampicillin was used against the same bacteria. The tested concentration of Ampicillin was effective against all the tested bacteria however all the extracts showed less inhibitory effect on those bacteria.

Amphotericin B was used as a positive control against the same fungal strains. The tested concentration of Amphotericin B was effective against all the tested fungal strains, however all the extracts showed no inhibitory effect.

We could not detect any antifungal activity of the various extracts of our studied *A. Tenuifolius*. This result was reported previously by Dangi *et al.*, 2013 [40].

The antimicrobial activity against both Gram positive and Gram negative bacteria and *Candida sp.* Strains could be related to the presence of several bioactive compounds with pronounced antimicrobial properties. In fact, flavonoids are known to possess antifungal, antiviral and antibacterial properties [41]. In particular, apigenin and kaempferol derivatives are generally considered the most responsible for such activities [42-43].

This result implies that the extract of *A. Tenuifolius* contains some potential therapeutic compounds against some of the medically important bacteria.

The minimal inhibitory concentrations (MIC) and the minimal bactericidal concentrations (MBC) of *A. Tenuifolius* extracts were summarized in **Table V.3**.

MIC generally ranged from 0.58 to 37.5 mg/ml for the Chloroform extract, from 0.39 to 25 mg/ml for the Butanol extract, from 0.78 to 50 mg/ml for the Ethyl acetate extract against all bacterial strains, for the fungal strains it was ranged from 18.75 to 37.5 mg/ml for the Chloroform extract, from 12.5 to 25 mg/ml for the Butanol extract and at 25 mg/ml for the Ethyl acetate extract. Independently of strains, results indicated that the Chloroform extract was the most effective organ as compared to the rest of extracts.

As regards MBC, high concentrations were needed to eliminate the growth of all tested bacterial and fungal strains with values ranging from 2.34 to > 75 mg/ml for the Chloroform extract, from 1.56 to > 50 mg/ml for the Butanol extract, from 3.12 to > 100 mg/ml for the Ethyl acetate extract. Results did not show difference between Gram-positive and Gram-negative strains.

Table V.3. Antibacterial and antifungal activities (expressed as diameter of Inhibition Zone (IZ), on mm), MIC and MBC values (mg/ml) of the different extracts from *A. tenuifolius* (Values expressed as the means IZ ± SD).

Code	Strains	Chloroform Extract			Butanol Extract			Ethyl Acetate Extract			Crude Extract			Ampicillin (10 mg/ml)		
		IZ ± DS	MIC	MBC	IZ ± DS	MIC	MBC	IZ ± DS	MIC	MBC	IZ ± DS	MIC	MBC	IZ ± DS	MIC	MBC
Bacteria																
SP ₃	<i>Staphylococcus epidermidis</i> CIP 106510	13 ± 2	0.58	2.34	6±0	25	>50	6±0	50	>50	6±0	1.56	6.25	21.33±0.57	0.078	0.625
SP ₁	<i>Staphylococcus aureus</i> ATCC 25923	9.67±0.58	2.34	9.37	9.67±0.58	3.12	6.25	6±0	25	>50	6±0	1.56	6.25	26.66±0.57	0.078	0.625
SP ₁₃	<i>Vibrio parahaemolyticus</i> ATCC 17802	8.67±1.15	18.75	75	6±0	25	>50	6±0	50	>50	6±0	25	>25	13.33±0.57	0.011	3
SP ₆	<i>Listeria monocytogenes</i> ATCC 19115	6±0	37.5	>75	6±0	0.39	1.56	6±0	0.78	3.125	6±0	0.048	0.39	12.33±0.57	0.023	0.093
SP ₁₁	<i>Bacillus cereus</i> ATCC 11778	6±0	4.68	18.75	6±0	25	>50	6±0	50	>100	6±0	25	>25	26±1	0.078	0.625
SP ₁₀	<i>Salmonella typhimurium</i> DT 104	19.3±1.15	18.75	37.5	10,7±2.08	3.12	6.25	6±0	50	>50	6±0	12.5	25	*	*	*
SP ₉	<i>Salmonella typhimurium</i> ATCC 1408	6±0	18.75	75	6±0	12.5	>25	6±0	50	>50	6±0	25	>25	18±1	0.023	0.093
SP ₅	<i>Escherichia coli</i> ATCC 35218	6±0	9.37	37.5	6±0	25	>50	6±0	50	>50	6±0	12.5	25	12.33±0.57	0.023	0.093
Yeast														Amphotericin B (10 mg/ml)		
														IZ ± DS	MIC	MBC
C ₁	<i>Candida krusei</i> ATCC 6258	6±0	37.5	>75	6±0	25	>50	6±0	25	>50	6±0	12.5	25	12±0	0.097	0.195
C ₂	<i>Candida albicans</i> ATCC 2019	6±0	18.75	75	6±0	12.5	25	6±0	25	>50	6±0	12.5	25	12.66±0.57	0.024	0.781
C ₃	<i>Candida parapsilosis</i> ATCC 22019	6±0	37.5	>75	6±0	25	>50	6±0	25	>50	6±0	25	>50	10.33±0.57	0.195	0.39
C ₄	<i>Candida tropicalis</i> 06-085	6±0	37.5	>75	6±0	25	>50	6±0	25	>50	6±0	25	>50	12±0	0.39	6.25

According to the scheme proposed by Marmonier, 1990 [44] and Boulaaba *et al.* 2015 [45], an extract is bacteriostatic when the ratio MBC/MIC ≥ 4 and bactericidal if the ratio MBC/MIC < 4 . Based on this report, it can be advanced that the Chloroform extract of *A. Tenuifolius* have a bacteriostatic effect on all pathogens used in this study.

V.3. Cytotoxic activities

Medicinal plants are assumed to be non-toxic and regarded safe due to their natural origin and long use in traditional medicine to treat various forms of diseases [46]. Their preparations are administered with the hope of promoting health and treating various diseases such as infections, colds, inflammation, insomnia, depression, heart diseases, diabetes, cancer and liver diseases has increased in recent times. However, scientific studies on efficacy and safety of some medicinal plants indicated that there are many phytochemicals that have cytotoxic, genotoxic, and carcinogenic effects when used chronically [47]. It should also be kept in mind that if a different extractant is used, the safety ascribed to traditional use based mainly on aqueous extracts may not be relevant at all. The adverse effects of medicinal plant use arise due to organ toxicity, adulteration, contamination, contents of heavy metals, herb-drug interactions, poor quality control and inherent poisonous phytochemical [48]. Some medicinal plant phytochemicals are associated with toxicities of the heart, liver, blood, kidney, central nervous system, gastrointestinal disorder and less frequently carcinogenesis [48]. In the formal herbal industry the toxicity problems of medicinal plants are attributable to insufficient quality assurance and non-compliance to the standards of Good Manufacturing Practice. As part of ethnopharmacological studies of medicinal plant available literature should be searched for known toxic properties of plants of interest before embarking on biological activity studies. However, where toxic effects are unavailable, the inclusion of cytotoxicity and other toxicity protocols in the study are useful in detecting potential toxicity.

The aim of this study is to determine the potential risk of the different extracts of *A. tenuifolius* by evaluating the cytotoxicity using Vero cell lines.

The cytotoxicity of the extracts was evaluated on VERO (African green monkey kidney) cells line. 10^4 Vero cells per well were seeded in 96-well plates and grown in Eagle's Minimum Essential Medium (MEM) supplemented with 5% Fetal Bovine Serum (FBS), 100 units/ml of penicillin, 100 $\mu\text{g/ml}$ of streptomycin and 0.25 $\mu\text{g/ml}$ of Amphotericin B at 37°C under 5% CO₂ atmosphere. After 24 hours incubation, confluent monolayers of Vero cells were exposed to decreasing concentration of the extract (from 3333 $\mu\text{g/ml}$ to 1 $\mu\text{g/ml}$) diluted in MEM supplemented with 2% FBS. After 48 hours of incubation, cell viability was observed in inverted microscope. The 50% Cytotoxic Concentration (CC₅₀), defined as the concentration of the extract able to reduce of 50% the cell viability, was determined by regression analysis in comparison to negative control.

V.3.1. Results & Discussion

The evaluation of the toxic action of plant extracts is indispensable in order to consider a treatment safe; it enables the definition of the intrinsic toxicity of the plant and the effects of acute overdose [49].

The extracts demonstrated activity at or below 100 µg/ml, were categorized as having strong cytotoxic activity, the extracts had LC₅₀ values between 100 µg/ml and 500 µg/ml, were categorized as having moderate cytotoxicity, the extracts had LC₅₀ values between 500 µg/ml and 1000 µg/ml, were considered to have weak cytotoxic activity [50], while the extracts had LC₅₀ values greater than 1000 µg/ml were considered to be non toxic [51].

In the presented study, the different extracts obtained from *A. tenuifolius* were evaluated for their cytotoxicity on VERO (African green monkey kidney) cell lines based on MTT assay. The CC₅₀ values are presented in (Table V.4.)

Table V.4. The CC₅₀ of the cytotoxicity assay of *A. tenuifolius* extracts on VERO cells.

Extracts	CC ₅₀ (µg/ml)
Chloroform	400
Ethyle Acetate	333
BuOH	1340
Crude	200

The highest cytotoxicity among all extracts (CC₅₀ = 200 µg/ml) was observed for the crude extract. Chloroform and ethyl acetate extracts showed a moderate cytotoxicity on VERO cell line with CC₅₀ values of 400 and 333 µg/ml, respectively, indicating the presence of cytotoxic compounds responsible for the observed toxicological activity. The Butanol extract showed a very weak or a non cytotoxicity with a CC₅₀ value of 1430 µg/ml.

V.4. Antiviral activity

The number of antiviral studies using plant extracts has increased in the last decades, and the results have shown that plants are potential sources of compounds that are able to inhibit and/or decrease viral infections. The selection of these plants by ethnopharmacological criteria increases the probability of finding new substances with significant pharmacological and biological activities.

The search for antiviral drugs more effective and affordable is one of strategies to control the viral infections [52-54]. Plants and their derivatives may serve as promising sources of novel antiviral compounds [55-59].

The antiviral activity was evaluated on Coxsackievirus B-3 (CVB-3) and Herpes Simplex Virus type 2 (HSV-2). The viruses were propagated on Vero cells in MEM

medium supplemented with 2% FBS at 37°C under humidified 5% CO₂ atmosphere. The infectious titer of the stock solution was 2.10⁷ TCID₅₀/ml (50% tissue culture infectious doses/ml) for CVB-3 and 8.10⁵ PFU/ml (plaque formation units/ml, PFU) for HSV-2. A MOI (multiplicity of infection) of 0.01 for CVB-3 and 0.1 for HSV-2 was seeded into cells monolayers cultivated in 96-well culture plates (2.10⁴ cells/wells), with different concentrations of the extracts starting from the CC₅₀. Plates without virus or extract were used as negative and positive controls, respectively. After 48 hours incubation, the inhibition of the cytopathic effect (CPE) for CVB-3 and the plaque virus for HSV-2 was observed in inverted microscope. The 50% inhibitory concentration (IC₅₀) defined as the concentration of the extract able to reduce 50% the CPE or plaque virus was determined by regression analysis in comparison to positive control. The selective index (SI) was calculated from the ratio CC₅₀/IC₅₀. A compound is considered as active if the calculated SI is higher than 10 [60].

In any case no extract was active, despite the high number of polyphenols reported in literature to possess inhibitory activity against viruses [61].

V.5. MTT assay

MTT assay was used to evaluate the potential anti-proliferative and cytotoxic activity in A375 (human melanoma) cancer cell line. The cells were incubated for 48 hours with increasing concentration of compounds **11** and **12** (5 μM to 50 μM) and, cell viability was determined by MTT proliferation assay.

V.5.1. Cell Viability Assay.

A375 cells, human melanoma cell line (American Type Culture Collection, Manassa, VA), were cultured in Dulbecco's modified Eagle (DMEM), supplemented with 10% (v/v) FBS, 2mM L-glutamine and antibiotics (100 U/mL penicillin, 100 μg/mL streptomycin) at 37°C in humidified atmosphere with 5% CO₂. To ensure logarithmic growth, cells were sub-cultured every 2 days. A375 cells were seeded in triplicate in 96 well-plates (1 x 10⁴/ well) and incubated for the 48 hours in the absence or presence of different concentrations (5 μM to 50 μM) of **11** and **12** or DMSO (0,1% v/v). Stock solutions of compounds (50 mM in DMSO) were stored at 20°C and diluted just before addition to the sterile culture medium. The number of viable cells was determined by using a [3-4, 5-dimethyldiazol-2-yl]-2, 5-diphenyl tetrazolium bromide (MTT, Sigma-Aldrich) conversion assay, as described [62]. IC₅₀ values were calculated from cell viability dose-response curves and were defined as the concentration resulting in 50% inhibition of cell survival, compared to control cells treated with DMSO.

V.5.2. Analysis of Cell Cycle and Hypodiploidy by Flow Cytometry.

Cell DNA content was measured by propidium iodide (PI) incorporation into permeabilized cells, as described by Nicoletti *et al.*, 1991 [63]. Briefly, the cells were harvested after treatment with our molecules used at concentrations of 10, 20 and 40 μM , washed with cold PBS and incubated with a PI solution (0.1% Sodium citrate, 0.1% Triton X-100 and 25 $\mu\text{g}/\text{ml}$ of prodium iodide, Sigma-Aldrich, 10 $\mu\text{g}/\text{ml}$ Rnase A) for 30 min at 4°C. Data from 10.000 events for each sample were collected by a FACScalibur flow cytometry (Becton Dickinson, San Josè, CA) and cellular debris was excluded from analysis by raising the forward scatter threshold. Percentage of cells in the sub G_0/G_1 phase, hypodiploid region, was quantified using the CellQuest software (Becton Dickinson). The distribution of cells in G_0/G_1 , S, G_2/M phases was determined using ModFit LT cell cycle analysis software (Becton Dickinson).

Proliferation of A375 cells was inhibited by treatment with compound **11** and **12** in a concentration-dependent manner, with IC_{50} values of 20.6 ± 0.8 and 23.2 ± 1.1 μM , respectively.

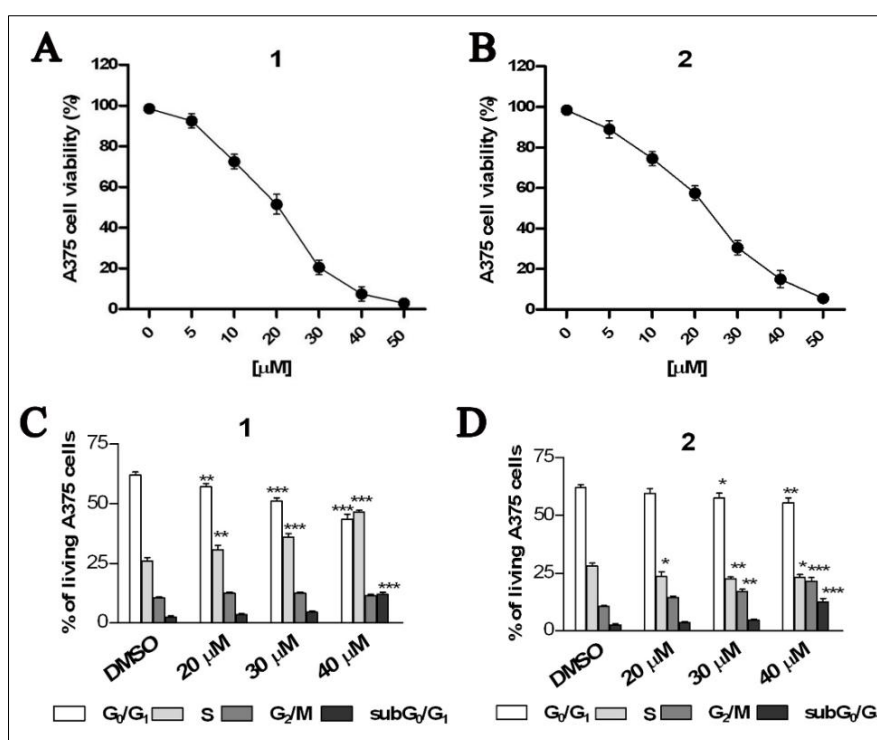


Figure V.4. Compounds **11** and **12** affects A375 human melanoma cell viability and cell cycle progression.

The cells were treated for 48 h with compound **11** (A) or **12** (B), used in different concentrations (5 to 50 μM) and processed for cell proliferation determination by the MTT assay. PI stained viable and hypodiploid A375 cells were analyzed by flow cytometry after the exposure to compound **11** (C) or **12** (D), for 48 h. Results are

expressed as means \pm SD of two experiment performed in triplicate (*P < 0.05, **P < 0.005, ***P < 0.001).

To establish the mechanism of action underlying the inhibition of cancer cell viability caused by the treatment, the cell cycle progression of A375 cancer cells was analyzed by flow cytometry. The cells were incubated for 48 hours with concentrations close to the IC₅₀ values or higher of compounds **11** and **12** (20, 30 and 40 μ M). The effects of compound treatment on cell cycle progression diverged significantly. The treatment with compound **11**, used in increasing concentrations, caused a progressive cell accumulation in S phase with a G1 phase decrease. (**Fig. V.4.C**), whereas compound **12** induced primarily a G2/M arrest with a slight cell decrease in G1 and S phases (**Fig. V.4.D**). Moreover, the treatment with high concentrations of compounds **11** and **12** increased the percentage of melanoma cells with hypodiploid nuclei ($13.2 \pm 1.0\%$ and $12.2 \pm 0.7\%$, respectively). These results indicated a different cytostatic effect concentration-dependent in human melanoma cells of metabolites and a similar pro-apoptotic effect when they were used at higher doses.

V.5.3. CONCLUSION

The *in vitro* activity of these two compounds **11** and **12** was evaluated in human melanoma A375 cells and both the metabolites inhibited the cell proliferation in a concentration-dependent manner, with IC₅₀ values of $\approx 20.0 \mu$ M.

REFERENCES

- [1] Verma, A. R., Vijayakumar, M., Rao, C. V., Mathela, C. S., *Food and Chemical Toxicology*, **2010**, *48*, 704-709.
- [2] Kannan, R. R. R., Arumugam, R., Anantharaman, P., *Asian Pac. J. Trop. Med.*, **2010**, *3*, 898-901.
- [3] Liu, J., Wang, C., Wang, Z., Zhang, C., Lu, S., Liu, J., *Food Chem.*, **2011**, *126*, 261-269.
- [4] Tepe, B., Degerli, S., Arslan, S., Malatyali, E., Sarikurkcu, C., *Fitoterapia*, **2011**, *82*, 237-246.
- [5] Mariod, A. A., Ibrahim, R. M., Ismail, M., Ismail, N., *Food Chem.*, **2010**, *118*, 120-127.
- [6] Tsaliki, E., Lagouri, V., Doxastakis, G., *Food Chem.*, **1999**, *65*, 71-75.
- [7] Erkan, N., Ayranci, G., Ayranci, E., *Food Chem.*, **2008**, *110*, 76-82.
- [8] Skerget, M., Kotnik, P., Hadolin, M., Hras, A. R., Simoncic, M., Knez, Z., *Food Chem.*, **2005**, *89*, 191-198.
- [9] Amarowicz, R., Naczek, M., Shahidi, F., *Journal of American Oil Chemists Society*, **2000**, *77*, 957-961.
- [10] Chang, L. W., Yen, W. J., Huang, S. C., Duh, P. D., *Food Chemistry*, **2002**, *78*, 347-354.
- [11] Janaszewska, A., Bartosz, G., *Scand. J. Clin. Lab. Invest.*, **2002**, *62*, 231-236.
- [12] Bauzaite, R., Venscutonis, P. R., Gruzdiene, D., Tirzite, D., Tirzitis, G., *In Food Technology and Quality Evaluation. Dris R, Sharma A, Science Publishers, In3, United States*, **2003**, 183-193.
- [13] Moon, J. K., Shinamoto, T., *J. Agric. Food Chem.*, **2009**, *57*, 1655-1666.
- [14] Brand-Williams, W., Cuvelier, M. E., Berset, C., *Lebensm. Wiss. Technol.* **1995**, *28*, 25-30.
- [15] PeyratMaillard, M. N., Bonnely, S., Berset, C., *Talanta*, **2000**, *51*, 709-716.
- [16] Huang, D. J., Ou, B. X., Prior, R. L., *J. agric. Food chem.*, **2005**, *53*, 1841-1856.
- [17] Villano, D., Fernandez-Pachon, M. S., Moya, M. L., Troncoso, A. M., Garcia-Parilla, M. C., *Talanta*, **2007**, *71*, 230-235.
- [18] Hanato, T., Kagawa, H., Yasuhara, T., Okuda, T., *Chem. Pharm. Bull.*, **1988**, *36*, 1090-1097.
- [19] <http://www.baltic-analytics.de/index.php?id=40>.
- [20] Espin, J. C., Soler-Rivas, C., Wichers, H. J., *Journal of Agricultural and Food Chemistry*, **2000**, *48*, 648-656.
- [21] Patro, B. S., Bauri, A. K., Mishra, S., Chattopadhyay, S., *Journal of Agricultural and Food Chemistry*, **2005**, *53*, 6912-6918.
- [22] Chaouche, T. M., Haddouchi, F., Ksouri, R., Atik-Bekkara, F., *Journal of the Chinese Medical Association*, **2014**, *77*, 302-307.
- [23] Krinsky, N. I., Johnson, E. J., *Mol. Aspects Med.*, **2005**, *26*, 459-516.
- [24] Rodriguez-Amaya, D. B., Kimura, M., Godoy, H. T., Amaya-Farfan, J., *J. Food Compos. Anal.*, **2008**, *21*, 445-463.

- [25] Jayaprakasha, G. K., Jaganmohan-Rao, L., *Zeitschrift fur Naturforschung C-A Journal of Biosciences*, **2000**, *55*, 1018-1022.
- [26] Jayaprakash, G. K., Selvi, T., Sakariah, K. K., *Food Research International*, **2003**, *36*, 117-122.
- [27] Wise, R., Hart, T., Cars, O., *British Medical Journal*, **1998**, *317*, 609-610.
- [28] Fransworth, N. R., *Journal of Ethnopharmacol*, **1993**, *38*, 145-152.
- [29] Houghton P. J., *Journal of Altern and Complement Med*, **1995**, *1*, 131-143.
- [30] Dubey, N. K., Kumar, R., Tripathi, P., *Current Science*, **2004**, *86*, 37-41.
- [31] Runyoro, D., Matee, M., Olipa, N., Joseph, C., Mbwambo, H., *BMC Complement Altern. Med.*, **2006**, *6*, 11-11.
- [32] Shahidi, B. H., *Asian J. Plant Sci.*, **2004**, *3*, 82-86.
- [33] Reddy, P. S., Jamil, K., Madhusudhan, P., *Pharmaceutical Biol.*, **2001**, *39*, 236-238.
- [34] Jayaprakasha, G. K., *Food Research International*, **2003**, *36*, 117-122.
- [35] Hirasawa, M., *Sing. Int. J. Antimicrob. Agents*, **1999**, *11*, 151-157.
- [36] Ríos, J. L., Recio, M. C., *J. Ethnopharm.*, **2005**, *100*, 80-84.
- [37] Snoussi, M., Noumi, E., Trabelsi, N., Flamini, G., Papetti, A., De Feo, V., *Molecules*, **2015**, *20*, 14402–14424.
- [38] Parveen, M., Ghalib, R. M., Khanam, Z., Mehdi, S. H., Ali, M., *Nat. prod. Res.*, **2010**, *24*, 1268-1273.
- [39] Gomez, A., Bozari, S., Yanmis, D., Gulluce, M., Sahin, F., Agar, G., *Pol. J. Microbiol.*, **2015**, *64*, 121-127.
- [40] Dangi, A. S., Aparna, Madhu S., Yadav, J. P., Arora, D. R., Uma, C., *Journal of Evolution of Medical and Dental Sciences*, **2013**, *2*, 5663-5667.
- [41] Cushnie, T. P., Lamb, A. J., *International Journal of Antimicrobial Agents*, **2005**, *26*, 343-356.
- [42] Basile, A., Giordan, S., Lopez-Saez, J. A., Cobianchi, R. C., *Phytochemistry*, **1999**, *52*, 1479-1482.
- [43] Rauha, J. P., Remes, S., Heinonen, M., Hopia, A., Kähkönen, M., Kujala, T., Pihlaja, K., Vuorela, H., Vuorela, P., *Int. J. Food. Microbiol.*, **2000**, *56*, 3-12.
- [44] Marmonier, A. A., *Introduction aux techniques D'étude des antibiotiques. In: Bactériologie Médicale. Techniques Usuelles, Doin, Paris*, **1990**, 227-236.
- [45] Boulaaba, M., Snoussi, M., Saada, M., Mkadmini, K., Smaoui, A., Abdelly, C., Ksouri, R., *Industrial Crops and Products*, **2015**, *76*, 1114-1122.
- [46] Fennell, C. W., Lindsey, K. L., McGaw, L. J., Sparg, L. G., Stafford, G. I., Elgorashi, E. E., Grace, O. M., Van-Staden, J., *J. Ethnopharmacol*, **2004**, *94*, 205-217.
- [47] Ernst, E., *pharmacoepidemiology and drug safety*, **2004**, *13*, 767–777.
- [48] Jordon, S. A., Cunningham D. G., Marles, R. J., *Toxicology and Applied pharmacology*, **2010**, *243*, 198-216.
- [49] Padmaja, R., Arun, P. C., Prashanth, D., Deepak, M., Amit, A., Anjana, M., *Fitoterapia*, **2002**, *73*, 508-510.

- [50] Clarkson, C., Vineshm, J. M., Neil, R. C., Olwen, M. G., Pamisha, P., Motlalepula, G. M., Niresh, B., Peters, J. S., Peter, I. F., **2004**, *J. Ethnopharmacol*, **92**, 177-191.
- [51] Oketch-Rabah, H. A., Dossaji, J. F., Mberu, E. K., *Pharm. Biol.*, **1999**, **37**, 329-334.
- [52] Chattopadhyay, D., Naik, T. N., *Mini Reviews in Medicinal Chemistry*, **2008**, **7**, 275-301.
- [53] Cos, P., Vlietinck, A. J., Vanden Berghe, D., Maesa, L., *Journal of Ethnopharmacology*, **2006**, **106**, 290-302.
- [54] Martim, K. W., Ernest, E., *Antiviral Therapy*, **2003**, **8**, 77-90.
- [55] Brandão, G. C., Kroon, E. G., Dos Santos, J. R., Stehmann, J. R., Lombardi, J. A., De Oliveira, A. B., *Revista Brasileira de Farmacognosia*, **2010**, **20**, 742-750.
- [56] Cowan, M. M., *Clinical Microbiology Reviews*, **1999**, **12**, 564-582.
- [57] Jassim, S. A. A., Naji, M. A., *J. Applied Microbiology*, **2003**, **95**, 412-427.
- [58] Martim, K. W., Ernest, E., *Antiviral Therapy*, **2003**, **8**, 77-90.
- [59] Rates, S. M. K., *Toxicon*, **2001**, **39**, 603-613.
- [60] Snoussi, M., Trabelsi, N., Dehmeni, A., Benzekri, R., Bouslama, L., Hajlaoui, B., Al-Sieni, A., Papetti, A., *Industrial Crops and Products*, **2016**, **89**, 533-542
- [61] Selway, J. W. T., *Antiviral activity of flavones and flavans*. In: Cody, V., Middleton, E., Harborne, J.B. (Eds.), *Plant Flavonoids in Biology and Medicine: Biochemical, Pharmacological, and Structure Activity Relationships*. Alan R. Liss, Inc., New York, NY. **1986**.
- [62] Terracciano, S., Chini, M. G., Vaccaro, M. C., Strocchia, M., Foglia, A., Vassallo, A., Saturnino, C., Riccio, R., Bifulco, G., Bruno, I., *Chem. Commun. (Camb.)*, **2016**, **52**, 12857-12860.
- [63] Nicoletti, I., Migliorati, G., Pagliacci, M. C., Grignani, F., Riccardi, C., *J. Immunol. Methods*, **1991**, **139**, 271-279.

General Conclusion

The principal subject of this study was the isolation and structural elucidation of the secondary metabolites from *A. tenuifolius* plant collected from the region of Bechar in south west of Algeria, followed by the evaluation of their biological potential. Various chromatographic techniques (HPLC, CC, TLC...), were used for separation and purification of 17 pure natural compounds from the Chloroform and ethyl acetate extracts whose 14 compounds were identified, two compounds were reported for the first time in *A. tenuifolius* specie and two other new compounds reported for the first time in literature. The structures identifications of the isolated compounds were determined by the combination of the different spectral methods: UV-Visible spectrophotometry, NMR 1D and its two-dimensional sequences: COSY, HSQC, HMBC, as well as the ECD Spectra, ESI-MS and HR-MS mass spectrometry data.

Quantitative estimation by spectrophotometric methods of total polyphenols content (TPC) and total flavonoids content (TFC) showed that the CHCl₃ extract has a high content of polyphenols and flavonoids compared to Ethyl acetate and Butanol extracts.

The phytochemical study of both Chloroform and the ethyl acetate extracts allowed the separation and the identification of:

β-Sitosterol (**1**),
Trans-N-feruloyltyramine (**2**),
Asphodeline (**3**),
Luteolin (**4**),
Luteolin-7-*O*-glucosyl (**5**),
Chrysophanol (**6**),
Quercetin-3-*O*-rutinoside (Rutin) (**7**),
5, 7, 4'-trihydroxyflavone (Apigenin) (**8**),
Caffeic acid (**9**),
10, 14-dicaffeoylquinic acid (**10**)
10'-oxanthrone-(*M*, 10'*S*)-*β*-glucopyranosyl asphodelin (**11**),
10'-oxanthrone-(*P*, 10'*S*)-*β*-glucopyranosyl asphodelin (**12**)
Asphodelin-10'-oxanthrone-(10'*R*)-*β*-*D*-xylopyranoside (**13**)
Asphodelin-10'-oxanthrone-(10'*S*)-*β*-*D*-xylopyranoside (**14**).

Various biological activities on the different organic extracts of *A. tenuifolius* plant were studied, the evaluation of the antioxidant activity using DPPH radical scavenging and *β*-Carotene Bleaching assay showed that all these extracts confirmed their free scavenger potency, this activity is largely related to the composition of the extracts and their richness in phenolic compounds. The analysis of the antibacterial activity using 8 strains of bacteria showed an activity only against some ones like *Staphylococcus epidermidis* CIP 106510, *Staphylococcus aureus* ATCC 25923, *Vibrio parahaemolyticus* ATCC 17802 and *Salmonella typhimurium* DT 104 for the

Chloroform extract. The antifungal activity was tested against 4 yeasts, no extract give an activity against all the yeasts.

The antiviral activity showed a negative result too with all the extracts. For the cytotoxic activity, it was moderate to very weak with the different studied extracts.

Finelly, The *in vitro* activity of two new isolated compounds (**11** and **12**) was evaluated on human melanoma A375 cells and both the metabolites inhibited the cell proliferation in a concentration-dependent manner with an IC₅₀ value of $\approx 20.0 \mu\text{M}$.

Abstract

The works presented in this manuscript is a continuation of the phytochemical research carried out by our phytochemistry group affiliated to the VARENBIOMOL research unit from many years on medicinal and aromatic plants growing in different regions of the country, including the vaste Sahara.

The first aim of this research is to value the biological resources related to the plant biodiversity of the Algerian flora and the knowledge associated with this flora in terms of traditional use in medicine, and the second one is the separation and identification of new bioactive compounds with interesting biological activities.

The choice of *Asphodelus tenuifolius* specie for a phytochemical and a biological study in this thesis was based mainly on the fact that this specie belongs to the Liliaceae family known for its richness in various secondary metabolites with a good biological and pharmacological interest, as well as for the good reputation of using this plant in local traditional medicine.

For this purpose, the organic extracts of *A. tenuifolius* specie were studied chemically using various chromatographic methods (TLC, CC, preparative plates, HPLC...) to lead the isolation and the identification of seventeen pure compounds using various spectroscopic analysis, 1D and 2D NMR (^1H , ^{13}C , COSY, HSQC, HMBC ...), ECD analysis, HRESI-MS and ESI-MS spectroscopy, UV-Visible, IR and also with comparison with the literature data. All These data allowed us especially to characterize two new structures of anthraquinones isolated from the Chloroform extract with ten other known compounds dividing into two flavonoids, one sterol, one nitrogen phenolic compound, an anthraquinone and two glycoside anthraquinones with three more compounds in the process of identification, most of these classes are known with their therapeutic benefit and interesting biological activities.

Phytochemical study of Ethyl Acetate extract of this specie allowed also the isolation of six known compounds: two phenolic acids, three flavonoids and one anthraquinone.

Quantitative estimation of total polyphenols and flavonoids contents (TPC and TFC) showed that the Chloroform extract has a high content of polyphenols and flavonoids compared to Ethyl acetate and Butanol extracts.

The biological activities assays like: antioxidant, antibacterial, antifungal, cytotoxic and antiviral performed for the different organic extracts, as well as a cytotoxic activity in A375 (human melanoma) cancer cell line carried out on the two new isolated compounds, confirm the pharmacological and the therapeutic properties of this specie and give an explication of their traditional uses.

Key Words: Liliaceae, *Asphodelus tenuifolius*, anthraquinones, polyphenols, HPLC, NMR 1D, 2D, HR-ESIMS, ECD, biological activities, cytotoxic activity, MTT assay, anti-proliferative potential.

ملخص

العمل المقدم في هذه الأطروحة يدخل في إطار مواصلة البحوث الفيتو كيميائية المنجزة من طرف وحدة البحوث VARENBIOMOL منذ سنوات حول النباتات الطبية و العطرية المتواجدة في مختلف مناطق الوطن و خاصة الصحراوية منها.

الغرض أو الهدف الأول من هذه الدراسة هو تثمين النباتات و المصادر البيولوجية المرتبطة بتنوع الغطاء النباتي في الجزائر و تحصيل المعارف المتعلقة بالاستعمال التقليدي لها من جهة و من جهة أخرى الفصل و التعرف على البنية الكيميائية لمركبات نباتية جديدة ذات نشاط بيولوجي هام.

اختيار نبتة *Asphodelus tenuifolius* لهذه الدراسة الفيتوكيميائية و البيولوجية يعتمد أساسا على انتمائها لعائلة Liliaceae المعروفة بغناها الكبير بالأبيض الثانوي ذو الفائدة البيولوجية الكبيرة و كذا على استعمالها المختلف محليا في الطب البديل بالأعشاب.

لأجل ذلك قمنا بدراسة كيميائية على مختلف المستخلصات العضوية للنبتة باستعمال مختلف طرق الفصل الكروماتوغرافي (كروماتوغرافيا العمود, كروماتوغرافيا الطبقة الرقيقة, كروماتوغرافيا HPLC) و الذي مكن من فصل 17 مركبا نقي تم التعرف على البنية الكيميائية للمركبات المفصولة باستعمال مختلف الطرق المطيافية كالرنين المغناطيسي و تطبيقاته 2D (COSY, HSQC and HMBC...) و 1D (^1H و ^{13}C) إضافة إلى تحاليل ECD, الأشعة فوق البنفسجية, مطيافية الكتلة HR-ESIMS و كذا المقارنة مع مختلف المراجع و المعطيات السابقة.

مكننا فصل مستخلص ثلاثي كلور الميثان أو الكلوروفورم من التحصل على مركبين جديدين لأول مرة من فئة الأنثراكينون (anthraquinone) مع فصل عشر مركبات أخرى معروفة من نفس المستخلص: اثنان من فئة الفلافونويدات, ستيروول, مركب أزوتي, مركب من فئة أنثراكينون و مركبين من فئة الأنثراكينون السكري بالإضافة إلى ثلاث مركبات مفصولة لم يتم تحديد بعد بنيتها الكيميائية. كل هذه المركبات تنتمي إلى فئات كيميائية معروفة بآثارها العلاجية و نشاطها البيولوجي الكبير.

الدراسة الفيتو كيميائية لمستخلص خلات الايثيل مكننا كذلك من فصل ستة مركبات, ثلاثة من فئة الفلافونويدات, حمضين فينول و مركب من فئة الأنثراكينون.

كما تم أيضا تحديد المحتوى الكمي الكلي للفينولات, الفلافونويدات الكلي لكل المستخلصات العضوية للنبتة المدروسة أين أظهر مستخلص ثلاثي كلور الميثان أو الكلوروفورم أكبر نسبة لهذا المحتوى مقارنة مع المستخلصات العضوية الأخرى.

دراسة خصائص البيولوجية لمضادات الأكسدة, مضادات البكتيريا, مضادات الفطريات, النشاط السام للخلايا و النشاط المضاد للفيروسات لكل المستخلصات العضوية و كذا النشاط السام للخلايا للمركبين النقيين المفصولين لأول مرة و كل النتائج المحصل عليها أظهرت و أكدت الخصائص الطبية و الدوائية للاستعمال التقليدي لهذه النبتة ما قد يساهم في إعطاءها أهمية علمية كبيرة قد تساعد على استغلالها بشكل أفضل.

الكلمات المفتاحية: *Liliaceae, Asphodelus tenuifolius*, المركبات الفينولية, كروماتوغرافيا HPLC, مطيافية الكتلة HR-ESIMS, الفعالية البيولوجية, النشاط السام للخلايا.

Résumé

Les travaux présentés dans cette thèse s'inscrivent dans la continuité des recherches phytochimiques effectuées par notre groupe de phytochimie affilié à l'unité de recherche VARENBIOMOL depuis des années sur des plantes médicinales et aromatiques poussant dans différentes régions du pays notamment le Sahara.

Cette recherche vise, premièrement à valoriser les ressources biologiques liées à la biodiversité végétale de la flore algérienne et les connaissances associées à cette flore en matière d'utilisation en médecine traditionnelle, et d'autre part la découverte et la séparation de nouveaux composés bioactifs susceptibles de posséder des activités biologiques intéressantes.

Le choix de l'*Asphodelus tenuifolius* dans le cadre de ce travail de thèse repose principalement sur l'appartenance de cette espèce à la famille des Liliacées connue par sa richesse en divers métabolites secondaires d'un grand intérêt biologique, ainsi que pour la bonne réputation de l'utilisation de cette plante dans la médecine traditionnelle locale.

A cet effet, les extraits organiques de l'espèce *A. tenuifolius* ont été étudiés chimiquement en utilisant des méthodes chromatographiques (CCM, CC, Plaques préparatives et CLHP) pour conduire à l'isolement de 17 composés naturels à l'état pur en utilisant de diverses analyses spectroscopiques RMN 1D et 2D (^1H , ^{13}C , COSY, HSQC, HMBC...), analyses ECD, HRESI-MS et ESI-MS, UV-Vis, IR et en comparant avec la littérature. Ceci a permis la caractérisation de 2 nouveaux produits isolés pour la première fois à partir de l'extrait Chloroforme et appartenant à la classe des anthraquinones ainsi 10 autres produits connus se répartissant en : deux flavonoïdes, un stérol, un composé phénolique azoté, une anthraquinone et deux autres anthraquinones glycosidées avec 3 autres produits en cours d'identification, dont la plupart sont réputés pour leurs vertus thérapeutiques et activités biologiques intéressantes.

L'étude phytochimique réalisée sur l'extrait Acétate d'éthyle de cette espèce nous a permis d'obtenir 6 produits connus : deux acides phénoliques, trois flavonoïdes et une anthraquinone.

L'estimation quantitative des polyphénols et des flavonoïdes totaux a montré que l'extrait CHCl_3 admet une forte teneur en polyphénols et en flavonoïdes par rapport aux autres extraits organiques.

Les tests de recherche des activités biologiques: antioxydante, antibactérienne, antifongique, cytotoxique et antiviral des différents extraits organique de cette espèce, ainsi qu'un test de l'activité cytotoxique effectuées sur les deux nouveaux produits, qui ont été réalisées confirment les propriétés pharmacologiques de cette espèce et donnent une explication sur son utilisation dans la médecine traditionnelle.

Mots Clés : Liliacée, *Asphodelus tenuifolius*, anthraquinones, polyphénols, CLHP, RMN 1D et 2D, HR-ESI-MS, activités biologiques, activité cytotoxique, potentiel antiproliférative.

Glucopyranosylbianthrone from the Algerian *Asphodelus tenuifolius*: Structural Insights and Biological Evaluation on Melanoma Cancer Cells

Ayoub Khalfaoui,^{†,||} Maria G. Chini,^{‡,||} Mohamed Bouheroum,[†] Soumia Belaabed,[†] Gianluigi Lauro,[‡] Stefania Terracciano,[‡] Maria C. Vaccaro,[‡] Ines Bruno,[‡] Samir Benayache,[†] Ines Mancini,[§] and Giuseppe Bifulco^{*,‡,§}

[†]Department of Chemistry, Research Unit, Development of Natural Resources, Bioactive Molecules, Physicochemical and Biological Analysis, University Mentouri Constantine, Route Ain ElBey, 25000, Constantine, Algeria

[‡]Department of Pharmacy, University of Salerno, Via Giovanni Paolo II 132, 84084 Fisciano (SA), Italy

[§]Department of Physics, University of Trento, Via Sommarive 14, I-38123 Povo-Trento, Italy

S Supporting Information

1. Isolation, extraction, and structural characterization

2. Stereoassignment:

- ✓ QM calculation of TS
- ✓ QM calculation of ECD curves
- ✓ QM calculation of NMR parameters

3. In vitro assays on human melanoma cancer cells

4. Inverse Virtual Screening study

1 (M, 10'S) $\Delta G^\ddagger = 24.0$ kcal/mol

2 (P, 10'S) $\Delta G^\ddagger = 21.5$ kcal/mol

ABSTRACT: Two new glucopyranosylbianthrone (1 and 2) were isolated from the aerial part of the plant *Asphodelus tenuifolius*, collected in Southwest Algeria. The 2D structures of 1 and 2 were defined by NMR analysis, HRESIMS data, and comparison with literature data. The comparison of experimental and calculated electronic circular dichroism and NMR data led to characterization of the (*M*) and (*P*) atropisomeric forms of the glucopyranosylbianthrone, asphodelins (1) and (2), respectively. The in vitro activities of these two metabolites were evaluated in human melanoma A375 cells, and both the compounds inhibited cell proliferation at a concentration-dependent manner, with IC₅₀ values of 20.6 ± 0.8 and 23.2 ± 1.1 μM, respectively. Considering their biological profile, an inverse virtual screening approach was employed to identify and suggest putative anticancer interacting targets.

Anthraquinones are a class of aromatic compounds with a 9,10-dioxanthracene core.¹ Many of these are common in plants belonging to the families Fabaceae (Cassia), Liliaceae (Aloe), Polygonaceae (Rheum, Rumex), Rhamnaceae (Rhamnus), Rubiaceae (Asperula, Coelospermum, Coprosma, Galium, Morinda, and Rubia), and Scrophulariaceae (Digitalis).²

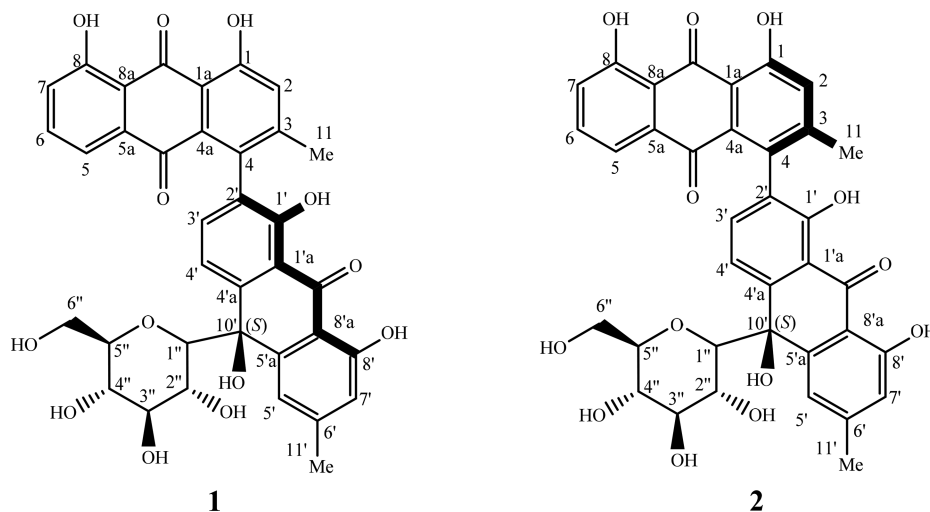
Natural anthraquinones and preanthraquinones are considered important chemotaxonomic markers for plants belonging to the Asphodelaceae (Liliaceae) family.³ *Asphodelus* is a circum-Mediterranean genus, which includes 16 species. It belongs to the Asphodelaceae or Liliaceae family, which comprises 187 genera and 2500 species.⁴ *Asphodelus tenuifolius* Cav. is an annual weed, native to the Mediterranean region, Asia, and the Mascarene Islands. It is known as onion weed⁵ and used as a vegetable.⁶ Seeds, roots, and whole plants are used for medicinal purposes and in the treatment of several

pathologies such as diabetes⁷ and paralysis.⁸ Phytochemical investigations revealed that the plant contains alkaloids, phenols, flavonoids, tannins, steroids, and anthraquinones, including chrysophanol, aloemodin, and anhydrorugulosin. Three bianthraquinones and 8-*O*-(β-D-glucopyranosyloxy)-chrysophanol have also been isolated from this plant.^{9,10} The chemical features of anthraquinones have been linked to their involvement in a series of biological oxidative processes. In addition, their structural features may allow them to strongly interact with DNA, and this can explain the favorable correlation between their cytotoxicity potency and DNA affinity. Anthraquinones with dimeric structure have been shown to act as potential bis-intercalating agents with an increased cytotoxicity activity.¹¹ In particular, the activity

Received: March 20, 2018

Published: July 31, 2018

Chart 1



against melanoma cancer cells exhibited by these molecules has prompted interest in the discovery of more potent agents able to treat this kind of cancer, which is one of the most resistant to classical chemotherapy.

Here we report the isolation and structural characterization of the (*M*) and (*P*) atropisomers of a glucopyranosylbianthrone isolated from the aerial parts of the Algerian plant *A. tenuifolius* Cav. and their cytotoxicity against human melanoma cells.

RESULTS AND DISCUSSION

The CHCl_3 extract of the aerial part of *A. tenuifolius* Cav. was subjected to purification by sequential silica gel chromatography and RP-18 HPLC to yield the two metabolites (**1** and **2**, Chart 1). After the determination of their 2D structures, a quantum-mechanical (QM)/electronic circular dichroism (ECD)/NMR combined protocol was applied to determine their correct stereostructures (vide infra). Such approach provided (1) evidence of possible atropisomerism arising from the hindered rotation about the biaryl axis; (2) comparison of experimental and calculated ECD spectra to define the (*M*) and (*P*) atropisomers; and (3) comparison of calculated and experimental ^{13}C NMR chemical shifts to define the absolute configuration at C-10'.

Compound **1** (Chart 1) was obtained as a yellowish, amorphous powder. Its HRESIMS analysis gave an $[\text{M} - \text{H}]^-$ ion at m/z 669.16353 (calculated for $\text{C}_{36}\text{H}_{29}\text{O}_{13}$, 669.16081), consistent with the molecular formula $\text{C}_{36}\text{H}_{30}\text{O}_{13}$, accounting for 22 indices of hydrogen deficiency. The structure was elucidated by NMR analysis including ^1H , HMBC, and HSQC data. The ^{13}C NMR spectrum of **1** showed 36 carbon resonances, including two methyl groups (δ_{C} 21.9 and 22.9), an oxymethylene (δ_{C} 62.9), eight aromatic methines, five sp^3 oxymethines, 12 quaternary carbons, four oxygenated sp^2 tertiary carbons, three carbonyl carbons (δ_{C} 194.5, 182.6, and 193.4), and one oxygenated sp^3 tertiary carbon. Accordingly, the ^1H NMR spectrum showed eight deshielded resonances ascribable to eight aromatic protons and two singlets at δ_{H} 2.13 and 2.47 assigned to two aromatic methyl groups (Table 1). The ^1H NMR spectrum showed the presence of a hexose unit characterized by five oxymethine protons at δ_{H} 3.45 (d, 9.3), 3.30 (t, 9.3), 3.57 (t, 9.3), 3.15 (t, 9.3), and 3.27 (m) and an oxymethylene at δ_{H} 3.57 (m), 3.77

(m) coupled to their neighbors in this order, as suggested by the COSY experiment. In addition, the ^1H NMR spectrum showed four highly deshielded singlets at δ_{H} 11.87, 12.03, 12.12, and 12.58, indicative of four exchangeable hydrogens bound to oxygen, and assigned to four phenolic groups (δ_{C} 162.9, 162.2, 159.3, and 162.7).¹² The HMBC correlations shown in Figure 1 indicate the cross-peaks between each phenolic group and their respective neighboring carbons, thus permitting their placement at C-1, C-8, C-1', and C-8'.

The arrangement of the aromatic protons, as deduced by COSY and HMBC correlations, indicated the presence of an ABX spin system at δ_{H} 7.59 (1H, d, $J = 8.2$ Hz, H-5), 7.60 (1H, t, $J = 8.2$ Hz, H-6), and 7.24 (1H, d, $J = 8.2$ Hz, H-7), an AX pattern at δ_{H} 7.25 (1H, d, $J = 8.2$ Hz, H-3') and 7.55 (1H, d, $J = 8.2$ Hz, H-4'), two *meta*-coupled protons at δ_{H} 7.20 (1H, s, H-5') and 6.84 (1H, s, H-7'), separated by the C-11' methyl group (HMBC correlation in Table 1 and Figure 1), and an isolated singlet at δ_{H} 7.27 (s, H-2) showing correlation with the methyl protons at δ_{C} 21.9 (C-11). Comparison of the NMR data of **1** with those of reported compounds suggested that it was closely related to asphodaside A,¹² a xylopyranosylbianthrone¹² containing a pentose unit linked at C-10' instead of the hexose moiety revealed and deduced by comparison of the ESIMS and NMR data of **1**. The aromatic singlet at δ_{H} 7.27 (H-2) with the biosynthetically anticipated methyl signal at δ_{C} 21.9 (C-11), as well as the ABX spin system, was assigned to the anthraquinone substructure and was supported by the long-range H–C correlation patterns (H-5/C-10, H-7/C-8a, H-2/C-1a, Table 1). The remaining $^1\text{H}/^{13}\text{C}$ resonances and in particular the AX system (H-3' and H-4') and the pair of *meta*-coupled protons, separated by the 11'-methyl group, were attributed to the oxanthrone substructure. The correlations between the tertiary carbinol at δ_{C} 77.3 (C-10') and H-4' and H-5' were diagnostic for this assignment. The presence of a β -glucopyranosyl unit in compound **1** was supported by (i) the presence in the ESIMS data of an ion at m/z 506, due to the loss of a hexosyl unit from $[\text{M} - \text{H} - 162]^-$, and (ii) the multiplicity of the sugar signals and the $J_{\text{H-H}}$ values were in good agreement with those reported for other β -glucopyranosyl moieties.^{13,14} Finally, analysis of the long-range C/H correlations established the link between the anthraquinone, oxanthrone, and β -glucopyranosyl moieties. In particular, the correlation between C-4 (δ_{C}

Table 1. ^1H (600 MHz) and ^{13}C (150 MHz) NMR Data of Compounds **1** and **2** in CDCl_3^a

position	1			2	
	δ_{C}^b	$\delta_{\text{H}}^{b,c}$	HMBC (H \rightarrow C)	δ_{C}^b	$\delta_{\text{H}}^{b,c}$
1	162.9			164.1	
2	125.6	7.27, s	C-11, C-1a, C-4, C-1	125.6	7.29, s
3	150.4			151.2	
4	131.5			132.5	
5	120.5	7.59, d (8.2)	C-10, C-7	120.0	7.52, d (8.1)
6	137.4	7.60, t (8.2)	C-5a, C-8	137.1	7.56, t (8.1)
7	124.2	7.24, d (8.2)	C-8a, C-5	124.1	7.23, d (8.1)
8	162.2			163.2	
9	194.5			194.1	
10	182.6			183.7	
1a	115.0			116.1	
4a	131.5			132.5	
5a	134.5			135.5	
8a	116.3			116.8	
1'	159.3			159.4	
2'	129.6			130.9	
3'	135.4	7.25, d (8.2)	C-4, C-4'a, C-1'	135.9	7.28, d (8.1)
4'	116.2	7.55, d (8.2)	C-10', C-2', C-1'a	116.0	7.55, d (8.1)
5'	118.5	7.20, s	C-11', C-8'a, C-7', C-10'	119.3	7.17, s
6'	147.9			148.9	
7'	118.3	6.84, s	C-11', C-8'a, C-5', C-8'	118.5	6.85, s
8'	162.7			163.5	
9'	193.4			192.8	
10'	77.3			77.9	
1'a	116.3			117.2	
4'a	145.7			146.8	
5'a	146.7			144.4	
8'a	114.2			115.3	
1''	83.8	3.45, d (9.3)	C-10', C-4'a, C-5'a, C-3''	83.5	3.34, d (9.3)
2''	71.7	3.30, t (9.3)	C-10', C-1'', C-3''	71.4	3.30, t (9.3)
3''	78.8	3.57, t (9.3)	C-2'', C-4'', C-5''	78.7	3.53, t (9.3)
4''	70.7	3.15, t (9.3)	C-3'', C-5'', C-6''	70.5	3.15, t (9.3)
5''	81.0	3.27, m	C-3'', C-1''	79.4	3.04, m
6''	62.9	3.57, m, 3.77, m	C-4''	62.9	3.44, m, 3.56, m
11	21.9	2.13, s	C-3, C-2, C-4	21.5	2.13, s
11'	22.9	2.47, s	C-6', C-5', C-7'	23.0	2.47, s
1-OH		12.58	C-1, C-2, C-1a		12.85
8-OH		12.03	C-8, C-7, C-8a		12.03
1'-OH		12.12	C-1', C-2', C-1'a		12.02
8'-OH		11.87	C-8', C-7', C-8'a		11.72

^aAssignments were based on ^1H , ^1H COSY, HSQC, and HMBC experiments. ^bValues in ppm. ^cMultiplicity and coupling constants (J in Hz) are indicated in parentheses.

131.5) and H-3' (δ_{H} 7.25) defined the linkage between the anthraquinone and oxanthrone substructures (C-4/C-2'), while the correlation between C-10' (δ_{C} 77.3) and the anomeric proton provided evidence of the location of the sugar moiety (Table 1) as well as the type of glucosidic linkage, as supported by the shielded anomeric carbon resonance at δ_{C} 83.8 (C-1''). The IR absorption bands for carbonyl (1604

cm^{-1}), hydroxy (3405 cm^{-1}), and aromatic functionalities (1423 cm^{-1}) supported the anthraquinone-type structure. Collectively, these data defined the structure of **1** as shown in Chart 1.

Compound **2** (Chart 1) was obtained as a yellowish, amorphous powder. Its HRESIMS analysis gave an $[\text{M} - \text{H}]^-$ ion at m/z 669.16345 (calculated for $\text{C}_{36}\text{H}_{29}\text{O}_{13}$, 669.16081), the same as compound **1**. The ^1H and ^{13}C NMR data of compound **2** are similar to those of **1** (Table 1), suggesting the same 2D structure for both.

After defining the 2D structure of the two C-glucosidic metabolites and assuming the presence of a D-glucose, two issues were considered in order to establish the correct stereostructures of **1** and **2**, i.e., atropisomerism around the biaryl axis and the absolute configuration at C-10' (**1a**, **1b**, **2a**, and **2b**, Figure 2).

A conformational search related to the possible diastereoisomers of **1** and **2** (**1a**, **1b**, **2a**, and **2b**, Figure 2), required for the subsequent phases of computation of the ECD spectra and NMR parameters, was performed at the empirical level (molecular mechanics, MM), combining Monte Carlo molecular mechanics (MCM), low-mode conformational sampling (LMCS), and molecular dynamics (MD) simulations (see the Experimental Section). In addition, to corroborate atropisomerism due to the hindered rotation about the biaryl axis,^{15,16} the MM sampled conformers of the possible atropisomers for each diastereoisomer were subjected to geometry and energy optimization steps at the MPW1PW91/6-31G(d) density functional level of theory (DFT).

After geometry optimization, the conformers were visually inspected in order to avoid redundant conformers. DFT calculations were employed for predicting the rotational energy barrier related to the interconversion between the atropisomers (Experimental Section) for both the (10'R) and (10'S) configurations. This parameter was calculated for the **1b** (*M*, 10'R) and **2b** (*P*, 10'R) atropisomers, obtaining $\Delta G^\ddagger = 24.0$ and 21.5 kcal/mol, and referred to the difference between the most stable conformers of **1b** and **2b** and the related energy of the transition state, respectively. Such high rotational barriers are compatible with the hindered rotation about the biaryl bond.¹⁵ Similar results were found for the **1a** (*M*, 10'S) and **2a** (*P*, 10'S) atropisomers, obtaining values of $\Delta G^\ddagger = 23.1$ and 20.6 kcal/mol, thus corroborating the presence of atropisomerism and the related hindered interconversion.

Next, the calculated and experimental ECD spectra were compared to predict the atropisomeric forms of **1** and **2**. Starting from the conformers related to the diastereoisomers featuring both the (10'R) and (10'S) absolute configurations and the *M/P* atropisomeric forms (**1a**, **1b**, **2a**, and **2b**, Figure 2), the ECD curves were calculated at the MPW1PW91/6-31G(d,p) functional/basis set in EtOH (IEFPCM) to reproduce the effect of the solvent.¹⁷ Comparison of the experimental and calculated ECD curves of **1** and **2** (Figure 3) showed that the calculated spectra of the (*M*) atropisomeric forms (**1a** and **1b**) are similar to the experimental ECD of **1**. On the other hand, the simulated spectra of atropisomeric forms (*P*) (**2a** and **2b**) are superimposable to the experimental ECD spectrum of **2**, regardless of the relative configuration at C-10'. Therefore, these results suggest that the Cotton effects are not influenced by the 3D arrangement at C-10', further supporting the hindered rotation of the biaryl bond. These results highlighted an important result in the stereoassignment

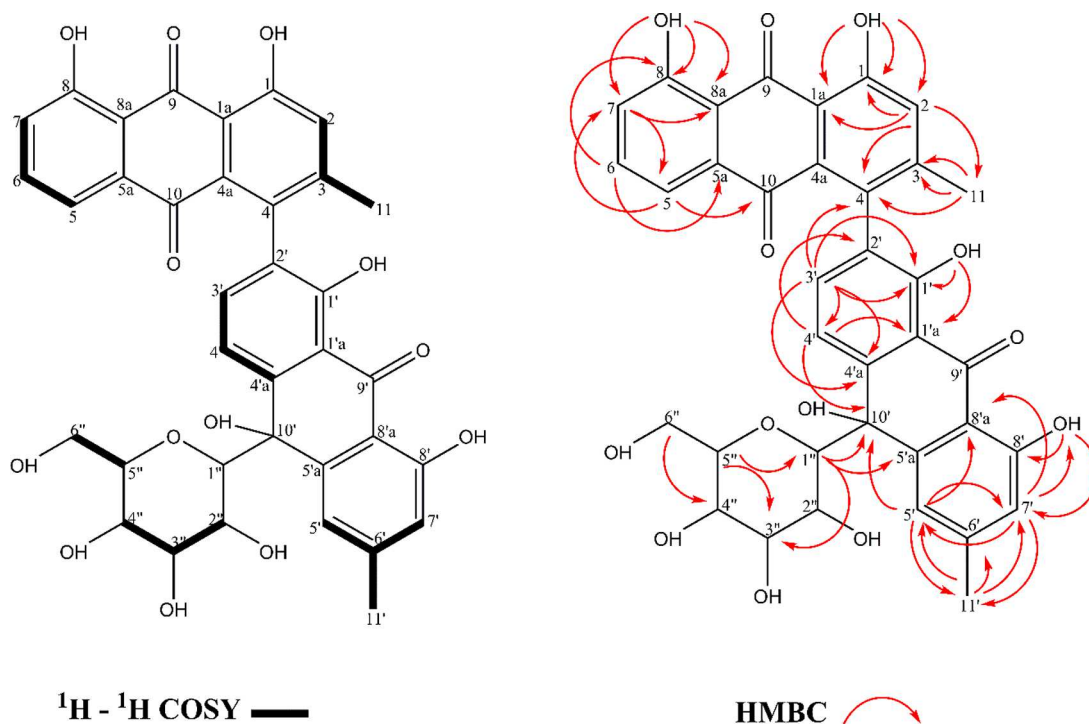


Figure 1. 2D NMR correlations of compounds **1** and **2**, $^1\text{H}-^1\text{H}$ COSY coupling (bold face bonds), and HMBC correlations.

process: the real structure of **1** is restricted to those of **1a** and **1b**, whereas **2** will correspond to **2a** or **2b**. Consequently, in order to assign the C-10' configuration, we applied a DFT/NMR approach that has been successfully used in the characterization of unknown stereostructures by us^{18–22} and by other research groups.²³ For both pairs of possible diastereoisomers (**1a** or **1b** vs **1**, and **2a** or **2b** vs **2**), the Boltzmann-weighted averages of the predicted ^{13}C NMR chemical shifts were computed at the MPW1PW91/6-31G(d,p) level, accounting for the energies of each sampled conformer on the final Boltzmann distribution. Furthermore, the multistandard approach (MSTD)^{24,25} was employed, using tetramethylsilane (TMS) and benzene as reference for sp^3 and sp^2 ^{13}C atoms. For each atom, the experimental and calculated ^{13}C NMR chemical shifts were compared and the mean absolute errors (MAEs) for the pairs of possible diastereoisomers were computed.

The results highlighted the better fit with the experimental data (Table 1) of **1a** (^{13}C MAE = 2.8 ppm) versus **1b** (^{13}C MAE = 4.4 ppm) and of **2a** (^{13}C MAE = 2.1 ppm) versus **2b** (^{13}C MAE = 4.5 ppm), suggesting the (10'S) absolute configuration for both atropisomers (Tables S1 and S2, Supporting Information, for comparison between the experimental and calculated ^{13}C NMR chemical shift data). Accordingly, the structures of **1** (*M*, 10'S) and **2** (*P*, 10'S) were defined as shown in Chart 1.

After this phase of structural characterization, the MTT assay was used to evaluate the potential antiproliferative and cytotoxic activity in the A375 (human melanoma) cancer cell line. The cells were incubated for 48 h with increasing concentrations of compounds **1** and **2** (5–50 μM), and cell viability was determined using the MTT proliferation assay. Proliferation of A375 cells was inhibited by treatment with compounds **1** and **2** in a concentration-dependent manner, with IC_{50} values of 20.6 ± 0.8 and 23.2 ± 1.1 μM , respectively (Figure 4A,B).

To establish the mechanism of action of the inhibition of cancer cell viability caused by treatment with **1** and **2**, the cell cycle progression of A375 cancer cells was analyzed by flow cytometry. The cells were incubated for 48 h with concentrations close to the IC_{50} values or higher of compounds **1** and **2** (20, 30, and 40 μM). The effects of the treatment with both compounds on cell cycle progression diverged significantly. Specifically, the treatment with compound **1**, used in increasing concentrations, caused a progressive cell accumulation in the S phase with a G1 phase decrease (Figure 4C), whereas compound **2** primarily induced a G2/M arrest with a slight cell decrease in G1 and S phases (Figure 4D). The treatment with high concentrations of compounds **1** and **2** increased the percentage of melanoma cells with hypodiploid nuclei ($13.2 \pm 1.0\%$ and $12.2 \pm 0.7\%$, respectively). These results indicated a different concentration-dependent cytostatic effect in human melanoma cells of the two metabolites and a similar pro-apoptotic effect when they were used at higher doses. Starting from these results, an inverse virtual screening (IVS) approach was used as a tool for the rapid selection of the most promising targets for these bioactive natural compounds.^{27–30} In this phase, the aglycone portion (**3**, Chart 2) was screened against 306 targets (Table S3, Supporting Information) involved in cancer and inflammation pathologies, by means of molecular docking calculations.

After the normalization process, a ranking with the most promising interacting targets was obtained (the first 30 identified targets are reported in Table S4, Supporting Information). Analysis of the ligand/protein complexes at a molecular level highlighted several interacting targets, for which their correlation with melanoma was reported. In the first position of the IVS ranking (Table S4, Supporting Information), adenosine A_{2A} , a receptor playing a key role in melanoma, was identified.³¹ Indeed, A_{2A} antagonism has been reported as a useful strategy to directly interfering with the protumor effects of adenosine in melanoma tissue. Further-

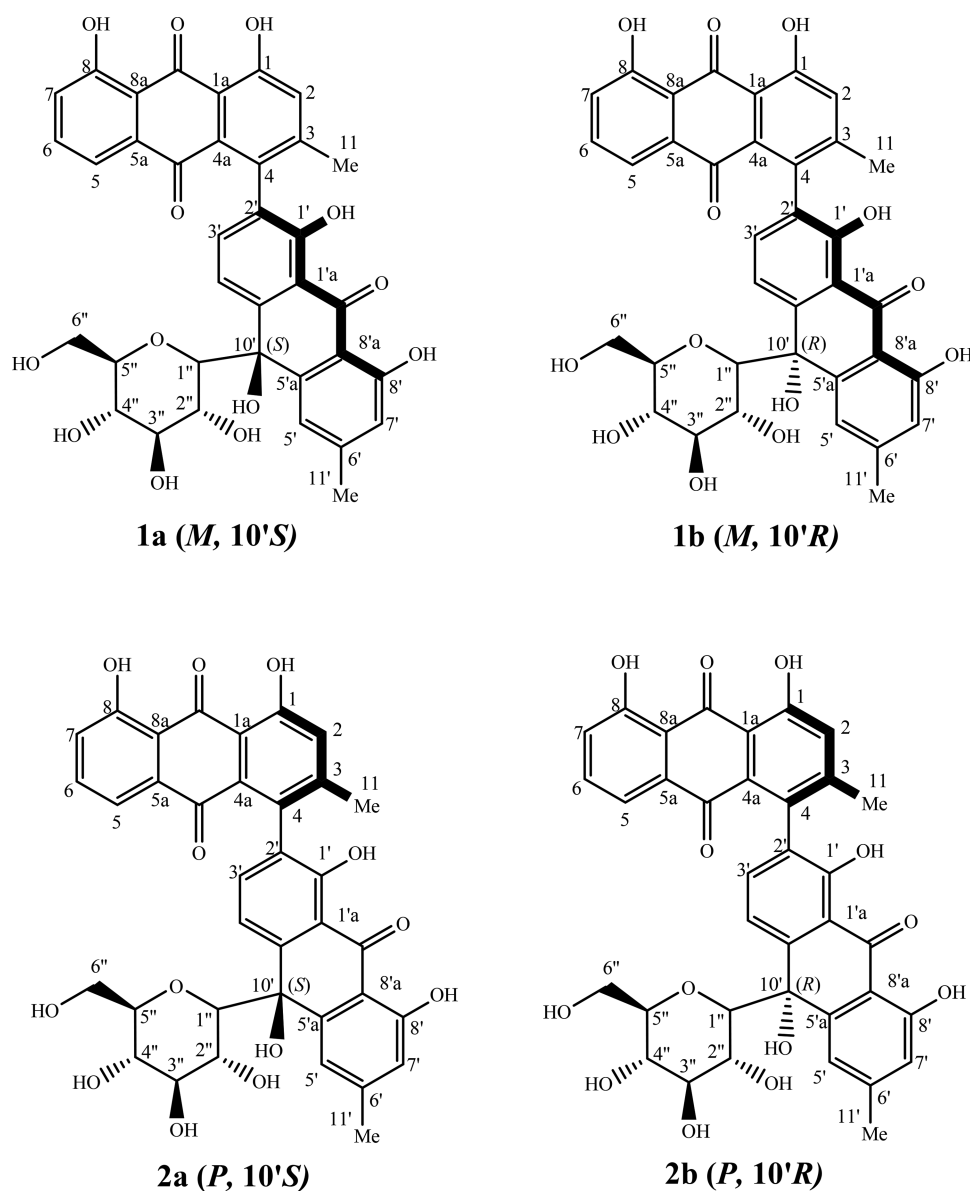


Figure 2. Molecular structures of the four possible diastereoisomers of **1** and **2** (**1a**, **1b**, **2a**, and **2b**).

more, inhibition of glycogen synthase kinase (GSK)-3 β , identified as the third best target by IVS, is correlated with the reduction of the motile and invasive behavior of melanoma cells.³² Polo-like kinase 1 (PLK1, the fourth target identified by IVS) expression is dynamically regulated during the cell cycle in human melanoma, and the combined inhibition of PLK1 and MAPK has been reported as a potentially attractive strategy in melanoma therapy.³³ The results from the IVS are in agreement with the disclosed specific antimelanoma biological activity, and further biological evaluations are ongoing in our laboratory to corroborate the virtual outcomes.

In summary, a multistep protocol was applied to the isolation and structural and biological characterization of two novel compounds isolated from the aerial parts of *A. tenuifolius*. The 2D structures of **1** and **2** were defined following the standard combination of isolation, purification, and characterization of the natural products using the general techniques (HPLC, NMR, etc.). The correct stereoassignment of these two metabolites was determined with the comparison of the experimental and calculated ECD curves and NMR param-

eters, allowing the assignment of **1** (*M*, 10'*S*) and **2** (*P*, 10'*S*) as two atropisomeric forms of the same glucopyranosylbiantnone. Furthermore, the evaluation of their biological activity disclosed their interesting effects on melanoma cancer cells, prompting us to further investigate this aspect through the application of the inverse virtual screening methodology. From this *in silico* study, a panel of 30 interacting targets involved in inflammatory and tumoral events was identified, and these outcomes will be followed by further biological study to confirm the antitumoral activity of the reported compounds.

EXPERIMENTAL SECTION

General Experimental Procedures. Optical rotations were determined with an Autopol IV instrument. FT-IR (Fourier-transform infrared) spectra were recorded by using an FT-IR Bruker Tensor 27/37 spectrometer equipped with an attenuated transmitter reflection device at 4 cm⁻¹ resolution in the absorption region ΔV 4000–1000 cm⁻¹. NMR spectroscopic data were acquired on a Bruker DRX-600 spectrometer at 300 K. 2D NMR spectra were acquired in CDCl₃ in the phase-sensitive mode with the transmitter set at the solvent resonance and time proportional phase increment used to achieve

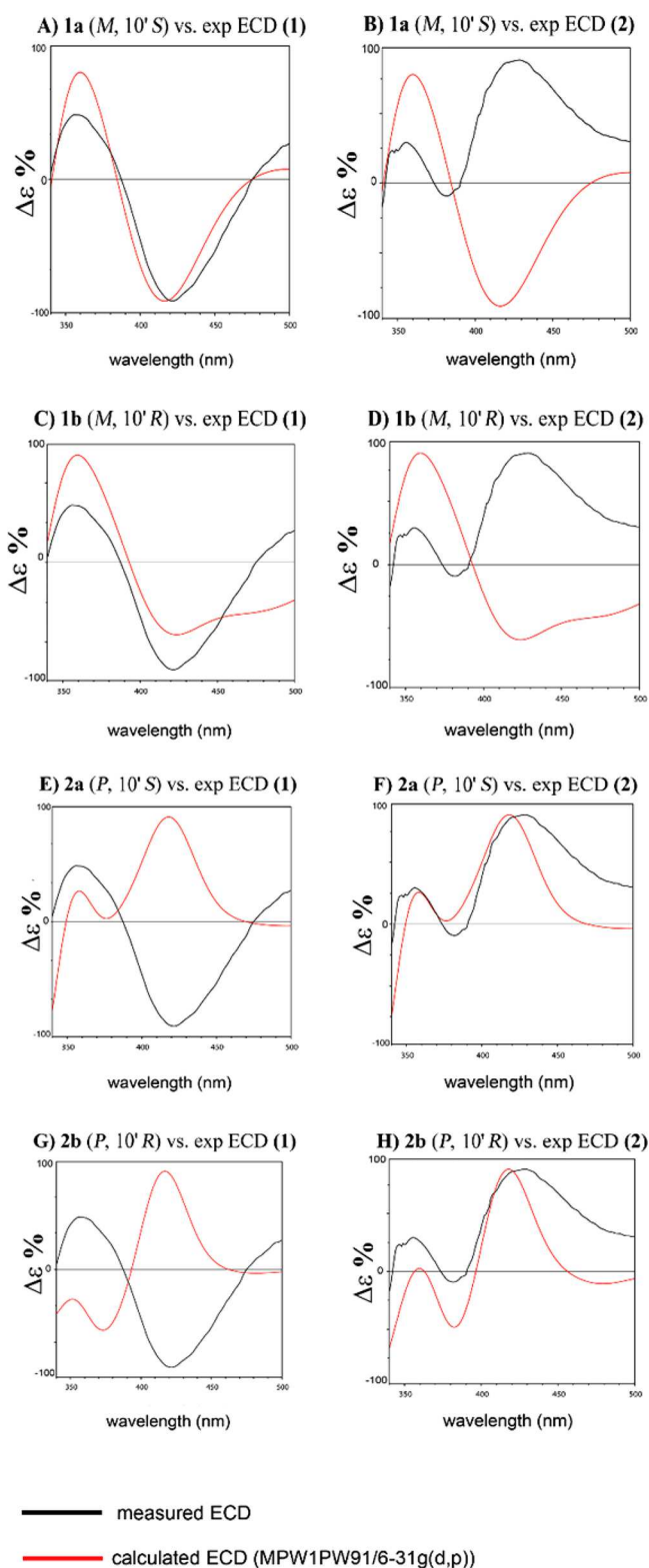


Figure 3. Comparison of the experimental ECD spectra of **1** and **2** with the TDDFT-predicted curves of compounds **1a**, **1b**, **2a**, and **2b**. The region of interest (350 to 500 nm) as reported for other known similar glucosyl anthraquinones is shown.^{12,14,26}

frequency discrimination in the ω_1 dimension. The standard pulse sequence and phase cycling were used for DQF-COSY, HSQC, and HMBC. Electrospray ionization (ESI) mass spectra were recorded on a Bruker Esquire-LC spectrometer equipped with an electrospray ion source used in positive or negative ion mode by direct infusion of a

methanolic solution of the sample, under the following conditions: source temperature 300 °C, drying gas N₂, scan range 100–1000 *m/z*. HRESIMS data were acquired on an LTQ Orbitrap XL mass spectrometer (Thermo Fisher Scientific, San Jose, CA, USA) operating in negative ion mode. Column chromatography (CC) was performed on silica gel (63–200 μm , Merck, Darmstadt, Germany); TLC was performed on precoated Kieselgel 60 F₂₅₄ plates (0.2 mm, Merck, Darmstadt, Germany); the mobile phases used for TLC analyses were CHCl₃/MeOH (9.5:0.5) and CHCl₃/MeOH (9:1), and the spots were detected by treating with a Ce(SO₄)₂/H₂SO₄ (Sigma-Aldrich, Milano, Italy) solution. Preparative TLC was carried out on silica gel GF254 (20 × 20 cm, 1 mm thickness). HPLC was done with a Merck Hitachi L-6200 equipped with a UVIDEC 100-V detector using a Phenomenex Luna RP-18 column (5 μm , 250 mm, 4.60 mm).

Plant Material. Aerial parts of *A. tenuifolius* were collected in May 2010 in Southwest Algeria. The plant was identified by M. Mohamed Benabdelhakem (Ex-Director of the National Agency of Preservation of Natural Resources, Bechar, Algeria). An authenticated voucher specimen, with the identification number AS10TEN, was deposited at the Herbarium of the VARENBIOMOL research unity, University Mentouri of Constantine, Algeria.

Extraction and Isolation. A total of 1860 g of air-dried and powdered aerial parts of *A. tenuifolius* was extracted with EtOH/H₂O (80:20 v/v × 3, 48 h) three times at room temperature. After filtration, the filtrates were concentrated using a rotary evaporator. The combined ethanolic extract was evaporated at 38 °C to give a residue (105.5 g), which was suspended in distilled water. Each resulting solution was extracted successively with CHCl₃ (3 × 400 mL), EtOAc (3 × 400 mL), and *n*-BuOH (6 × 400 mL). The organic phases were filtered using common filter paper and concentrated under vacuum at 38 °C to obtain the following dry organic extracts: CHCl₃ (5.60 g), EtOAc (7.77 g), and *n*-BuOH (14.41 g). The residue from the CHCl₃ extract (5.60 g) was dissolved in 5 mL of CHCl₃ and subjected to CC on silica gel (63–200 mesh, 170 g) eluted with *n*-hexane/EtOAc gradient elution and then with increasing percentages of MeOH. Fractions of 50 mL were collected to yield 28 fractions (F1–F28) obtained by combining the different eluates based on TLC analysis. Fractions 14 and 15 were combined (101.90 mg) and subjected to CC on silica gel eluting with CHCl₃/MeOH with an increasing polarity to yield six subfractions according to their TLC behavior. After purification on preparative TLC (silica gel₂₅₄, CHCl₃/MeOH, 9.0:1.0), subfraction 3 (55.1 mg) gave a mixture containing two major compounds. A 35 mg amount of this mixture was subjected to semipreparative HPLC analysis on a reversed-phase Phenomenex Luna C₁₈ column (250 mm × 4.6 mm, 5 μm particle diameter), using MeCN/H₂O (50:50 v/v) at a flow rate of 1.0 mL/min and detection at 254 nm to give compounds **1** (4 mg, *t_R* = 28 min) and **2** (5 mg, *t_R* = 19 min), respectively.

(*M*,10'*S*)-1',4,5,8',10'-Pentahydroxy-2,6'-dimethyl-10'- β -glucopyranosyl-[1,2'-bianthracene]-9,9',10(10'*H*)-trione, **1**: yellowish, amorphous powder, detected as a single spot on silica gel TLC with CHCl₃/MeOH (9:1) at *R_f* 0.80; IR (KBr) ν_{max} 3405, 2923, 2852, 1604, 1423, 1361, 1282, 1093 cm⁻¹; [α]_D²⁵ -270 (*c* 0.01, MeOH); ECD 422 ($\Delta\epsilon$ -1.34), 356 (+0.71), 317 (-0.99), 256 (-3.76), 213 (+5.26); ESI (-) MS *m/z* 668.9 [M - H]⁻, 505.9 [(M - H - (C₆H₁₂O₆)]⁻; HRESIMS *m/z* 669.16353 [(M - H)⁻, calcd for C₃₆H₂₉O₁₃, 669.16081]; ¹H (CDCl₃, 600 MHz) and ¹³C NMR (CDCl₃, 150 MHz) data, see Table 1.

(*P*,10'*S*)-1',4,5,8',10'-Pentahydroxy-2,6'-dimethyl-10'- β -glucopyranosyl-[1,2'-bianthracene]-9,9',10(10'*H*)-trione, **2**: yellowish, amorphous powder, detected as a single spot on silica gel TLC with CHCl₃/MeOH (9:1) at *R_f* 0.70; IR (KBr) ν_{max} 3409, 2919, 1600, 1420, 1355, 1280, 1091 cm⁻¹; [α]_D²⁵ +4.6 (*c* 0.1, MeOH); ECD 428 ($\Delta\epsilon$ +2.98), 382 (+0.81), 356 (+0.77), 320 (-3.78), 249 (+9.88), 230 (-1.60), 233 (+0.77), 212 (-12.99); ESI (-) MS *m/z* 668.9 [M - H]⁻, 505.9 [(M - H - (C₆H₁₂O₆)]⁻; HRESIMS [M - H]⁻ *m/z* 669.16345 [(M - H)⁻, calcd for C₃₆H₂₉O₁₃, 669.16081]; ¹H (CDCl₃, 600 MHz) and ¹³C NMR (CDCl₃, 150 MHz) data, see Table 1.

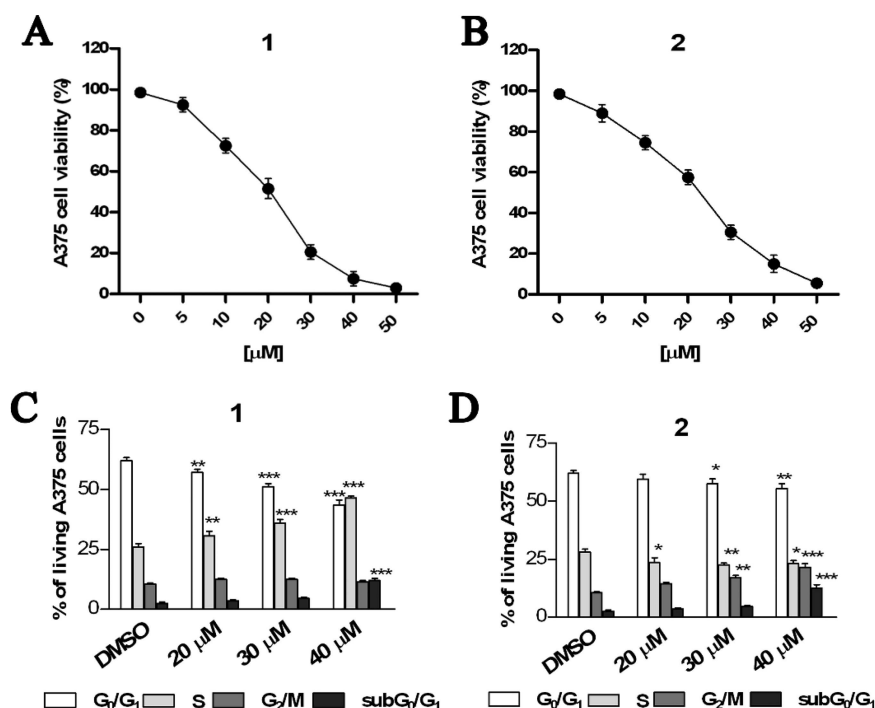
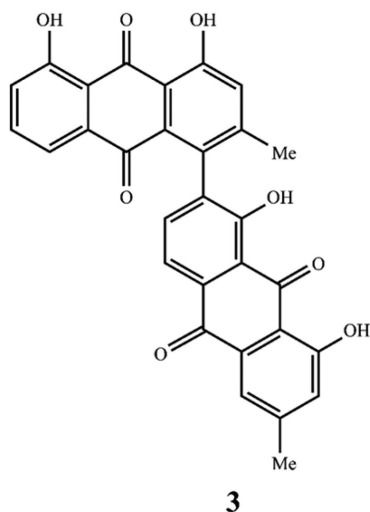


Figure 4. Compounds 1 and 2 affect A375 human melanoma cell viability and cell cycle progression. The cells were treated for 48 h with compound 1 (A) or 2 (B), used in different concentrations (5–50 μM) and processed for cell proliferation determination by the MTT assay. Propidium iodide-stained viable and hypodiploid A375 cells were analyzed by flow cytometry after exposure to compound 1 (C) or 2 (D), for 48 h. Results are expressed as means \pm SD of two experiments performed in triplicate (* $P < 0.05$, ** $P < 0.005$, *** $P < 0.001$).

Chart 2



Computational Details. Maestro 10.2³⁴ was used for generating the starting 3D chemical structures of the possible diastereoisomers of compounds 1 and 2 (1a, 1b, 2a, and 2b, Figure 2). As a first step exhaustive conformational searches at the empirical MM level with the MCM method (50 000 steps) and LMCS method (50 000 steps) were performed, in order to allow a full exploration of the conformational space. Furthermore, molecular dynamics simulations were performed at different temperatures (450, 600, 700, 750 K), with a time step of 2.0 fs, an equilibration time of 0.1 ns, and a simulation time of 10 ns. All the conformers were minimized using the OPLS force field³⁵ and the Polak–Ribier conjugate gradient algorithm. The “redundant conformer elimination” module of MacroModel 10.2³⁴ was used to select nonredundant conformers. For compounds 1 and 2, MM conformational searches produced both sets of atropisomers, which were separated after visual inspection once the hindered

rotation along the biaryl axis was assessed by means of QM calculations (vide infra). The QM calculations were performed using Gaussian 09 software.³⁶ The conformers were optimized at the QM level using the MPW1PW91 functional and the 6-31G(d) basis set.³⁷ The atropisomerism arising from the hindered rotation along the biaryl axis was evaluated via computation of the rotational energy barrier required for the interconversion between the 1a (*M*, 10'*S*) and 2a (*P*, 10'*S*), and 1b (*M*, 10'*R*) and 2b (*P*, 10'*R*) atropisomers (Figure 2). Specifically, the starting geometry model representing the transition state was built with the two phenyl moieties roughly in the same plane, which was subsequently optimized at the QM level using the Bery algorithm, the MPW1PW91 functional, and the 6-31G(d) basis set, followed by vibrational frequency calculations. Analysis of the vibrational frequencies showed that the optimized structure was correctly associated with the transition state, since the two phenyl moieties slightly moved along the biaryl axis, producing the two different atropisomeric forms at each oscillation. Comparison of the energies between the lowest energy-associated conformer found for 1a (*M*, 10'*S*) and 2a (*P*, 10'*S*), and 1b (*M*, 10'*R*) and 2b (*P*, 10'*R*), and the transition states confirmed the hindered rotation along the biaryl axis, and then the different atropisomers were separately considered for the subsequent computation of the ECD spectra and NMR spectroscopic parameter calculations. Afterward, assuming the presence of a β -glucopyranosyl unit, the prediction of the ECD spectra was performed using all the significant conformers and performing QM calculations at the TDDFT (NStates = 40) MPW1PW91/6-31G(d,p) level in EtOH (IEFPCM) to reproduce the effect of the experimental solvent.¹⁷ The final ECD spectra of 1a, 1b, 2a, and 2b were built considering the influence of each conformer on the total Boltzmann distribution and taking into account the relative energies and were graphically plotted using SpecDis software.³⁸ In order to simulate the experimental ECD curve, a Gaussian band-shape function was applied with an exponential half-width (σ/γ) of 0.20 eV. After proving the presence of atropisomerism, the selected conformers for the different pairs of diastereoisomers of compounds 1a and 1b versus 1, and 2a and 2b versus 2, were used for the subsequent computation of the ¹³C NMR chemical shifts, using

the MPW1PW91 functional and the 6-31G(d,p) basis set. Final ^{13}C NMR values for each of the diastereoisomers were calculated considering the influence of each conformer on the total Boltzmann distribution taking into account the relative energies. Calibrations of calculated ^{13}C NMR chemical shifts were performed following the multistandard approach^{29,30} (see above). The data were evaluated considering the $|\Delta\delta|$ parameter (absolute differences in experimental vs calculated ^{13}C NMR chemical shifts) and the MAE parameter ($\text{MAE} = \sum(|\delta_{\text{exp}} - \delta_{\text{calc}}|)/n$) (summation through n of the absolute values of the differences in the corresponding experimental and calculated ^{13}C NMR chemical shifts).

Cell Viability Assay. A375 cells, a human melanoma cell line (American Type Culture Collection, Manassa, VA, USA), were cultured in Dulbecco's modified Eagle, supplemented with 10% (v/v) fetal bovine serum, 2 mM L-glutamine, and antibiotics (100 U/mL penicillin, 100 $\mu\text{g}/\text{mL}$ streptomycin) at 37 °C in a humidified atmosphere with 5% CO_2 . To ensure logarithmic growth, cells were subcultured every 2 days. A375 cells were seeded in triplicate in 96-well plates ($1 \times 10^4/\text{well}$) and incubated for 48 h in the absence or presence of different concentrations (5–50 μM) of **1** and **2** or DMSO (0.1% v/v). Stock solutions of compounds (50 mM in DMSO) were stored at –20 °C and diluted just before addition to the sterile culture medium. The number of viable cells was determined by using the MTT [3-(4,5-dimethylthiazol-2-yl)-2,5-diphenyltetrazolium bromide] conversion assay (Sigma-Aldrich).³⁹ IC_{50} values were calculated from cell viability dose–response curves and were defined as the concentration resulting in 50% inhibition of cell survival, compared to control cells treated with DMSO.

Analysis of Cell Cycle and Hypodiploidy by Flow Cytometry. The cell DNA content was measured by propidium iodide (PI) incorporation into permeabilized cells.⁴⁰ Briefly, the cells were harvested after treatment with compounds **1** and **2** used at concentrations of 10, 20, and 40 μM , washed with cold phosphate-buffered saline, and incubated with a PI solution (0.1% sodium citrate, 0.1% Triton X-100, and 25 $\mu\text{g}/\text{mL}$ of PI, Sigma-Aldrich, 10 $\mu\text{g}/\text{mL}$ Rnase A) for 30 min at 4 °C. Data from 10 000 events for each sample were collected by FACScalibur flow cytometry (Becton Dickinson, San José, CA, USA), and cellular debris was excluded from analysis by raising the forward scatter threshold. Percentage of cells in the sub G_0/G_1 phase, hypodiploid region, was quantified using the CellQuest software (Becton Dickinson). The distribution of cells in G_0/G_1 , S, and G_2/M phases was determined using ModFit LT cell cycle analysis software (Becton Dickinson).

Statistical Analysis. All data represent the mean \pm SD of at least three independent experiments performed in triplicate. The statistical significance of cell cycle distribution results was performed by two-way analysis of variance (ANOVA) with Bonferroni post-test analysis using GraphPad Prism 5 software. The P value ≤ 0.05 was considered significant.

Inverse Virtual Screening. The chemical structures of compound **3** and eight “blank” compounds were built with Maestro (version 10.2) Build Panel.³⁴ The panel of targets (306 protein 3D structures) was built downloading the .pdb files from the Protein Data Bank database (www.rcsb.org, Table S3, Supporting Information). Molecular docking calculations were performed using the Autodock-Vina software.⁴¹ In the configuration files linked to 3D structures of the protein are coordinates and dimensions along the x , y , z axes of the grid related to the site of presumable pharmacological interest, with a spacing of 1.0 Å between the grid points. The exhaustiveness parameter⁴¹ was set to 64, saving 10 conformations as a maximum number of binding modes. For all the investigated compounds, all acyclic bonds were treated as active torsional bonds. A starting set of promising interacting proteins of **3** was selected setting a predicted binding affinity cutoff = –7.5 kcal/mol. The identified proteins (253 items) were then also screened against the eight “blank” molecules, the latter needed for the normalization of the binding affinities of **3**, as reported in eq 1:

$$V = V_0/V_R \quad (1)$$

where V represents the normalized value of **3**, V_0 is its predicted binding affinity from docking calculations (kcal/mol), and V_R is the average value of binding energy calculated on all the “blanks” (kcal/mol). It is important to note that V is a dimensionless number and, thus, may be used to predict the interacting targets of a case-study compound, rather than to have precise indications about the related binding affinities. A final ranking was obtained from the most to the least promising target. Normalized values and predicted binding energies for **3** are reported in Table S4 (Supporting Information).

■ ASSOCIATED CONTENT

📄 Supporting Information

The Supporting Information is available free of charge on the ACS Publications website at DOI: 10.1021/acs.jnatprod.8b00234.

IR, HRESIMS, ^1H NMR, HSQC, HMBC, and COSY spectra for compounds **1** and **2** of the chloroform extract of the aerial part of the plant *A. tenuifolius* Cav; comparison between experimental and calculated ^{13}C NMR chemical shifts for **1** and **2**; PDB codes of 306 targets and final ranking of 30 interacting targets obtained by an inverse virtual screening study of **3** (PDF)

■ AUTHOR INFORMATION

Corresponding Author

*Tel: +39 089969741. Fax: +39 089969602. E-mail: bifulco@unisa.it.

ORCID

Giuseppe Bifulco: 0000-0002-1788-5170

Author Contributions

^{||}A. Khalfaoui and M. G. Chini contributed equally to this work.

Notes

The authors declare no competing financial interest.

■ REFERENCES

- Chien, S. C.; Wu, Y. C.; Chen, Z. W.; Yang, W. C. *Evid. Based Complement. Alternat. Med.* **2015**, *2015*, 357357.
- Seigler, D. S. *Plant Secondary Metabolism*; Springer-Verlag New York Inc., 2012; p 759.
- Van Wyk, B. E.; Yenesew, A.; Dagne, E. *Biochem. Syst. Ecol.* **1995**, *23*, 23.
- Lifante, Z. D.; Aguinagalde, I. *Am. J. Bot.* **1996**, *83*, 949–953.
- Aslam, N.; Janbaz, K. H.; Jabeen, Q. *Bangladesh J. Pharmacol* **2016**, *11*, 11.
- IUCN. *A Guide to Medicinal Plants in North Africa*; IUCN Centre for Mediterranean Cooperation: Malaga, Spain, 2005; p 256.
- Ahmed, N.; Mahmood, A.; Tahir, S. S.; Bano, A.; Malik, R. N.; Hassan, S.; Ashraf, A. J. *Ethnopharmacol.* **2014**, *155*, 1263–1275.
- Abu-Rabia, A. *Chin. Med.* **2012**, *3*, 157–166.
- Abdel-Mogib, M.; Basaif, S. A. *Die Pharmazie* **2002**, *57*, 286–287.
- Hammouda, F. M.; Rizk, A. M.; Seif el-Nasr, M. M. *Die Pharmazie* **1974**, *29*, 609–610.
- Taher, A. T.; Hegazy, G. H. *Arch. Pharmacol Res.* **2013**, *36*, 573–578.
- Ghoneim, M. M.; Elokely, K. M.; El-Hela, A. A.; Mohammad, A. E.; Jacob, M.; Radwan, M. M.; Doerksen, R. J.; Cutler, S. J.; Ross, S. A. *Phytochemistry* **2014**, *105*, 79–84.
- Adinolfi, M.; Corsaro, M. M.; Lanzetta, R.; Parrilli, M.; Scopa, A. *Phytochemistry* **1989**, *28*, 284–288.
- Yang, Y.; Yan, Y. M.; Wei, W.; Luo, J.; Zhang, L. S.; Zhou, X. J.; Wang, P. C.; Yang, Y. X.; Cheng, Y. X. *Bioorg. Med. Chem. Lett.* **2013**, *23*, 3905–3909.

- (15) Bringmann, G.; Price Mortimer, A. J.; Keller, P. A.; Gresser, M. J.; Garner, J.; Breuning, M. *Angew. Chem., Int. Ed.* **2005**, *44*, 5384–5427.
- (16) Smyth, J. E.; Butler, N. M.; Keller, P. A. *Nat. Prod. Rep.* **2015**, *32*, 1562–1583.
- (17) Tomasi, J.; Mennucci, B.; Cammi, R. *Chem. Rev.* **2005**, *105*, 2999–3093.
- (18) Chini, M. G.; Malafronte, N.; Vaccaro, M. C.; Gualtieri, M. J.; Vassallo, A.; Vasaturo, M.; Castellano, S.; Milite, C.; Leone, A.; Bifulco, G.; De Tommasi, N.; Dal Piaz, F. *Chem. - Eur. J.* **2016**, *22*, 13236–13250.
- (19) Bifulco, G.; Dambruoso, P.; Gomez-Paloma, L.; Riccio, R. *Chem. Rev.* **2007**, *107*, 3744–3779.
- (20) Cerulli, A.; Lauro, G.; Masullo, M.; Cantone, V.; Olas, B.; Kontek, B.; Nazzaro, F.; Bifulco, G.; Piacente, S. *J. Nat. Prod.* **2017**, *80*, 1703–1713.
- (21) Masullo, M.; Cantone, V.; Cerulli, A.; Lauro, G.; Messano, F.; Russo, G. L.; Pizza, C.; Bifulco, G.; Piacente, S. *J. Nat. Prod.* **2015**, *78*, 2975–2982.
- (22) Di Micco, S.; Chini, M. G.; Riccio, R.; Bifulco, G. *Quantum Chemical Calculation of Chemical Shifts in the Stereochemical Determination of Organic Compounds: A Practical Approach*; Springer Netherlands: Handbook of Marine Natural Products, 2012; pp 571–599.
- (23) Willoughby, P. H.; Jansma, M. J.; Hoye, T. R. *Nat. Protoc.* **2014**, *9*, 643–660.
- (24) Sarotti, A. M.; Pellegrinet, S. C. *J. Org. Chem.* **2009**, *74*, 7254–7260.
- (25) Sarotti, A. M.; Pellegrinet, S. C. *J. Org. Chem.* **2012**, *77*, 6059–6065.
- (26) Zhu, J. J.; Zhang, C. F.; Zhang, M.; Bligh, S. W.; Yang, L.; Wang, Z. M.; Wang, Z. T. *J. Chromatogr. A* **2010**, *1217*, 5384–5388.
- (27) Lauro, G.; Romano, A.; Riccio, R.; Bifulco, G. *J. Nat. Prod.* **2011**, *74*, 1401–1407.
- (28) Lauro, G.; Masullo, M.; Piacente, S.; Riccio, R.; Bifulco, G. *Bioorg. Med. Chem.* **2012**, *20*, 3596–3602.
- (29) Gong, J.; Sun, P.; Jiang, N.; Riccio, R.; Lauro, G.; Bifulco, G.; Li, T. J.; Gerwick, W. H.; Zhang, W. *Org. Lett.* **2014**, *16*, 2224–2227.
- (30) Giordano, A.; Forte, G.; Massimo, L.; Riccio, R.; Bifulco, G.; Di Micco, S. *Eur. J. Med. Chem.* **2018**, *152*, 253–263.
- (31) Montinaro, A.; Iannone, R.; Pinto, A.; Morello, S. *Pharmacol. Res.* **2013**, *76*, 34–40.
- (32) John, J. K.; Paraiso, K. H.; Rebecca, V. W.; Cantini, L. P.; Abel, E. V.; Pagano, N.; Meggers, E.; Mathew, R.; Krepler, C.; Izumi, V.; Fang, B.; Koomen, J. M.; Messina, J. L.; Herlyn, M.; Smalley, K. S. *J. Invest. Dermatol.* **2012**, *132*, 2818–2827.
- (33) Jalili, A.; Moser, A.; Pashenkov, M.; Wagner, C.; Pathria, G.; Borgdorff, V.; Gschaidner, M.; Stingl, G.; Ramaswamy, S.; Wagner, S. N. *J. Invest. Dermatol.* **2011**, *131*, 1886–1895.
- (34) *Maestro 10.2*; Schrödinger LLC: New York NY, 2015.
- (35) Piazza, G.; Fanikos, J.; Zayaruzny, M.; Goldhaber, S. Z. *Thromb. Haemostasis* **2009**, *102*, 505–510.
- (36) Frisch, M. J.; Trucks, G. W.; Schlegel, H. B.; Scuseria, G. E.; Robb, M. A.; Cheeseman, J. R.; Scalmani, G.; Barone, V.; Mennucci, B.; Petersson, G. A.; Nakatsuji, H.; Caricato, M.; Li, X.; Hratchian, H. P.; Izmaylov, A. F.; Bloino, J.; Zheng, G.; Sonnenberg, J. L.; Hada, M.; Ehara, M.; Toyota, K.; Fukuda, R.; Hasegawa, J.; Ishida, M.; Nakajima, T.; Honda, Y.; Kitao, O.; Nakai, H.; Vreven, T.; Montgomery, J. A., Jr.; Peralta, J. E.; Ogliaro, F.; Bearpark, M.; Heyd, J. J.; Brothers, E.; Kudin, K. N.; Staroverov, V. N.; Kobayashi, R.; Normand, J.; Raghavachari, K.; Rendell, A.; Burant, J. C.; Iyengar, S. S.; Tomasi, J.; Cossi, M.; Rega, N.; Millam, J. M.; Klene, M.; Knox, J. E.; Cross, J. B.; Bakken, V.; Adamo, C.; Jaramillo, J.; Gomperts, R.; Stratmann, R. E.; Yazyev, O.; Austin, A. J.; Cammi, R.; Pomelli, C.; Ochterski, J. W.; Martin, R. L.; Morokuma, K.; Zakrzewski, V. G.; Voth, G. A.; Salvador, P.; Dannenberg, J. J.; Dapprich, S.; Daniels, A. D.; Farkas, Ö.; Foresman, J. B.; Ortiz, J. V.; Cioslowski, J.; Fox, D. J. *Gaussian 09, Revision A.02*; Gaussian, Inc.: Wallingford, CT, 2009.
- (37) Cimino, P.; Gomez-Paloma, L.; Duca, D.; Riccio, R.; Bifulco, G. *Magn. Reson. Chem.* **2004**, *42*, S26–S33.
- (38) Bruhn, T.; Schaumlöffel, A.; Hemberger, Y.; Bringmann, G. *Chirality* **2013**, *25*, 243–249.
- (39) Terracciano, S.; Chini, M. G.; Vaccaro, M. C.; Strocchia, M.; Foglia, A.; Vassallo, A.; Saturnino, C.; Riccio, R.; Bifulco, G.; Bruno, I. *Chem. Commun. (Cambridge, U. K.)* **2016**, *52*, 13515.
- (40) Nicoletti, I.; Migliorati, G.; Pagliacci, M. C.; Grignani, F.; Riccardi, C. *J. Immunol. Methods* **1991**, *139*, 271–279.
- (41) Trott, O.; Olson, A. J. *J. Comput. Chem.* **2010**, *31*, 455–461.